COALFIELD GEOLOGY COUNCIL OF NEW SOUTH WALES

Geological Hazards

Proceedings of a Symposium held at Newcastle 15-16th November 2001

Edited by
Rod Doyle & Julie Moloney

Geological Hazards – The Impact On Coal Mining

Coalfield Geology Council of New South Wales

Executive
Chairman: Michael Creech, Powercoal
Secretary: Michael Armstrong, NSW Department of Mineral Resources
Past Chairman: Andrew Newland Newtuk Consulting Pty Ltd
John Lea, Groundsearch Australia Pty Ltd
John Edwards, Consulting Geologist - Collective Experience

Postal Address
The Secretary
Coalfield Geology Council of New South Wales
NSW Department of Mineral Resources
PO Box 536
St Leonards NSW 2065
Australia

LIST OF SPONSORS

The Coalfield Geology Council of NSW extends its deep appreciation to our sponsors. Without their generous support the necessary seed money to hold this conference would not have been available.

GeoGAS

Valley Longwall Drilling
ACARP

Engineering Computing Services International (ECSI)
Carbon Consulting International (CCI)
McElroy Bryan Geological Services (MBGS)
Reeves Wireline
Mitchell Drilling

COALFIELD GEOLOGY COUNCIL OF NEW SOUTH WALES

GEOLOGICAL HAZARDS

The Impact on Coal Mining

Proceeding of a Symposium held at Lake Macquarie, New South Wales
15-16th November 2001

Edited by

Rod Doyle & Julie Moloney

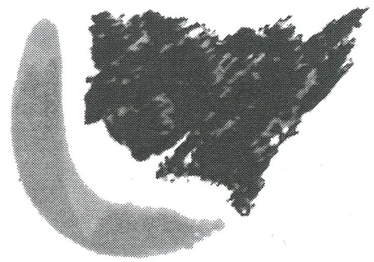

ORGANISED BY THE

COALFIELD GEOLOGY COUNCIL OF NEW SOUTH WALES

in conjunction with

NEW SOUTH WALES DEPARTMENT OF MINERAL RESOURCES
SYDNEY BASIN COAL GEOLOGIST GROUP

First published in 2001 for the Coalfield Geology Council of New South Wales

ISBN 0-9579774-0-9

National Library of Australia Cataloguing-in-Publication data:
Geological Hazards : The Impact On Coal Mining
Proceedings of a symposium held at Lake Macquarie,
New South Wales, 15-16th November 2001.

Bibliography
1. Mineral industries – Geological Hazards – Congresses.
2. Doyle, Rod. 1956-
3. Coalfield Geology Council of New South Wales.

Cover design, typeset and compact disc set up by Lee Moore-Sam
Freeform Marketing & Design – email address **freeform@hunterlink.net.au**

Cover photograph: A thin (<20cm thick) siderite dyke at Dartbrook Coal, showing possible compaction deformation. Here it crosscuts the WUB1 formation – a volcanic tuff within the Wynn Upper seam.

Printed in Australia

Contents

The Chairman's Comment

Geological Hazards is the third symposia organised by the Coalfield Geology Council of NSW concerned with the interaction between the science of geology and coal mining. The first in 1996 (Geology in Longwall Mining) dealt with a wide range of issues from strata control to resource delineation. The second in 1997 concentrated on the role of geology and geologists in mine safety issues. Both symposia were well attended and many excellent papers were presented. The symposia volumes will remain a valuable resource on any geologist's bookcase.

In keeping with the primary role of the Coalfield Geology Council, this symposium continues the same basic theme, with the emphasis turning to the management and identification of geological hazards. Although many of these hazards have been impacting on mining for many years the tools and methods that enable geologists to better understand these features are always improving. As a result, it is essential that we all keep up to date and have some understanding of the relative strengths and weaknesses of each technique. The best way of keeping up to date with these issues is to attend a symposium like this, where you can hear the presentations, read the symposium volume and talk to your peers.

The Coalfield Geology Council of NSW is a body established with the aim of bringing together geological knowledge from government, individuals, private companies and academic groups to assist the NSW coal industry. The Council's roles include: liaison between industry and government, the revision and publication of codes and standards, and the standardisation of geoscience techniques and terminology. This is the 40th anniversary of this body whose members currently total 50, representing a wide range of interested bodies. In recent years the Council has been involved in promoting the "JORC Code for Resources and Reserves" and formulating the "Guidelines for the Estimation and Reporting of Australian Black Coal Resources and Reserves". It has also been involved in regional stratigraphic correlation and assessments of structure across the Sydney Basin. I urge every company directly involved in coal mining in NSW to be active in the Council and provide an active representative.

The Council would like to acknowledge the contribution of the sponsors that have made the running of this conference possible, as well as the editors and the many contributors who, in the current climate must generally contribute their personal time to prepare their presentations. These contributions along with the anticipated attendance at this conference will, I am sure, attest to the relevance of this symposia series.

Michael Creech
Chairman

SESSION ONE — CHANGES

Geological Hazards — The impact to mining 15-16 November 2001, eds Doyle, Moloney, pp 3-8

Climate changes – a geologist's view

CLAUS F.K. DIESSEL

C.F.K. & L.J. Diessel

Because of the potential severity of the problem of climate change for future generations, it is unfortunate that the debate of current climatic trends and their causes has been shifted from the realms of detached rationality to the prophecies of various interest groups who exert pressure on our political masters to do something about it even though the prescribed medicine might not be helpful. Much of this debate is concentrated on the recent increase in global temperature of approximately 0.6°C since the end of the 19th Century, while little attention is paid to the numerous climate changes that preceded the current temperature rise. Yet, the study of our climate would greatly benefit from a wider application of the Principle of Uniformitarianism because most of what is happening now has happened before without any anthropogenic interference.

WHAT IS CLIMATE?

The Chambers Science and Technology Dictionary defines climate as "the statistical ensemble of atmospheric conditions characteristic of a particular locality over a suitably long period (e.g. 30 years) including relevant parameters such as mean and extreme values, measures of variability, and descriptions of seasonal variations." Aspects considered include:

- humidity,
- rainfall,
- solar radiation,
- cloud,
- wind, and
- atmospheric pressure.

All seven parameters vary with geographic altitude, latitude and longitude such that local and seasonal values may differ considerably from the global means of +15°C for the average surface temperature, or 1 bar for the average surface pressure.

THE COMPOSITION OF THE ATMOSPHERE

Apart from solar radiation which is as much part of the climatic condition as it is a major extraterrestrial cause of it, the other six parameters are intimately linked to the composition of our atmosphere. The current atmospheric composition can be summarised as follows:

Nitrogen (N_2) content	78.09%
Oxygen (O_2) content	20.95%
Argon (Ar) content	0.93%
Carbon Dioxide (CO_2) content	0.036%
Neon (Ne) content	0.002%
Helium (He) content	0.0005%
Water Vapour (H_2O)	0.01 to 5.0%

Additional components of very small proportions are methane (CH_4), nitrous oxide (N_2O), sulfate aerosols, ozone, and several largely man-made gases, e.g. CFCs, carbontetrachloride and others.

The atmosphere functions like the glass cover of a greenhouse, and it has been calculated (Lean and Rind, 1996; Bayer, 2001) that without this cover, the mean surface temperature on Earth would be –18°C rather than the previously mentioned +15°C. The atmospheric components mainly responsible for this difference are (in order of importance) water vapour, carbon dioxide, methane and some of the other gases mentioned above. They all come under the generic term of greenhouse gases because they store heat by letting solar radiation pass through the atmosphere on its way to Earth, while absorbing the long-wave radiation that is reflected back from Earth's surface. Exceptions are ozone and airborne sulfates which are cooling agents.

Neither the current composition of the atmosphere, nor the previously mentioned atmospheric conditions have been static throughout Earth's history, and there is a strong possibility of the existence of a causal link between atmospheric composition and atmospheric condition. Indeed, the popular assumption that anthropogenic greenhouse gases are the cause of the current global warming is based on the idea that such a link exists.

Before we can intelligently discuss the extent of the current climatic changes and their causes, it is essential to try to understand the history of Earth's atmosphere. With few exceptions, neither the composition, nor the climatic properties of the atmosphere of past geological periods can be measured directly. Palaeoclimatic research relies therefore largely on palaeontological, petrological and sedimentological evidence contained in the rock record. This evidence tells us that the climate has undergone many changes in the geological past. Naturally, the resolution of these often cyclic changes decreases with geological age.

THE ORIGIN OF THE ATMOSPHERE

It is reasonable to assume that the first atmosphere formed from the gaseous exhalations of ancient volcanoes and other sources of fluid lava. It is further reasonable to assume that the composition of these gases was not fundamentally different from the exhalations that still today emanate from volcanoes, i.e. water vapour, carbon dioxide, nitrogen and sulphur dioxide. The lack of free oxygen in modern volcanic exhalations, as well as astronomic and lithologic evidence suggest that the Archaic atmosphere was oxygen-free but enriched in carbon dioxide, probably not unlike the approximately 95% carbon dioxide that make up the atmospheres of our two planetary neighbours, Mars and Venus.

The precipitation of water vapour to form the ancient oceans on Earth, and the development of photosynthesis, some 3Ga ago, brought about a fundamental change in the composition of our atmosphere. Water is capable of dissolving large quantities of most gases which, in the case of carbon dioxide means that there are 60 times more CO_2 contained in ocean water than in the atmosphere. This means that the formation of oceans caused the first major reduction in atmospheric carbon dioxide. The second reduction began with the development of life, when marine algae started to tap into the rich source of carbon dioxide which they synthesised with water to form carbohydrates and other organic compounds. This had a major effect on atmospheric composition, because not only was carbon dioxide stored temporarily in organisms, but the formation of organic and inorganic limestone began to withdraw vast quantities of CO_2 from the early carbon cycle as well.

The development of photosynthesis, initially by marine algae, had another profound effect on atmospheric composition. Due to the gas exchange between the hydrosphere and the atmosphere, the used-up carbon dioxide was not only replenished from the atmosphere but oxygen, the by-product of photosynthesis, found its way from the hydrosphere into the atmosphere. As long as life was restricted to water, the concentration of atmospheric oxygen increased only very slowly. Oxygen began to increase more rapidly from the end of the Silurian Period, when the plant kingdom had developed an effective vascular system that allowed it to spread across the continents.

The formation of land-based vegetation caused a further reduction in atmospheric carbon dioxide, particularly by locking up carbon in peatlands and tropical rain forests. Today, the latter contain 42% of all plant-based carbon compared with only 1% in agricultural vegetation. The ongoing reduction in forest cover, mainly by burning, not only returns large quantities of CO_2 to the atmosphere, but the reduced evapotranspiration also means that less solar energy is used up in biomass production, which adds to global warming.

CLIMATIC CHANGES IN GEOLOGICAL TIME

A survey of past climates reveals a story of constant changes. These changes will be identified in the address by means of a set of temperature and relative-sea-level charts with varying resolution, starting with the Phanerozoic (essentially the last 600Ma) and ending with the climatic events and their effects on human development over the last 600 years.

Considering that systematic measurements of temperature and precipitation only began in the middle of the 19th Century, all assessments of earlier temperatures must rely heavily on proxy data. These cover a wide range including determinations of the CO_2 and CH_4 content, as well as temperature-dependent oxygen isotope ratios in fluid and gas inclusions of ice cores and rocks. In many instances, these actual measurements are supplemented by anecdotal evidence from past human activity, such as the carefully kept diaries dating the beginning of the annual rye harvest in Norway or, very importantly, the five-hundred year old record of the spring-ice thaw in the harbour of the Estonian city of Tallinn (Tarrand and Nordli, 2001). Other information comes from sedimentology, micro-stratigraphy, palaeontology, particularly palynology, and the annual growth rings of trees. By the proportion of the ^{14}C isotopes contained in the growth rings and their width, cold and warm, dry and wet growth periods that can be dated back for some 45 000 years. Similar work has established varve chronology covering approximately 12 000 years.

The results of the various surveys show that at least since the Proterozoic Era, Earth's climate has been affected by frequent changes from cold to warm periods often with far more extreme temperatures than we experience today. There were times when the whole globe appears to have been frozen and, alternatively, throughout much of the Mesozoic Era, the poles appear to have been without any ice caps. Indeed, sub-tropical conditions with luxurious forests existed during parts of the Cretaceous Period in today's arctic portions of America.

The currently available geological record also suggests that our present time, which has been called the Modern Optimum (or Maximum in reference to the high incidence of sunspot activity), may be just another relatively warm and climatically balanced portion of the Holocene Interglacial that, eventually, will lead to another ice age.

THE POSSIBLE CAUSES OF CLIMATIC CHANGES

The climatic changes that have affected our planet are the product of the mutual influence of various factors, properties and components. These involve:

- the gas content of the atmosphere including its cloud cover,
- the varying intensity of solar radiation,
- its albedo, i.e. the ratio of incident to reflected solar radiation,
- the distribution of precipitation,
- air and marine currents,
- the degree of atmospheric contamination by volcanic and anthropogenic dust, as well as
- gaseous volcanic exhalations and others.

Any equilibrium that may be established between the many factors influencing the lithosphere, atmosphere, hydrosphere and biosphere cannot be static but must be highly mobile and delicately balanced. This equilibrium is disturbed with varying effects and rapidity when the conditions of any one of the "spheres" change, or when the equilibrium is disturbed by an extra-terrestrial event, such as a large meteor impact or a change in solar radiation. Some of the changes are episodic and possibly long-lasting, such as the development of photosynthesis and other one-off events like the break-up of the Gondwana continent and the establishment of new patterns of ocean circulation. Other effects are cyclic in nature, such as the wobble of Earth's axis of rotation or the eccentricity of Earth's orbit around the Sun.

Much of the recent discussion of climate change has centred on anthropogenic causes, in particular the so-called greenhouse gases. Although water vapour generates heat from a much wider wave spectrum and is far more common in the atmosphere than carbon dioxide, the latter has been regarded more than any other agent as the main cause of climatic changes. Our brief survey of the factors that might have been responsible for past and present climatic changes begins therefore with carbon dioxide.

The role of CO_2

As mentioned above, the atmosphere has been warming up by about 0.6°C since the end of the so-called Little Ice Age in the middle of the 19th Century. This has been closely paralleled by an increase of atmospheric carbon dioxide from 0.029% in 1850 to the present 0.036% (Bayer, 2001). Despite the fact that the trend lines for global temperature, atmospheric CO_2 content, and relative sea-level variations have roughly similar configurations, completely opposing interpretations have resulted. According to the most vocal camp, variations in the amount of atmospheric carbon dioxide, in conjunction with other greenhouse gases, are the main causes of variations in temperature and relative sea level. This hypothesis was first developed in 1896 by Arrhenius who regarded CO_2 depletion as the cause of the Quaternary ice ages. Support for this hypothesis has come from many quarters. For example, Retallack (2001) observed that Pleistocene Ginkgo leaves had more stomata (air intake pores) than they have today. By experimenting with growing Ginkgo plants, he found that the stomata density adjusts itself inversely to the available carbon dioxide content, and he concludes therefore that there was less CO_2 in the Pleistocene air than we have today. However, does this conclusion really prove that the Pleistocene glaciations were caused by a reduction in atmospheric carbon dioxide? Unfortunately, cause and effect are not always convincingly put, as shown by the following quotation from Lean and Rind (1996): "Between 1850 and 1990 the global-mean temperature at the surface of the Earth warmed by approximately 0.5°C (about 1°F). During the same period, the amount of carbon dioxide measured in the Earth's atmosphere increased by about 25%, **as a consequence of our ever-increasing use of fossil fuels.** This **raises the possibility that the two trends are directly connected**, and that the century-long warming is a long-anticipated sign of the climate system's response to human activities" (my bolding).

There is no similarly simple alternative viewpoint, and the only unifying principle that holds the opposing camps together is the conviction that the role of CO_2 is either negligible or has reversed causality (Veizer et al., 2000). The latter view holds that variations in atmospheric carbon dioxide are symptoms not causes of climatic variation, i.e. the proportion of CO_2 increases because the oceans, the main reservoir of this gas, release it to the atmosphere as their water warms up.

Changes in the emission of solar radiation

Considering that without solar radiation, both the hydrosphere and biosphere would not exist at all, and the lithosphere and atmosphere would have evolved quite differently, the Sun must have a profound effect on Earth's climate. For practical purposes, a distinction is made between changes in the amount of radiation emitted by the Sun and variations in the amount of solar radiation received by Earth because of changes in its position or trajectory around the Sun.

Radiation is emitted from the Sun's surface at a temperature of between 5000 and 8000°C and reaches Earth's upper atmosphere with a power of approximately 1.37kw/m^2. Its wavelength covers the whole of the visible spectrum and extends beyond the infra-red range into radio waves, and beyond the ultra-violet region

into x- and gamma-rays, respectively. While much of the ultra-violet and shorter-wave radiation is absorbed by the upper atmosphere, most of the visible and infra-red light reaches Earth's surface, which retains approximately 70% of the incoming radiation. The short-wave portion of the 30% that is reflected from the ground moves back into space while its long-wave component is absorbed by the greenhouse gases contained in the lower atmosphere to give us the previously mentioned global average of currently +15°C.

The intensity of solar radiation varies in short, medium and long terms. Long-term changes in solar radiation are related to the evolution of the Sun itself which over the last 3Ga has decreased in size but increased in radiation. Concurrently, Earth's rotation has slowed from a 21-hour day during the Cambrian Period to the present 24 hours, while its annual trajectory around the Sun decreased from about 420 days to the present 365 days. These secular changes may have had an influence on climate, although their significance is uncertain.

In contrast, short-term variations in solar radiation are related to increased sunspot and solar flare activity that covers periods of only 5 to 15 years with a mean of 11 years (Schwabe Cycle). Both are related to periodic disturbances in the Sun's magnetic field. They raise solar radiation mainly in the UV and shorter wavelengths as well as in very long radio waves. The visible spectrum is less affected, but a rise in temperature of several tenths of a percent has been recorded. This temperature increase becomes more significant in times of clustered sunspot activity, as happened many times in the past.

Actual observations of sunspot activity reach back to the time of Galilei at the end of 16th Century, but systematic measurements of this phenomenon began only in 1860 at the Zürich Observatory (Berner et al., 2000). However, proxy data can be obtained from the above-mentioned measurements of radiocarbon (^{14}C) isotopes in the annual growth rings of trees and from ^{10}Be in ice cores. These isotopes are formed in smaller than normal quantities during periods of high solar activity when the Sun's distorted magnetic field shields Earth from cosmic radiation.

Direct measurements and radiocarbon determinations of sunspot frequency have revealed clusters of increased solar activity mainly in cycles of 80 to 90 years (Gleissberg Cycle) and a longer cycle of 208 years (Berner et al, 2000). Alternatively, there have been pause periods of reduced sunspot activity which follow a similar pattern and may last for several decades. Best-known examples are the Spörer, Maunder and Dalton Minima which climaxed in the years 1500, 1710 and 1800, and are low-temperature punctuations of the Little Ice Age that lasted from the middle of the 15th to the middle of the 19th Century. Conversely, the present Modern Optimum (or Maximum, see above) of global temperatures coincides with an increase of all three cycles of sunspot activity (Berner et al., 2000):

- the current 11-year (Schwabe) cycle began in 1996 and should have peaked about now, only to wane again until approximately 2007,
- the 80 to 90-year (Gleissberg) cycle is still waxing and should peak around the year 2020, and
- the 208-year cycle should reach its maximum in a few decades.

The movements of Earth and Sun

The geological record suggests that the occurrence of past warm and cold periods, at times when anthropogenic causes were out of the question, might have been caused by the additive or subtractive superposition of sunspot cycles of varying periodicity. In addition, the radiation received by Earth could have been further amplified or diminished when taking into account the movement of Earth and its trajectory around the Sun.

Obliquity and precession of Earth's rotational axis

Earth's rotational axis is tilted at an angle of currently 23° 26' 34" against the plane of its trajectory around the Sun (obliquity of the ecliptic). This tilt causes the seasonal changes on Earth but, similarly to the movement of a spinning top, the angle of the axis of rotation is not constant. It wobbles by an angle of 2.8° over a period of approximately 41 000 years. This precession of the rotational axis causes the Tropics of Cancer and Capricorn to shift between 22 and 24.8°. When the tilt angle is low, the distribution of solar flux is more balanced between the two hemispheres and seasonal changes are less pronounced. Conversely, when the axial tilt is high, the density of solar radiation that reaches high latitudes is great during summer and very low during winter resulting in hotter summers and colder winters.

The Eccentricity of Earth's trajectory around the Sun

Earth rotates around the Sun in an elliptic trajectory that causes the distance between Sun and Earth to vary between 147 and 152 Million kms over the period of one year. Currently, Earth is closest to the Sun on 2nd January, i.e. during the northern winter and southern summer, while on 2nd July, during the northern summer and southern winter, the distance is greatest. This has a balancing effect on the seasonal changes in the Northern Hemisphere while the opposite is true for the Southern Hemisphere, where the above-mentioned sunspot-generated increased solar flux is further magnified in summer by the comparative closeness of the Sun. This means that, excluding all other influencing

factors, southern summers should be hotter than northern summers at comparable latitudes.

Because the orbit of Earth around the Sun has its own precession, the points of greatest and smallest distance between Earth and Sun shift in time over a period of 100 000 years. This time frame relates closely to the period of Pleistocene glacial and interglacial cycles. Additional cycles with a periodicity of 19 000 and 23 000 years of increasing and decreasing amounts of solar radiation received by Earth result from the superposition of Earth's rotational and trajectory movements.

The cyclic nature of some climatic variations is probably the main reason why recurring fluctuations in solar radiation, and the waxing and waning of the flux received by Earth, in response to its rotational and trajectory movements (Milankovitch Cycles), have been looked at as the most likely causes for changes in global temperature and relative sea level. Periods of warm temperature do correlate with increased sunspot activity and, in the absence of anthropogenic causes, larger-scale cycles, such as the Maunder and other climatic minima, as well as the repeated ice ages and their intervening warm periods, can probably be attributed to variations in solar radiation (Crowley, 1996).

The effect of Earth's tectonism and volcanism on climate

Geological evidence tells us of former sea-level highstands that are far in excess of what we see today. For example, the mid-Cretaceous relative sea level was 250m higher than it is at present, and 85% of Earth's surface was then flooded compared with today's 71%. Considering that a complete melting of all the present terrestrial ice in Antarctica, Greenland and mountain glaciers elsewhere would raise the sea level by only 70m, additional or different forces must have been at play to accomplish some of the extreme highstands of the past. According to Kothen and Knufinke (2001), sea-floor spreading and its associated vulcanicity are the main causes of variations in relative sea level, global temperature and carbon dioxide content. These authors suggest that the above-mentioned excessive mid-Cretaceous relative sea-level rise was caused by accelerated sea-floor spreading that culminated in the formation of large systems of mid-oceanic ridges. Heat transfer from the ascending magma through the thin oceanic crust, then by sub-marine lava to seawater, and from there to the atmosphere, are seen as the main cause of extensive global warming. The water ascending from the vast areas of submarine vulcanicity was replenished at depth by cold water descending from circum-polar regions, while the surface water was further warmed by solar radiation in equatorial latitudes from where it moved pole-ward (e.g. present-day Gulfstream) and created warm-temperate conditions in high latitudes.

According to Kothen and Knufinke (2001), the Cretaceous model has general application, i.e. at times of intensive magmatism and sea-floor spreading, the poleward warm-water transfer is very effective thus causing climatic maxima in high latitudes. The increase in atmospheric carbon dioxide from volcanic exhalations as well as from the release of CO_2 from the warm sea water is seen to be a side-effect of the general warming, not its cause. According to this model, the subsequent reduction in magmatism and sea-floor spreading and the subsidence of the aging sea floor cause the relative sea level to be lowered again as, for example, happened towards the end of the Cretaceous and Early Tertiary Periods.

The changing distribution of land and sea associated with the opening and closing of oceans and the birth and decay of mid-oceanic ridges also affect our climate by redirecting ocean currents and atmospheric circulation with all the consequences of creating regions of high and low rainfall. Ice, snow and clouds reflect the incoming solar energy more efficiently than wet land, and wet land more than dry land, and the latter more than water. Because of this, variations in the proportion of land and sea, and dry, wet and glaciated regions are bound to have far-reaching consequences for Earth's energy budget.

SUMMARY AND CONCLUSIONS

A review of the evolution of Earth's climate reveals a pattern of constant changes at all levels of analytical resolution. They have been a natural part of our planet's geological development for at least 2.3Ga, which is the oldest age of what appear to be glacial moraines. Many of the climate changes that happened since then were so extreme that they profoundly affected biological evolution. Conversely, the development of life on Earth affected our climate, for example, by reducing the amount of atmospheric carbon dioxide and the release of molecular oxygen from silicates as a side effect of evapotranspiration. Humans have not escaped the effects of climatic variations either. Great social upheavals, like the ancient waves of human migration in search of better land, occurred mainly in times of climatic pessima. So did peasant uprisings and religious changes. Great battles were either won or lost, because they were fought at times of either favourable or unfavourable climatic conditions rather than because of the ingenuity or lack of it of the military leaders.

Human history was not only affected by climatic changes, but human activities also contributed to them. The almost total deforestation of the Mediterranean countries in Roman times is repeated today, here and in

equatorial regions with similar effects of accelerating desertification. Pollution of air, water and land increasingly interferes with the natural evolution of both biosphere and atmosphere. In view of the enormous social consequences of climate changes, we should do everything to recognise both short- and long-term trends and endeavour to distinguish between natural and anthropogenic causes. The Intergovernmental Panel on Climate Change (IPCC) has modelled a mid-range global warming of 1 to 3°C for the next 100 years on the basis of greenhouse gas emission alone. Considering that there are still severe doubts about cause and effect in climate modelling, and that the current density of observation points is inadequate to forecast weather conditions for more than a few days, climate predictions still have a long way to go. In spite of this uncertainty, it would be presumptuous to assume that the delicate balance between the many forces that control our climate would not be affected by human activity, by what we put into the soil, the water and the air. The geological record shows us that Earth's climate is capable of changing from one extreme to the other, and Hegel's dialectic teaches us that large changes may often be the result of accumulated small causes. Translated to the climate problem, this means that carbon dioxide might not be the cause of global warming, but given a trend in that direction, such as the currently increased solar radiation, it may well have an amplifying effect.

REFERENCES

BAYER, A. 2001. Von Wolkenschichten, Wärmespeichern und Vulkanen – einige Aspekte zur “Klimakatastrophe.” http://www.unierlangen.de/docs/FAU/fakultaet/natIII/geol appl/klima.htm

BERNER, U. & STREIFF, H. eds. 2000. *Klimafakten*. E. Schweizerbartsche Verlagsbuchhandlung (Nägele und Obermiller), Stuttgart.

CROWLEY, T.J. 1996. Remembrance of things past: Greenhouse lessons from the geological record. *In:* Eddy, J.A. ed. Consequences - The Nature & Implications of Environmental Change, Vol 2/1: http://gcrio.ciesin.org/consequences/winter96/geoclimate.html, pp. 10.

KOTHEN, H. & KNUFINKE, H.U. 2001. Ursachen der Warm- und Kaltphasen und der Meeresspiegelschwankungen sowie die Rolle des CO_2. http:home.tonline.de/home/heinz.kothen/dttext.htm

LEAN, J. & RIND, D. 1996. The Sun and climate. *In:* Eddy, J.A. ed. Consequences - The Nature & Implications of Environmental Change, Vol 2/1, http://gcrio.ciesin.org/consequences/winter96/sunclimate.html, pp. 10.

RETALLACK, G.J. 2001. A 300-million-year record of atmospheric carbon dioxide from fossil plant cuticles. *Nature* **411**, pp. 287 - 290.

TARRAND, A. & NORDLI, P.Ø. 2001. The Tallinn temperature series reconstructed back half a Millennium by use of proxi data. *In:* Ogilvie, A.E.J. and Jonsson, T. eds. *The Iceberg in the Mist: Northern Research in Pursuit of a "Little Ice Age"*. Kluwer Academic Publishers, Spec. issue of Climatic Change **48**, pp. 189 - 199.

VEIZER, J., GODDERIS, Y. & FRANCCEDILOIS, L.M. 2000. Evidence for decoupling of atmospheric CO_2 and global climate during the Phanerozoic Eon. *Nature* **408**, pp. 698 - 701.

Geological Hazards — The impact to mining 15-16 November 2001, eds Doyle, Moloney, pp 9-22

A history of the Standing Committee on Coalfield Geology of NSW and its successor, the Coalfield Geology Council of NSW

ANTON CROUCH

School of Geology, *University of New South Wales*

We are travelling in the footsteps of those who've gone before (**Trad "When the saints go marching in")**

ARCHAEAN

The writing of a history of the Standing Committee on Coalfield Geology of New South Wales and its successor, the Coalfield Geology Council of New South Wales was first raised in September 1997 and progress was, for some time, very slow. It was not until June 2000, when details of publishing options were discussed, that the work began to acquire some momentum and the approach of the 40th anniversary of the committee/council was seen as a realistic target to aim for.

The story is almost the history of the phrase *coal geology* in New South Wales. It is a story of determined scientific and technical development and a story of comradeship that exists in few professions other than geology. Geologists are truly the salt of the earth and I am indebted to the following people who helped me during the writing of this work.

Mike Armstrong (DMR)	Julie Moloney (DMR)
Kim Bayly (DMR)	Imelda Mosher
Cathy Brown (AGSO)	Tony Osman
John Cramsie (DMR)	Michelle Smyth
Michael Creech (Powercoal)	Brian Vitnell
Rod Doyle (Dartbrook Coal)	Colin Ward (UNSW)
Bruce Kirby (DMR)	Ken Wood
Cliff McElroy	Sharon Zwi (USyd).

I hope I have all the facts right but if not, then I alone am responsible for the errors. I have not avoided drawing my own conclusions in places and it must be realised that not all members of the committee/council, whether past or present, will agree with me.

This is a story that could be sub-titled *Things ain't what they seem to be*. In common usage, seam implies a join or a boundary but no geologist who has spent any time working in a coal mine can be other than indoctrinated with the concept of coal seam as a bed of material with a significant thickness. This is understandable — you literally work **in it**. You also know that when coal can be seen in outcrop or in a bore core, someone is likely to ask, "Can it be mined?" Coal is a rock that is always a potential commodity. That mining terminology should collide with stratigraphy is not surprising. This story starts with such a collision.

NEOPROTEROZOIC (PRE OCTOBER 1961)

Is a coal seam more than it seems to be? By early 1961 the geologists of the Geological Survey of New South Wales thought so. Why couldn't a coal seam be a recognised stratigraphic unit? *Seam*, as applied to a stratum of coal, is at least as old as the first half of the 18th century and was universal as a coal mining term in New South Wales in the 19th century. For some stratigraphers, however, *seam* in particular and coal terminology in general were a problem — seam names were thought to be so entrenched in the mining industry that it was considered unrealistic to subject coal seam naming to the Australian Code of Stratigraphic Nomenclature. The 3rd edition of the code (1959) noted that "rules should not be laid down for coal seam nomenclature" (Prefatory d) and "It is considered inadvisable to lay down rules for coal seam nomenclature" (Clause 32). The Code did allow that "The term 'Coal Measures' may be used, where appropriate, instead of 'Group' or 'Sub-Group'" (Clause 16).

For administrative purposes, the Geological Society of Australia's *Code of Stratigraphic Nomenclature* was "owned" by the Bureau of Mineral Resources, Geology and Geophysics (BMR) in Canberra. The BMR's position on coal terminology reflected an attitude that was, and still is, part of the nature of science itself — "pure" science differs from "applied" science. That the BMR had taken a stand on the use of coal seam names in formal stratigraphy is not surprising — coal seam names were applied inconsistently, both locally and regionally, and the problem was to get worse with the development of the black coal export industry and the emergence of seam names as "brand" names.

The correspondence between the Stratigraphic Nomenclature Committee (of the Geological Society of Australia(GSA)) and the Geological Survey of NSW during 1961, on the matter of coal seam terminology, has not been located but it is probable that there was some friction between the two groups. As became apparent some years later, the friction was largely due to a certain narrowness of view on both sides. Why did the BMR

not see that *coal* is a perfectly good lithological name and hence, unremarkable as part of the formal name for a formation or member? Why did the Geological Survey not see that *seam* is a mining term and too imprecise to be used formally?

Cliff McElroy, Senior Geologist in the Geological Survey of NSW, was secretary of the NSW branch of the Stratigraphic Nomenclature Committee of the Geological Society of Australia in 1961 and "was frustrated at that committee's inability to handle coal problems" (McElroy, 1998). As discussed later in this history, the "problems" were essentially twofold — the perceived need by the Geological Survey to use *seam* as a formal term and a reluctance to change the names of many coal measure units when the long-established names were invalid under the Australian Code of Stratigraphic Nomenclature. McElroy discussed the matter with Joe Whiting (Geological Survey of NSW) and Ken Mosher (Joint Coal Board) and all agreed that the NSW Department of Mines should establish a "Standing Committee on Coal (or Coal Seam) Nomenclature".

During the first half of 1961, McElroy prepared a submission to this effect and it was forwarded to Fred Booker (NSW Government Geologist) above the signatures of McElroy and Whiting. Booker took the matter to heart, "pushed it along" (McElroy, 1998) and put a submission to C. St J. Mulholland, Under Secretary for Mines. Mulholland responded on 31 July 1961, writing to The Secretary, Joint Coal Board and advising that it was "proposed to establish a Standing Committee on Nomenclature of NSW Coal Measures" (Mulholland, 1961). Reference was made to the fact that the "Geological Society of Australia Sub-committee on Stratigraphic Nomenclature specifically excludes from consideration the nomenclature of coal seams". The first meeting of the Standing Committee on Coalfield Geology of New South Wales took place at the Department of Mines on 6 October 1961.

EARLY PALAEOZOIC (OCTOBER 1961 TO OCTOBER 1968)

The first meeting of the committee was held at the Department of Mines offices in Goldsborough House, Loftus Street, near Circular Quay on Friday 6 October 1961. The building no longer stands, the site now being a small park.

Government Geologist Fred Booker formally opened the meeting and drew attention to "the long standing need for uniform treatment of coalfield problems in their many aspects" (Whiting, 1961). Those present were:

- Jeannette Adrian (Joint Coal Board),
- Allan Carter (representing GSA stratigraphic nomenclature sub-committee),
- Arthur Hams (NSW Combined Colliery Proprietors' Association),
- Fred Loughnan (University of NSW),
- Cliff McElroy (Geological Survey of NSW),
- Peter McKenzie (BHP Ltd, Newcastle),
- Ken Mosher (Joint Coal Board),
- John Smith (NSW Department of Mines coal mines inspectorate),
- Jack Stuntz (Australian Oil and Gas Corp. Ltd),
- Dennis Tompkins (University of Sydney),
- Joe Whiting (Geological Survey of NSW), and
- Ron Wilson (Australian Iron and Steel Pty Ltd, Wollongong).

Joe Whiting was elected chairman, Cliff McElroy secretary and Jeannette Adrian assistant secretary, after which Fred Booker left the meeting saying that he did not wish to take a formal part in the committee's activities due to "many commitments". The formal name *Standing Committee on Coalfield Geology of NSW* was adopted and the difference between this name and the informal name used prior to the meeting (*Standing Committee on Coal (seam) Nomenclature*) shows that the participants were taking a broad view of the committee's function from the beginning. Hereafter, the committee will be referred to by the abbreviation SCCG.

The aims of the SCCG were established as:

- bringing together detailed knowledge of the various coalfields,
- correlation studies of coal seams and coal measures generally with associated nomenclatural aspects, on both local & regional basis,
- standardisation of coal terms,
- methods of calculation and calculation of coal reserves,
- the appropriate distribution of the results of its activities, and
- a method of working adopted.

The working method to be "That the committee operate on the principle of sub-committees, generally of 2 to 4 members; the full committee having power to co-opt both to the full committee and the sub-committees; the sub-committees having power to co-opt to the sub-committees; all findings of the sub-committees to be ratified by the full committee before issue."

Sixteen sub-committees were established and the needs to draft a set of rules and examine the boundaries of coal districts were raised. The minutes of the first meeting also contain an oblique reference to the friction between the GSA and Geological Survey of NSW, hypothesised in the previous section. There is mention of a GSA letter of 5 September 1961 and a minuted response of "no action taken". Further support for the "friction" hypothesis is provided by the minutes of the second meeting of the SCCG which record that "no further action" be taken with respect to the SCCG/GSA relationship and a reference to "imperfections" in the Australian Code of Stratigraphic Nomenclature. The second meeting, held three weeks after the first, was at the offices of the Joint Coal Board (JCB) — a collection of vintage huts at the corner of Goulburn and Brisbane streets, and part of the site now occupied by the Sydney Police Centre. The business of the meeting

included an expansion of aim (c) above, to *exchange of ideas on geological techniques and terms employed in coalfield geology with a view to standardization ¾* again, evidence that the SCCG was thinking of its role as being more than deliberating on coal nomenclature. This second meeting also saw a discussion of the use of geological terms compared to those used by mining engineers, and the adoption of rules and a schedule of quarterly meetings on the first Fridays of March, June, September and December, at 2pm.

Sub-committee work during the last quarter of 1961 was intense:

- rules were drawn-up,
- work began on a "Stratigraphical code for coalfield geology in NSW,
- a revised stratigraphy of the Newcastle Coal Measures was prepared by Dick Britten (JCB) and Peter McKenzie (BHP, Newcastle),
- a revised stratigraphy of the Greta Coal Measures in the Cessnock area was submitted by Kazys Kemezys (JCB),
- a proposed revision of the Tomago Coal Measures was submitted by Brian Robinson (JCB),
- suggested rules for calculating and reporting coal reserves in NSW (Ken Mosher and Ernie Wright, JCB) were foreshadowed, and
- co-operation between the SCCG and Standards Association of Australia (SAA) was with members of the SCCG serving on the SAA sub-committee preparing the draft of standard coal terms.

It is clear that this period of activity reflected the existence of a large amount of work that was already "in the pipeline" and waiting for the emergence of a body such as the SCCG. The prominence of the JCB in the SCCG's workings is apparent at this early stage — a position that was to last for almost 30 years.

Within a year of its establishment, the SCCG had:

- ratified a stratigraphic code (referred to informally in early records as *nomenclature rules*),
- prepared a draft code for the calculation of coal reserves, and
- come to an agreement with SAA on a set of coal and petrographic terms.

The draft code for the calculation of coal reserves was a very tentative document indeed, with references to its being a "guide", not a "binding specification" and particular attention paid to the idea of distances between outcrops and bore holes (the term *points of observation* had not yet been coined) being "desirable", rather than mandatory. The reserves code was to be a long time coming — it was not formally presented for discussion until September 1967 and was not ratified until June 1968. At this time, the SCCG did however affirm that the scope of the SCCG referred to coal **field** geology, not coal **measure** geology.

The *nomenclature rules* were a continuing worry to the SCCG and there is evidence that the SCCG was loath to "go it alone". The rules, as first circulated at the end of 1961, make it clear that the material was intended to be supplementary to the Australian code. The three "difficulties" which such a supplementary code would address included:

- the retention of names for seams and coal measure units which did not comply with the Australian code,
- the avoidance of "unwieldy" classifications due to the variability of both coal and intervening sediments, and
- the need for "special provisions', established by the detailed information of the sedimentary sequence within coal measures.

A copy of the SCCG rules was sent to the NSW branch of GSA in June 1962, asking that the rules be added to the Australian code as a supplement. There is no record of a response, but it is probable that the SCCG continued to hope for a change in the GSA's approach to coal terms. Such a change never came and by 1964 the Australian Code of Stratigraphic Nomenclature included a reference to the work of the SCCG, but the Australian code was overtaken by the adoption of the international code (Hedberg, 1976) before any formal resolution could occur. Australia adopted the International Stratigraphic Guide *in toto* as a replacement for the 4th edition of the Australian code in 1978 (Staines, 1985), and the only mention of coal terminology is a note (Note 15, p 98) which records the Australian practice of accepting *Coal Measures* as a formal term and the informal nature of *seam*. Although the SCCG had difficulties with the Australian code it could not be said that the SCCG was unanimous in its own approach to nomenclature. As early as December 1962, two JCB geologists (Owen Shiels and Helena Basden) wrote to the SCCG, disagreeing with the view that the Australian code could not be applied to NSW coalfield terminology without modification. They wrote as individuals and they could not have been more direct — "the needs of the industry should not be allowed to intrude into formal stratigraphy to its detriment".

The scope of the membership of the SCCG had to be considered in 1962, when two members changed jobs (Ken Mosher to Conzinc Rio Tinto and Cliff McElroy to University of NSW). The rules were changed to allow company membership additional to BHP, AIS and AOG, and Conzinc Rio Tinto and Clutha Ltd were admitted.

At the second general meeting of the SCCG in March 1963 Ken Mosher was elected chairman and the office bearers of the SCCG were referred to as "the executive" for the first time. The second general meeting also marked a turning point in that, on the subject of the *nomenclature rules*, a letter to the SCCG from Norm Fisher of the BMR was discussed and taken as sufficient reason for the SCCG to proceed with its own code of stratigraphic nomenclature for coal measure sequences. This meeting also seems to be the first occasion on which the matter of the word *seam* was discussed at length and the concept of *coal formation* suggested. This year also saw the establishment of the procedure for holding meetings in "the field', ie outside Sydney. The first such meeting was at BHP, Newcastle

in May 1963. At this meeting the stratigraphies of the Tomago Coal Measures at East Maitland, the Singleton Coal Measures, and the Muswellbrook Coal Measures were ratified. Also, the concept of a stratigraphy of a Central Coalfield was raised (with some dissention) and the term *tuff* adopted as a valid term for the Newcastle Coal Measures.

After the first two years of almost explosive action, activity decreased somewhat — only 5 people attended the August 1963 meeting. The decision to include a "symposium" on a specific topic as part of each meeting was made, but it seems that the "symposium" on the South-western and Southern Coalfields, scheduled for the December 1963 meeting, did not occur. True symposiums on coalfield geology topics had to wait until the establishment of the coal geology specialist group of the GSA in 1978 but the idea of the SCCG meetings including a talk on a specific topic did survive and is now a feature of current meetings.

The SCCG acquired its own letterhead in December 1963 and, with regard to new work, 1964 proved to be a period of quiescence. Matters that were dealt with in this period include:

- further work with SAA on standard methods for sampling coal in situ and from bore cores,
- the adoption of the JCB's new standard code for rock and coal symbols,
- a procedural change to allow conveners of sub-committees to be people other than the secretary and assistant secretary, and
- Coal and Allied Industries Limited was admitted as a member, with Brian Vitnell as representative.

Despite the March 1963 "go it alone" decision on stratigraphic nomenclature there was a continuing interaction between the SCCG and the GSA. On the subject of stratigraphic nomenclature, there are references during 1964 to "pursuing the matter" with GSA, "detailed consideration" of the GSA's position and, with reference to the SCCG's own position, the absence of "finality on several major principles". By September 1964 the SCCG was hoping to have the impending 4th edition of the Australian Code of Stratigraphic Nomenclature include a "supplementary code" on coal nomenclature, ie the SCCG's code. This did not occur but the GSA included a reference to the SCCG 's "Stratigraphic Code for Coalfield Geology in NSW" in the 4th edition of the Australian code (1964).

Work on coalfield geology included the ratification of the Cessnock-Greta stratigraphy (with *Seam* as a formal term) and the subdivision of the Illawarra Coal Measures into two sub-groups (Sydney and Cumberland). The impending GSA journal volume on the geology of NSW was noted and it was hoped that the work of the SCCG could be included in this volume. This did in fact happen, but in a hybrid way. The GSA volume (Packham, 1969 was not published until November 1969, by which time the SCCG had decided to use the formal terms *Formation* and *Member* for stratigraphic units and limit *seam* to informal use. With regard to the Permian of the Sydney Basin the GSA volume is a mixture of formal and informal naming — groups and non coal measure formations comply with the Australian code but coal beds are *Seams*, regardless of whether the units are formations or member. Interestingly, work on the Illawarra Coal Measures in the Southern and South-western Coalfields at this time was the beginning of a trend to consolidation of stratigraphies that continues to the present day. During the early 1970s, Ron Wilson (AIS) occasionally joked that the Southern Coalfield, having "taken over" the South-western in 1970, had its sights on the Western Coalfield. What was said, originally in jest, soon came to pass and we now have a "one basin – one stratigraphy" approach to coalfield geology in NSW.

Major controversy arose at the end of 1964 — a proposal to modify the past three years' approach to coal seam nomenclature. Helena Basden (JCB) pointed out that there was no reason why the GSA code could not be used for coal measure sequences, with the word *seam* used informally. Basden even went so far as to suggest that the term *Coal Measures* not be used. Her position was impeccable scientifically (she pointed out, as an example, that the formal Wallarah Formation could contain the informal Wallarah seam and that the Newcastle Coal Measures should be renamed the Newcastle Group) but it did not carry the day. The SCCG decided to drop the idea of a "supplementary code" and submitted Basden's views to the GSA, perhaps hoping that **it** might take up the matter again. Interestingly, Basden did not advocate an abandonment of the principle of the SCCG having its own rules for coal measure nomenclature — she merely pointed out the compatibility of the Australian code with the SCCG approach. Reading her December 1964 "Guide for coalfield geologists" today makes one wonder what all the fuss was about. Basden's proposals were rigorous, and with the exception of the group/coal measure issue, are in accordance with current practice.

The somewhat confused reaction to Basden's proposals was well demonstrated over the next year — at the same time as Basden's views were being submitted to the GSA, the Newcastle Coal Measures type sections were ratified with *Seam* used. Soon thereafter the SCCG resolved to adopt *Seam* as a formal term, retain the use of *Coal Measures* as in the Australian code, and ask the GSA to incorporate the use of *Seam* in the Australian code. Having so resolved, the SCCG then ratified the Basden-prepared "Guide for coalfield geologists", ignoring the boldness of the remarks on the use of *seam*. During this time the organisational aspects of the SCCG were modified by allowing for alternative or substitute representatives, giving the chairman a deliberate and casting vote, and expanding the membership to "any other company representative who, in the opinion of the committee, is eligible for membership". Technical aspects first raised during this period were the use of the term *laminite*, the establishment of an editorial sub-committee, the need for standardisation in lithological logging and the retention of core samples in a core library.

After the drama of the use of *seam*, matters were

peaceful during 1966 and 1967, with a great deal of attention to detail in many areas. Activities included:

- the name "American Creek Formation" in the Southern Coalfield was replaced by "Allans Creek Formation,
- a suggestion that duplication of geographic names be allowed was defeated,
- sedimentary terminology was tightened up with *grit* proscribed, *laminite* defined, shale/mudstone usage clarified, *tuff* revisited and the matter of *carbonaceous shale* raised,
- the universities of Macquarie, Newcastle and New England were invited to join the SCCG,
- a reserves code reached the stage of formal discussion with a view to ratification,
- it was observed (as a clear indicator of the maturity of the SCCG) that "many young workers were often closer to geological problems than some members of the committee, and hence it might be profitable to hear their views in sub-committee",
- consideration of the depth and thickness limits for coal reserves (3000 feet and 3 feet, respectively were suggested),
- the possibility of duplication of formal stratigraphic names in the Newcastle – Singleton area when all of Australia was considered,
- uniformity of terminology in describing splitting properties of rocks was considered, and
- a formal definition of coal, based on SG (RD) and/or % of non-carbonaceous material given.

The SCCG had the sad task, in its March 1967 annual report, of noting the death of one of its founding members — Peter McKenzie (died October 1966).

The meeting of 7 June 1968 saw the presentation and ratification of the SCCG's first code for calculating and reporting coal reserves. This was a major achievement and the rigour imposed by this code was to have a significant and beneficial effect on the quality of coal exploration during the "boom" years that followed. The SCCG can be truly proud of this code — it not only paved the way for an Australian code but it also had some influence on international practice by eschewing the logically absurd concept of "undiscovered" reserves and resources.

The minutes of this meeting also reveal a small surprise — the *seam* issue had not gone away. The final draft of the stratigraphy of the Southern Coalfield was being held up while the merits of using *seam* were being argued! The matter came to a head at the October (sic) meeting with voting on a motion on notice by Ken Wood and Ken Mosher. The motion "**That the term *seam* shall not be used in a formal stratigraphic sense for either formation or member, and that in accordance with the Australian Code of Stratigraphic Nomenclature, (Article 16, proposed 5th Edition) such terms as Bulli Coal and Balgownie Coal Member shall be applied, and further that any previous recommendations made by the Standing Committee to G.S.A. in this matter be rescinded and G.S.A. notified accordingly**" was agreed to.

After 7 years the SCCG had come full circle. Perhaps it is no coincidence that the resolution of the *seam* issue came with the consideration of the Southern Coalfield — a formation such as the Wongawilli Coal, with its mine working section (the Wongawilli seam), is a fine example of how the formal and the informal can coexist.

LATE PALAEOZOIC (OCTOBER 1968 TO JUNE 1984)

The SCCG finalised the matter of the use of *seam* in December 1968 by accepting the stratigraphy of the Southern Coalfield and affirming that the decision on the use of *seam* applied to all coalfields.

Although it now occupied the high stratigraphic ground, the SCCG was under considerable stress organisationally. As the mining "boom" of the late 60s developed there was a flight of geologists from the public service and universities, which had a significant effect on the membership of the SCCG. Between June 1968 and September 1970 there were numerous resignations and on two occasions there was no meeting — one seems to have not been called and one lapsed for want of a quorum. The position of assistant secretary was not filled when Jeannette Adrian resigned in June 1968 and no minute has survived of the biennial election in March 1969.

The period September 1969 to June 1971 seems to have been one of some dichotomy. On one hand the SCCG, probably encouraged by the publication of the GSA's volume on the geology of NSW, was clearly eager to have its resolutions published, and on the other hand, was troubled by the small number of people attending meetings. It was decided to publish articles in the Records of the Geological Survey of NSW. First to be published included:

- the reserves code,
- the decision on the use of *seam*,
- the report on sedimentary terminology, and
- the stratigraphy of the Illawarra Coal Measures in the Southern and South-western Coalfields.

This material appeared in *Rec. Geol. Surv. NSW* **13** (2), 1971 — almost exactly 10 years after the establishment of the SCCG. At this time Helena Basden was appointed as convener of the Editorial sub-committee, a position she was to occupy with distinction for many years. There was also a feeling of a need to "tidy-up" the areas of activity. For the first time, the relationship of coal districts (a JCB statistical concept) to coalfields (an operational and partly geological concept) was discussed and it was decided to base sub-committee work on the coalfield concept.

The publication of the stratigraphy of the Illawarra Coal Measures led to a small controversy, which was to occupy the SCCG on-and-off for the next five years and which, in a somewhat desultory manner, occupies it even now. The issue was the status of the Bargo Claystone and the Darkes Forest Sandstone. The SCCG

had decided to include these two units as members in the Appin Formation and was probably unaware that a "revised stratigraphy" (Bowman, 1970), giving the two units formation status, was in the pipeline. Bowman's work clearly had priority (manuscript dated December 1969, published December 1970) over the SCCG's work (ratified June 1970, published December 1971). Harry Bowman wrote to the SCCG in December 1970 drawing attention to the anomaly but the only recorded response from the SCCG was a request for comment from the Geological Survey. It is not clear if such a request was actually made and the matter did not come to a head until late 1975.

The records of the SCCG's activities in the first half of 1971 suggest that personal issues may have been significant at this time. Surviving minutes of the June 1971 meeting are incomplete — 2 pages have been removed and the remaining (hand-written) page is cryptic with regard to the membership of some people. With a decline in the turbulence caused by the nickel-led mining boom and the election of Ken Mosher as chairman there was a return to stability and a concentration on "bread and butter" issues, such as coalfield stratigraphy and the need to modify the reserves code to take into account the approach of metrification of measurement units. Dick Britten's comprehensive work on the Singleton Coal Measures became the major issue for discussion at this time and the SCCG even arranged a special meeting (8 October 1971) at the Department of Mineral Resources' core library at Londonderry. The Singleton Coal Measures (Super Group) proposals clearly polarised the SCCG — the value of the synthesis from a large amount of data was certainly appreciated but many members were not prepared to go as far as recognising the equivalence of the Wollombi and Wittingham Coal Measures with the Newcastle and Tomago Coal Measures of the Newcastle Coalfield. Ratification, with claims for equivalence removed, was forthcoming and it is ironic that, some 30 years later, the use of coal seam names from the Newcastle Coalfield is now accepted, without comment, in the Wollombi Coal Measures.

As the membership of the SCCG increased in the first half of the 1970s, a significant influence on the SCCG's work came from the coal producing companies. The decreasing influence of the Geological Survey is well shown by the return of the Bargo Claystone/Darkes Forest Sandstone issue in 1975. The Geological Survey had maintained its position on this issue (see, for example, Bunny, 1972) but when the paper on the slope stability of the Wollongong area (Bowman, 1972) was eventually published, the SCCG took a stance and wrote, in October 1975, to the Geological Survey, noting "deviations" from the SCCG's position. The "deviations" were twofold — the use of the term *mudrock* as a lithological descriptor and the status of the Bargo Claystone and Darkes Forest Sandstone as formations. The reply from Neville Markham, Director, (November 1975) was polite but blunt — *mudrock* was a perfectly acceptable alternative to *mudstone* (it was used by Robert Folk, one of the authorities that the SCCG referred to in its own report on sedimentary terminology) and Bowman (1970) had precedence with regard to the status of the Bargo Claystone and the Darkes Forest Sandstone. That the Geological Survey's position was entirely reasonable was of no consequence to the SCCG as a whole, even after taking to account the fact that some members of the SCCG agreed with the Survey's view on the formation status of the rock units in question.

More constructive aspects of the SCCG's work in the mid 1970's were:

- the modification of the reserves code to take into account metrification (2nd edition, ratified March 1973),
- publication of the comprehensive report on the stratigraphic nomenclature of the Northern Coalfield (both as *Rec. Geol. Surv. NSW* **16** (1), 1975), and
- the definitions of the coalfields of the Sydney and Gunnedah basins (*Rec. Geol. Surv. NSW* **17** (2), 1975).

The report on the stratigraphy of the Northern Coalfield was a particularly welcome event. It reinforced the distinction between the informal use of *seam*, and the formal use of *Formation* and *Member*. Further, it brought together in a single publication the stratigraphies of the Greta Coal Measures, the Tomago Coal Measures, the Newcastle Coal Measures, and the Singleton Super-group.

Other matters that were considered at this time were:

- the work of the AusIMM on ore reserves,
- the application of confidence levels to estimates of coal reserves, and
- the influence that an international code of stratigraphic nomenclature might have on the Australian code.

An interesting aspect of the SCCG's operations in the 1970s and early 1980s is the way that delays in publishing the SCCG's findings overtook the implementation of some of the findings. Two examples stand out – a June 1975 decision to discontinue the use of the term *Coal Measures* fell by the wayside (September 1976 saw the ratification of the stratigraphy of the Coorabin **Coal Measures**), and the decision to delete the reserves category of *Assumed* (March 1983) was reversed when the concept of differentiating between *Resources* and *Reserves* was adopted with the 5th edition of the code (June 1984).

The above examples are indicative of the rapid evolution of the SCCG in the late 1970s. There was a concentration on technical expertise and scientific rigour, in part reflecting the changes that were taking place in the coal mining industry in NSW and Queensland. As the formation of a coal specialist group of the GSA was mooted (September 1976), the SCCG was thinking about the need to have specific guidelines for coal extracted by open cut. During 1977 the SCCG arranged technical talks on radiometric logging, the use of a gamma probe to study the roof strata of underground mines, and the potential use of in-seam radar.

A radical move came in June 1977 when the SCCG decided (by a margin of a single vote) to allow the calculation of recoverable reserves only from the measured and indicated categories. The appropriateness of this decision was demonstrated when an attempt at a rescission motion failed to get a seconder at the September 1977 meeting. This was also a period of increasing membership and the expression of some concerns at the proportion of consultants on the SCCG.

Published during this period were the 3rd edition of the Code for calculating and reporting coal reserves (ratified June 1977, published in *Rec. Geol. Surv. NSW* **18** (2), 1978), suggested procedures for coal bore titles (ratified December 1976, published as above) and the 4th edition of the reserves code (ratified December 1979, published in *Rec. Geol. Surv. NSW* **19** (2), 1980). The appearance of two editions of the reserves code in such a short time reflected the rapid change in attitude to this matter. The 3rd edition took the step of allowing the calculation of recoverable reserves only from the measured and indicated categories for possible underground mining, and only from the measured category for possible open cut mining. The 4th edition went further by adding a pro-forma "public statement of reserves", intended for use in cases of public statements claiming the authority of the code. Some mining company representatives were alarmed by the extent of the disclosure required by the public statement provisions but the SCCG's views were very much in line with the spirit of regulation that was abroad in the mining industry,

The other major issue at this time was an awareness that the SCCG had reached a turning point in its functioning. Relationships with coal mining groups in other states, the size of the SCCG, and the effect this had on the traditional sub-committee structure — these were all seen as being in need of examination. For the first and only time in its history, the SCCG held a two day meeting in December 1979 with the express purpose of examining "a different method of managing its affairs". The meeting was notable for two things — ratification of the 4th edition of the reserves code (with 2 company representatives voting no!) and a re-drafting of the constitution to provide, *inter alia*, for the establishment of an executive. An executive was established to allow the making of decisions between quarterly meetings and it is a measure of the egalitarianism and democracy of the SCCG that the executive has never been seen as an elected "board of directors".

The early 1980s was a period of consolidation in the coal industry in NSW and it saw the establishment of a Coal Strategy Division within the NSW Department of Mineral Resources (DMR). There were some rumblings when coal geology, after more than 100 years as part of the Geological Survey, was transferred to the new division. The SCCG concentrated on the refining of coalfield stratigraphies and examining ways in which the matter of reserve calculations for proposed open cut operations could be improved, including use of the results of down-hole geophysical logs. Membership of the SCCG was 55 in March 1982 and at that time the stratigraphy of the Southern Coalfield had been revised. The revision (ratified June 1981, published in *Rec. Geol. Surv. NSW* **21** (2), 1983) merged the previous Southern and South-western Coalfields but steadfastly continued to assign member status to the Bargo Claystone and Darkes Forest Sandstone.

Environmental aspects of coal exploration were of some concern in the early 1980s. The SCCG became embroiled in the middle of a small rumpus, between the NSW Department of Environment and Planning (DEP) and the NSW Coal Association. The DEP had prepared a document called "Guidelines for the conduct of coal exploration programmes" and had sent it to the NSW Coal Association for comment. The Coal Association's response had come to the SCCG, with the original document, but when the SCCG's executive advised the DEP that their document would be discussed by the full SCCG, it was rewarded with a terse letter from the DEP saying that the document was a confidential internal report and "was apparently improperly handed to your committee"! Not surprisingly, at the September 1983 meeting, the SCCG agreed that it was entirely proper that the SSCG consider the document and so advised the DEP.

Other matters considered at this time were:

- the revision of the guidelines for sedimentary terminology (Colin Ward was a member of the team which was producing a photographic "core book" of Sydney Basin sedimentary rocks),
- an agreement that the SCCG should not "set itself up financially", and
- preparations for input to a proposed national code for the calculation of coal reserves.

There is no record of the SCCG reaction when it was reported that the co-ordinating body for the proposed national code might be the BMR, but it is known that the Queensland Geological Survey vetoed the idea. John Cramsie (then Chief Coal Geologist, NSW DMR Coal Strategy Division, later Director of the Geological Survey of Victoria and now Director of the Geological Survey of NSW) suggested that the Government Geologists Conference be the vehicle for consideration of a national code and this was the procedure adopted. Tony Galligan (NSW DMR) and Charlie Mengel (Geological Survey of Queensland) had carriage of the project after it was taken up by the Government Geologists Conference in 1984. As mentioned before, the category of assumed reserves was deleted from the SCCG reserves code in March 1983 but this change was short lived — the possibility of a national code led to the introduction of the distinction between resources and reserves and this distinction was used to re-introduce the concept of assumed *resources*. Despite this minor illogicality, the 5th edition of the SCCG's resources and reserves code was a major advance and was to prove to be a very good basis for a national code.

A substantial body of work was published at this

time in *Rec. Geol. Surv. NSW* **22** (1), 1986 including:

- guide to the calculation of confidence limits for an estimation of coal reserves (ratified September 1982), terminology for classification and description of coalfield rocks (ratified June 1963),
- code for calculating coal resources and reserves, 5th edition (ratified June 1984),
- stratigraphy of the Jerrys Plains Subgroup of the Wittingham Coal Measures in the Singleton-Muswellbrook coal district of the Hunter Valley (ratified December 1984),
- stratigraphic subdivision of the Illawarra Coal Measures in the Western Coalfield (ratified December 1984), and
- redefinition of coalfields, in the Sydney and Gunnedah Basins (ratified March 1985.

MESOZOIC (JUNE 1984 TO DECEMBER 1994)

September 1984 saw the JCB in new premises (the former Qantas building in Chifley Square) and for the geological staff the new offices must have seemed almost luxurious, when compared with the 19th century "charm" of the Bulletin Place premises. As is the case with life forms, however, exoticism is sometimes a prelude to extinction. By early 1992 most of the board's technical functions, including geology, had been disbanded. The organisational vacuum left by the JCB's technical demise was filled by the DMR.

The national reserves code was a major consideration between 1984 and 1986. Galligan and Mengel were to report to the Government Geologists Conference in March 1985 and it seemed that progress would be smooth. It was — Queensland was happy to use the 5th edition of the NSW code as a base and a final product was completed by February 1986, ratified by the Government Geologists Conference in April 1986 and published in July 1986 (*Minfo* **12** pp. 33-36). An interesting aspect of the national code, now titled *Australian code for reporting identified coal resources and reserves*, is that although there is no mention of an *assumed* category it is there under a new name — *Inferred Resources, Class 1*. The definition of *coal resources* as, "all of the **potentially** (my emphasis) usable coal in a defined area" passed un-noticed at the time of the ratification of the 5th edition of the NSW code, but was the subject of some discussion when work on the national code commenced. It was realised that this had financial implications, eg in the calculation of front end payments. The definition was retained and the implications of it were to emerge again in a quite different setting in the 1990s — the procedures for calculating coal compensation payments under the NSW coal compensation scheme.

If the smooth progress on the formulation of a national reserves code is one of the high points of the SCCG's existence, the same period saw a low point – a member objecting to the actions of fellow members of a sub-committee. At issue was the publication of material that was still being worked on by the sub-committee. The matter was raised at the December 1984 meeting and the discussion centred on two issues — the release of conclusions based on confidential information, with no consultation with the suppliers of the material, and the criticising of other's unpublished work with no prior reference to them. The SCCG moved a motion of regret at what had happened and it is perhaps not surprising that, when the material was ratified and published by the SCCG, there was no reference to the earlier publication in Quarterly Notes of the Geological Survey of NSW **57.**

By the time the Australian resources and reserves code was finalised, the DMR was active in re-visiting the stratigraphy of the Hunter Coalfield and was well established with a programme on the Gunnedah Basin. Other work being commenced at this time was attention to special provisions for calculating reserves for open cut mining and standardisation of codes for the use of computers in lithological logging. The Sydney Basin "core book" was published by the Earth Resources Foundation of Sydney University at the end of 1986.

December 1986 was the 25th anniversary of the SCCG and this was celebrated by a lunch in the dining room of the Royal Commonwealth Society (cnr Bent and Bligh Streets). Egalitarianism is a distinguishing feature of geological social events but on this occasion it did have one slightly embarrassing consequence — the seating capacity of the "top table" was not large and one geologist, keen to engage a "distinguished guest" in conversation, occupied a seat to the exclusion of another "distinguished guest". The supplanted one remarked afterwards that he found the conversation of the *hoi polloi* quite invigorating.

By the start of 1987 the SCCG was commencing one of its periodic soul searching episodes. The statutory role (or more correctly, the lack thereof) of geologists in the coal mining industry was raised, and it was suggested that an effort be made to have the role of the mine geologist codified in the Coal Mines Regulation Act. This was an entirely worthy proposition but the probability of it ever coming to pass was then (as it is now) small. Other examples of the SCCG looking to expand its horizons were suggestions that a study of geology in longwall operations be undertaken, and that an application be made for a NERDCC grant (to complete the Hunter Coalfield study). A more down-to-earth suggestion was that the SCCG should conduct a survey of member's opinions on the operations of the SCCG.

The results of the survey of member's opinions were:

- only 15 out of over 50 members responded,
- all thought that there was a continuing role for the SCCG,
- most were happy with the existing constitution,
- most thought that the long-established areas of work (eg stratigraphy and reserves codes) should be continued,

- new areas of work suggested were structural mapping and computer applications,
- all thought that the SCCG's role was different to that of the Coal Geology Group of the GSA,
- most thought that there was no need for the SCCG to change the way it operated,
- all thought that the link with the DMR should be retained,
- most thought that the frequency of meetings (every 3 months) was satisfactory,
- a majority thought that some meetings should be held outside Sydney,
- most thought that there was no need to change the format of meetings,
- most thought that the basis for membership should not be changed, and
- most did not want the SCCG to engage in any financial activities.

With the benefit of hindsight it can be seen that the SCCG's somewhat introspective approach to its operations reflected an actual change of the environment in which the SCCG operated.

The changes included:

- long-time members died (Dick Britten in 1989; Ken Mosher in 1990),
- the JCB wasted away between 1989 and 1991,
- the hoped-for standardisation of computer data sets was always imminent but never quite achieved at the industry-wide scale,
- medium scale coalfield mapping was reduced in priority, and
- the attempt to contribute geologically to the increasing installation of longwall units went nowhere.

This last project was a particularly frustrating aspect of the SCCG's operations from 1988 to 1995 and is discussed in more detail later. On the brighter side, work on the guide to the evaluation of open cut reserves continued productively, as did revisions of the stratigraphies of the Hunter, Newcastle and Southern Coalfields. New areas of interest were environmental matters and the rise to importance of the Gunnedah Basin.

The demise of the JCB's technical functions made it necessary for the SCCG to change its constitution — it contained references to named positions that no longer existed in the JCB. This process began in December 1993 and the changes were approved at the meeting in December 1994. Not only did the SCCG change its constitution it also re-invented itself with a new name, the **Coalfield Geology Council of New South Wales**. This rebirth also saw the advent of a wonderful new logo produced by Harry Bowman and representing, New South Wales in the form of a lump of coal, together with a blue boomerang not only recognizing our State's heritage, but also representing our coal products going 'overseas'.

CAINOZOIC (DECEMBER 1994 TO PRESENT)

The SCCG's longwall project between 1988 and 1995 is an interesting example of how a good idea can lead to a long and frustrating experience in a case where the project group does not have control of the supply of the information on which the project is to be based. The idea was first raised in 1987 and was based on the sound premise that geological input to the design of longwall operations would be required. Such geological input was standard procedure overseas, and today, is commonplace in the Australian industry. The first phase, in late 1988, had identified a wide variation in the amount of geological work done before longwall extraction, and significantly, that it was uncommon for geologists to have control of the pre-extraction exploration phase. A questionnaire was distributed to 35 longwall operators (by Frans Bos), seeking information on what actually happened with regard to geological input to the longwall mining process but the response was disappointing — only 11 were returned by March 1989. By June 1990, when no further returns had been received, there were doubts as to whether the quantity of information was sufficient for a meaningful study and whether the data was reliable. A synopsis of the data was prepared by June 1991 but no further activity occurred until June 1993, when the sub-committee was reactivated. Again, due to doubts about the reliability of the "old" data, nothing happened until December 1995, when it was decided to hold a symposium on the role of geology in longwall mining.

The symposium was held at the University of New South Wales in November 1996 and was a success — demonstrating that the CGC was most effective when it had control of the inputs to its activities. The success of the 1996 symposium emboldened the CGC and another successful symposium was held in Newcastle in November 1997 (*Safety in mines ¾ the role of geology*). In order to retain control of the financial surpluses from these symposiums, the CGC briefly considered incorporating in 1998 but the clear general view was that such a move would have far more disadvantages than benefits.

Holding meetings alternatively in Sydney and country venues was well established during this period and the procedure is now seen as a valuable exercise in bringing members into contact with the work environments of colleagues. A major innovation was the establishment of the CGC's **Award for excellence in coal geology** in 1993. This award, conferred in December each year, recognises outstanding work by coal geologists (not necessarily members of the CGC) and includes the presentation of a handsome trophy carved from torbanite from the Greta Coal Measures at Muswellbrook Colliery.

The end of the 20th century saw two major publication events — the first Bulletin of the CGC, and a revision of the Australian resources and reserves code, referenced in the Joint Ore Reserves Committee of the AusIMM (JORC) Code. The Bulletin marked a radical departure from previous SCCG publications by

identifying the authors of the material ratified by the CGC. *Coalfield Geology Council of New South Wales, Bulletin* **1**, 1999 is subtitled "Collected papers by committees and working parties of the Council" and contains papers on:

- computer-based resource/reserve estimates,
- guide to systematic evaluation of open cut coal reserves,
- environmental considerations for coal geologists,
- Permian stratigraphy of the Gunnedah Basin,
- stratigraphy of the Greta Coal Measures, Muswellbrook Anticline area, Hunter Coalfield,
- coal seam nomenclature application in the Hunter Coalfield,
- revision of the stratigraphy of the Newcastle Coal Measures, and
- stratigraphy and terminology for the Southern Coalfield the Bargo Claystone and Darkes Forest Sandstone have formation status!

Work on revisions to the Australian resources and reserves code began in 1994, with a significant addition to the scope of the code — the introduction of the requirement that public statements of coal resources and reserves be made by a *competent person* (later to be called an *estimator*). A great deal of time was spent on the criteria for defining a *competent person*. By June 1998 a significant number of people in both NSW and Queensland had come to the conclusion that the proposed revision of the JORC code made the Australian coal code redundant with respect to stock exchange reporting. The CGC agreed and, at the June 1998 meeting, endorsed the use of the JORC code for stock exchange reporting and decided to develop guidelines on calculating coal resources and reserves compliant with the JORC Code. At its September 1999 meeting the CGC endorsed "Guidelines for the estimation and reporting of Australian black coal resources and reserves", the JORC code having come into force. The detail of these guidelines contained a significant scientific change — for the first time, the estimated Indicated and Measured Resources categories included a reference to an expected % error range. In another first, publication of the guidelines was, metaphorically, instantaneous – the material was posted on the DMR web site in December 1999. The speed of this publication took some coal geologists by surprise and there followed a period of further discussion, culminating in the publication (on the DMR web site) of revised guidelines in December 2000. These revised guidelines make no reference to % error, and contain a provision for periodic review.

The other major issues that occupied the CGC's time in this period were the matters of coal seam methane, and education. The CGC grappled with the education issue for some years before coming to the conclusion that it had no real influence in this area, either at the level of teaching geology or in the wider field of "educating" the general public in the benefits of geology to modern society. The sub-committee was disbanded in 2001. The coal seam methane work is ongoing and to date has covered methods of determining the gas content of coal seams and the reproducibility of the fast desorbtion and quick crush methods.

As a further example of the CGC's more out-going approach to its role, the matter of a memorial lecture in honour of Ken Mosher was raised in March 1988. Ken was one of the founding fathers of the CGC and to date two lectures have been given – by Brian Vitnell (1999) and Colin Ward (2000), both as part of the Newcastle Symposium. (A presentation of this paper in the 'Geological Hazards' conference will mark the 3rd in the series. Eds.)

To finish this story, we can note a similarity between the Standing Committee on Coalfield Geology of NSW/Coalfield Geology Council of NSW and the now venerable Geological Society of London. That august body was formed in November 1807, "for the purpose of making geologists acquainted with each other, of stimulating their zeal, of inducing them to adopt one nomenclature, of facilitating the communication of new facts, and of contributing to the advancement of geological sciences" (Winchester, 2001). Almost 200 years later this is a pretty good description of the CGC. When we consider that the London society first met in a tavern and described itself as "a little talking geological Dinner Club" the comparison is even more apt. Whether discussing the merits of chocolate ice-cream cake at lunch in a Sydney restaurant or arguing about the Denman Formation over a decent red in the Hunter Valley, we have acted with zeal and companionship. "Adopt one nomenclature"? That may take a little more time but we will all be privileged to be part of the process.

PALAEONTOLOGY

BOWMAN, H.N. 1970. Palaeoenvironment and revised nomenclature of the upper Shoalhaven Group and Illawarra Coal Measures in the Wollongong-Kiama area, New South Wales. *Records of the Geological Survey of NSW* **12** (2), pp. 163-182.

BOWMAN, H.N. 1972. Natural slope stability in the City of Greater Wollongong. *Records of the Geological Survey of NSW* **14** (2), pp. 159-222.

BUNNY, M.R. 1972. Geology and coal resources of the southern catchment coal reserve, southern Sydney Basin, New South Wales. *Geological Survey of NSW, Bulletin **22***. Committee on Stratigraphic Nomenclature, 1959. Australian code of stratigraphic nomenclature (third edition). *Journal of the Geological Society of Australia* **6** (1), pp. 63-70. Committee on Stratigraphic Nomenclature of the Geological Society of Australia, 1964. Australian code of stratigraphic nomenclature (fourth edition). *Journal of the Geological Society of Australia* **11** (1), pp. 165-171. Committee on Stratigraphic Nomenclature of the Geological Society of Australia, 1973. Australian code of

stratigraphic nomenclature (fourth edition, amended). *Journal of the Geological Society of Australia* **20** (1), pp. 105-112.

HEDBERG, H.D.(ed), 1976. *International stratigraphic guide – a guide to stratigraphic classification, terminology, and procedure.* John Wiley and Sons, New York.

MCELROY, C.T. 1998. *Letter to the author*, 29 March 1998.

MULHOLLAND, C. St J. 1961. *Letter to The Secretary, Joint Coal Board*, 31 July 1961.

PACKHAM, G.H.(ed), 1969. Geology of New South Wales. *Journal of the Geological Society of Australia* ***16*** *(1).*

STAINES, H.R.E. 1985. Field geologist's guide to lithostratigraphic nomenclature in Australia. *Australian Journal of Earth Sciences* **32** (2), pp. 83-106.

WHITING, J. 1961. Annual report of the Standing Committee on Coalfield Geology of NSW. In *Annual report of the NSW Department of Mines*, 1961.

WINCHESTER, S. 2001. *The map that changed the world*. Viking, Harmondsworth (UK).

PUBLICATIONS OF THE SCCG/CGC

Records of the Geological Survey of NSW, ***13****(2), 1971, pp. 101-130* ¾ Introduction, Code for calculating and reporting coal reserves, Resolution regarding formal seam nomenclature, Report of subcommittee on sedimentary terminology, and Report of combined subcommittees for Southern and South-western coalfields.

Records of the Geological Survey of NSW, ***16****(1), 1975, pp. 5-105* ¾ Code for calculating and reporting coal reserves (2nd edition), and Report of subcommittee for the Northern Coalfield – stratigraphic nomenclature.

Records of the Geological Survey of NSW, ***17****(2), 1975, pp. 85-86* ¾ Definition of coalfields, Sydney and Gunnedah basins.

Records of the Geological Survey of NSW, ***18****(2), 1978, pp. 139-152* ¾ Stratigraphy of the Coorabin Coal Measures, Coal bore titles – suggested procedures, and Code for calculating and reporting coal reserves (3rd edition).

Records of the Geological Survey of NSW, ***19****(2), 1980, pp. 273-278* ¾ Code for calculating and reporting coal reserves (4th edition).

Records of the Geological Survey of NSW, ***21****(2), 1983, pp. 443-447* ¾ Report of subcommittee for Southern Coalfield.

Records of the Geological Survey of NSW, ***22****(1), 1986, pp. 99-161* ¾ A guide to the calculation of confidence limits for an estimation of coal reserves, Terminology for classification and description of coalfield rocks, Code for calculating and reporting coal reserves (5th edition), Stratigraphy of the Jerrys Plains Subgroup of the Wittingham Coal Measures in the Singleton-Muswellbrook Coal District of the Hunter Valley, Stratigraphic subdivision of the Illawarra Coal Measures in the Western Coalfield, and Redefinition of coalfields in the Sydney and Gunnedah basins.

Minfo, ***12****, 1986, pp. 33-36* ¾ New resources/reserves code for Australia.

Bulletin of the Coalfield Geology Council of NSW, ***1****, 1999, 52 p.* ¾ Computer-based resource/reserve estimates, Guide to systematic evaluation of open cut coal reserves, Environmental considerations for coal geologists, Permian stratigraphy of the Gunnedah Basin, Stratigraphy of the Greta Coal Measures, Muswellbrook Anticline area, Hunter Coalfield, Coal seam nomenclature application in the Hunter Coalfield, Revision of the stratigraphy of the Newcastle Coal Measures, and Stratigraphy and terminology for the Southern Coalfield.

OFFICE BEARERS

Chairperson

Joe Whiting	Oct 1961 – Mar 1963 Geological Survey of NSW
Ken Mosher	Mar 1963 – Mar 1965 Joint Coal Board
Cliff McElroy	Mar 1965 – Mar 1967 University of NSW
Ron Wilson	Mar 1967 – Mar 1969 AIS, Wollongong
Owen Shiels	Mar 1969 – Jun 1971 Joint Coal Board
Ken Mosher	Jun 1971 – Mar 1973 Conzinc Rio Tinto
Bill Parkhill	Mar 1973 – Mar 1975 BHP, Newcastle
Michelle Smyth	Mar 1975 – Mar 1977 CSIRO
Brian Robinson	Mar 1977 – Mar 1979 Joint Coal Board
Peter Goodwin	Mar 1979 – Jun 1981 BP Clutha
Brian Vitnell	Jun 1981 – Jun 1983 Coal & Allied
Anton Crouch	Jun 1983 – Jun 1985 Anton Crouch and partners
Colin Ward	Jun 1985 – Jun 1987 University of NSW
Frank Stoddart	Jun 1987 – Jun 1989 BHP, Newcastle
Rod Davis	Jun 1989 – Jun 1991 MEGS
Carl Weber	Jun 1991 – Jun 1993 Pacific Power
Beau Preston	Jun 1993 – Jun 1995 Coal & Allied
Harry Bowman	Jun 1995 – Jun 1997 Coal Compensation Board
Rod Doyle	Jun 1997 – Jun 1999 Shell
Andrew Newland	Jun 1999 – Jun 2001 Newtuk
Michael Creech	Jun 2001

Powercoal

Secretary

Cliff McElroy	Oct 1961 – Jun 1962
Rowley Brunker	Jun 1962 – Sep 1962
Ken Wood	Sep 1962 – Sep 1969
Mal Bunny	Sep 1969 – Jun 1970
Ian Menzies	Jun 1970 – Mar 1977
Jenny Thomson	Mar 1977 – Jun 1981
Carl Weber	Jun 1981 – Sep 1984
Vic Tadros	Sep 1984 – Jun 1985
Chris Baker	Jun 1985 – Jun 1991
Mike Armstrong	Jun 1991

Assistant Secretary

Jeannette Adrian	Oct 1961 – Jun 1968

Executive

Anton Crouch	Ron Wilson Dec 1979 – Jun 1981
Ken Mosher	Ron Wilson Jun 1981 – Jun 1983
Brian Vitnell	Colin Ward Jun 1983 – Jun 1985
Anton Crouch	Frank Stoddart Jun 1985 – Jun 1987
Ken Brown	Colin Ward Jun 1987 – Jun 1989
Ken Brown	Bill Knox Jun 1989 – Jun 1991
Beau Preston	Andy Williams Jun 1991 – Jun 1993
Harry Bowman	John Rogis Jun 1993 – Jun 1995
Ron Boyd	Tony Osman Jun 1995 – Jun 1997
Adrian Hutton	Andrew Newland Jun 1997 – Jun 1999
Michael Creech	Ted Houston Jun 1999 – Jun 2001
John Edwards	John Lea Jun 2001

Recipients of award for excellence in coal geology

John Anderson	Kembla Coal & Coke December 1993
Claus Diessel	University of Newcastle December 1994
Barry Lay	Mining & Exploration Geology Services December 1995
Konrad Moelle	University of Newcastle December 1996
Winton Gale	Strata Control Technology December 1997
Colin Ward	University of NSW December 1998
Vic Tadros	NSW Dep't of Mineral Resources December 1999
Ray Williams	GeoGAS December 2000

Cliff McElroy (December 1962).

Ken Mosher (circa 1960).

Andrew Newland (Chair), Mike Armstrong (Secretary) and Ted Houston share a light-hearted moment during an Executive Meeting held at COAL's Tuggerah office (3/03/00).

Geological Survey of NSW (December 1958)
Seated (l to r): Phil Lavers; Ted Rayner; Miss Matters; Carmel Fitzgerald; Joe Whiting
Standing (l to r): Warwick Jones; Paul Coss; Don Nicholson; Col Adamson; Len Hall; Russ Griffin; Don Pinkestone; Jack Harrison; Graham Wallis; Des Wynn; Dick Relph (*back*); Jim Lloyd (*front*); Milton Coleman; Cliff McElroy; Norm Trueman; Ken Wood; Rowley Brunker; Anton Crouch (*back*); Dave Flack (*front*); Danny ? (*Visiting Indonesian geologist*). Many of the people involved in the establishment and maintenance of the SCCG in its early years are present in this photo.

Geological hazards — The impact to mining 15-16 November 2001, eds Doyle, Moloney, pp 25-30

The Influence of Coal-Mine Geology on Seismic Data Quality in the Bowen Basin

TROY PETERS & STEVE HEARN

Velseis Processing Pty Ltd, tpeters@velpro.com.au and Velseis Pty Ltd and University of Queensland, steveh@velseis.com.au

Over the past two decades numerous seismic surveys have been undertaken to assist with exploration over Australian coal mines. More recently this has been extended to assist with mine design and coal extraction. This latter application is placing increasing demands on the quality and resolution achievable with the seismic method. We present a number of examples of seismic surveys conducted in the Central and Northern Bowen Basin which illustrate that seismic data quality is strongly influenced by localised mine geology. Unfavourable near-surface conditions including variable weathering and the presence of basalt or other high-velocity layers can drastically impact on image quality. The stratigraphy of the target coal seams also affects the definition of the target seam. We comment on various ways of reducing the adverse effects of unfavourable mine geology. By incorporating knowledge of mine geology in the acquisition design and by utilising appropriate processing solutions, it is possible to obtain high quality seismic imagery.

INTRODUCTION

Numerous seismic surveys have been conducted over Australian coal mines in the last twenty years. Whilst the majority have been successful in meeting objectives, some results, particularly in the earlier years, were less convincing. In retrospect, it appears that such failures were sometimes associated with incomplete understanding of regional and local geological variations, and of how these factors impact data quality. An improved understanding of these issues over the past decade has enabled the seismic method to move from the exploration arena to become the primary geophysical tool for mine design and coal extraction.

In this paper we present typical examples of situations where seismic data quality is influenced by variations in the localised mine geology. Perhaps the most striking geological influence relates to the near surface, where drastic degradation in the seismic image can result from lateral variations in topography and weathering, or from the presence of basalt or other high velocity layering. In addition the interpretability of the coal structures depends on the depth, and stratigraphic nature, of the coal itself.

The examples presented here are from the Bowen Basin, the major coal-producing basin in Australia. However, the broad conclusions have also been observed in surveys from other Australian coal regions. Figure 1 identifies the geographical location of the Bowen Basin within central Queensland, and shows the approximate locations of the examples considered here.

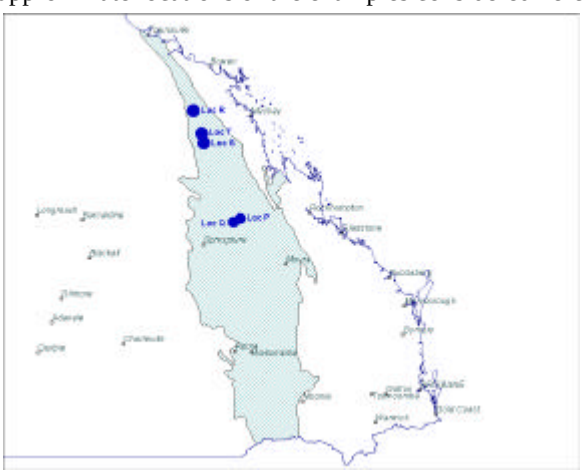

Figure 1 Geographical location of the Bowen Basin and the five example locations considered.

Locations P (Cook Colliery) and Q (South Blackwater Mine) are in the southern central basin. Location R (Newlands Mine) is in the northern basin. Locations S and T are in the northern central Basin. These different sites provide a range of near-surface conditions, as well as different coal depths and stratigraphies.

NEAR-SURFACE GEOLOGY

Locations P and Q are separated by less than 20km. The coal seam geology is virtually identical, namely a dual seam with the mining horizon uppermost in the sequence stratigraphy. However, these locations exhibit quite different near surface geologies. Location P has a simple geology of shallow uniform weathering on top of fresh Permian sediments. On the other hand, Location Q has deep variable tertiary cover with topographical highs containing sub-surface hard bands (high velocity layers).

The impact of the different surficial geologies on seismic quality is illustrated in Figure 2. The raw record from Location P (Figure 2(a)) exhibits simple refractor behaviour, and strong, well-defined reflectors. This 'classic' form is typical of areas of simple near surface geology. On the other hand, the raw record from Location Q (Figure 2(b)) indicates the thickness of the tertiary layer through the lower velocity refracted energy. The 'leg jump' feature seen on the first arrivals is the typical manifestation of the velocity inversion associated with the hard band overlying unconsolidated tertiary. The reflection energy is much less obvious on the field record from Location Q, compared to that from P.

Figures 2(c) and 2(d) show frequency spectra averaged over the traces in the field records from Figures 2(a) and (b) respectively. In these and subsequent spectral plots the non- reflection events have been muted, and the analysis window has been chosen to emphasise target reflectors. Figure 2(a) illustrates the excellent frequency bandwidth available in the Location P data. The complex near surface at Location Q is manifested by a significant reduction in reflection signal bandwidth. Figures 2 (e) & (f) are the resulting stacked sections from the two locations. Location P exhibits superior data quality with excellent fault definition. (The data from this region is consistently among the highest quality throughout the Bowen Basin.) The stack response over Location Q is of poorer quality, with the likelihood of accurate fault identification reduced.

This problem of obtaining good penetration beneath high-velocity, or multi-layered, surface situations is widely observed (e.g. Papworth, 1985; Roth et al, 1998; Evans and Ursovic, 1995; Battig, 2000). Recent modelling work on the Denison Trough (Battig and Hearn, 2001) supports the view that in such situations much of the shot energy is trapped as reverberatory noise in the near surface layers.

COAL SEAM GEOLOGY

We now give examples of how the seismic image is influenced by the stratigraphy of the coal itself. Firstly, we comment briefly on the effect of seam depth.

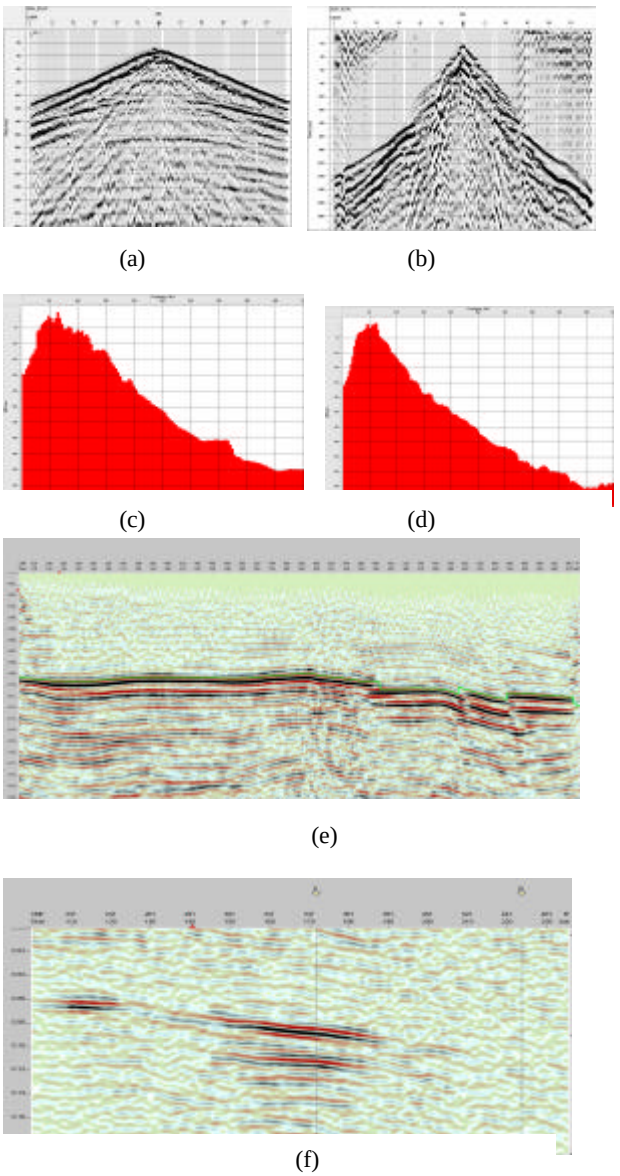

Figure 2 (a) Field record Location P, (b) field record Location Q, (c) target-reflector spectral analysis Location P (horizontal axis 50Hz increments, vertical axis –5Db increments), (d) spectral analysis Location Q, (e) stacked section Location P, (f) stacked section Location Q.

Location R, from the northern basin, provides a situation similar in most respects to that seen at Location P. For practical purposes, this is a single seam stratigraphy, since the mining horizon is the uppermost, and dominant, seam. As with Location P, this site is characterised by simple surficial geology. No thick weathering layers, or interbedded basalts, are present. The target seam at Location R is of comparable thickness to that at Location P. However the seam at Location R is at considerably greater depth (300m) than at Location P (100m).

Figure 3 (a) illustrates that the quality of shot records at Location R is excellent, comparable to that seen at Location P. The reflection spectral bandwidth is only slightly reduced (Figure 3(b)) compared to that seen at Location P. Presumably there is a slight increase in scattering due to longer path lengths. Figure 3(c) shows that the stack quality is very good. In summary, provided surface conditions are favourable, image quality for simple seam situations should decrease only marginally with increasing seam depth.

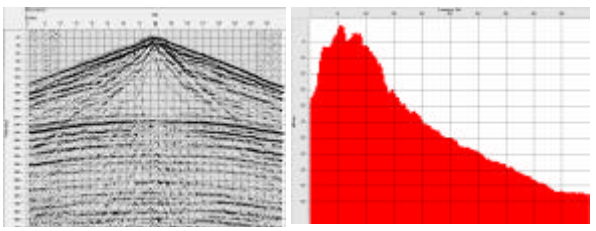

(a) (b)

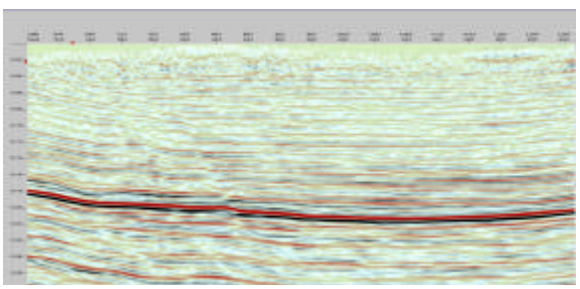

(c)

Figure 3 (a) Location R: Field record, (b) target-reflector spectral plot, (c) stacked section.

We now consider the situation where the target seam lies within a more complex coal stratigraphy. Locations S and T, situated in the northern central Bowen Basin, exhibit a multi-seam stratigraphy. Figure 4 shows a synthetic seismogram analysis for the area, and includes sonic, density and reflectivity curves. The mining horizon in this instance, is identified by the orange line in Figure 4. Note that a number of well defined seams overly the target. These shallower seams exhibit strong reflectivity at their upper and lower boundaries.

Figures 5 (a), (b) and (c), show a typical field record, spectral analysis (focussing on the target reflector), and stacked section, from Location S. At this site the near surface conditions are conducive to the seismic technique, i.e. shallow uniform weathering on fresh Permian sediments. The field record is characteristically simple in form, due to this favourable near-surface geology. Note however that the target reflector in this case is less clearly imaged, and has a reduced spectral bandwidth, compared with Locations P and R. This can be explained by transmission loss of the seismic wave as it penetrates the high-reflectivity seams shallower in the sequence.

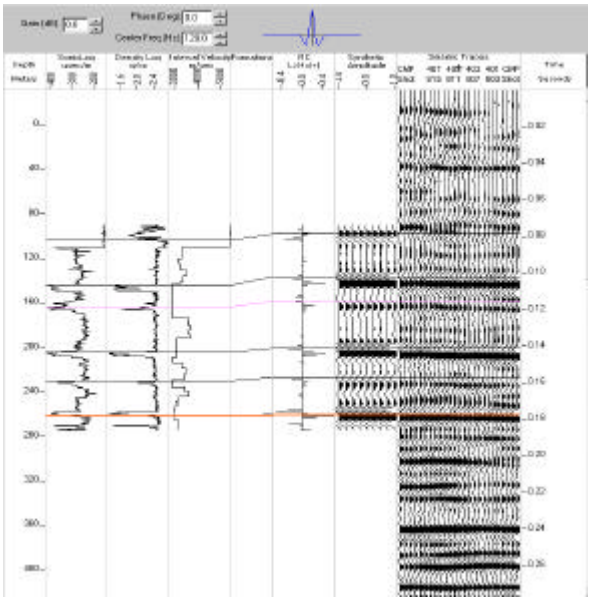

Figure 4 Synthetic Seismogram analysis from northern central Bowen Basin (Locations S, T). The quantities plotted are, from left to right: sonic, density, smoothed interval velocity, reflectivity, synthetic seismogram, real seismic section. (The real seismic section has been selected from a zone where all seams are well imaged, for purposes of tying to the synthetic. The image quality on lower seams is atypical.)

CUMULATIVE EFFECTS

As our final example, Location T illustrates the combined influence of unfavourable surface conditions and a multi seam stratigraphy. Location T has a similar coal stratigraphy and depth to that seen at Location S. However, now the surface comprises a severely variable Tertiary layer often in excess of 80m thick. In addition, this site has inter-bedded basalt stringers, typically following ancient river channels and underlain by unconsolidated river sands. Such adverse surface conditions are manifested in the raw records of Figure 6(a). As seen at location Q, the thick Tertiary layer is evident in the low-velocity refractor. A velocity inversion is again apparent on the refracted arrivals as a leg jump. The target spectral content (Figure 6(b)) has been reduced due to the combined effects of an unfavourable surface and transmission loss through multiple coal seams.

The left-hand portion of the stacked section of Figure 6(c) exhibits the loss of quality caused by the combined effects of unfavourable surface conditions and multiple seams above the target. On the right hand portion of the section the surface geology is more favourable, although the target image quality is still adversely affected by transmission loss through the overlying seams.

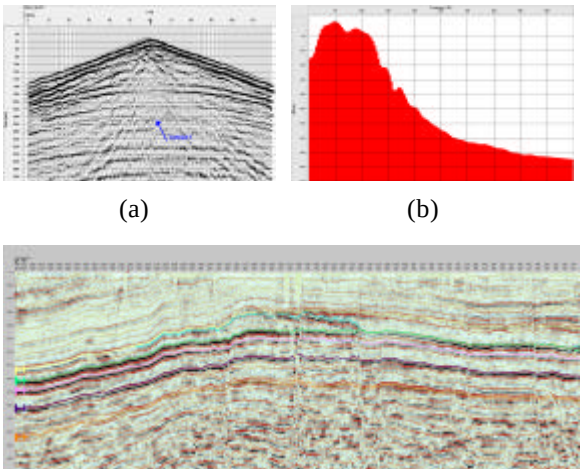

(a) (b)

(c)

Figure 5 Location S: (a) field record, (b) target-reflector spectral analysis, (c) stacked section.

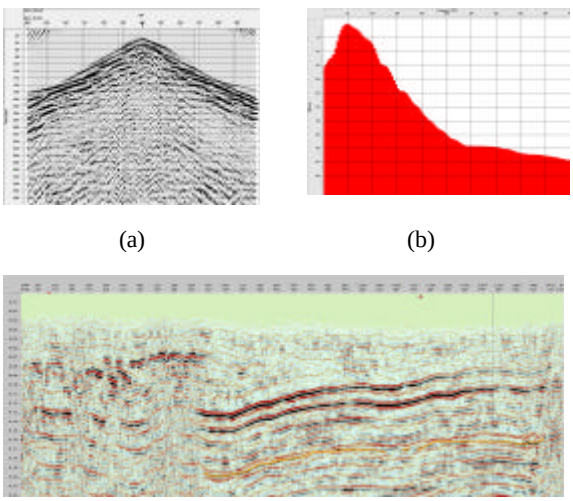

(a) (b)

(c)

Figure 6 Location T: (a) field record, (b) target-reflector spectral analysis, (c) stacked section.

SOLUTIONS

In the preceding sections we have given examples of how coal seismic quality is influenced by both near-surface geology, and the depth and stratigraphy of the coal seams themselves. We now comment briefly on potential means of reducing the adverse effects of certain mine geologies.

In the case where thick variable Tertiary or interbedded basalt is encountered one option is to make an effort to position the source below these anomalies. This would ensure maximum energy is directed down to the coal seams under investigation. An example of this is shown in Figure 7 below.

Figure 7(a) shows reflection quality obtained at BHP-Billiton's Crinum Mine, over terrain with favourable surface conditions. Figure 7(b) shows a section from an adjacent area at the same mine, where interbedded basalts occur near the surface. Mine staff were aware of the negative impact basalt would have

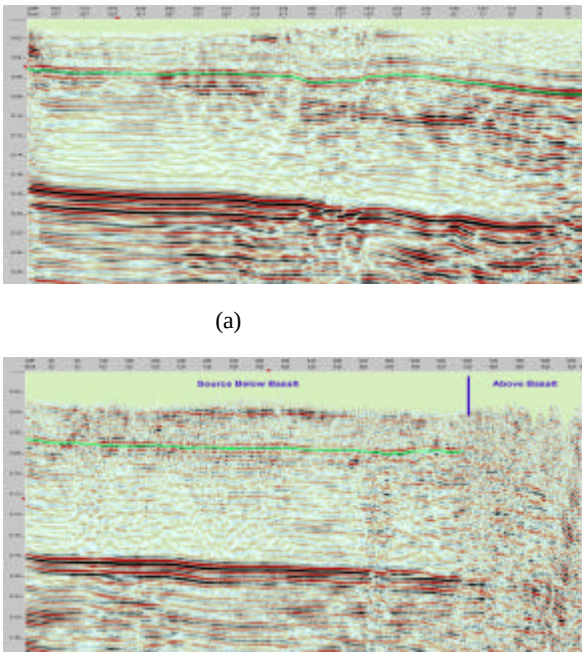

(a)

(b)

Figure 7 (a) Stacked data, no surface basalt, (b) Stacked data, surface basalt.

on survey objectives, so an effort was made to position the source sub-basalt. As Figure 7(b) shows, this was successful for most of the line with good data quality through the entire sequence. Unfortunately it was not possible to always position shots below the thick basalt layer. The right most third of this line shows how data quality deteriorated when the shot was detonated in the basalt sequence.

In some circumstances, 3D recording provides improved scope for imaging below surface anomalies. This may be the case, for example, where the surface anomalies are restricted in lateral position, so that some ray paths in each bin provide useful reflection energy. This azimuthal variation in ray paths may also yield improved refraction statics solution.

As an example, recall Figure 2(f) from Location Q (South Blackwater Mine). As previously discussed the data quality has been compromised by thick Tertiary and interbedded hard bands. Figure 8 is a section extracted from a 3D volume, and identical in location to the 2D line. Neglecting the effects of reduced CMP fold towards the extremities, the 3D line exhibits superior Signal-to-Noise and continuity.

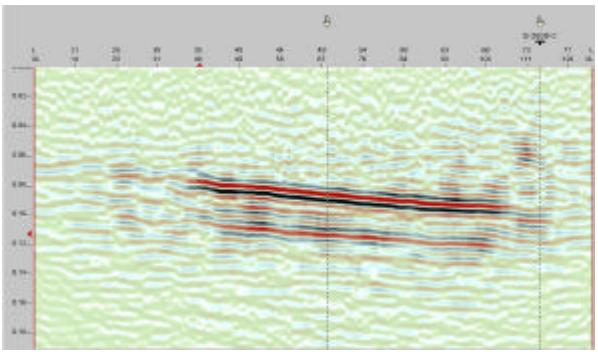

Figure 8 Location Q: Section extracted from 3D volume at the same location as the 2D line from Figure 2(f).

CONCLUSION

We have shown several examples which illustrate how localised mine geology can have a significant influence on reflection quality, and hence on the outcome of coal-mine seismic programs. The near-surface geology is often the most important factor, although the depth and configuration of the coal seams will also affect image quality. Mine planning staff often have a wealth of information on Tertiary/weathering thickness, and the presence or absence of basalt: this should be fully exploited in the acquisition and processing design. With this approach it is possible to obtain viable imagery in situations previously considered unsuitable for seismic exploration. There is future potential for addressing the problems illustrated here with newer technologies, originating from the petroleum sector. These include wave equation datuming, pre-stack migration, and mode-converted reflection.

ACKNOWLEDGEMENTS

The authors would like to thank Newlands Coal, Cook Colliery and BHP-Billiton Coal for permitting us to use data acquired over their holdings.

REFERENCES

BATTIG, E (2000). Seismic wave propagation in basalt terrains: A numerical modelling approach. Hons. Thesis, Univ of Qld.

BATTIG, E. & HEARN, S. (2001). Numerical modelling of seismic wave propagation in basalt terrains: Extended Abstracts, ASEG 15th Conference and Exhibition.

EVANS, B. & URSOVIC, M. (1995). The potential of surface and down-hole seismic in multi-layer basalts: 1995 Bowen Basin Symposium, pp. 55-63.

PAPWORTH, T.J. (1985). Seismic exploration over basalt covered areas in the UK. First Break, 3(4), pp. 20-32.

ROTH, M., HOLLIGER, K., & GREEN, A.G. (1998). Guided waves in near-surface seismic surveys: Geophys. Res. Lett. 25, pp. 1071-1074.

Geological hazards — The impact to mining 15-16 November 2001, eds Doyle, Moloney, pp 31-44

Determination of Geological Hazards using Downhole Acoustic Logs

D. R. GREEN

Green Exploration & Mining Services Pty Ltd

The definition of discontinuities, stress, and geomechanical units are all critical for determining geological hazards to mining. There is an increased requirement for geotechnical data in mine planning (layout direction, fault location etc). Various methods are available, but these are often costly and time consuming.

The slimline acoustic scanner is a relatively new device that can be used in exploration drilling to detect weak or strong zones, discontinuities, bedding partings, caving, and breakout. It can provide precise details on the depth, dip and direction of these features, and can enable determination of the principal stress direction. It can also be used as an indicator of immediate roof and floor conditions, as well as potential goaf delamination horizons. These expected conditions can then be displayed with other appropriate logs in a visually effective presentation.

Numerous features were interpreted from the acoustic scanner at four sites and were rigorously compared with those observed in standard geological, geotechnical and geophysical logs. A comparison of results and costs of stress direction determinations from the scanner was made with other methods. This demonstrated that the slimline acoustic scanner is a cost effective tool.

INTRODUCTION

Whilst a number of methods and tools are available to determine the geomechanical features of overburden and its response to longwall mining there is not sufficient yet known about the specific delamination features which control roof conditions. Determination of rock mass properties and categorisation are helpful, but do not predict the location and nature of those features that directly influence goaf formation. Numerical modelling is currently the favoured method for predicting caving behaviour. However, assumptions need to be made about the location of delamination planes.

As the geomechanical features controlling roof conditions and goaf formation are poorly understood and their determination is often expensive, any method which provides cost effective knowledge of these features is critical to determining overburden behaviour on longwall faces and for defining appropriate support levels in gateroads.

The slimline acoustic scanner is a relatively new device that utilises the amplitude and travel time of an acoustic pulse to generate an image of the borehole wall (Figure 1). Consequently it is able to depict weak or strong zones, discontinuities, bedding partings and stratification (Figure 2) as well as provide information on the borehole geometry such as caving, breakout (Figure 3) and ellipticity. As it is an oriented tool, it provides precise details on the depth, dip and direction of these features (Figure 4).

Whilst the sonic log is used routinely to make assessments about the relative strengths of different lithological units, bore core is still required to define those discontinuities which may be more significant in determining potential failure mechanisms. The industry is also familiar with standard geotechnical logging practices and the presentation of results in various formats.

The slimline acoustic scanner is potentially a more cost effective means of providing and displaying important geotechnical parameters. However, a perennial problem with any new remote sensing geophysical survey tool is establishing reliable relationships between the generated geophysical response and the tangible evidence of observation and measurement.

As the slimline acoustic scanner had not previously been rigorously tested against observed features and other methods, its full potential for interpretation and use had not been established. In order to gain widespread acceptance and usage there was a need for fundamental evaluation against borecore and other downhole investigative methods. This was carried out as part of ACARP Project C9003.

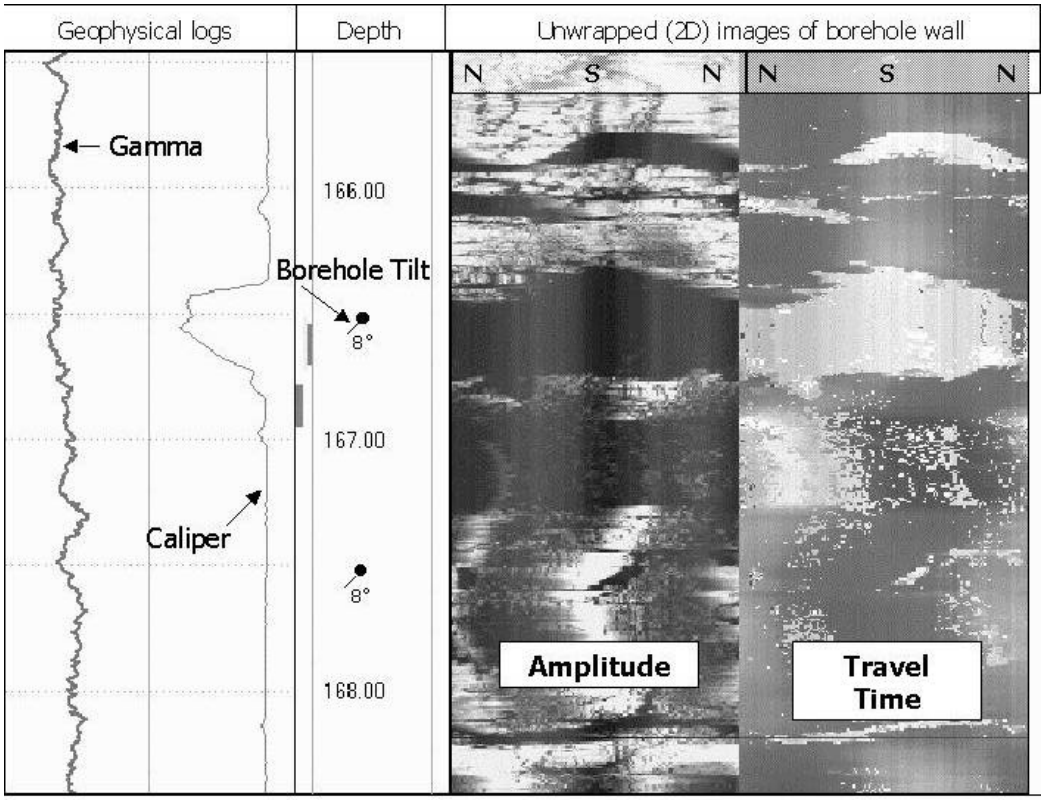

Figure 1 Acoustic Scanner output.

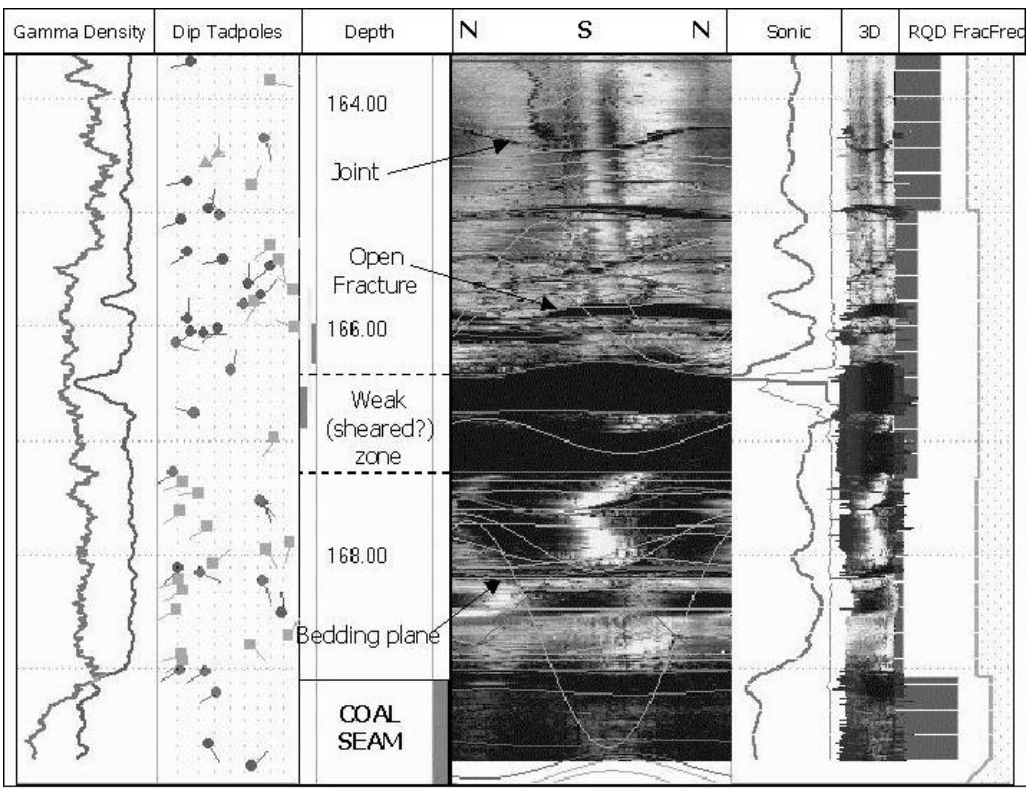

Figure 2 Structural features interpreted from Scanner image.

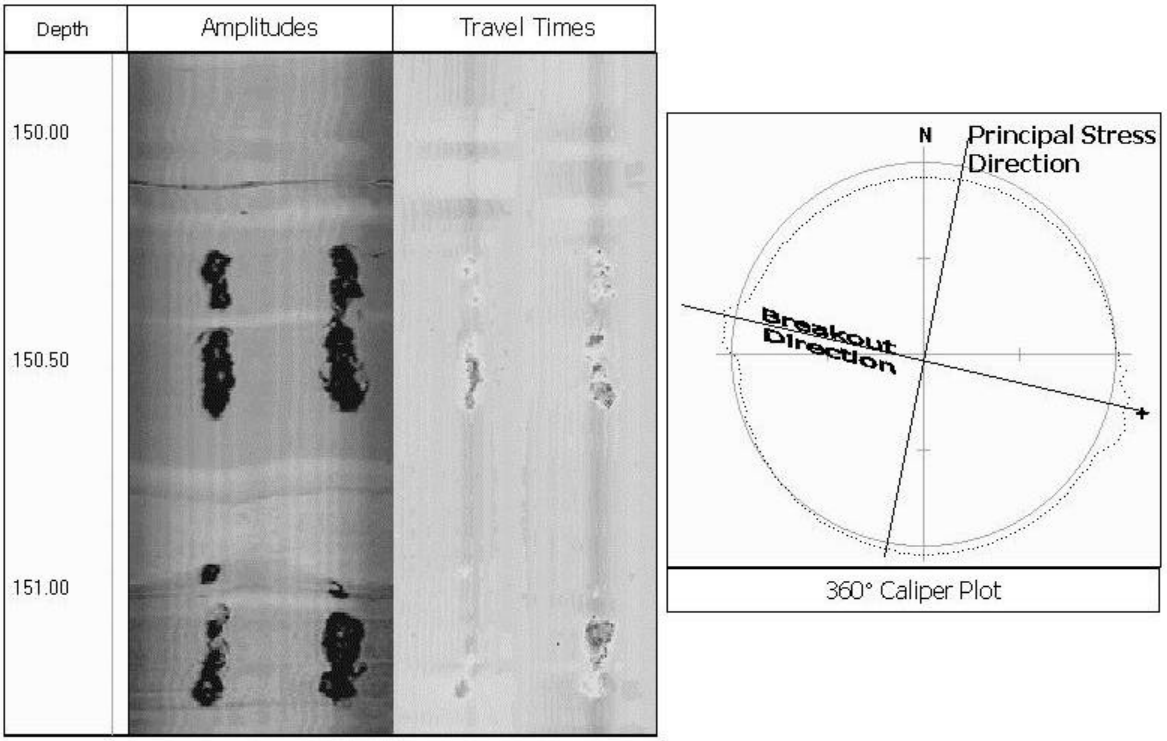

Figure 3 Breakout interpreted from Scanner image.

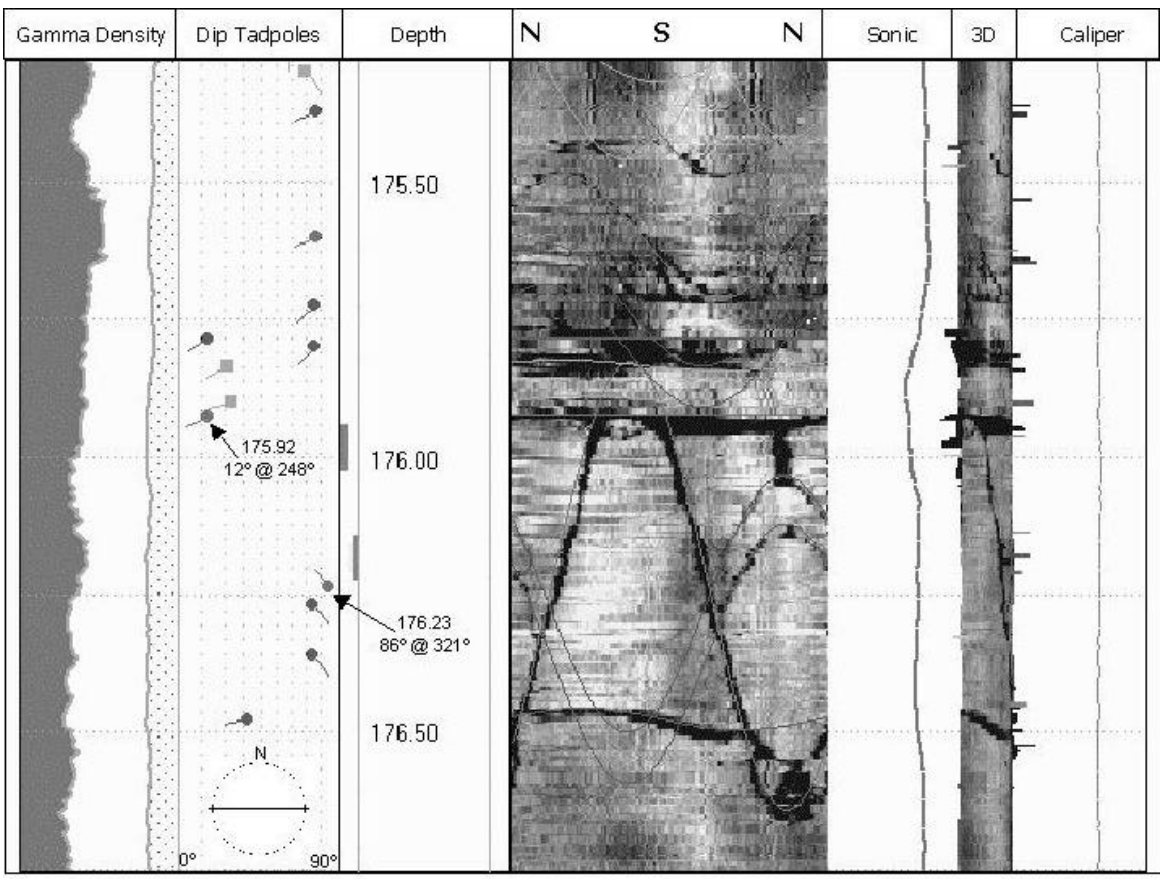

Figure 4 Depth, dip and direction interpretation of Scanner features.

METHODS

Nearly 1000m of core from three Bowen Basin sites (Moranbah/ German Creek Coal Measures) and one Sydney Basin site (Whittingham Coal Measures) was geotechnically logged. This provided data on numerous fractures (bedding breaks, joints, faults, veins, etc.) and geomechanical features from a variety of strata types and roof conditions. Features were interpreted from the acoustic scanner logs with different confidence levels applied (High where feature visible across >75% of image, Medium where >50%, and Low where <50%). These features were then compared with the core log and other geophysical logs.

Fractures from the core logging were matched where possible by depth and dip angle with interpreted scanner features. This revealed a number of core features that were not matched with an interpreted scanner feature and vice versa. Where possible unmatched features were searched for in core or photos and the scanner log was inspected again. Investigations were made into the reasons for the lack of a match and some comparison statistics were determined.

All possible instances of breakout were recorded and compared to stress direction determination results obtained from other methods. A comparison of costs of different methods was undertaken.

Post caving data was collected to evaluate the effect of particular discontinuities on goaf formation. An investigation was made into the presentation of scanner logs with other borehole logs in various software systems.

RESULTS

More than 2000 features were interpreted from 16 boreholes. Only one third of all bedding plane breaks

	PERCENTAGE OF ALL FEATURES BY TYPE					
	% of Core features seen by Scanner by type		% of Scanner features seen in Core by confidence type			
HOLE	**BP**	**JOINT**	**High**	**Med**	**Low**	**TOTAL**
A001	42	50	40	41		41
A002	54	59	40	35		39
A003	51	50	50	24		38
Site A total	**49**	**55**	42	33		**39**
B001	35	65	79	61	69	68
B002	12	17	80	90	73	80
B003	55		100	71	33	67
B004	43	80	57	40	50	50
B005	54	50	91	80	70	81
Site B total	**31**	**58**	78	62	66	**68**
C001	38	61	38	50	39	40
C002	34	53	62	59	57	60
C003	36	68	49	33	21	43
Site C total	**35**	**59**	49	48	40	**47**
D001		69				
D002	41	59	50	46	31	46
D003	68	41	60	29	39	47
D004	100	77	57	25	35	36
D005	100	56	40	100	40	54
Site D total	**56**	**56**	39	35	38	**38**
TOTAL	**38**	**58**	49	46	50	**48**

Table 1 Match of core log with scanner interpreted figures.

were matched by features seen by the scanner, whilst the scanner detected nearly 60% of all joint features seen in core. This result varied slightly from site to site and with core and scanner quality. Nearly 50% of scanner features from all sites were recognised in the core. A summary of these results is provided in Table 1 and discussion of them follows. A better result was expected but there are some clear reasons for the lack of match between core and scanner interpreted features and these are discussed in the next section.

There was no significant distinction in detection between the three confidence levels applied suggesting it is not sufficient to only interpret high or medium confidence features. Clear joint sets were defined with a good comparison with features logged in core (Figure 5). Comparison with direct joint mapping shows that the scanner is a reliable tool for determination of the known joint sets, with the advantage that it is not biased to any particular face direction.

Nine of the sixteen boreholes showed breakout and gave comparable results for principal stress direction with underground overcoring, hydraulic fracturing (Figure 6) and downhole wireline overcoring (Sigra method). There were also comparable results between the UCS strength of units displaying breakout with the stress magnitude obtained from other methods.

The large number of values that can be obtained from the scanner enables a greater statistical determination of the principal stress direction. An evaluation of the costs associated with various methods clearly shows a cost advantage to using the acoustic scanner for principal stress direction determinations (Table 2). Other advantages such as the ability to obtain stress direction data in a number of locations, for different stratigraphic horizons, and related to major structures, contribute to the cost effectiveness of this tool.

Features in core not scanner

There are some clear reasons for the lack of matching features due to the nature of the borehole conditions and the data acquisition.

If there is smearing or caking in the borehole a poor scanner image can result. If there are very high angle features, the scanner may not be able to resolve them. Where the feature is too tight (ie there is a poor strength contrast) it will not be displayed. It is also possible that some of these features are drilling induced. Obviously if the feature is drilling induced (or due to stress relaxation of the core) there will not be a corresponding scanner feature. This is clearly a reason for the lack of matches of bedding breaks, which can obviously be induced by drilling and handling procedures of a 63mm core.

Features in scanner not core

Whilst it can be demonstrated that the acoustic scanner defines the principal joint sets it is necessary to know whether it also produces spurious results. Consequently numerous examples of unmatched scanner features were examined to find a reason and determine the impact on scanner interpretation.

The most significant number of unmatched features were related to bedding features or lithology changes which did not correspond to a bedding break (eg siderite lenses or mudstone bands in coal seams). Carbonaceous fragments and lenses also have the same appearance as weak planes on the scanner image and can give misleading information (Figure 7).

A large number of features were identified from the scanner where core had been sampled before having being logged, or where there was core loss or core was broken. Some features occurred at the end of a core run and were not logged. These are four critical reasons for the use of the scanner, as core cannot provide data on fractures if it is damaged or removed (Figure 8).

The acoustic scanner also revealed significantly more joints or cleats in coal seams which were apparently more difficult to see or define from the core (Figure 9). There were also a number of features interpreted in tuff units that appear to have been rehealed and were not visible as fractures in the core (Figure 10). It is clear from this that the scanner provides significant additional information to that obtained from the core (Figure 11).

At two sites in the study it was possible to examine the core after conducting the scanner interpretation which allowed unmatched scanner features to be searched for in the core. This revealed errors in the original core log and a number of features which were not seen or recorded whilst logging (Figure 12). In some cases depths of features were incorrect (due perhaps to errors in depth adjustment of core loss or drillers depths), whilst recorded dip angles were influenced by the angle of the borehole. The acoustic scanner is not influenced by the angle of the hole and hence interpreted dip angles are structurally correct.

Following relogging of the core of two boreholes the number of matched ‘joints’ were increased by 9% to 15% (Table 3). Even in well matched zones of joints the scanner recorded additional features which had not been logged.

Whilst the comparison percentage is still low and some individual features may not be detected, joint sets and major planes or zones of weakness are identified. Although 40% of joints are not detected in the scanner image (for the reasons above), the accurate definition of dip directions and position adds considerably to the data determined from core logging.

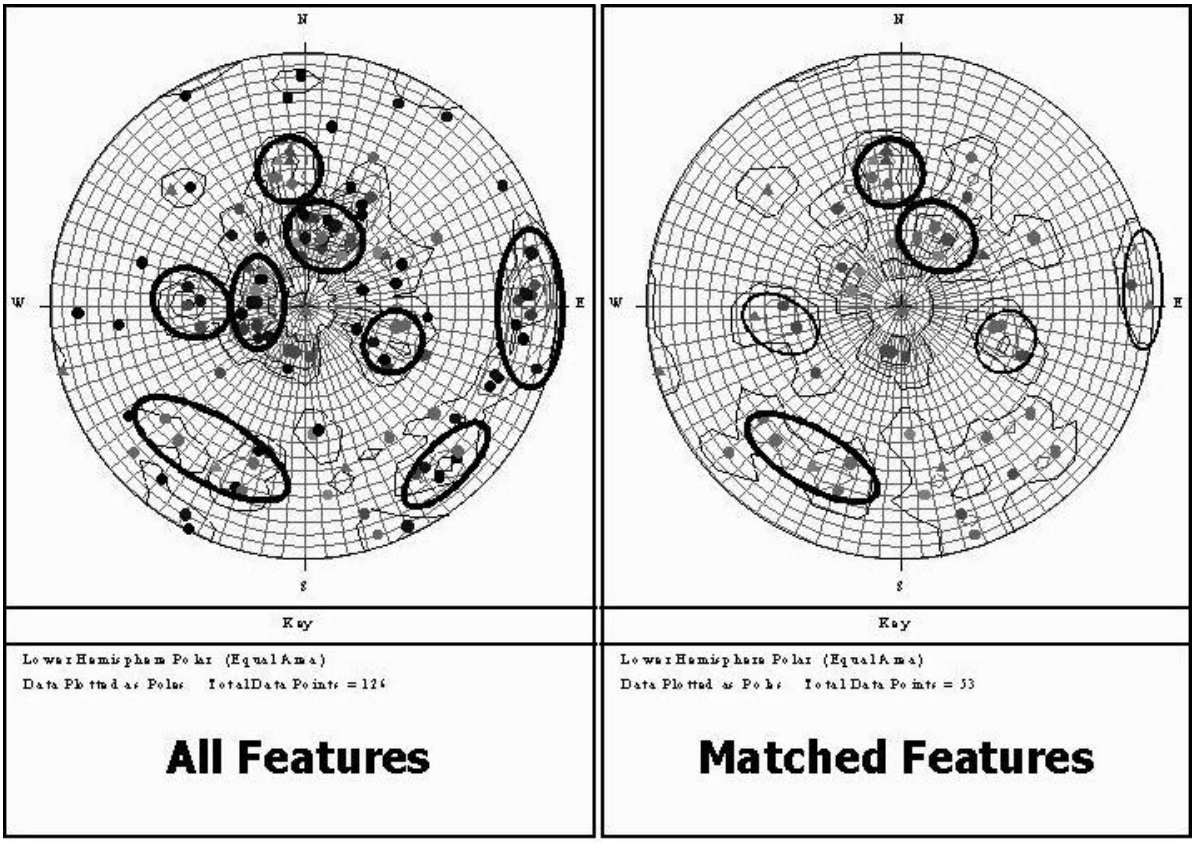

Figure 5 Stereo net comparison of All vs Matched features.

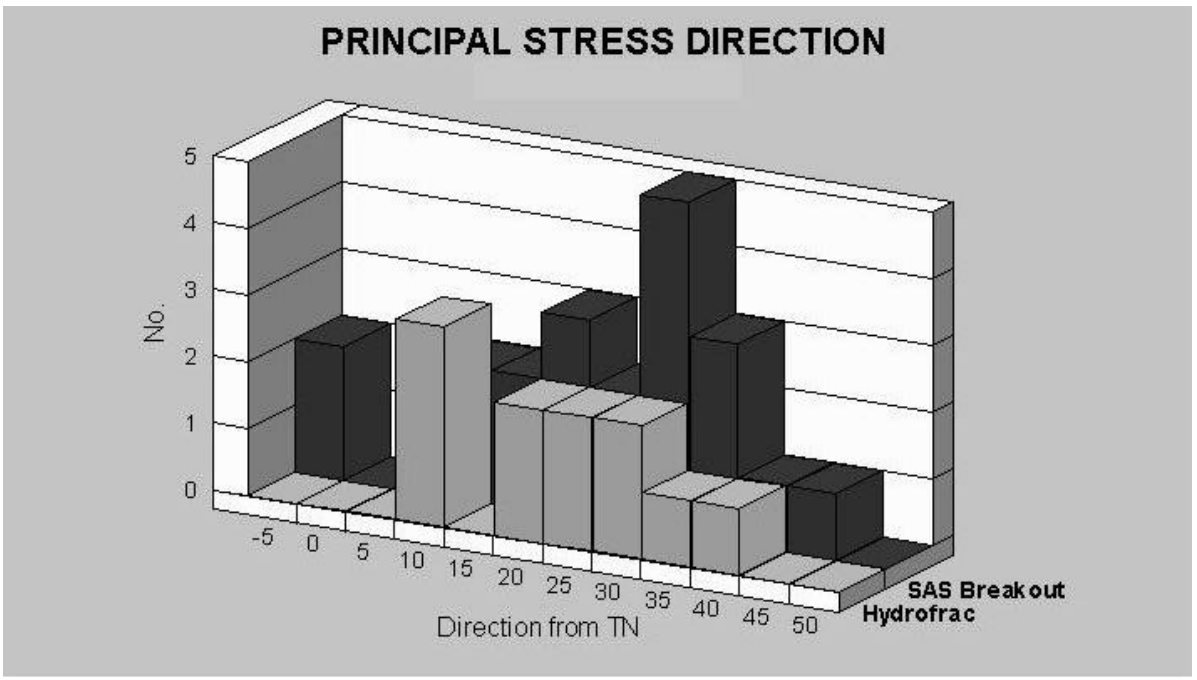

Figure 6 Principal Stress Direction method comparison.

BOREHOLE			INDICATIVE COSTS				
TD	**CORE**	**SCAN**	**Drilling**	**Gen Logs**	**Scanner***	**Sigra[x]**	**Hydrofrac[x]**
300m	35m	50m	$12,000	$1,200	$1,800	$15,000	$25,000
	Additional % cost to drilling			10%	15%	125%	208%
	TOTAL			$13,200	$15,000		
			= nearly 2 x Core (incl. Scanner)			$28,200	
			= nearly 3 x Core (incl. Scanner)				$38,200
					*incl. interp	[x]excl. extra drilling costs	

TD	Chip	SCAN	Drilling	Gen Logs	Scanner*
300m	300m	50m	$3,000	$1,200	$1,800
	TOTAL			**$4,200**	**$6,000**

2 x Core (incl. Scanner) = 5 x Chip (incl. Scanner)

2 x Core + Sigra Test = 9 x Chip (incl. Scanner)

1 x Core + Hydrofrac Test = 6 x Chip (incl. Scanner)

1 x Core + Hydrofrac Test = 1 x Core (incl. Scanner) + 4 x Chip (incl. Scanner)

Table 2 Comparison of Costs of Principal Stress Direction Determination methods.

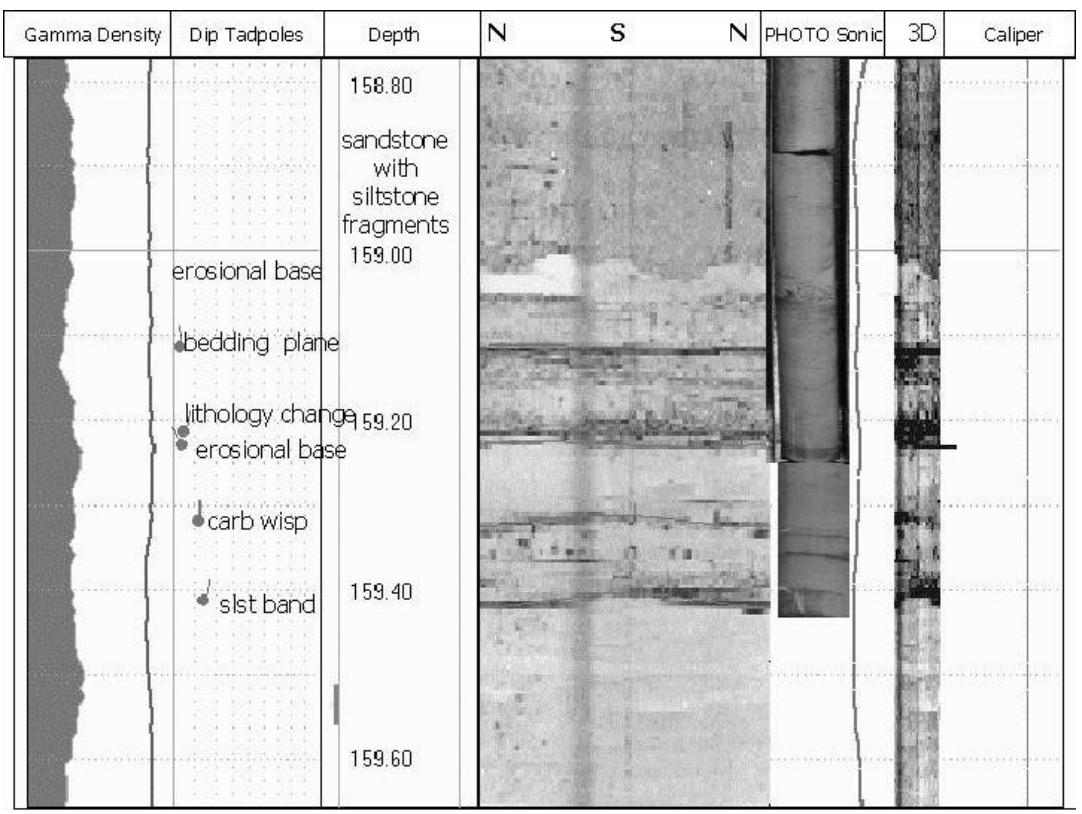

Figure 7 Sedimentary features as seen in Scanner image.

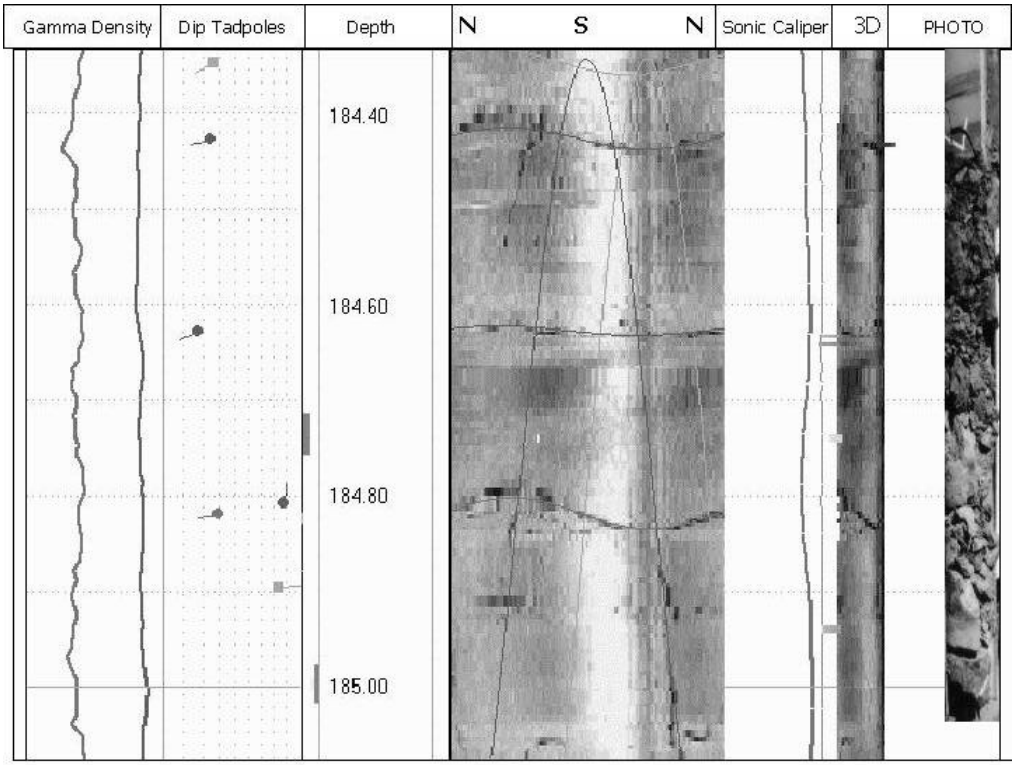

Figure 8 Feature in Scanner not Core: Broken Core.

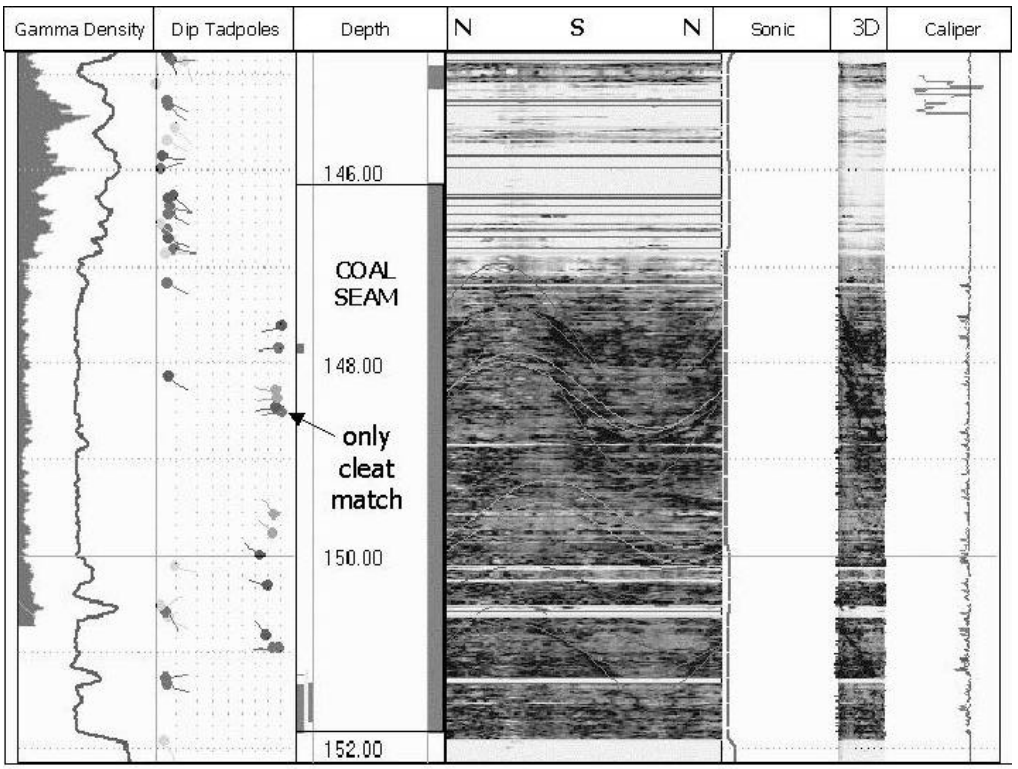

Figure 9 Feature in Scanner not Core: Extra Cleats.

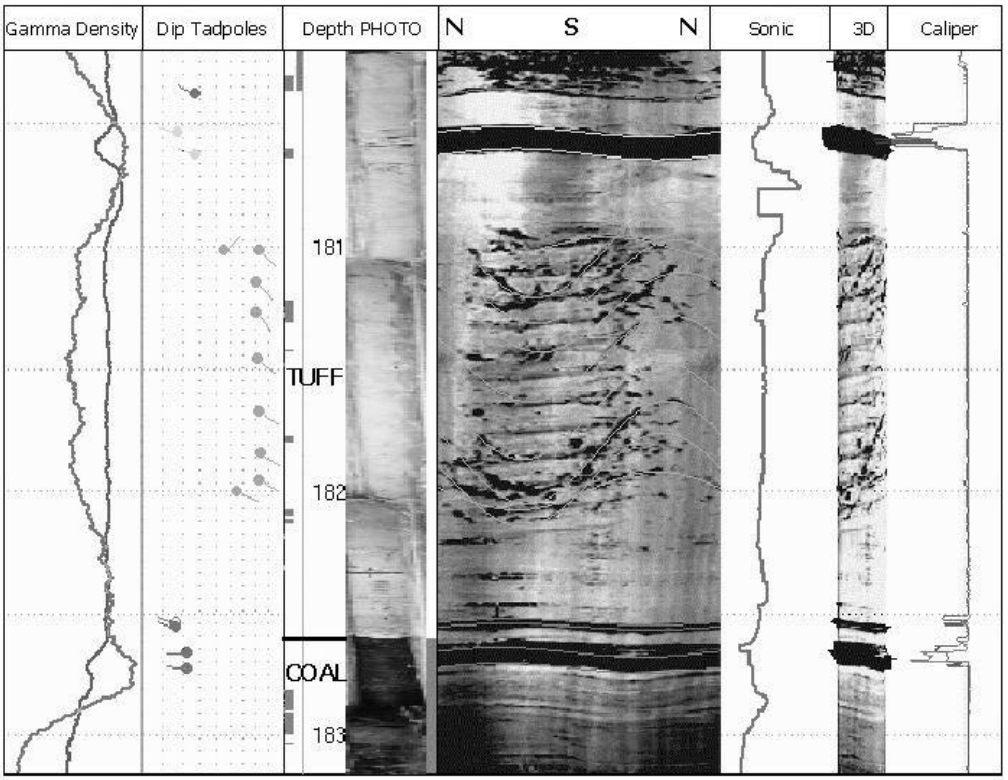

Figure 10 Feature in Scanner not Core: Tuff unit.

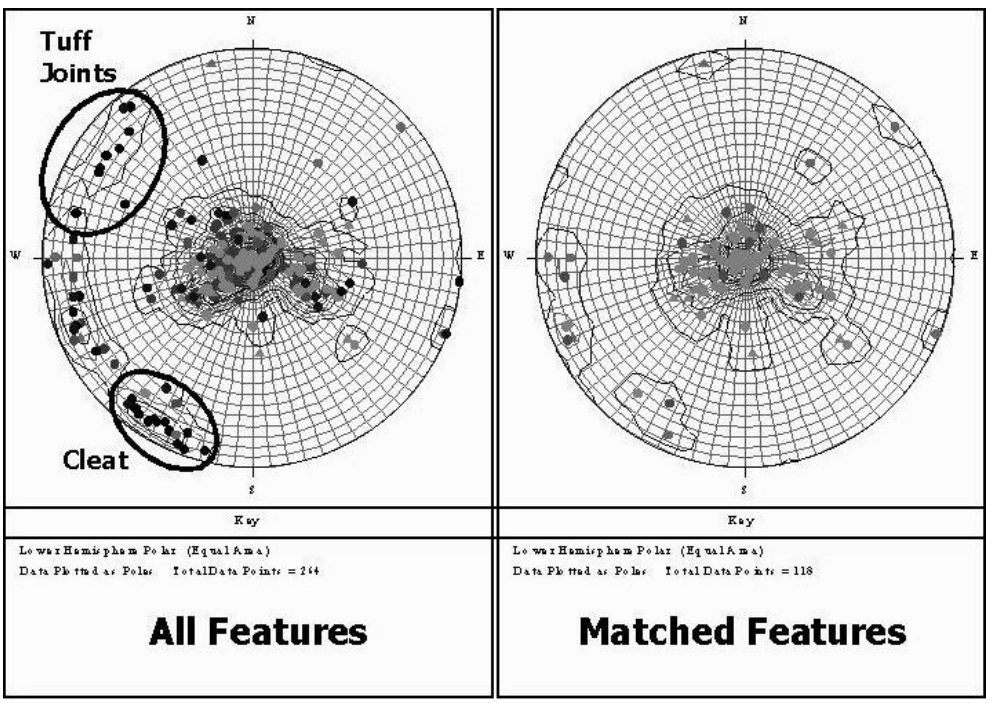

Figure 11 Stereo net comparison showing extra joint sets.

It is important to recognise that the acoustic scanner is a geophysical tool with certain limitations, is subject to interpretation, and consequently cannot be expected to be a replacement for hard physical evidence (ie core). However, it does add a significant level of accuracy and detail, which can be overlooked during core logging, and can be re-examined and reviewed frequently.

OPEN HOLES

Whilst the benefit of utilising the acoustic scanner in core holes has been demonstrated, it is also clearly advantageous to use it in open (chip) holes. As discussed, key geotechnical features can be more accurately defined by the scanner than from core. By running the acoustic scanner in open holes it is possible to reduce the cost and dependence of geotechnical assessment on coring (Table 2). This will then enable more widespread determination of important geotechnical parameters that are critical to understanding overburden characteristics which are critical to mining.

It is not possible to determine the reliability of the scanner interpretation in an open hole, but evaluation of scanner images suggests that significant features can be determined from a well drilled open hole. The best results have been obtained from hammer or PCD drilled holes that have been drilled a little slower than usual and are well flushed. The build up of any caking on the borehole wall severely reduces or eliminates the definition of any fractures by the scanner. Whilst the cost of an open hole is significantly lower than that of a cored hole, the value of it can be dramatically increased with the application of the acoustic scanner.

BEDDING BREAKS

Are bedding breaks a reliable indicator of weak horizons or does the acoustic scanner give a more reliable indicator of roof failure discontinuities? Which features are correct or more significant geotechnically?

The recording of bedding breaks and RQD is standard practice in geotechnical logging and is required to determine rock mass ratings. However bedding breaks do not necessarily predict the location and nature of those specific delamination features which control roof conditions and directly influence goaf formation.

Matching of bedding breaks in the core with weak planes (which may be bedding related or be low angle joints or shears) in the scanner image suggest that breaks do not always occur where there is the greatest strength contrast (Figure 13). Whilst core is subject to extreme and varied physical processes by the drilling and handling operations, a good scanner image provides a consistent representation of the strength of the strata. Therefore it would appear to offer a more reliable indication of where strata is most likely to delaminate in response to tensile stress.

WEAK UNITS

Weaker units are not always identifiable in core or from the standard sonic log. These units can either be thin planes, or not be visually distinct from other beds, and can be logged as the same strength (even stronger where coarser) as the surrounding lithology. Yet the acoustic scanner suggests some units are noticeably weaker (possibly indicating strong grains in weak

	PERCENTAGE OF ALL FEATURES BY TYPE					
	% of Core features seen by Scanner by type		% of Scanner features seen in Core by confidence type			
HOLE	BP	JOINT	High	Med	Low	TOTAL
INITIAL LOG						
D002	36	50	39	26	8	29
D003	67	26	54	25	18	36
POST SCANNER LOG						
D002	41	**59**	50	46	31	**46**
D003	68	**41**	60	29	39	**47**

Table 3 Match of features before and after logging.

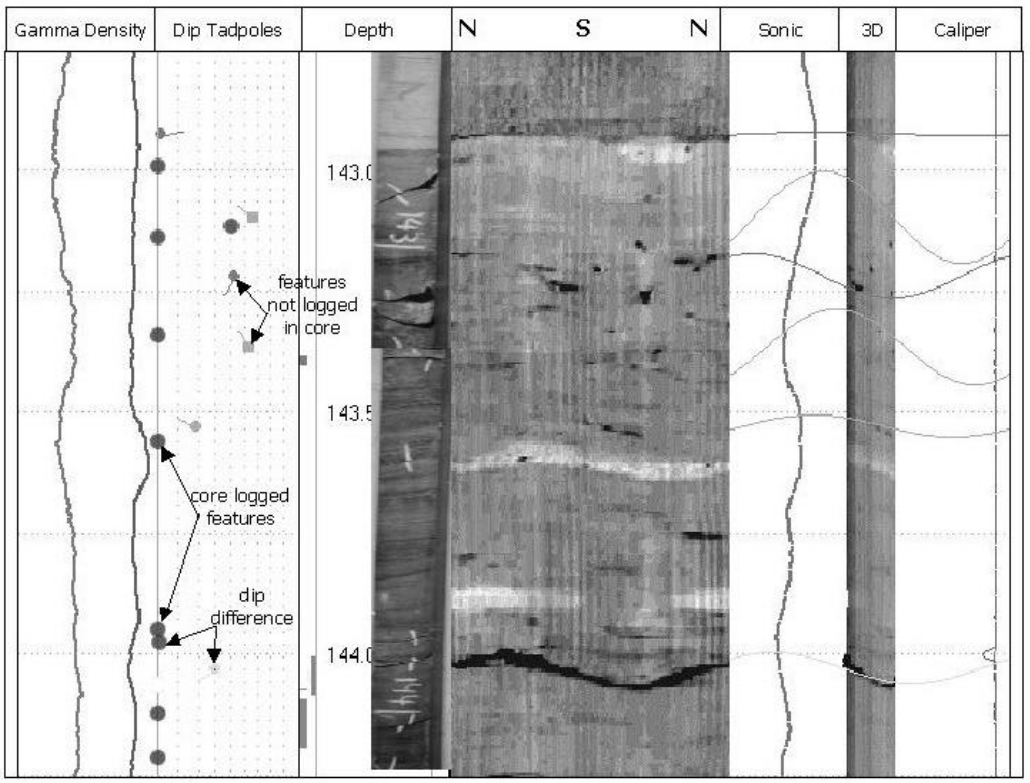

Figure 12 Feature in Scanner not Core: Logging errors.

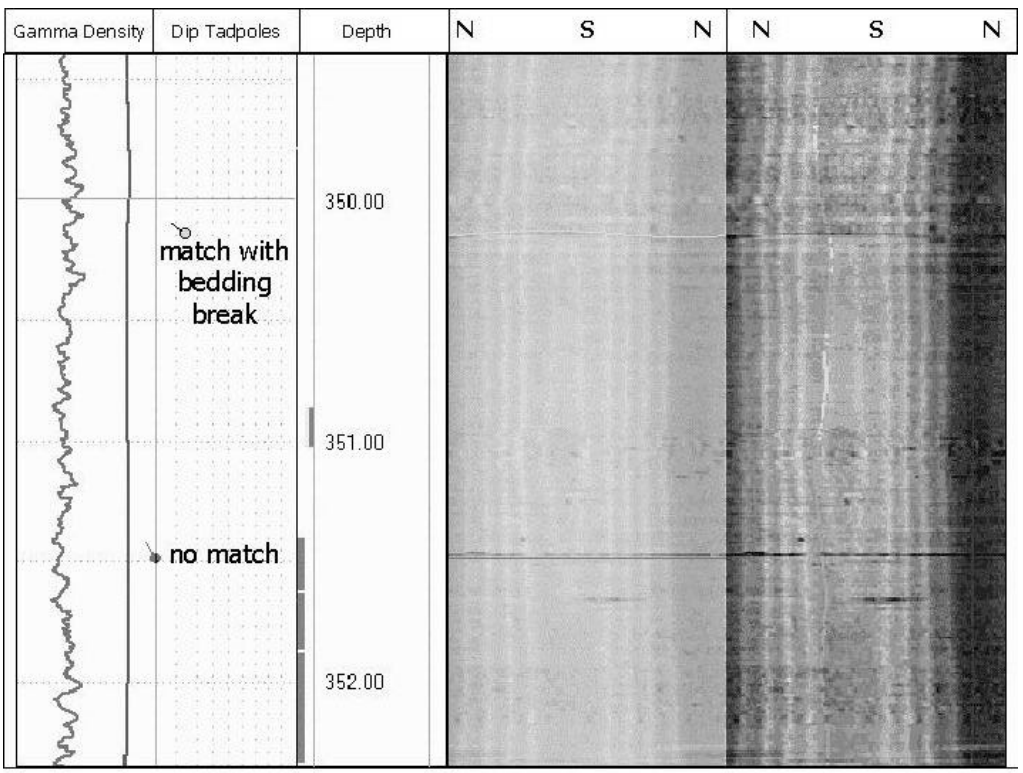

Figure 13 Comparison of Matched and Unmatched Bedding Breaks.

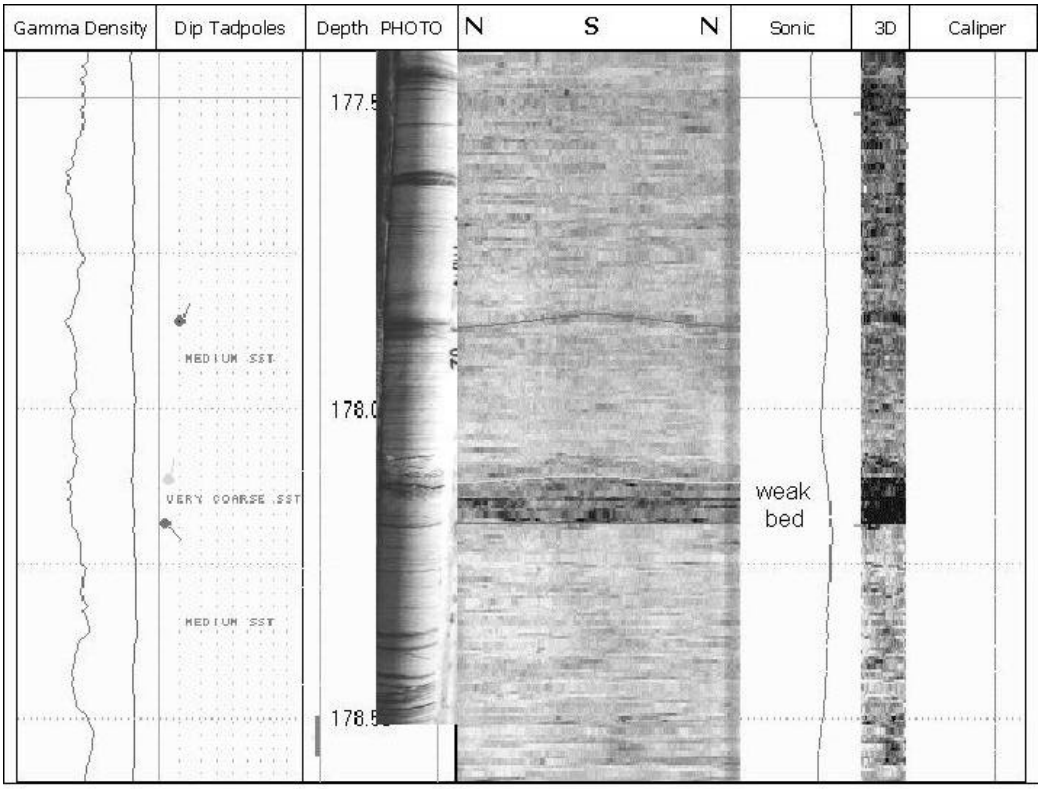

Figure 14 Detection of Weak beds from Scanner image.

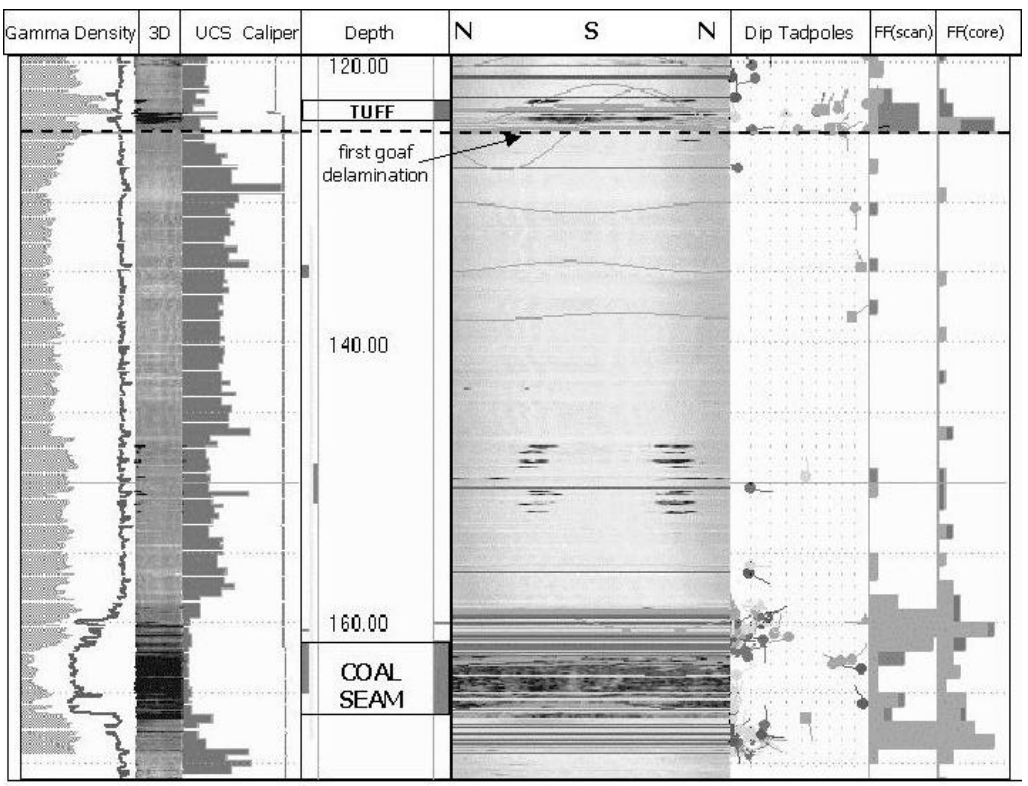

Figure 15 Fracture Frequency comparison.

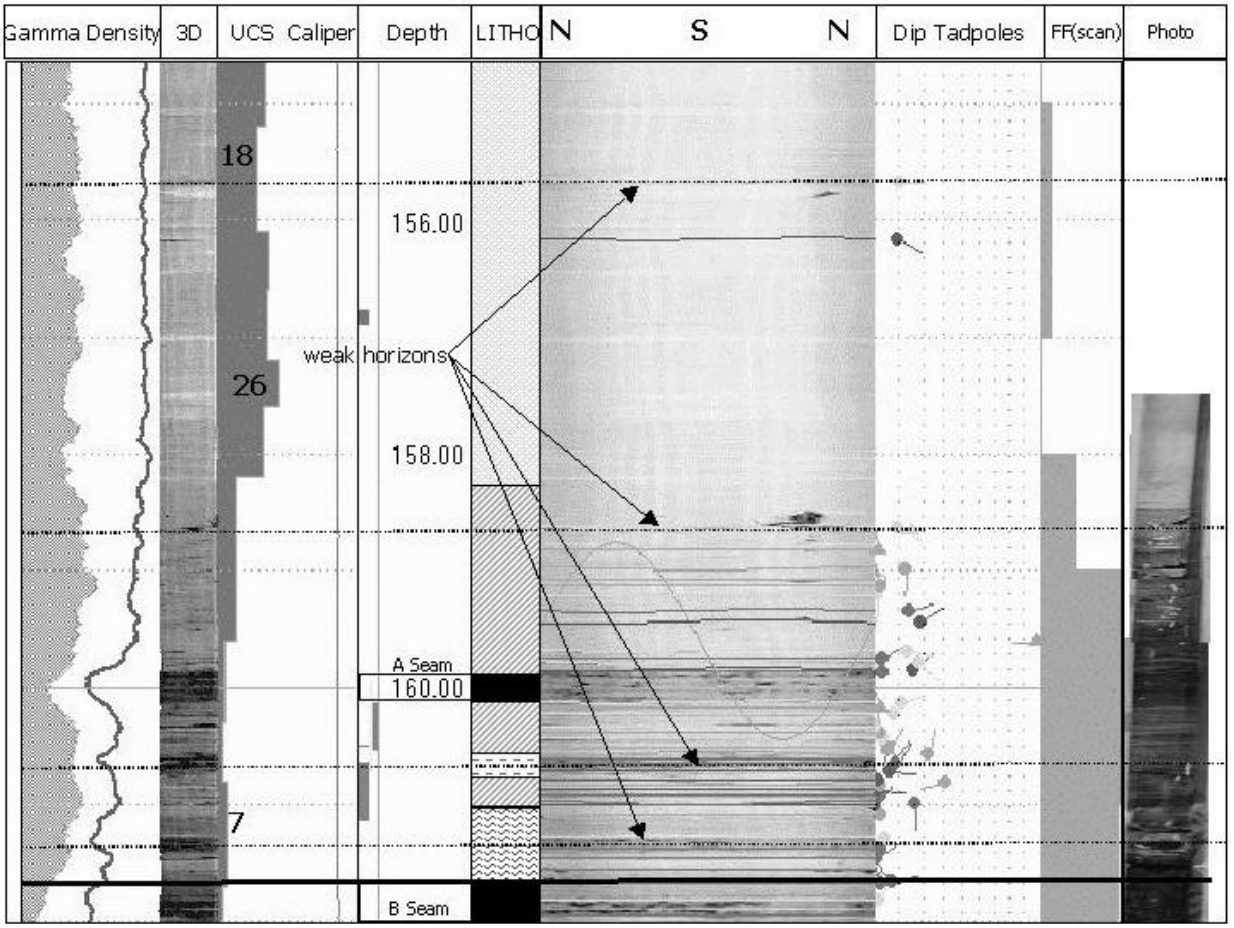

Figure 16 Presentation of Geotechnical data.

cement) (Figures 10 and 14). These interpreted features significantly enhance and even supersede the information gained from core.

By way of contrast, the size and shape of sideritic (or other hardened) units can also be readily described from the scanner image.

FRACTURE FREQUENCY

By systematically identifying weak beds and planes from the acoustic scanner image as well as joints and other fractures, it is possible to generate a Fracture Frequency log of low angle or all fractures [Figure 15 – FF(scan)]. This log has been compared to one generated directly from the core log [Figure 15 – FF(core)] and whilst an exact match is not obtained there is an obvious correlation (Figure 15). That is, the scanner clearly identifies zones of high or low fracture frequency in the same sections of the borehole as determined from the core log. If required, the spacing of any fracture or bedding set can also be determined from the scanner image.

This suggests the information from the scanner interpretation can be utilised directly in rock mass characterisation schemes. Assessments of roof conditions and potential roof failure or goaf formation zones can also be made. This information can then be incorporated into numerical models to improve predictions of roof and goaf behaviour. To confirm the usefulness of scanner interpretations they were compared to the known or measured behaviour of the goaf from other monitoring systems.

GOAF FORMATION

Extensometer data from one site indicates that all strata up to >30m above seam behaved as a single unit. Consequently none of the fractures or bedding planes/units identified in the core or scanner over this horizon contributed to goaf formation. However the scanner did identify significant features and a high fracture frequency in the tuff unit at this level and it is clearly recognised as a weaker unit (Figure 15). This confirmed the assessment made from the core, which showed massive sandstone strata without significant bedding or fracturing. Whilst sideritic units were

identified and create significant strength contrasts they do not appear to contribute to goaf formation.

The scanner did identify a number of features in the immediate roof and floor that could help determine the level of roof support required (Figures 15 and 16).

Conversely roof strata at another site is more laminated and the scanner detected numerous weak horizons. Microseismic monitoring at this site shows a number of horizons in the first 30m of roof where delamination occurs and contributes to goaf formation. The relatively high fracture frequency in scanner interpreted boreholes at this location suggest this behaviour is likely to continue and areas of heavy roof are unlikely.

It is to be hoped therefore that the scanner can be effectively used as a diagnostic tool in the definition of roof and goaf forming conditions.

PRESENTATION

"A picture tells a thousand words" is a well known saying which is not always applied to geotechnical data. Various logs, tables and histograms derived from core do not always adequately convey the location or nature of geological hazards which may impact on the mining process. A good 'picture' of the geotechnical conditions is possible from the acoustic scanner in conjunction with the display of other relevant logs. Such a picture can readily be used to communicate important information about potential roof conditions to a variety of people from managers to miners (Figure 16). It is also possible to extract information from the scanner in suitable formats for input to other display packages (eg virtual mine, major software packages) to show on sections, hazard plans etc. More extensive use of the scanner to gain and present this type of information may well assist in the management of geological hazards.

SUMMARY

The acquisition of accurate and relevant data is essential for the definition of geological hazards in all types of mining. Any tool which is able to provide data on the stress field, joint sets, and location of planes of weakness, from commonly drilled boreholes at a moderate cost, has to be extremely valuable. The slimline acoustic scanner is such a tool.

Whilst comparison of geotechnically logged core with interpreted acoustic scanner images suggest there is a poor match of bedding breaks to weak horizons, and a moderate match of joints to features on the scanner, there are some clear advantages to its use. Joint sets are clearly identified, and the scanner shows features normally unavailable due to core loss, breakage, sampling, errors etc. Breakout from the scanner gives a reliable indicator of the principal stress direction and an estimate of the stress magnitude can also be derived. Additional uses of the acoustic scanner to define and display expected roof and goaf conditions make this a very cost effective geotechnical tool.

ACKNOWLEDGMENTS

This paper is the result of research funded by ACARP, as part of project C9003. The following companies (and mine sites) assisted with data and mine support: Pacific Coal (Kestrel); MIM (Oaky Creek); Anglo Coal (Dartbrook and Moranbah North). Valuable software and technical support was provided by Reeves Wireline Services. Thanks are given to all site and office personnel for their assistance, and especially to Barry Ward for support, discussion, and review of this project and paper.

REFERENCES

FIRTH, D. 1999. Log analysis for mining applications. Reeves Wireline Services.

Geological hazards — The impact to mining 15-16 November 2001, eds Doyle, Moloney, pp 45-49

Electromagnetic Emissions Monitoring to Warn of Wind Blasts and Gas Outs
Results of ACARP Project at Moonee Colliery: C9005

K. VOZOFF & VLADIMIR FRID

V&A Geoscience Sydney, Ben Gurion University Israel

Electromagnetic signals are emitted by rocks as they fracture, in much the same way as acoustic signals, but by different processes and with different characteristics. The object of this project was to evaluate the potential usefulness of the electromagnetic emissions (EME) as warning signals, to complement the acoustic emissions (AE) which are now used in several mines in Australia and overseas. AE have some disadvantages as regards cost and flexibility, and are not completely reliable, so there is incentive to look for alternatives. Three sets of single channel EME measurements were collected between March and July 2001. Results were compared with fracture events in the mine and with the four channel AE records. In one of the three cases there was no response, in another there was a large response beginning before the seismic and lasting for some time. In the third case the EME showed only a small response. The conclusion is that EME show promise, but that additional measurements, preferably multichannel, are necessary before the true potential can be assessed.

WHAT ARE ELECTROMAGNETIC EMISSIONS?

EME are electromagnetic (EM) waves given off from rocks as they fracture, in the same way as microseismic emissions, although there is no general agreement on the cause. They are reported on size scales from single crystals and rocks in the laboratory (Hanson et al 1982, Brady & Rowell 1986 & Cress et al 1987), to the mine scale (Frid 1997a, Frid 1997b & Frid 2001), to earthquakes (King 1983 & Hayakawa 1993). Frequencies range from megahertz for small scales and hard rocks, to subaudio for earthquake precursors.

In the in-mine application, the first known publications in English are in Khatiashvili 1984, Nesbitt & Austin 1988, Frid 1997a & Frid 1997b. In Nesbitt & Austin 1988, EME were detected prior to rockburst. In Frid 1997a and Frid 1997b, EME were used to predict gas-outs and outburst in Russian coal mines. Frid refers to work done in coal and metalliferous mines and published in Russian. Using purpose built (analog) equipment tightly tuned to 100kHz, his group made measurements daily during a care and maintenance shift. The number of impulsive emissions measured in 5-minute intervals was compared with their traditional predictors, their Gum method, the volume of methane emitted into a short hole drilled into the rib, and found to be equally reliable and safer. Figure 1 is a result from reference Frid 2001, in which the EME results are compared with the Gum result in the lower seam, on a traverse beneath the pillar in the upper seam.

POTENTIAL BENEFITS OF EME

In principle, EME should be easier to work with than are microseisms since:

- sensors do not require mechanical coupling to the rocks so they should be able to move with the mine face, making them equally applicable for use during longwall and pillar extraction, and for indicating outburst, gas out, etc.,
- EME would be expected to propagate without attenuation in air, so they should not have to be located near the face,
- their components, the electric and magnetic fields, may provide directional information to indicate their source, and
- the sensors can be relatively cheap, so they can be made disposable.

The main *a priori* concern is the effect on the measurement of EM noise from mining machinery and power systems.

MEASUREMENT PROGRAM

The project plan was to observe on two sensors at Moonee Colliery, and to compare the results with the operating microseismic system, and mining events, and with each other. The problem at Moonee is windblast, which can arise from collapse of the strong roof left unsupported over too great a length. Two well-proven, battery operated IS PC data acquisition systems were

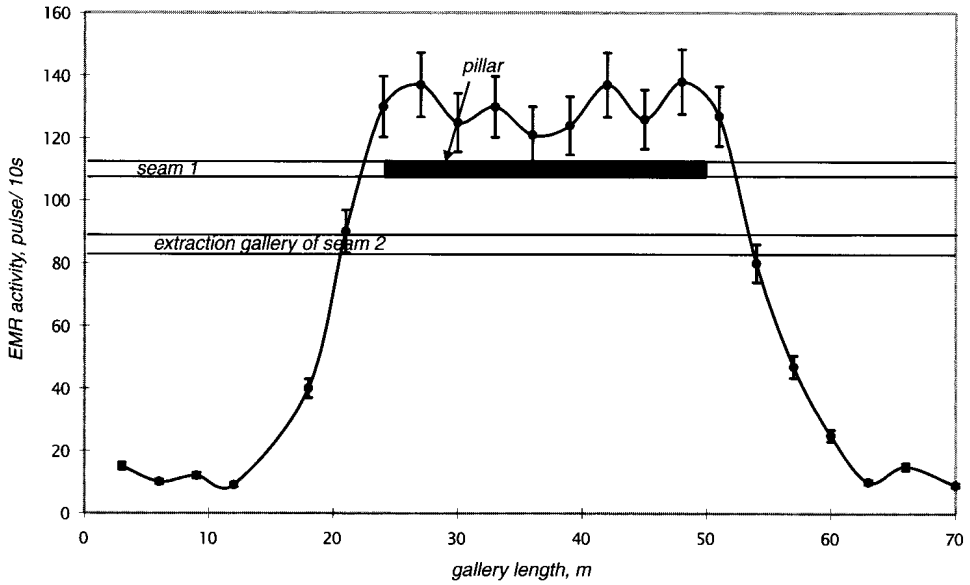

Figure 4
EMR profiling at the zone of pillar influence. The error in EMR activity is of the order of ±7.5%, while in gum value is of the order of ±0.5 l/m.

Figure 1 Results of EM and Gum profiling beneath a pillar (from V. Frid, ref n).

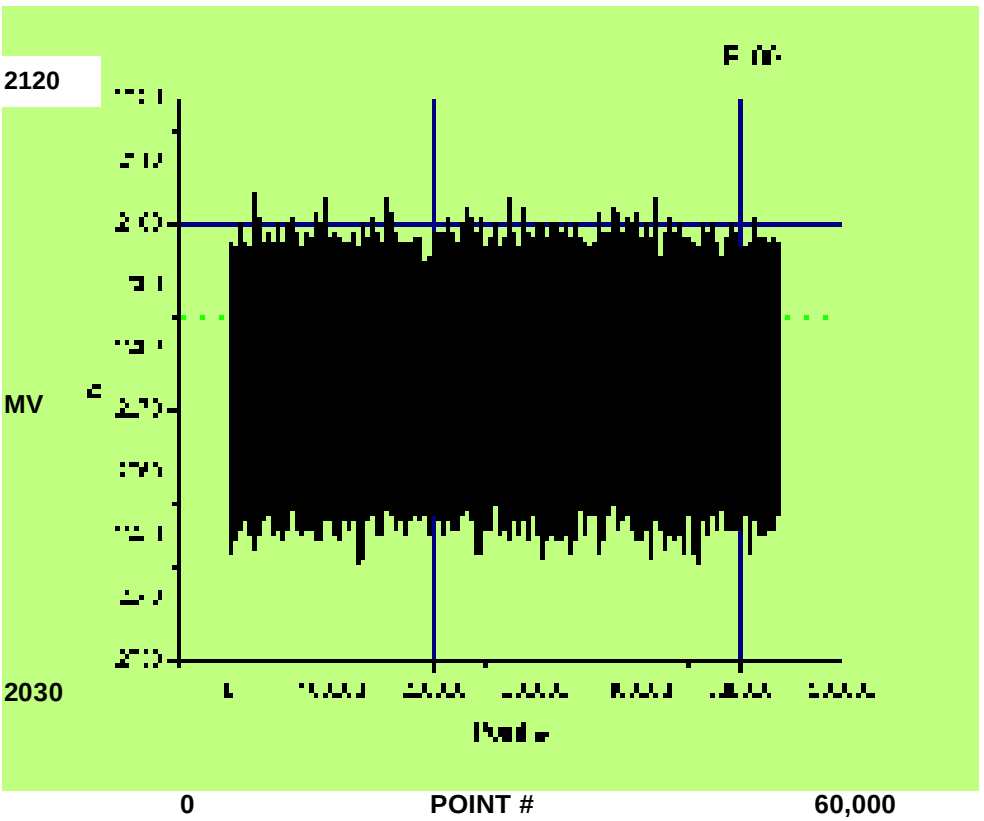

Figure 2 Typical data set acquired at Moonee Colliery. This contains 540,673 data points at 10 microsecond intervals, or 5 seconds of data.

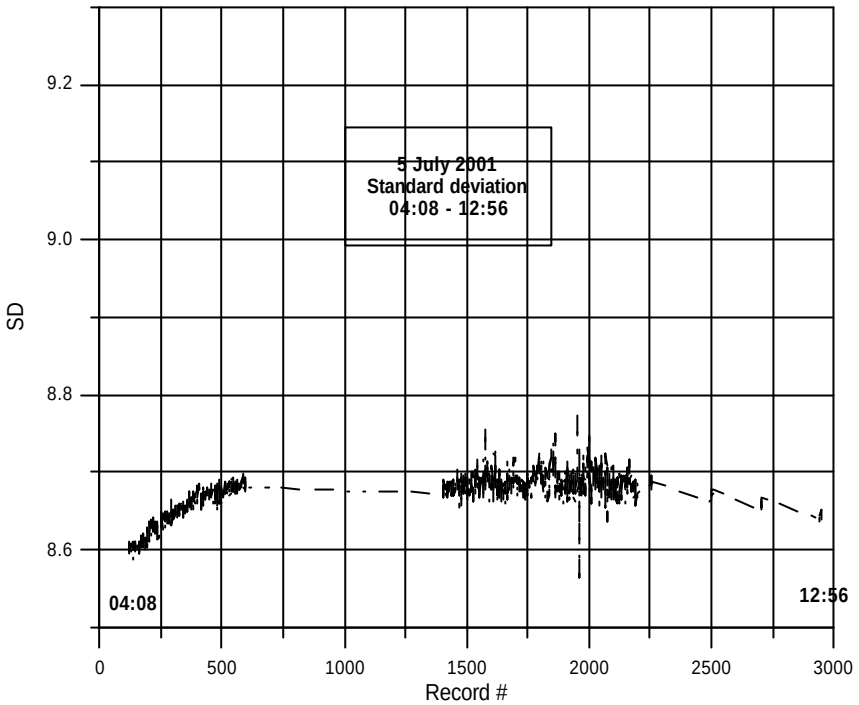

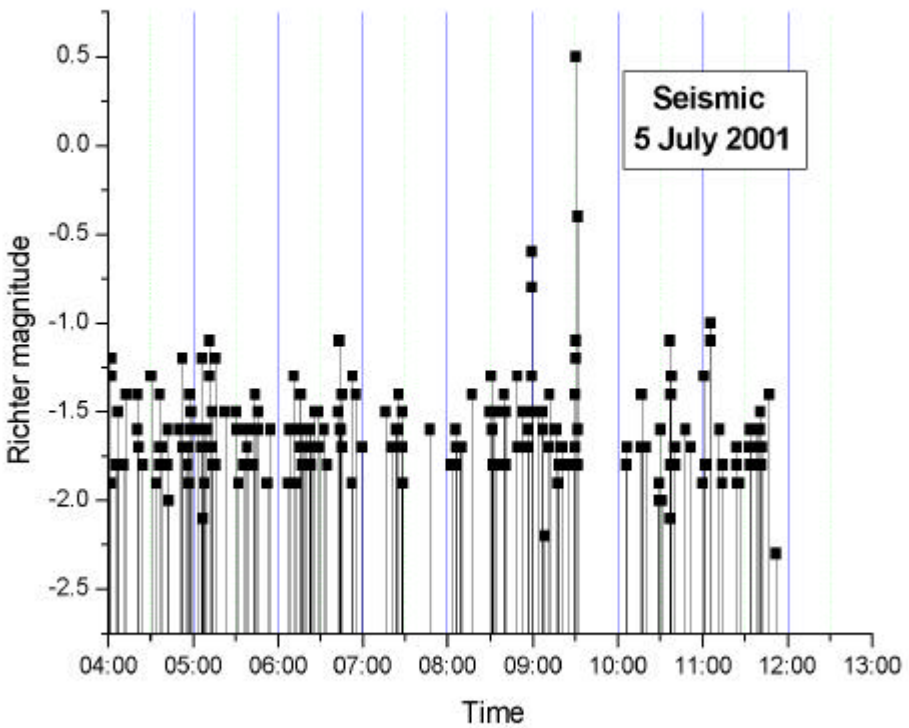

Figure 3 Comparison of standard deviation of the EME data with seismic events at Moonee Colliery on 5 July 2001. Seismic data were kindly provided by Andrew Newland. The time scales are not quite equivalent.

available from BHP Research. Their maximum A/D rate was only 100kHz, half of what was desired but still capable of providing useful data. Two magnetic field sensors — induction coils — were made up with approximately the same sensitivity as those used by Frid, and with passive bandpass filters peaking at 25kHz, for antialiasing and to reject low frequency power noise.

Two serious practical difficulties arose to force changes to the plan. IS approval for the battery power supplies of the PC's was withdrawn, so that it was necessary to operate the equipment in (200kg) flameproof boxes, and the windblast operating regime required that the sensors be bolted to the rib. The system was no longer very mobile. Even more serious was that the system was reduced from two channels to one, as funds were not sufficient for two flameproof boxes.

Systems were installed in the cut-through nearest the working face, at the intersection with the main gate. On average the sensor was ~75m from the centre of the working face. In order to minimise noises from mine machinery an effort was made to record during one of the weekly hydrofracs, which were instituted in order to keep the length of unsupported roof less than 50m. This was achieved in only one of the three data sets.

Eventually three full data sets were acquired, far fewer than desired. They consisted of 2000 to 3000 1MB files of 12 bit binary data, beginning when the system had been put in place and switched on, and continuing until the power supply battery had run down. Each file is approximately 5 seconds long. Once they had been converted to ASCII, each file consisted of 540,600 points. Figure 2 is a typical 5-second file after ASCII conversion.

DATA ANALYSIS

The signal looked very different from what had been anticipated and indicated a signal/noise ratio of only 1.2 or 1.3. That could almost certainly be substantially improved with larger sensors and more pre-amplification. The signals could not be characterised simply by visual inspection. Samples of the data were then plotted and various analyses were carried out. These included peak counts, simple statistics (mean, standard deviation and standard error, range), amplitude distribution plots and spectral analyses. The most useful results were the standard deviations. Of the three full data sets, one showed a very strong response to a fall, beginning earlier than the AE and with more spikes, another showed a weak response and the third showed no detectable response at all. Figure 3 shows the standard deviation and seismic events for the strongest EME event.

CONCLUSIONS & RECOMMENDATIONS

Although the sensor was located ~50m from the falls, at a site selected for convenience, positive results were obtained in one of the three sessions and weak results a second, supporting the initial premise that EME might be used more easily than AE. As well, the EME variations seem to have appeared earlier than the AE. There is therefore, a strong indication that the EM responses could be very useful in giving advance warning of large fracture particularly with more sensors in place.

In spite of the amount of data collected, the number of recording sessions, and the time spent analysing them, was inadequate to permit any more conclusions to be drawn from this hardware/software combination. A much better data acquisition/processing system would be:

- sharply tuned to at least one frequency of 100kHz or higher,
- include five channels, or at least three,
- do the preliminary processing in real time, obviating the need to save large volumes of data for later processing, and
- move with the face.

Such a system has been specified. Cost to build the data acquisition system, exclusive of sensors and software, was estimated to be $40,000.

ACKNOWLEDGMENTS

The work was sponsored by ACARP as project C9005. Indispensable help was provided by Phil Wolfenden of Moonee Colliery, Richard Danell, Ross Gibson and Lawrence Leung of (or formerly of) BHP Research, John Doyle and Andrew Newland of Geosensing Solutions, Nick Pain and Andy Williams of Oceanic Coal, and Michael Creech of Power Coal. We are deeply indebted to these men and their organisations.

REFERENCES AND READING

BAHAT, D., RABINOVITCH, A. & FRID, V. 2001. Fracture characterisation of chalk in uniaxial and triaxial tests by rock mechanics, fractographic and electromagnetic methods. J. Structural Geology, v 23, pp. 1531-1547

BRADY, B.T. & ROWELL, G.A. 1986. Laboratory investigation of the electrodynamics of rock fracture. Nature 321 (6069), pp. 488-492.

CRESS, G.O., BRADY, B.T. & ROWELL, G.A. 1987. Sources of electromagnetic radiation from fracture of rock samples in the laboratory. Geophys. Res. Lett. 14 (4), pp. 331-334.

FRID, V. 1997a. Rockburst hazard forecast by electromagnetic radiation excited by rock fracture. Rock Mech. Rock Eng., 30 (4), pp. 229-236.

FRID, V. 1997b. Electromagnetic radiation method for rock and gas outburst forecast. J. Appl. Geophys. 38, pp. 97-104.

FRID, V. 2000. Electromagnetic radiation method water-infusion control in rockburst-prone strata, J. Appl. Geoph. 43, pp. 5-13.

FRID, V. 2001 Calculation of electromagnetic radiation criterion for rockburst hazard forecast in coal mines. Pure Appl. Geophys. v 158 pp. 931-944.

FRID, V., BAHAT D., GOLDBAUM J. & RABINOVITCH A. 2000. Experimental and theoretical investigation of Electromagnetic radiation induced by rock fracture, Israel Journal of Earth Sciences, 49, pp. 9-19.

FRID, V., RABINOVITCH, A. & BAHAT, D. 1998. Electromagnetic radiation associated with induced triaxial fracture in granite. Phil. Mag. Lett. v 79, pp. 79-86.

GOLDBAUM, J., FRID, V., RABINOVITCH, A. & BAHAT, D. 2001. Electromagnetic Radiation Induced by Percussion Drilling. Int. J. Fract. 23, pp. 1531-1547

HANSON, D.R. & ROWELL, G.A. 1982. Electromagnetic radiation from rock failure. US Bureau of Mines Report of Investigations RI8594. 21p.

HAYAKAWA, M., TOMIZAWA, I. & OHTA, K. 1993. Direction finding of precursory radio emissions associated with earthquakes: a proposal. Phys. Earth Plan. Inter. 77: pp. 127-135.

KHATIASHVILI, N. 1984. The electromagnetic effect accompanying the fracturing of alkaline halide crystals and rocks. Izv. Earth. Physics. V20, pp. 656-661.

KING, C. Y. 1983. Electromagnetic emissions before earthquakes. Nature. V301, p. 377.

NESBITT, A. C. & AUSTIN, B. 1988. The emission and propagation of electromagnetic energy from stressed quartzite rock underground. Tran. Inst. Electr. Eng. 89: pp. 53-56.

RABINOVITCH, A., BAHAT, D. & FRID, V. 1995. Comparison of electromagnetic radiation and acoustic emission in granite fracturing. Int. J. Fracture, 71, pp. 33-41.

RABINOVITCH, A., FRID, V. & BAHAT, D. 1996. Emission of electromagnetic radiation by rock fracturing. Z geol. Wiss., 24 (3/4), pp. 361-368.

RABINOVITCH, A., FRID, V. & BAHAT, D. 1998a. A note on the amplitude-frequency relation of electromagnetic radiation pulses induced by material failure. (Pers. Comm.) 10p.

RABINOVITCH, A., FRID, V. & BAHAT, D. 1998b. Parameterization of electromagnetic radiation pulses obtained by triaxial fracture of granite samples. Phil. Mag. Lett., 77 (5) pp. 289-293.

RABINOVITCH, A., FRID, V. & BAHAT, D. 2001. Gutenberg-Richter type relation for laboratory fracture induced electromagnetic radiation. Physical Review E. (accepted).

RABINOVITCH, A., FRID, V., BAHAT, D. & GOLDBAUM, J. 2000. Fracture area calculation from electromagnetic radiation and its use in chalk failure analysis, Int. J. Rock Mech. Min. Sci. 37, pp. 1149-1154.

Geological hazards — The impact to mining 15-16 November 2001, eds Doyle, Moloney, pp 53-61

Basement controls on regional to minescale structure and sedimentation in the Moranbah Coal Measures: The super model 2000 case study

JOAN ESTERLE, RENATE SLIWA, GUY LEBLANC SMITH & JOEL YAGO

CSIRO Exploration and Mining, PO Box 883, Kenmore, Qld 4069

Regional geological models integrated from mine scale data in the Bowen Basin demonstrate the inter-relationship between structure and sedimentology. In particular they highlight seam splitting, the position of geotechnically massive sandstone bodies and weak flanking strata, faulting and poor ground conditions. The regional distribution of thick coal seam pods, seam splits, and thick sandstone lithofacies is controlled by subtle structural movements in the basement at the time of deposition, as well as differential compaction. Thick (>8m) merged seams stack over areas of stable basement, as interpreted from regional gravity surveys. Marginal to these areas, seams split across structural "hinge zones" and are interspersed with thick sandstone bodies. These were areas of prolonged subsidence throughout the Permian. Localised subsidence due to the differential compaction of the thick pods of peat, however, created accommodation space for thick, amalgamated, sandstone channels in the roof of the thick Goonyella Middle seam. Subsequently, the depositional fabric and the basement structure played a major role in partitioning subsequent deformation within the coal measures. Domains of consistent normal fault and cleat orientations appear to be bounded by the same structural "hinge zones" that controlled the distribution of thick sandstone bodies. During later deformation, the splayed edges of deeper-seated thrust faults tended to deflect around the more competent sandstone bodies. In areas where drilling is too sparse to accurately resolve small scale or laterally intermittent faulting, the association with more laterally continuous sedimentary domains in the interburden can be used to anticipate and investigate likely faulting and ground conditions.

INTRODUCTION

The purpose of a mine site geological model is to transform data into knowledge that can be integrated with engineering knowledge of rock mass behavior to avoid or mitigate hazardous conditions in advance of mining. Structure, stress and the distribution of strong and weak rock are three major factors that impact on ground control. These are inter-related and controlled by the geological history of the coal measures from sediment deposition through subsequent burial and deformation.

Many of the structural features manifested in the coal measures can be tracked back to basement dislocations and their repeated reactivation throughout deposition and deformation; few workers have pursued these relationships due to the difficulties of acquiring and integrating large and disparate regional data sets with mine scale information. The objective of the Super Model 2000 project was to integrate such a dataset and develop predictive models for the interaction of structure, stress and gas distributions within target seams of the Moranbah and German Creek Coal Measures on the western limb of the Bowen Basin in Queensland, Australia (Figure 1).

DATA AND APPROACH

Geological data sets and models across five adjacent leases covering an area of approximately 500km^2 were contributed to the project (Figure 2). More than 10,000 drill holes had been used by company staff to identify, correlate and construct computer models of the major coal seams and their splits across this area, as well as Tertiary incision and infill. The seams were correlated between leases for a common nomenclature and a composite model was generated. Seam structure was determined from this model and supplemented by structural mapping (fault, joint and cleat) conducted in open cut high wall exposures and active underground workings by mine staff and consultants.

A series of mine- and lease-scale studies were

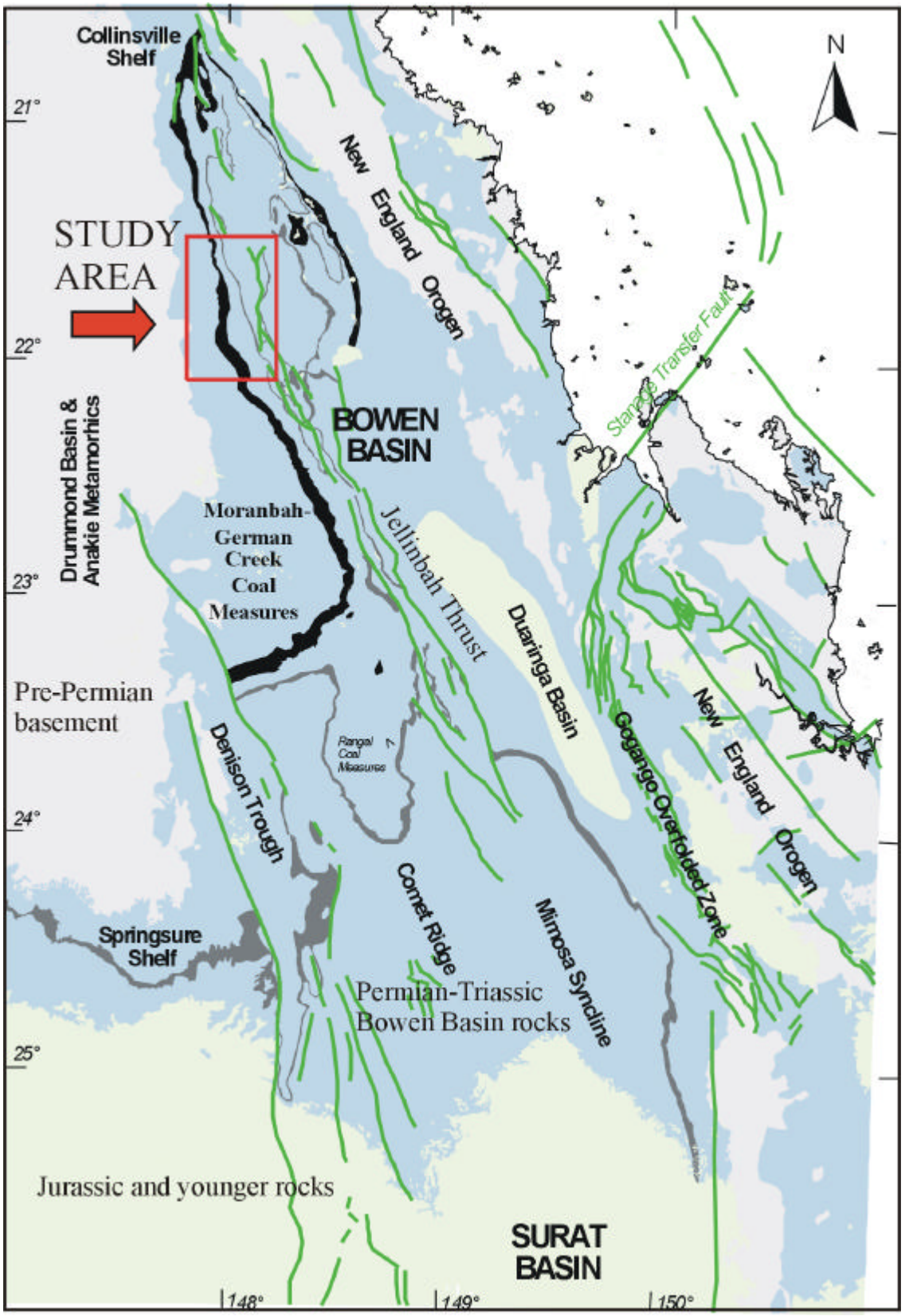

Figure 1 Location map of study area in Bowen Basin, Queensland, Australia showing outcrop (thick black) of Moranbah and German Creek Coal Measures and structural fabric of the basin.

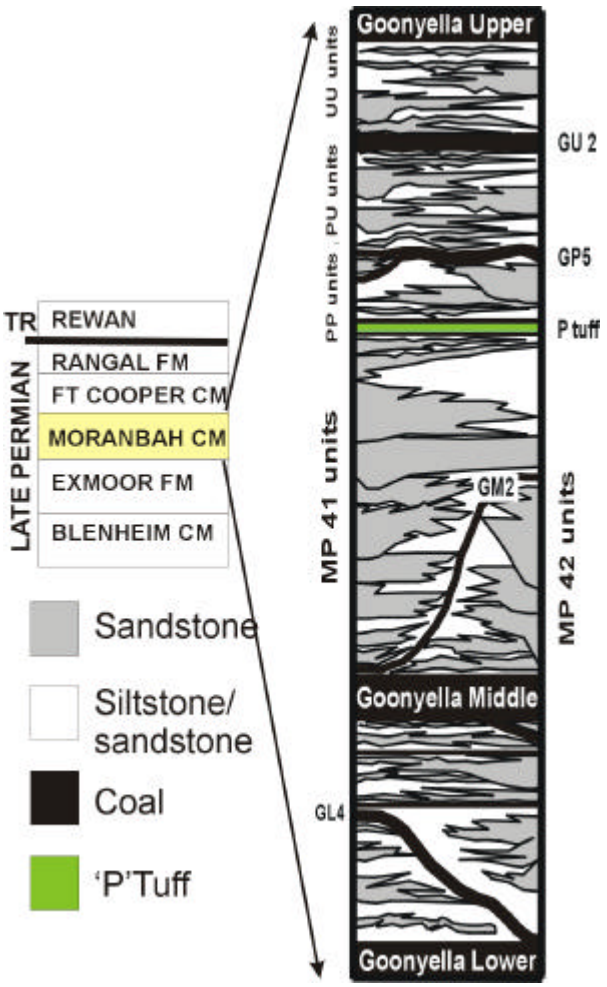

Figure 2 Stratigraphic location of the study interval within the Permian Moranbah Coal Measures.

conducted to characterize the sedimentary units occurring between the Permian age coal seams in the northern tile (Esterle, 1995; Esterle et al, 1999; LeBlanc Smith et al, 1998; 2000; Falkner, 1997). The laterally continuous sandstone units were correlated and coded for input to the existing coal seam model (Figure 2). Finer grained facies marginal to the sandstones were not modelled, nor were the very thin (<1m) and discontinuous sandstones. These facies provide the host or background to the coal seams and sandstones in the model. The geometry of sandstone and coal units was resolved by grid interpolation and contouring.

A 'roof zone' map was constructed for the stratigraphic interval most likely to participate in goafing for the Goonyella Middle seam currently mined by longwall methods in this area. Vertical sequences in sandstone distribution were interpreted from borehole geophysics and qualitatively grouped into one of six zones presented in Table 1, and also in Figure 3 where the zones are contoured. When overlain by interpreted fault systems, the zone map can be used to determine domains of similar roof conditions and potentially hazardous conditions.

Regional gravity data was obtained from the Australian Geological Survey Organisation (AGSO) and, along with interpretations from previous aeromagnetic studies (Bos and Pryer, 2000), used to formulate hypotheses about basement control on seam splitting, sandstone deposition and subsequent deformation.

RESULTS

Regional Patterns

The north-south cross section through the combined model demonstrates: the regional and local variability in coal seam thickness and splitting character, sandstone distribution, deformation in the Permian coal measures, and the levels of Tertiary incision and infill (Figure 4). The section demonstrates the lateral continuity of the main mineable seams, namely the Goonyella Lower (GL), Middle (GM) and Upper (GU) seams, and their associated splits. A broad east-west trending regional anticline dominates the area, with its crest underlying the Goonyella-Riverside lease where the GL and GM seams are thick (>8m) and close (15 to 30m) to one another. To the north and south of the limbs of the antiform, the GL and GM seams split into a series of thinner seams. An isopach map of the GM seam is presented in Figure 5 to show the geographic locality where it and the GL and GU seams are thickest.

In the crest area of the regional anticline the dip of the strata is gentle, around 3° to the east. To the north in North Goonyella and to the south in the Grosvenor area the axis of regional-scale folding swings from an E to a NE strike (see Figure 7). In these "structural hinge" zones the dip of the strata steepens to about 5°. Areas of thick Tertiary incision and infilling with sediments and basalts are associated with these areas.

Local folding occurs with wavelength of 4 to 6km. The departures of roof and floor splits from the GM seam are often associated with the hinges of the folds, as is the thinning of the GM to P Tuff interval. The apparent increase in fold amplitude in the Grosvenor-Moranbah South area is caused by a swing of the fold hinges to the northeast, i.e. they are no longer perpendicular to the section. Outcrop-scale folding and faulting occurs within the individual seams. Distribution of these features is controlled by the larger structures and the interburden makeup of the coal measures.

The thick amalgamated sandstone channel complexes (Zones A and B) in the GM to P Tuff interval tend to occur within broad synforms on the crest of the regional anticline. This is most evident at

Zone	Character	Interpreted facies	Potential impact on roof conditions
A	Very thick (>40m), amalgamated sandstone units without major bedding breaks	Repetitive channel depocentres	Massive roof, weighting
B	Very thick stacked sandstone units, each 15 to 25m thick but separated by 1 to 4m of weak carbonaceous mudstone	Repetitive channel depocentres	Massive roof, weighting, bridging of upper sandstone
C	Thick (15-25m) laminated to interbedded mudstone and siltstone overlain by >5m thick sandstone unit	Floodplain/channel margins	Weak roof overlain by massive roof, bridging
D	Thick (15-25m) single sandstone unit overlain by mudstone	Accessory channels and splays	Variable roof, strong to weak
E	Thin to thick (8-40m) interbedded mudstone and siltstone with minor sandstones <5m thick	Floodplain/lakes	Weak roof, potential faulting pathway, slope steepening or slickensides close to channel margins
F	Thin (<8m) carbonaceous and root-penetrated, slickensided mudstone that contains thin coals	Clastic mire	Weak roof; often overlain by thick channel in next interburden above P Tuff

Table 1 Roof zones occurring between GM and P Tuff.

Goonyella- Riverside and Moranbah North. Above this stratigraphic interval, sandstones are thinner and more wide-spread throughout, up to he GU seam. Sparse drilling above this sequence suggests that another series of thick amalgamated sandstones occurs above the GU seam in this area.

Sandstone Distribution

Although sandstones occur throughout the Permian sequence, the thickest (60m) and most widespread units (2 to 3km wide and more than 25km long) occur in the GM to P Tuff interburden. They are predominant in the area overlying thick GL and GM seams in the Goonyella-Riverside lease (Figure 6). The thick, amalgamated sandstones (Zones A and B) occur in S to SW oriented belts that represent a prolonged depocentre of channelised flow.

Thick sandstones also occur over the Moranbah North lease, but exhibit a different distribution. Here they are oriented west and southwestward, emanating as narrow channels that splay westward and distribute into smaller lobes or channels. Another set of thick sandstones occurs over the Grosvenor lease, but data are too sparse for patterning.

The thick channels taper rapidly into the adjacent fine-grained facies of Zones D to F and minor channels and splays occur in D. To the north of Goonyella-Riverside the GM to P Tuff interval stays consistently thick (30 to 45m), but is dominated by weaker siltstones and mudstones facies with minor sandstone channels. This facies is dominant over North Goonyella, whereas minor channels occur in Ward's Well.

In the south of Goonyella-Riverside, the GM to P Tuff interval undulates and the channel sandstones circumnavigate an "island" of slow deposition and low subsidence where the P Tuff occurs within 10m of the GM seam. The P Tuff actually merges with the GM seam in the southeast of Grosvenor. These islands define the margins of the major channel system and overly areas of stacked channel sequences occurring within the splits of the GL seam.

Structural Elements

Within the Bowen Basin most of the large faults recognized at a regional scale are east over west thrust faults that sole out at depth. The eastern margin of the study area is bordered by the Jellinbah thrust system (Figure 1), which has more than 600m throw and is the westernmost thrust front in the northern part of the

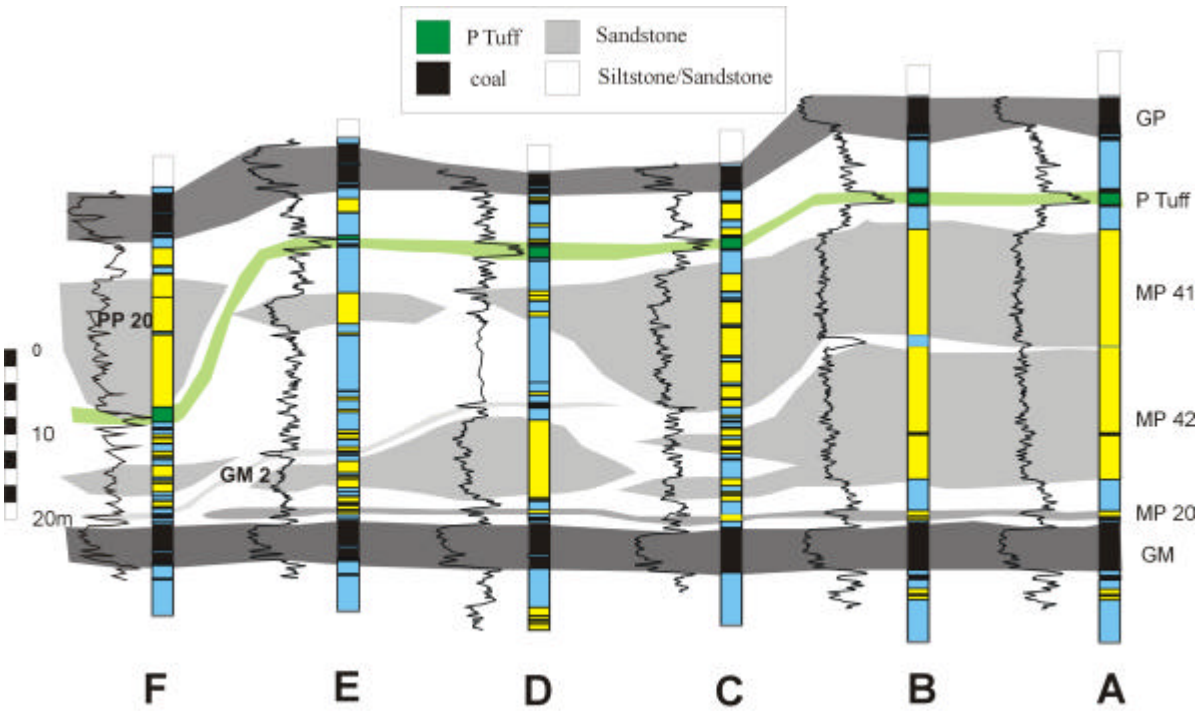

Figure 3 Schematic diagram showing the correlation of modelled sandstone bodies within the GM to P Tuff sequence, and the distribution of sandstones within roof zones.

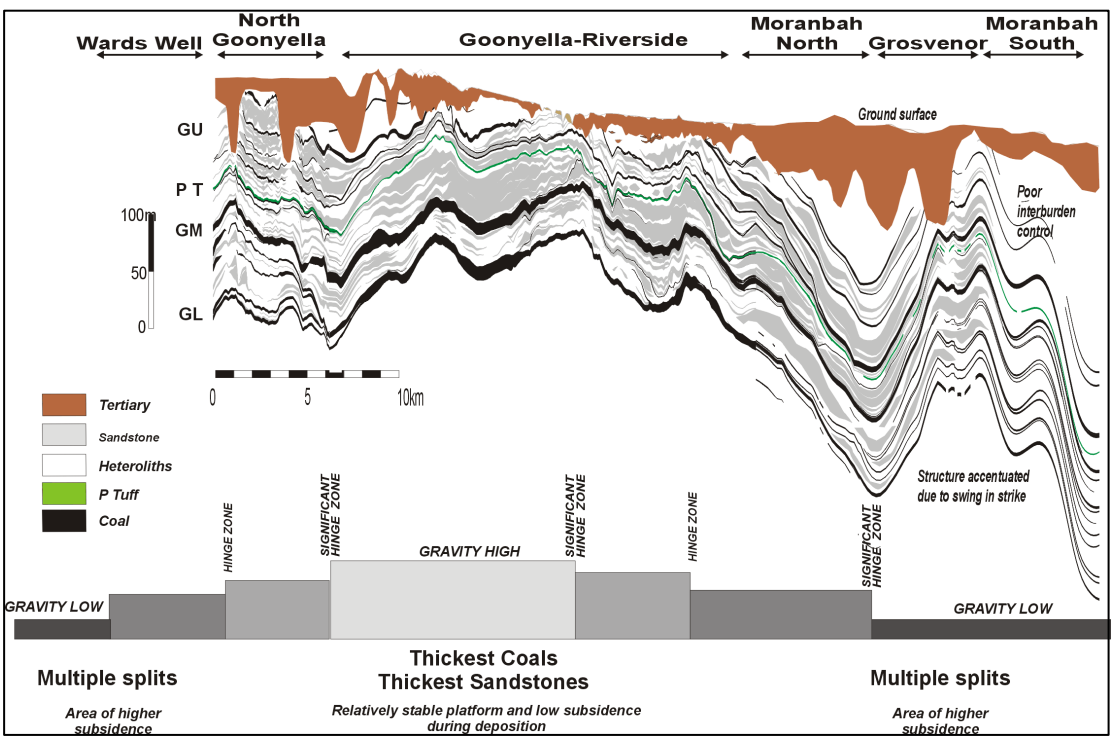

Figure 4 Cross-section through northern tile sedimentary model. Relationship to interpreted gravity signature shown in lower diagram.

basin. Evidence of early sets of normal/transfer fault systems exist and in many cases control the local structural and sedimentary fabric of the Moranbah Coal Measures (MCM).

Faults can be grouped into three general classes, depending on fault type, age and orientation. The largest, and most spectacular structures in the mines are thrust faults related to the Jellinbah fault system. They strike NS, with swings to the NNE or NNW common. Thrust zones are laterally continuous (>10km), but individual faults commonly partition into short en-echelon structures. The faults dip to the east, subparallel to bedding, but propagate up-sequence to the west. Mapping suggests that individual thrusts follow coal seams below the large sandstones and propagate upward in the succession along their margins. During compression, the weaker zones surrounding the more competent sandstones provide pathways for the upward migration of bedding plane shears, thrusting and potential redistribution of stress.

Normal faults occur in distinct sets that trend NE, EW and less commonly NW. They generally have less than 15m throw with a minor strike-slip component and are relatively short. While the NE and NW trending faults form an orthogonal set that is common throughout the Supermodel area, and is interpreted as a reactivation of early Permian extensional faults, the east-west trending faults are more cryptic and are restricted to the structural hinge zones in North Goonyella and Moranbah. Where they are exposed in highwalls normal faults are generally overprinted by reverse movements, suggesting that they formed early in the structural development prior to thrusting.

The third class of structure includes faults that are controlled by a strong NS grain in the basement to the coal measures. This grain is most notable in the regional orientation of the Comet Ridge, Southern Taroom Trough as well as the northern part of the Jellinbah thrust system. Across the whole of the Supermodel area, nearly all faults with >8m throw trend NS. The faults themselves can be thrust or normal faults, depending on the time of reactivation and propagation of the basement structures through the coal measures.

Face cleat in the study area also changes orientation from north to south. In the north it trends WNW, but swings to the WSW in the south (Faraj, 1997). The change in orientation coincides with the crest of the regional antiform, as well as with several mapped dykes and a large sill at the GM seam level. This suggests that the cleat highlights an important structural boundary at this position.

Interpreted Gravity Signature

Patterns observed in the structure and sedimentary sequences were assessed relative to interpreted signatures from gravity data (data courtesy of AGSO). The gravity image resolves the density contrasts in the region that can be interpreted as an estimate of sedimentary cover over crystalline basement. It is suggested that the basement exerted an influence on both the sedimentary and structural fabric in the overlying MCM.

The highest gravity anomaly occurs to the west of the MCM subcrop along the western flank of the study area (Figure 7). It is flanked by an extensive and broad zone of intermediate gravity that strikes NS beneath the North Goonyella to Moranbah North leases. This area coincides with the broad regional anticline observed in the modelled section and also in the structure contours on the GM seam floor overlain on the gravity image. This same area also coincides with the areas of thick and proximal GL and GM seams, suggesting that this area was a relatively stable platform during the deposition of these seams.

Zones of steep gradient in the gravity response are also associated with significant structural flexures where the GM seam shows significant changes in orientation and gradient. These are interpreted as "hinge zones" and are associated with the splitting patterns observed in the GL, GM and GU seams.

DISCUSSION

The Bowen Basin evolved in three phases (Fielding et al, 2000):

1. extension with associated rift volcanics (Early Permian),
2. passive thermal subsidence with associated marine conditions (Late Permian), and
3. foreland thrust loading from the west with associated uplift and continental conditions (Late Permian to Triassic).

Later uplift and associated mild deformation occurred during the Cretaceous, followed by sedimentation and volcanic activity during the Tertiary. The latter formed the extensive basalt flows that cap large portions of the study area (Figure 7). Based on interpretations of aeromagnetic surveys, Bos and Pryer (2000) suggested that the older basement structures controlled the location and nature of younger faults that intersect the Permian sequence. In particular, these later events reactivated various older structures, including the NW/NE extensional faults and the NS trending deep basement structures. They also suggested that a higher density of faulting is related to areas of shallow basement. This study corroborates, but extends this concept to suggest that areas of increased structural complexity occur in the "hinge zones" or areas of transition along basement blocks.

During the deposition of the MCM, major volumes

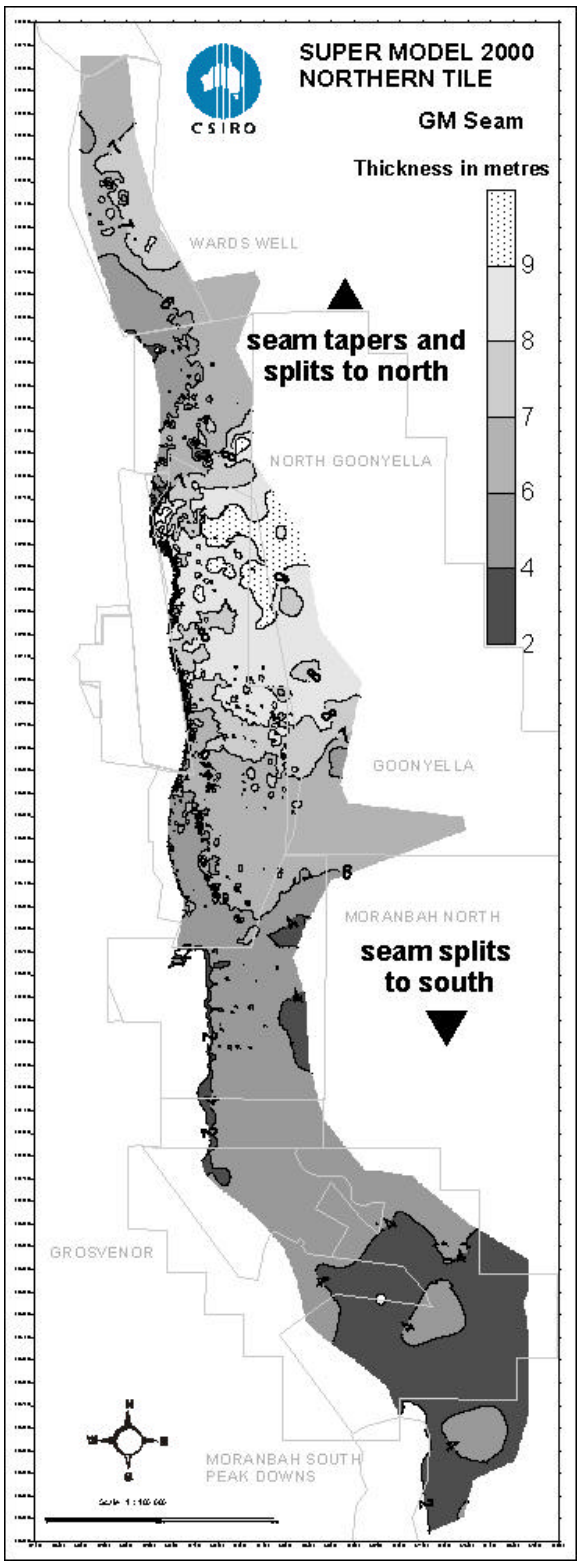

Figure 5 Isopach map of the GM seam within the northern tile study area.

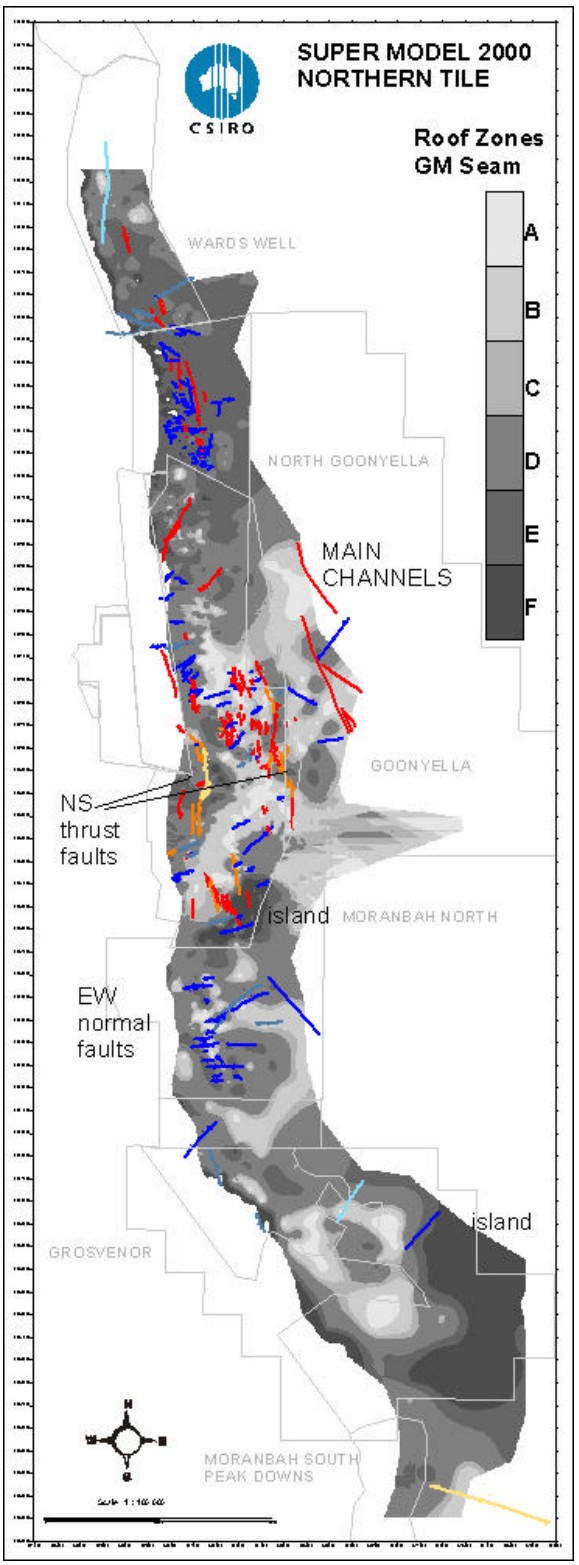

Figure 6 Distribution map of roof zones in the GM to P Tuff interval. Zones described in Table 1 and Figure 3.

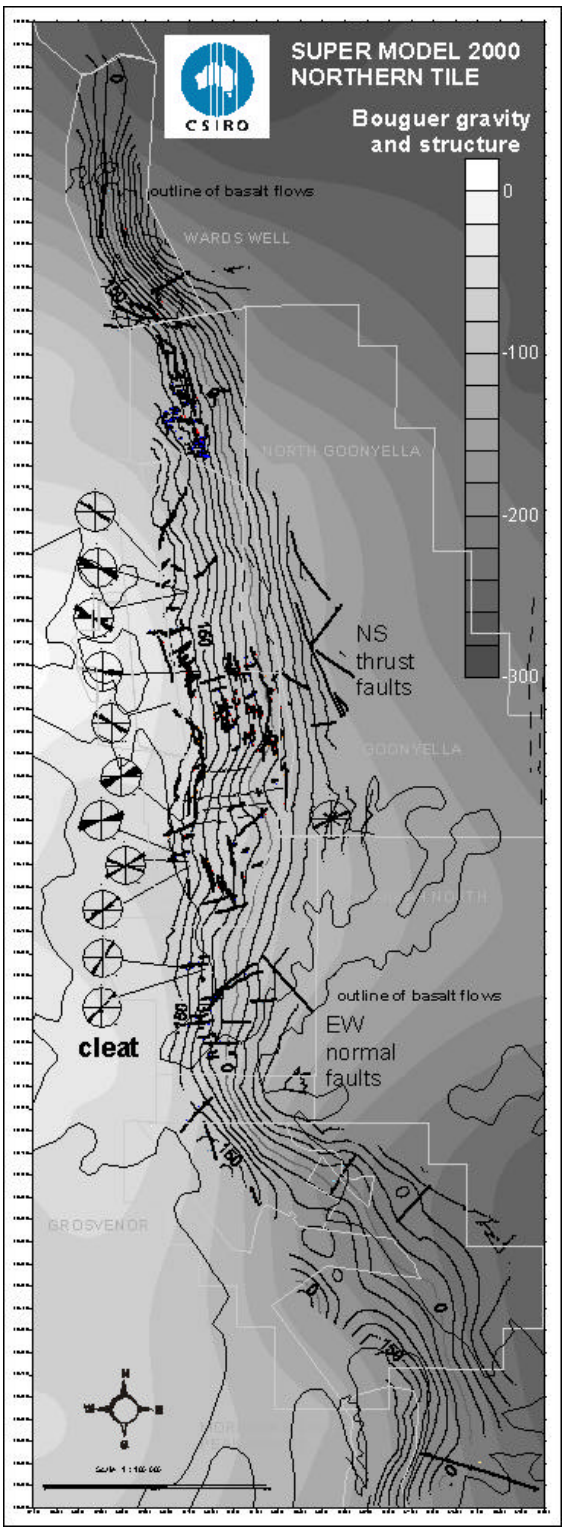

Figure 7 Gravity map overlain by structure contours on the GM seam floor, interpreted and mapped faults, dykes, cleat orientation roses and the outline of Tertiary basalt. Faults are described in the text.

of sediment were supplied from the north and northeast, forming a series of coal-capped alluvial sequences (Fielding et al, 2000). The thickest and merged coal seams occur in an area interpreted as relatively stable during deposition and are flanked bysignificant splitting associated with the structural hinge zones observed in the gravity image. Seam splitting occurs when the site of peat accumulation is inundated by sediment-laden water and, after sediments are deposited, peat mires reoccupy the site. As a result, the sites of maximum peat accumulation are delicately balanced between areas that are topographically "high" and those that are topographically "low", and hence easily inundated. Prolonged and repeated subsidence is interpreted in the areas of the gravity lows, resulting in more complex splitting and interfingering with channel sandstones, particularly in the GL seam. The above scenario is applicable to the GL and GM seam sequence, but a different mechanism may have controlled subsidence for deposition of the very thick, amalgamated channel system that occurs in the roof of the GM seam. Here the few hundred metres of peat and mud (allowing for a 10:1 compaction ratio from peat to coal and 7:1 to mudstone) began to compact relative to the flanking channel sands, creating accommodation for the progressive avulsion of the channel depocentre across the platform (discussed in Michaelson and Henderson, 2000).

Hence, the palaeotopography that controlled the juxtaposition of thick coals and thick sandstones was influenced locally by differential compaction, but in the long term by differential subsidence across these basement blocks. Subsidence would be lower over stable basement blocks, creating the platform for the repeated accumulation of thick peats. Subsidence would be higher, or exhibit sporadic changes in rate on unstable flanks, resulting in vertical stacking of thin coals and thicker sandstones throughout the Permian.

During the Triassic, the Hunter-Bowen Orogeny resulted in a major NE-SW shortening. Although the most significant deformation occurred on the eastern margin of the southern Bowen Basin (in the Gogango Overfolded zone), comparatively smaller thrusts propagated to the west throughout the northern basin. These include the Jellinbah Thrust system that bounds the eastern margin of the study area and many of the smaller (1 to 10m displacements) thrusts mapped within the coal mines. Although there is an association of smaller thrusts propagating through the sequence around the more massive sandstone channels, the deep and large-scale control on these structures suggests that their position is more likely controlled by earlier basement fabric.

During the Cretaceous, large-scale explosive volcanism formed the volcanic plugs and dykes of intermediate composition throughout the northern Bowen Basin. Many of the dykes are oriented either EW or NS, using prefabricated zones of weakness. This extension was followed by gentle compression and uplift of about 1500m during the Late Cretaceous and

was associated with the reactivation of most existing structures and the development of joint systems and coal cleat. During the Tertiary, terrestrial sediments were deposited across the Bowen Basin onto an incised erosional surface. The basement high appears to have remained a stable platform and topographic high, both at the base of the Tertiary and today. The most significant Tertiary incision and basalt infilling occur over the same low gravity flanks where Permian seam splitting is recurrent.

IMPLICATIONS FOR MINING

Integration of the sedimentary and structural models provides a framework in which to explain and predict differences observed in ground conditions at both the regional and the mine scale. Using the "zone map" approach, areas of potentially massive roof can be defined by amalgamated sandstone channel system that occurs above the working seam. The occurrence and severity of weighting that might occur beneath these thick sandstones would depend on their *in-situ* strength and bedding plane character, as well as the design of the chock support system. Monitoring and modelling of face and gate road conditions beneath one of these sandstones suggested that the most significant activity occurred in the transition zone as the channel tapered into weaker rock (Kelly et al, 2001; Weisenfluh and Ferm, 1991). In the Goonyella area, mapping demonstrated that individual thrusts tended to propagate up through the weaker sediments along the flanks of the more massive channels. Hence, severely faulted ground is less likely to occur under the thick, broad sandstones. Faulted ground would tend to exacerbate already weak roof conditions away from these channels. In areas where drilling is too sparse to accurately resolve small scale or laterally intermittent faulting, the association with more laterally continuous sedimentary domains in the interburden can be used to anticipate and investigate likely faulting and ground conditions.

ACKNOWLEDGEMENTS

The authors acknowledge BHP-Billiton Pty. Ltd, Anglo-Coal Pty. Ltd., North Goonyella Mining for access to data and permission to publish. In particular we thank Doug Dunn, Bob Coutts, Andrew Willson, Andrew Laws and Brett Garland. Financial support for the Super Model 2000 project comes from ACARP, BHP-Billiton, MIM-Oaky Creek Mine, Rio Tinto-Kestrel and Santos.

REFERENCES

BOS, F. & PRYER, L. 2000. The application of airborne geophysical surveys to structural interpretations at Moranbah North. *In* Beeston, J.W. ed. *Bowen Basin Symposium 2000 – the New Millennium – Geology*. Geological Society of Australia Inc. Coal Geology Group and the Bowen Basin Geologists Group, Rockhampton, October, 2000, pp. 279-286.

ESTERLE, J.S. 1995. Sedimentological analysis of exploration borehole data: Goonyella Ramp 0 underground: end of Phase I drilling. CSIRO Exploration and Mining Confidential Report 171c.

ESTERLE, J.S., DAMEN, P. & LAWS, A. 1999. Updated Sedimentary Model: Moranbah North Underground Mine. CSIRO Exploration and Mining Confidential Report 638c.

FALKNER, A. 1997. Sedimentological analysis, Wards Well. Falkner Geological Consulting Pty. Ltd. Confidential Report to BHP Coal Pty. Ltd.

FARAJ, B. 1997. Cleat mineralisation, coalification and tectonic history of Late Permian Blackwater Group in ATP 364P, Northern Bowen Basin, Queensland: Implications for coalbed methane exploration. BHP Coal Pty. Ltd. Confidential Report.

FIELDING, C., SLIWA, R., HOLCOMBE, R. & KASSAN, J. 2000. A new palaeogeographic synthesis of the Bowen Basin of Central Queensland. *In* Beeston, J.W. ed. *Bowen Basin Symposium 2000 – the New Millennium – Geology*, pp. 287-302.

KELLY, M., LUO, X. & CRAIG, S. 2001. A study of longwall geomechanics using a range of assessment tools. *Paper submitted to International Journal of Rock Mechanics and Mining Sciences*. In review.

LEBLANC SMITH, G. & ESTERLE, J.S. 1998. Sedimentary and structural geology assessment for potential underground mining sites: Eureka and Goonyella No. 2 areas, Goonyella-Riverside Mine. CSIRO Exploration and Mining Confidential Report 506c.

LEBLANC SMITH, G. & YAGO, J. 2000. Integrated geological model of the North Goonyella Coal Mine, Queensland. CSIRO Exploration and Mining Confidential Report 680c.

MICHAELSON, P. & HENDERSON, R.A. 2000. Facies relationships and cyclicity of high-latitude, Late Permian coal measures, Bowen Basin, Australia. *International Journal of Coal Geology*, **10** (1), pp. 19-48.

WEISENFLUH, G.A. & FERM, J.C., 1991. Roof control in the Fireclay Coal Group, Southeastern Kentucky. *Journal of Coal Quality*, **10** (3), pp. 67-74.

Geological hazards — The impact to mining 15-16 November 2001, eds Doyle, Moloney, pp 63-79

Utilisation of airborne geophysics and satellite imagery in the study of igneous intrusions and their impact on the coal resources in the Rylstone area

N. Z. TADROS

New South Wales Department of Mineral Resources.

The Rylstone area covers 300km^2 near the western edge of the Sydney-Gunnedah Basin (Figure 1). In ascending stratigraphic order, the Permian sequence in the area consists of the marine Shoalhaven Group and the Illawarra Coal Measures; the Triassic sequence consists of the Narrabeen Group. The Narrabeen Group sandstones form a massive plateau in the east incised by the westerly flowing Cudgegong River. The edge of the plateau is commonly characterised by cliffs up to 30m in relief. In the west and south of the area, the plateau gives way to undulating hills and broad valleys. The Illawarra Coal Measures are exposed on the western slopes and form rolling hills in the middle of the area. Much of the central and western areas are covered by Quaternary alluvium and, to a lesser extent, marine rocks of the Shoalhaven Group. The Illawarra Coal Measures contain five potentially mineable seams, of which the Lithgow seam has the highest potential for economic extraction. The area is estimated to contain an inferred in situ coal resource of 1.3 billion tonnes that is potentially amenable to mainly underground mining methods. The coal is suitable for the export and domestic thermal markets (Agnew and Bayly 1989). In the 1970's, Coalex Pty Ltd. and the Joint Coal Board (Shiels & Kirby 1977) independently carried out reconnaissance exploration drilling over the Rylstone area. In the 1980's, the New South Wales Department of Mineral Resources drilled the area extensively. Diatremes and basaltic plugs, caps and flows are abundant in the Rylstone area. Sills are exposed only at a few locations, but numerous intersections have been made in the drilling programs. In contrast, diatremes and basaltic plugs, which constitute barriers to underground mining, have escaped detection in the drilling. Field mapping (Carne 1908; Temby 1983; Bradley et al. 1984) identified numerous diatremes and plugs in outcrop, but many others could not be mapped because of surface cover or difficult access. Therefore, in 1997 the New South Wales Department of Mineral Resources completed a 5500 line-kilometre airborne geophysical survey over the Rylstone area. The survey was aimed at identifying and mapping in detail these igneous intrusions in order to facilitate the assessment of their impact on the coal resources and to provide the basis for the delineation of coal resource blocks suitable for mining.

IGNEOUS INTRUSIONS AND EXTRUSIONS

The Rylstone area was subjected to a high level of igneous activity during the Mesozoic and Tertiary periods. Bradley et al. (1984) positively identified 109 igneous features in the area and inferred 162 features interpreted from aerial photographs where access to outcrops was difficult. They also investigated basalt/dolerite plugs, basalt-free diatremes and an interconnecting system of dykes in Kandos No. 1 and No. 2 underground Collieries to the west of Rylstone area, and suggested that "future coal mining operations in the Rylstone area will encounter minimal problems adjacent to diatremes with no basalt".

However, Kandos Colliery (now closed) is small by modern standards; its annual production averaged less than 80,000 tonnes and mining was by the traditional bord and pillar method. This mining method can usually deal with problems such as those caused by igneous intrusions. In contrast, the coal resources of the Rylstone area are most likely to be amenable to modern longwall mining methods, which require large blocks of coal that are largely free of geological discontinuities/hazards such as structure, igneous intrusions and associated coal quality deterioration problems.

Types of Surface Igneous features in the Rylstone area

Diatremes, basaltic plugs and caps, flows, sills and dykes are the main igneous features in the Rylstone area.

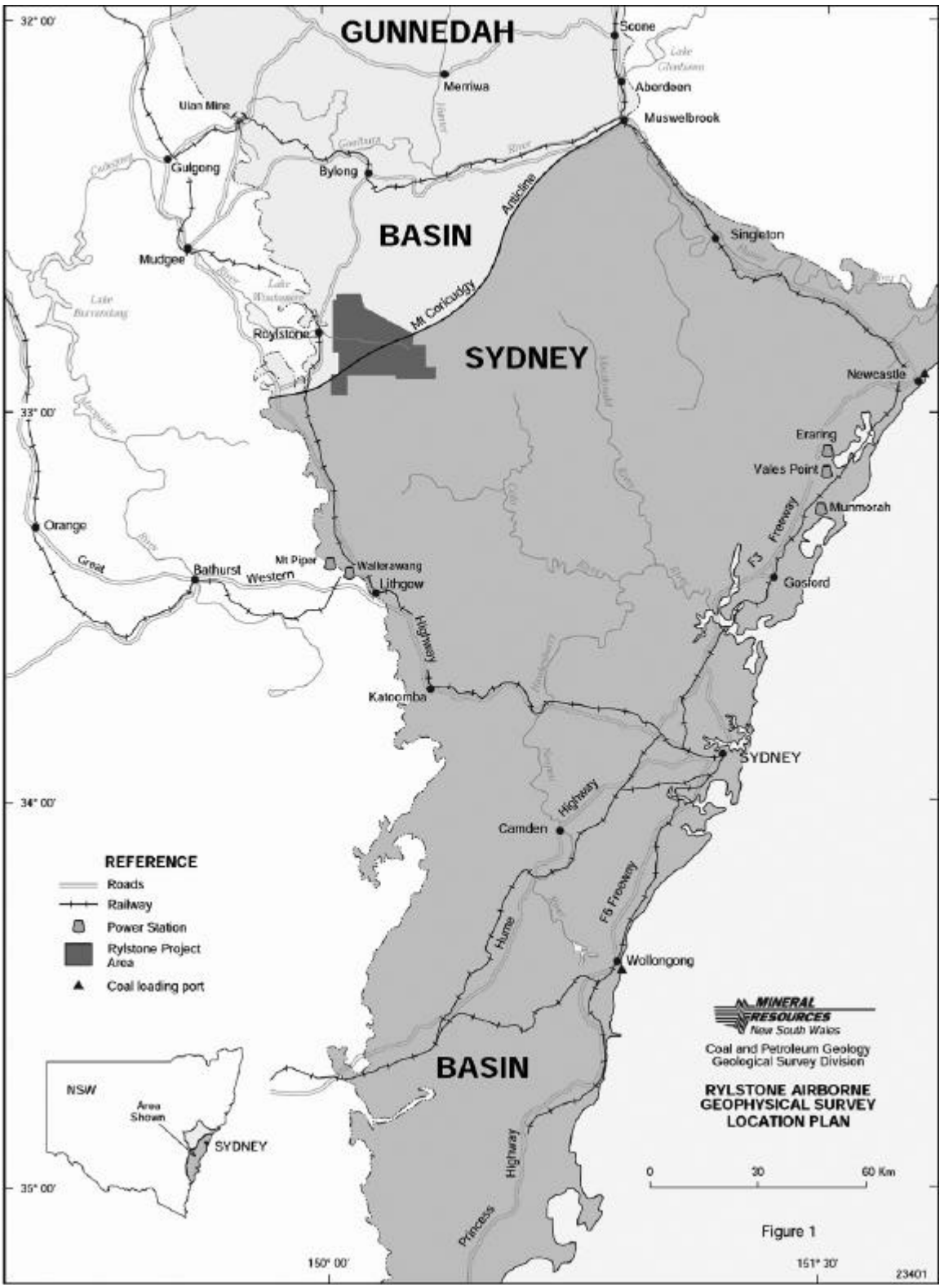

Figure 1 Location of the aeromagnetic and radiometric survey at Rylstone.

Diatremes

Diatremes are volcanic vents formed by explosive action and filled with angular fragments of pyroclastic debris (tuff, lapilli tuff and/or agglomerate), breccia containing blocks that were torn off vent walls (country rock) and rim rock, injected by the action of gas and other fluids. The vent tapers downward to a feeder zone, which usually tapped deep-seated, volatile-rich alkaline melts (Figure 2). The rising melt interacting with groundwater usually causes the explosive activity.

With a few exceptions, diatremes generally form negative topography (Figure 3). Diatremes that have basaltic or doleritic plugs and caps form significantly high hills.

The contact of the diatreme with the country rocks is generally characterised at the surface by a narrow zone of finely laminated ironstone "rim rock" and secondary ironstone replacement and/or silicification. The ironstone consists of fine continuous but kinked, crumbled and contorted layers of haematite or limonite. In many cases, the sandstone adjacent to vents is indurated and silicified and commonly has a silcrete-like appearance (Bradley et al. 1984).

Dips in sandstone up to 50° into some vents and up to 40° away from vents have been measured (Figure 3). In some cases, the sandstone at the contact has a contorted disordered appearance. In many cases the sandstone shows no structural disturbance right up to the breccia rim rock or the basaltic plug (Bradley et al. 1984).

Contact of the diatreme with the country rock shows the effects of very weak thermal alteration (less than 250°C, Crawford et al. 1980). As a result, diatremes have very limited heat effect on the coal seams except where basalt or dolerite had intruded the diatreme and ascended to the seam level or higher (Figure 2).

The two diatremes intersected in Kandos No. 2 Colliery are about 100m by 60m and 80m by 60m across respectively and have no basalt/dolerite plugs. Mining continued to the edge of the two diatremes without roof problems.

Plugs and Caps

Plugs form where basalt or dolerite feeder vents intrude into pre-existing diatremes and fill all or part of the old conduit (Figure 3). Typically, basalt/dolerite plugs taper-off downward from the surface and may have a rim of breccia.

A zone of cindered coal and poor roof conditions possibly 60-80 metres wide could be encountered surrounding basaltic plugs (Figure 2). For example, the two basalt/dolerite plugs encountered in Kandos No. 1 and No. 2 Collieries are 300m by 200m and 200m by 150m across respectively (Bradley et al. 1984). The smaller of the two plugs is rimmed by a 60m to 80m zone of cindered coal. A further example, the "Ovens Vent", one of the largest vents (with a basaltic plug) in the Rylstone area, is less than 100 metres from DM Kelgoola DDH 6. This drill hole intersected undisturbed coal measure sediments, including the Lithgow seam, which is not heat affected.

Bradley et al. (1984), accordingly, postulated that the width of this cindering zone will partly compensate for the downwards tapering of the plug when its surface area is used to estimate the coal sterilised at seam level (Figure 2) i.e. the area of coal sterilised at seam level will be no larger than that of the plug at surface level.

Basalt caps result from the preservation of basalt flows in the depressed area immediately overlying a diatreme and/or in palaeogeographic lows adjacent to diatremes and valley-fill basalt (Figure 3).

Basalt Flows

Although basalt flows have no direct impact on the coal seams, it is important to identify and map these features because of their relationship to their feeder pipes, which penetrate all strata including the coal seams. Large basaltic bodies covering, not only the entire feeder vent or diatreme, but also the surrounding area occur in several places, e.g. Mount Coricudgy flow, which has two feeder plugs. Some of the basalt flows are remnants of a more extensive sheet that is no longer connected to its feeder pipe.

Sills and Dykes

Of the many sills that have been intersected in drill holes, only a few have been mapped in outcrop. The two basaltic plugs and the two breccia vents in Kandos No. 1 and No. 2 Collieries are connected by a dyke system over 1.6 kilometres long and 2m to 20m thick and a branch dyke about 500m long. The dykes did not cause significant mining problems.

Drilling to date has not intersected igneous sills in the Lithgow seam. This is in contrast to the numerous basalt/dolerite sills that have been intersected within the coal measures and other coal seams at higher stratigraphic levels. However, the potential for sill emplacements in the Lithgow seam cannot be excluded. The extent and magnitude of structural disruption, heat effect and cindering of the coal are dependent on the size and thickness of the basaltic sills and their proximity to, and spatial relationship with, the coal seam. Thin sills intruded above or below the seam may cause little or no structural disruption of the coal, whereas, thick sills have domed-up the overlying strata. The extent and magnitude of the heat effect of a sill are generally less severe when it is emplaced above rather than below the seam.

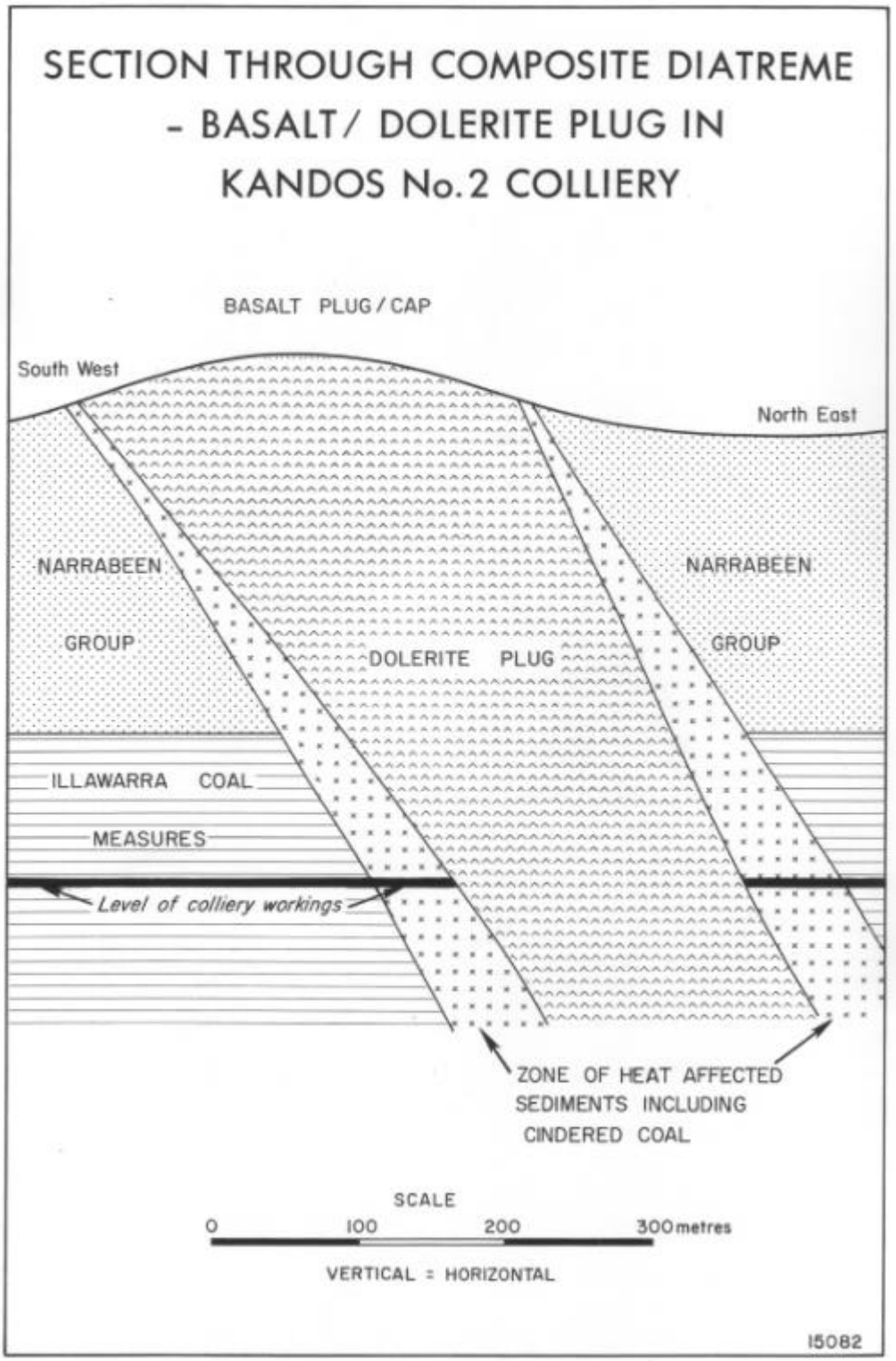

Figure 2 Structure and effect of a basalt/dolerite-intruded diatreme on a coal seam, Kandos No. 2 Colliery. (From Bradley et al. 1984).

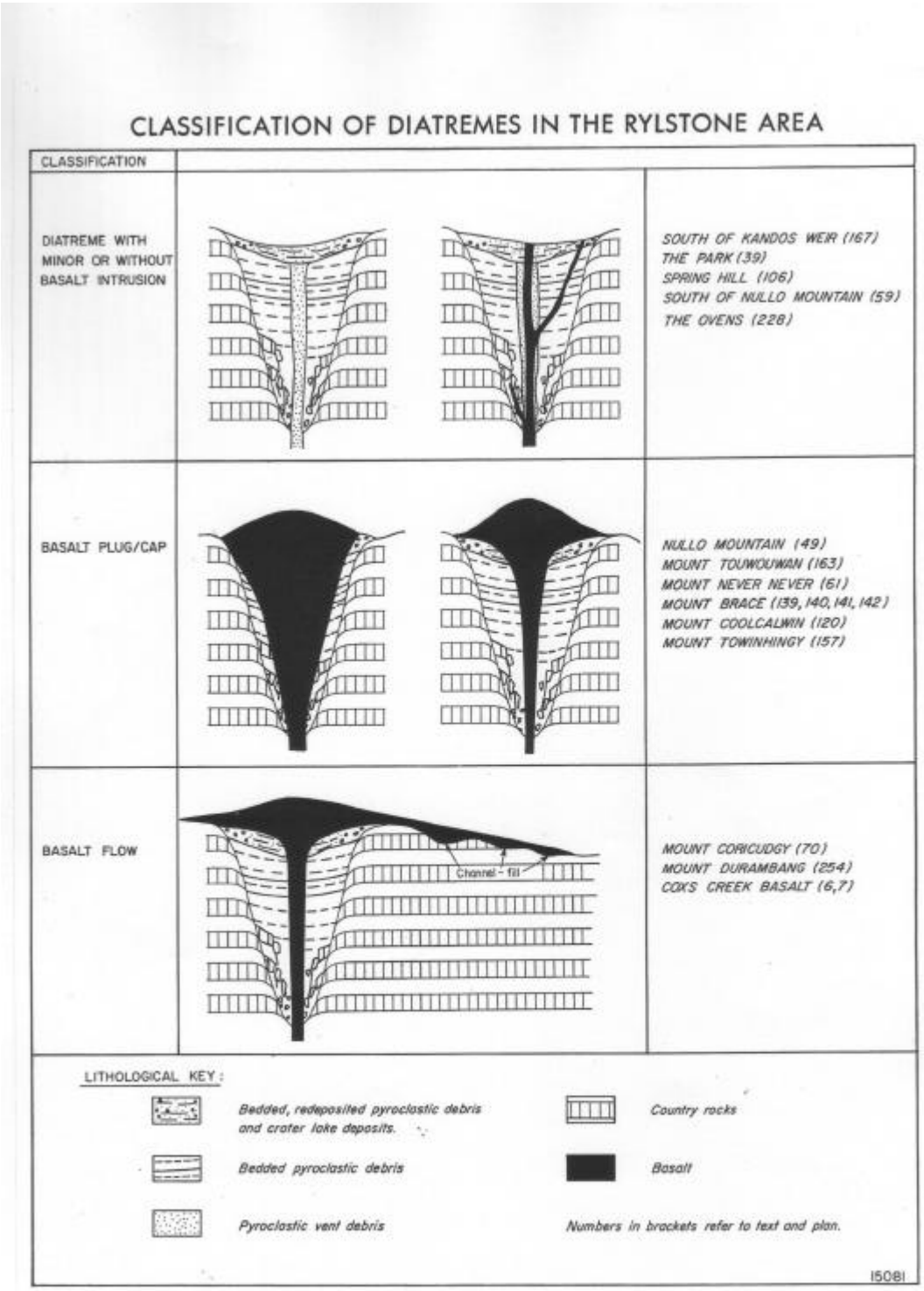

Figure 3 Types of diatremes in Rylstone area. (From Bradley et al. 1984; based on Lorenz 1975).

THE AEROMAGNETIC SURVEY

Difficult access to outcrops or the presence of thick alluvium cover hampered positive field identification of many geological features observed on aerial photographs (Bradley et al. 1984). Means of identifying these features and mapping new ones that were missed out in the early field mapping were canvassed in 1996. An airborne magnetic and radiometric survey was considered most appropriate (Tadros 1999).

The airborne survey was preceded by a ground magnetometer and spectrometer survey carried out along traverses over known outcrops of diatremes, plugs, sills and flows in the area. In addition, magnetic susceptibility measurements were made on core from two drill holes that intersected significant thicknesses of igneous intrusions. The measurements indicated that most types of intrusions contain ferromagnetic minerals and that an airborne magnetic survey would be useful in their detection. However, diatremes with no basaltic intrusive plugs recorded very low magnetic readings.

The spectrometer survey indicated that some diatremes produced gamma-ray values (for Potassium, Thorium and Uranium) well above background and has, thus, confirmed the importance of radiometric surveys in the detection of diatremes without magnetic signature.

The airborne magnetic and radioelement survey was designed to cope with the changes in topography with sharp relief in excess of 300 metres and the small diameter of the intrusive plugs. The survey was "drape-flown" at an altitude of 50 metres using a Squirrel helicopter. Traverses were flown in an east-west direction using an interline spacing of 100 metres. Tie lines were oriented in a north-south direction and spaced 1000 metre apart. Total magnetic intensity (TMI) field values were recorded every 0.1 second or 3-4 metres along the survey lines. A Multi-channel Gamma-Ray Spectrometer with a total crystal volume of 33.6 litres was used to acquire 256 channels of data once per second, or 30–40 metres along the survey lines. The Total Count, K, Th and U element responses were subsequently extracted from the data for analysis and display. Elevation and Terrain-clearance data were recorded using on board GPS and radar altimeter.

Satellite Imagery

Aerial photographs were used in the early 1980's with some success as a preliminary tool in mapping of surface igneous features in the Rylstone area (Bradley et al. 1984).

In this study, satellite imagery was preferred over aerial photographs as a basic tool for the study of the characteristics of surface igneous features and correlation with corresponding magnetic and radiometric anomalies. Satellite imagery consists of digital spectral information that lends itself to computer processing. In addition to topographic information, satellite imagery allows variations in surface composition (vegetation, soil, lithology etc.) to be enhanced and mapped.

A map-accurate geographic colour satellite image with 10m resolution was used. The image is an orthorectified merge of SPOT satellite Panchromatic (Pan) data and Landsat Thematic Mapper (TM) data. "SPOT Pan" is used to sharpen the spectral bands available from the 30m Landsat Thematic Mapper yielding 10m-resolution colour raster imagery. The spectral discrimination of Landsat TM combined with the spatial detail of SPOT Pan is an ideal match. Distortions in the raw imagery are removed through the use of ground control points and digital elevation data. The rectified image shows fine textural variations of the surface, which can be processed to enhance surface geology.

Image analyses of three TM colour band groups (123, 345 and 147) with SPOT Pan have been used to help identify igneous features particularly in the rugged terrain in the eastern part of the area. A merged image of Landsat TM bands 3,4 and 5 and SPOT Pan was used as a base on which filtered magnetic and radiometric images were superimposed to study and analyse the relationship between topography and the magnetic and radiometric anomalies.

RESULTS AND INTERPRETATIONS — MAGNETIC DATA

Foss and Pratt (1997) provided geophysical interpretations and modelling of the magnetic and radiometric data. Tadros (1999) reprocessed the data, provided geological interpretations and assessed the impact of the igneous intrusions on the coal resources in the area.

The airborne magnetic data revealed consistent anomaly character across the whole of the survey area. Anomalies sourced from magnetic intrusions exposed at the surface or at shallow depth with limited depth extent, such as sills, generally produce high gradient strong dipolar responses over the margins of the feature. Magnetic bodies that have greater depth extent and are exposed at or near the surface, such as basaltic plugs, also generally produce dipolar anomaly pattern with lower gradients than those for a shallow sill. Stacked profiles of the TMI data along the flight lines (Figure 4) show high amplitude, sharp gradient anomalies consistent with shallow source, highly magnetic igneous bodies. The broader lower amplitude variations indicate deeper sourced features. The exact source depth of these bodies (the shallow and the deep) within the sedimentary sequence is subject to

interpretation and requires extensive computer modelling (Foss & Pratt 1997). Figure 5 shows anomaly profiles over different magnetic bodies, e.g. a dyke, a thick sill with well defined (abrupt) boundaries and a tapered sill. The signals above the dyke and the thick sill with abrupt termination are sharp and well defined. However, the signal from the tapered sill is subtle and less well defined. This indicates the difficulty in interpreting the exact shape and size of this latter type of sill. The characteristics of the different anomaly types within the survey area are shown on the TMI image (Figure 6).

Image Enhancement of Magnetic Anomalies

The magnetic expression of some basaltic plugs and basalt-intruded diatremes and feeder pipes on the TMI image, in Figure 6, is masked by the magnetic response of shallow to outcropping sills and flows. Background noise can mask the less prominent, low amplitude response of smaller target features. Digital filtering and data enhancement techniques, using ER Mapper (version 5.5) software, have been applied to the data in an effort to reduce the effects of noise and to filter out the responses due to shallow or outcropping igneous sills and flows. Only the highest amplitude, sharp signature characteristic of the boundaries of thick, shallow sills can still be recognised on the filtered image as a "beaded" line marking the outside perimeter of these features, along with characteristic anomaly patterns for the larger intrusive bodies. The resultant application of a suitable filter is displayed in Figure 7. Investigation of a large number of these anomalies in the field has validated this technique. ER Mapper image-processing software was then used to enhance and display the filtered data and to generate line maps of the well-defined filtered anomalies (filtered anomaly map) that represent the diatremes and basaltic plugs. In addition, ER Mapper was used to calculate the cross sectional area of each igneous intrusion and the surrounding zone of heat affected and cindered coal.

Diatremes, Plugs and Cap Rocks

The magnetic anomalies on Figures 6 and 7 vary in size and intensity. Many are discrete and small in areal extent representing plugs and feeders exposed at the surface or at shallow depths. There are several large anomalies representing cap rocks or flows that are possibly remnants of more extensive sheets, which may or may not be connected to their feeder pipes. Several of the more prominent anomalies correlate with topographic highs associated with basaltic plugs and prominent basalt caps (Figure 8). However, some of the magnetic anomalies have no mappable surface geological sources suggesting that they may have been buried under surface cover. Further, mapped diatremes containing brecciated zones and tuffs, without associated basalts or iron oxide rim rock, have no magnetic expression.

Some of the anomalies are marginally offset from their mapped geological source. Foss and Pratt (1997) interpreted this offset as to have been caused either by lateral movement of weathering products on which geological mapping is partially based, or that small near-surface sources may also have north-south misplacements of up to 50 metres if they lie between flightlines. There is also a lateral displacement/offset between the observed TMI and the Reduced To Pole (RTP) calculated response, which provides a crude indication of depth to source.

Sills

Foss and Pratt (1997) interpreted some of the shallow-source magnetic anomalies to have been caused by thin horizontal sheets of high magnetic susceptibility, possibly of basaltic composition. These anomalies usually cover large areas and have a characteristic edge effect on the filtered anomaly image (Figure 7), particularly where they shallow upward towards a subcrop or outcrop zone. Field investigations and drill hole data indicate that these anomalies represent large basaltic sills, some of which may have feeders for which the magnetic expression is masked.

Geophysical modelling could not resolve the depths to, or confidently separate anomalies caused by, deep sills with great accuracy (Foss & Pratt 1997). This is due to the high noise levels produced by extensive near-surface sources. The problem is even greater with thin sills, overlapping thick and thin sills, or shallow and deep sills. Areas containing thin sills in proximity to major sills and plugs may indicate common feeder zones. Very thin magnetic and non-magnetic sills are likely to be present in the area, but could not be detected by the survey. However, integration of magnetic data, drill hole information and computer modelling is likely to produce the most reliable interpretation of the extent and distribution of igneous sills.

Dykes and Joints

The magnetic signal of a dyke is generally well defined (Figure 5). A few clearly identified dykes have been interpreted from the magnetic data. Modelling of several low-amplitude, high-frequency, north-trending, linear magnetic features suggest a shallow source associated with either thin highly magnetised igneous dykes, or magnetic minerals in joint zones. Foss and

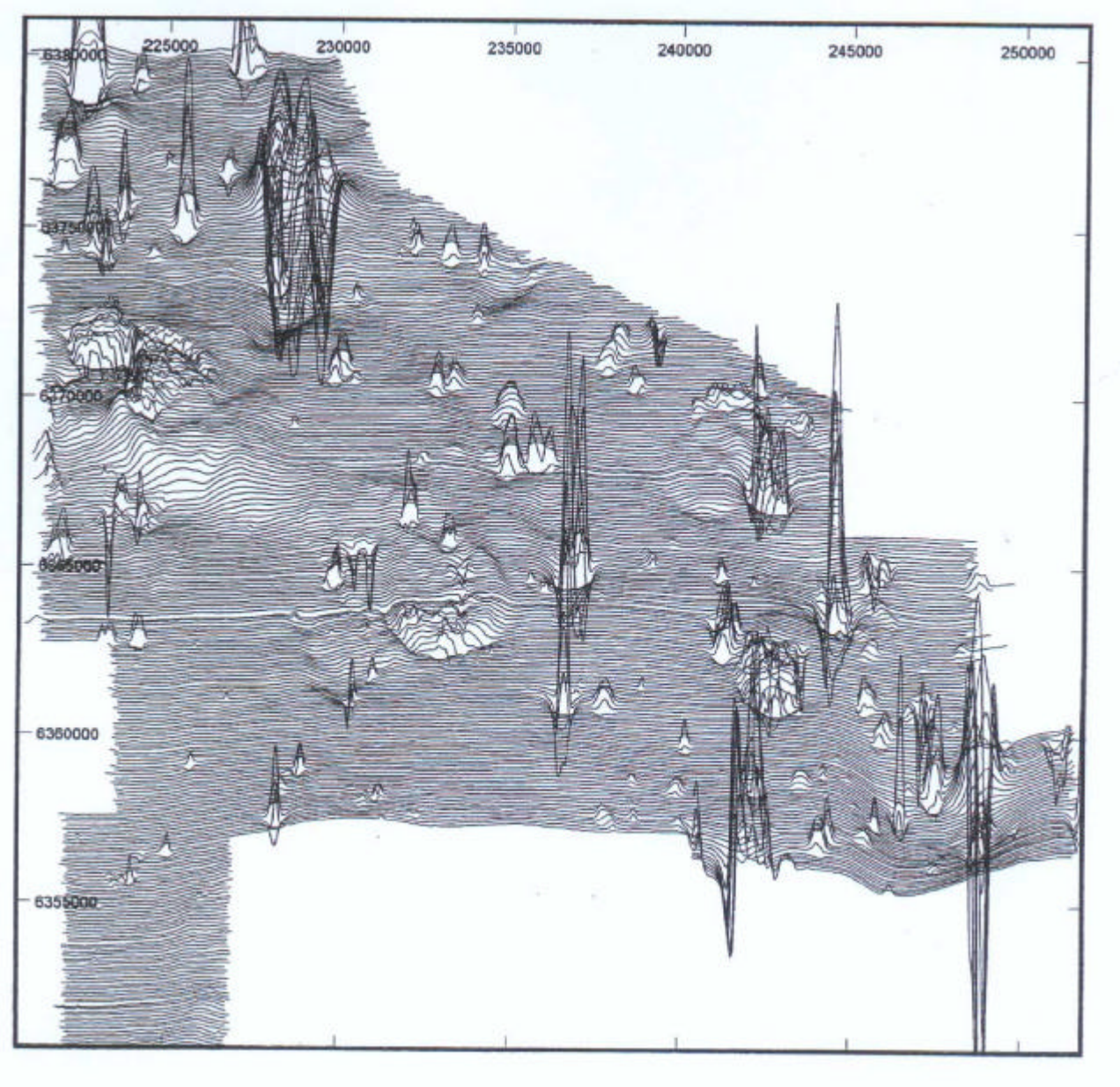

Figure 4 Total magnetic intensity stacked profile measured on the flight lines. (Foss & Pratt 1997).

Pratt (1997) preferred the latter interpretation because of the short strike length of these anomalies. The impact of dykes on the coal is dependent on their thickness, strike length and the hardness of their igneous rocks. Joints have less significant impact on the coal because of the low temperatures involved in the deposition of the iron oxides.

RESULTS AND INTERPRETATIONS - RADIOMETRIC DATA

The highest count on the total (Potassium, Thorium and Uranium) radiometric image occurs over low topography in the west and southwest in areas covered by clay-rich soil and alluvium. The image derived from the potassium channel is generally very similar to the total count because of the high potassium content in the clays, and thus the greatest contribution to the total count. Sandstone ridges over many parts of the project area are associated with low radiometric counts indicating that the sandstones are generally clean, i.e. with little or no clays.

The low count areas contain "islands" of relatively high radiometric counts, some of which have been directly correlated with exposed igneous intrusions. Topographic lows within the generally high sandstone country, such as in confluence areas of gullies and in flat low lying areas, also have high radiometric counts due to increased clay content resulting in difficult correlation with igneous intrusions. Potassium counts are relatively high (above the very low background count for the sandstone) and to a lesser extent thorium counts, over several of the coincident magnetic and topographic highs (basaltic plugs and cap rocks; Figure 8). Further, there is a zonation of high potassium and moderate thorium anomalies over some coincident magnetic and topographic highs (Foss & Pratt 1997). This zonation may be due to igneous differentiation or is a consequence of differentiation by weathering.

Subsequent analysis of the three main components of the radiometric image indicated that some non-magnetic, basalt-free diatremes produce very localised total radiometric counts higher than the surrounding sandstones. The analysis has also indicated that thorium counts were relatively high and thus can be used to map out diatremes that have escaped detection because of their low magnetic signature. Field investigation has subsequently confirmed the relationship between thorium anomalies and basalt-free diatremes. Some of these anomalies are shown on the thorium channel count image (Figure 9).

Similar to the potassium and thorium channels, the highest count on the uranium image also occurs over low topography in the west and southwest except that the image derived from the uranium channel is generally diffused and less predominant over the background. The relationship between the uranium anomalies and the basaltic intrusions and diatremes is not as clear, and consequently not as useful as for the potassium and thorium.

IMPACT OF IGNEOUS INTRUSIONS ON THE COAL RESOURCES

To assess the impact of the igneous intrusions on the coal resources of the Rylstone area, coal resource plans for the potentially mineable seams were superimposed on the filtered magnetic anomaly map using ER Mapper (Figure 10).

The Lithgow seam has the highest mining potential throughout the Rylstone area, with the exception of the northeastern corner. The seam is best developed towards the middle of the area beneath the Wollemi National Park. Drilling results indicate that the coal quality improves as the seam thickens. The resources of the Lithgow seam have been divided into four blocks determined by the thickness and quality parameters of the seam.

The magnetic anomaly map superimposed on the resource plan for the Lithgow seam on Figure 10 shows that the four Resource Blocks of the Lithgow seam are affected to variable degrees by basaltic plugs and diatremes.

The aggregate area affected by all igneous intrusions within the four resource blocks of the Lithgow seam is estimated to be about 21.5km^2, mainly in a working section ranging from 2.0-5.6m in thickness. These intrusions have reduced the in situ resource of the Lithgow seam by about 67.7 million tonnes or 8.4% to approximately 740 million tonnes.

Modern underground longwall mines require large resource blocks free of geological hazards and discontinuities such as igneous intrusions, structure and associated significant coal quality deterioration problems. Igneous intrusions impede longwall mining and, therefore, the mineability of the coal resource in the Rylstone area by this method will depend on the spatial distribution of the intrusions within each of the identified Resource Blocks.

It is evident from Figure 10 that Resource Blocks and associated significant coal quality A and B on the western side of the Wollemi National Park have the best mining potential by longwall methods as the coal is least affected by basaltic plugs and diatremes. Also, the coal seam is present at relatively shallow depths of less than 300 metres.

The potentially mineable section of the Lithgow seam in Resource Block C, although thicker and better in coal quality than in Resource Blocks A and B, is affected by numerous large intrusions and is deeper than 300 metres. However, the area covered by this block is very large and can accommodate two longwall

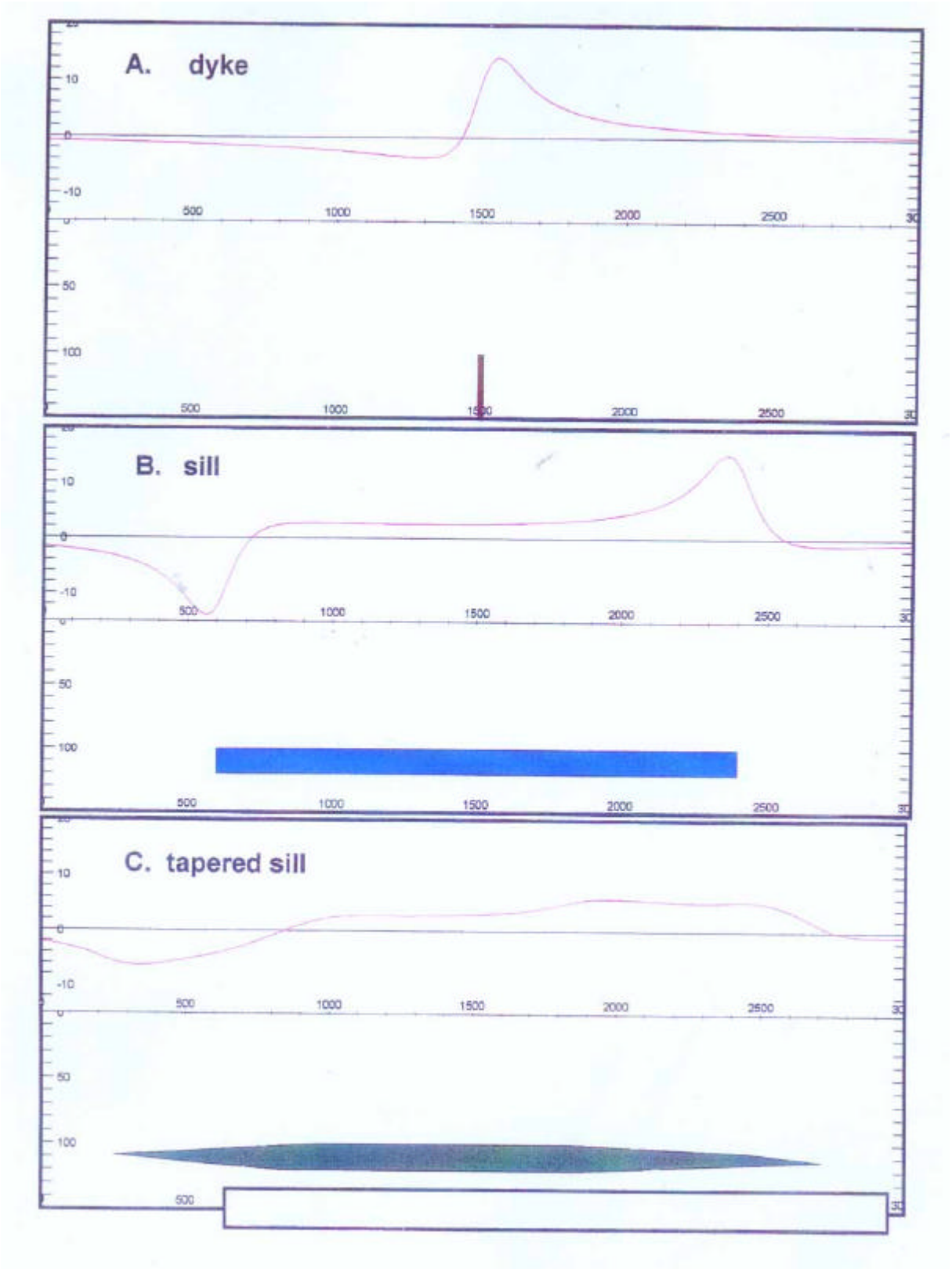

Figure 5 Types of magnetic anomalies sourced from a dyke, a thick sill with well-defined boundary and a tapered sill (Foss & Pratt 1997).

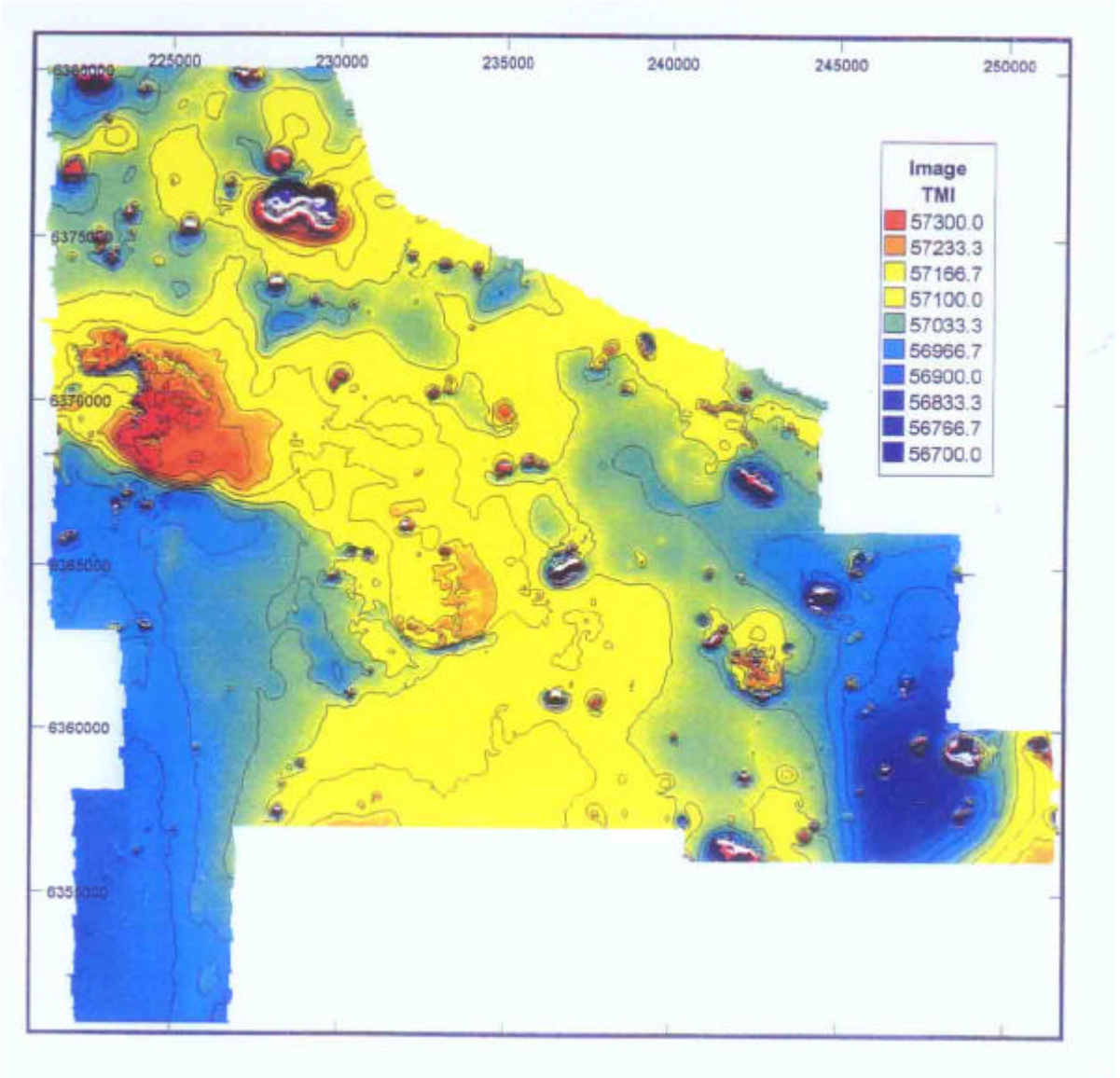

Figure 6 Total magnetic intensity image in Rylstone area (Foss & Pratt 1997).

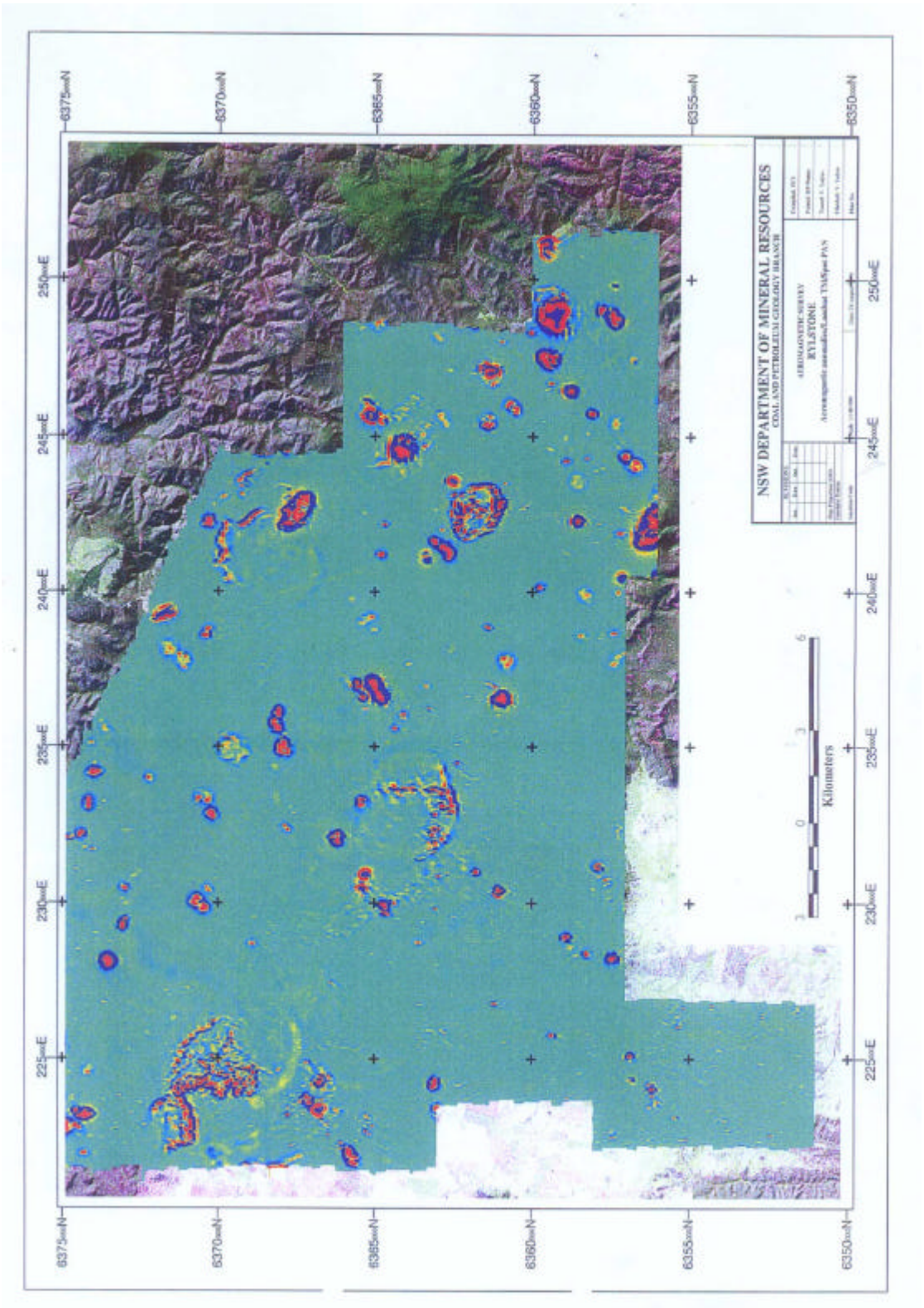

Figure 7 Total magnetic intensity image in Rylstone area (Foss & Pratt 1997).

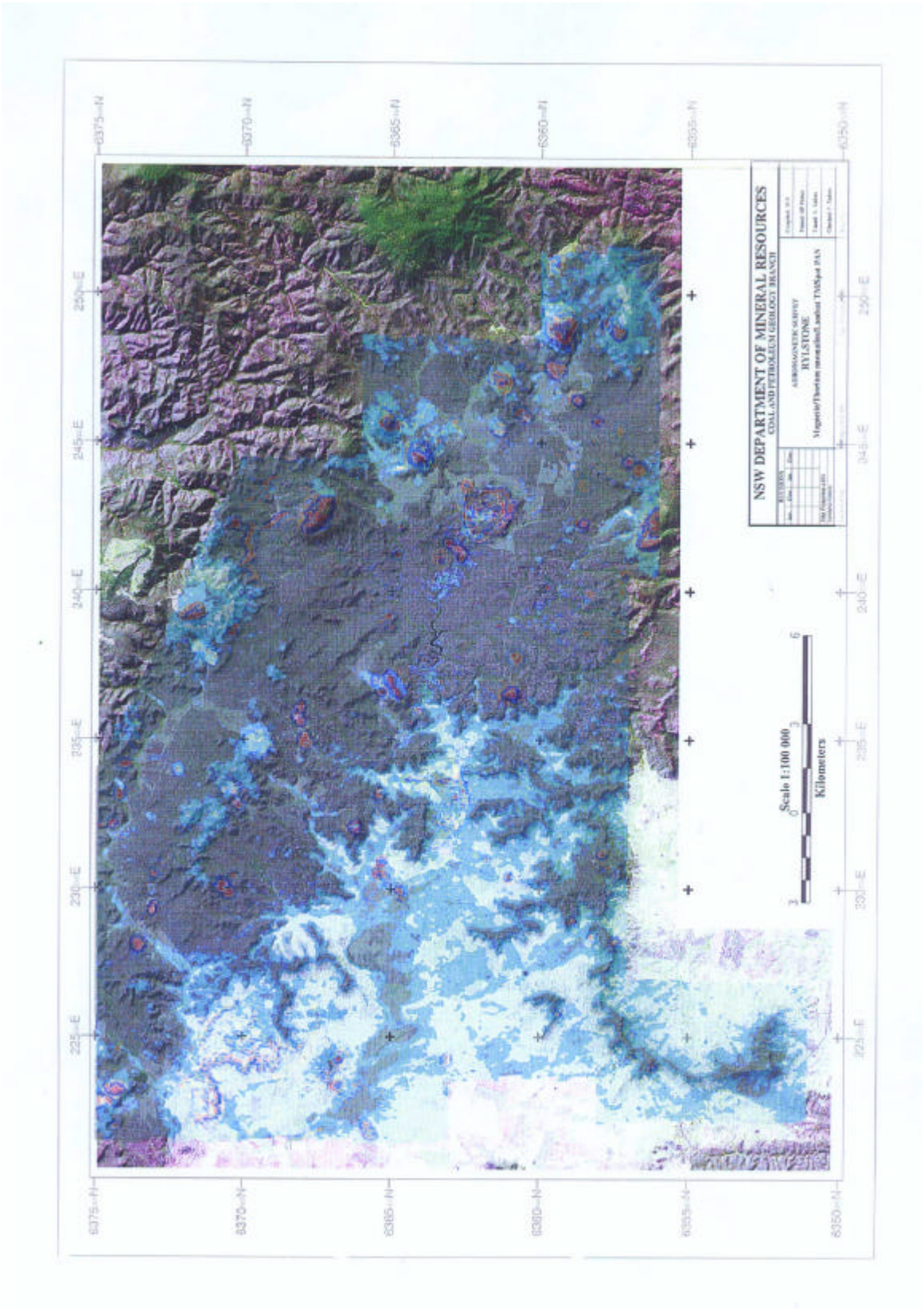

Figure 8 A three-layer composite image – filtered and enhanced magnetic (red) and thorium (pale blue) anomalies superimposed on a merged Landsat TM and SPOT Pan image. (Tadros 1999).

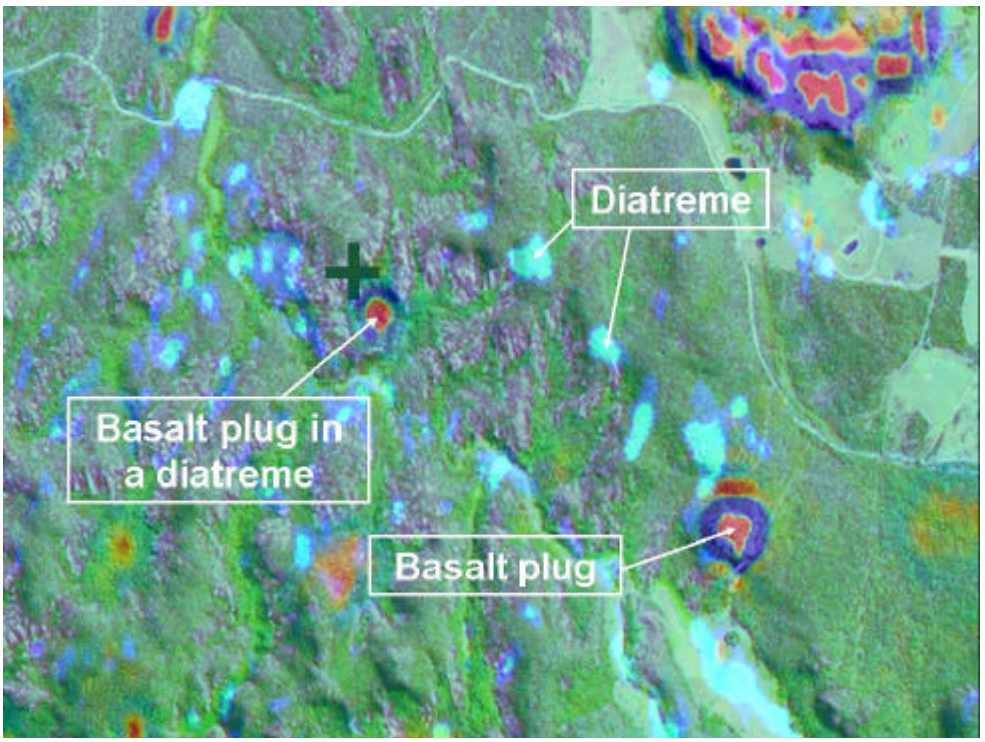

Figure 9a Thorium anomalies (pale blue) over basalt-free diatremes and magnetic anomalies over basaltic plugs.

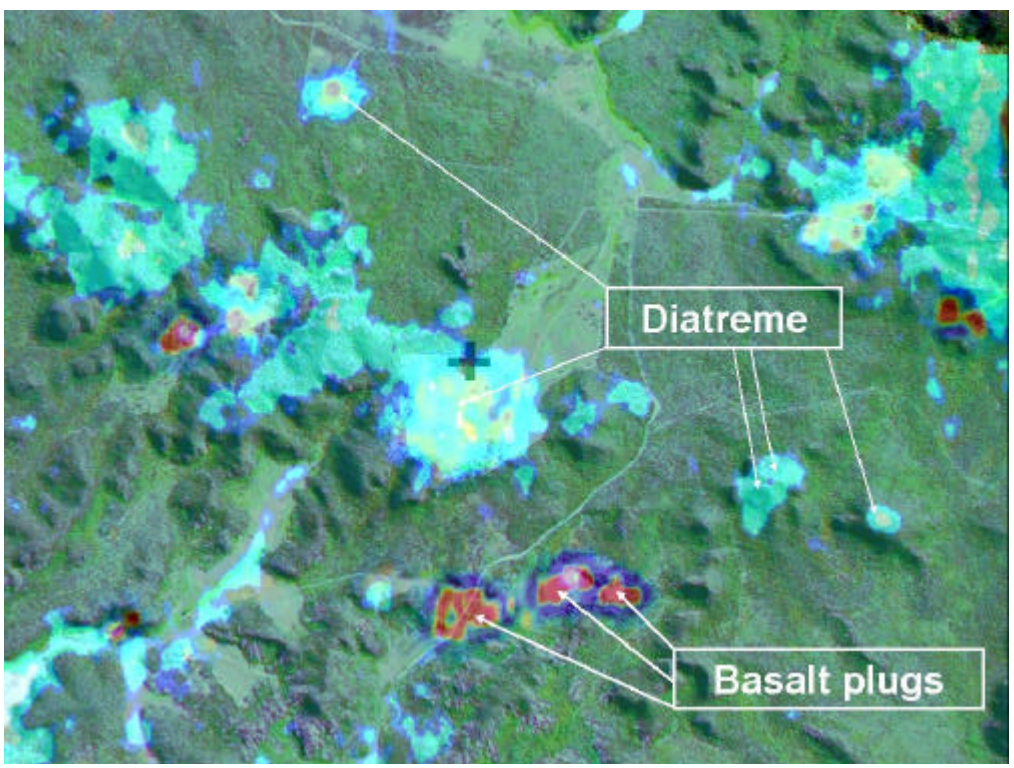

Figure 9b Thorium anomalies (pale blue) over intruded and basalt-free diatremes. The large thorium anomaly in the centre contains a weak magnetic anomaly indicating basalt at depth.

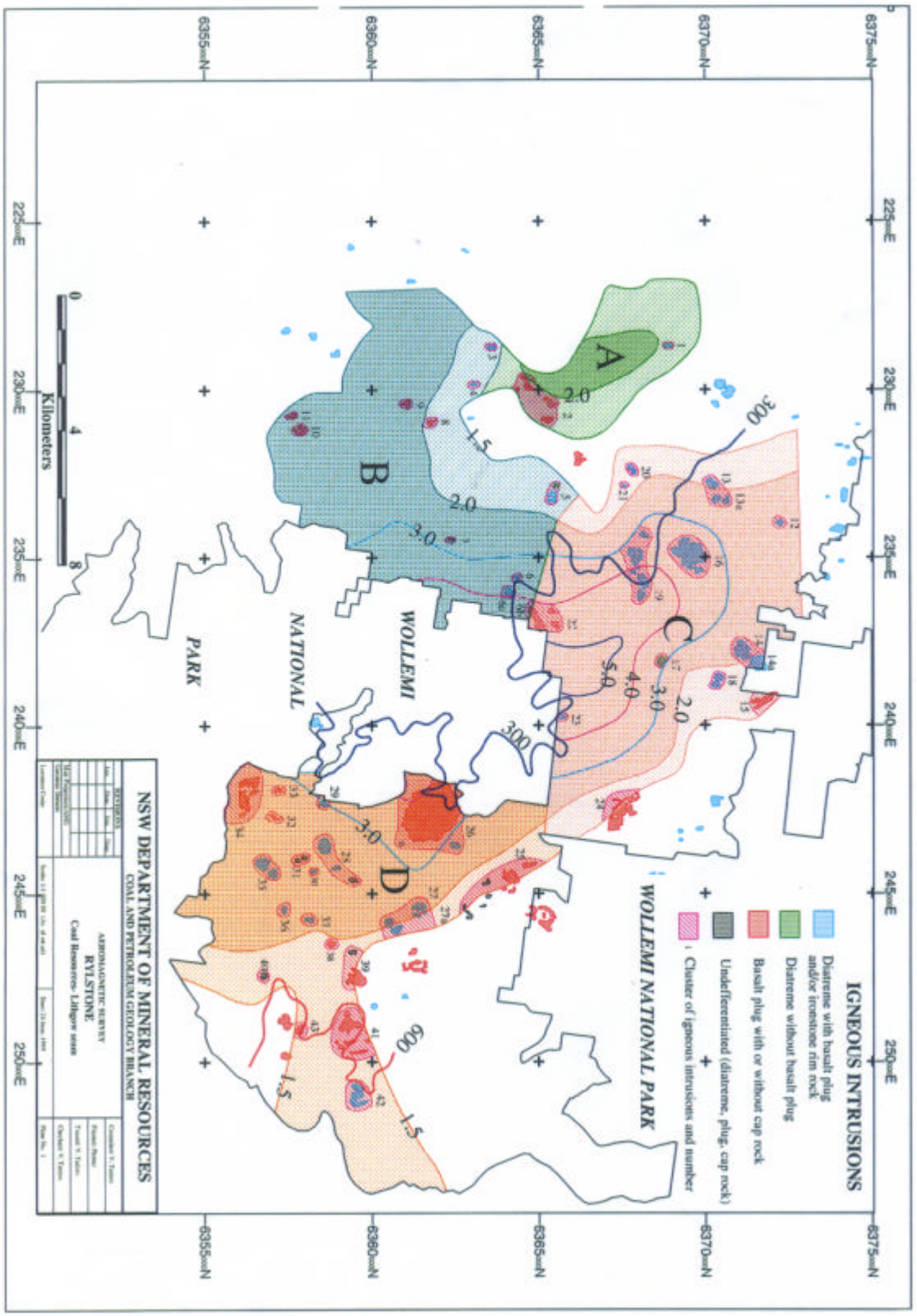

Figure 10 Impact of igneous intrusions (diatremes and plugs) on the coal resources of the Lithgow seam. (Tadros 1999).

mining areas, the largest of which could be up to 8 km long and up to 4km wide.

Resource Block D on the eastern side of the Wollemi National Park has the least longwall mining potential because the coal is disrupted by numerous basaltic plugs, many of which are clustered over large areas. In addition, the Lithgow seam is present at depths ranging from 350m to 700m and the coal quality is only moderate.

However, there are relatively small "pockets" in the shallowest parts in the north and south central areas within this Resource Block, which are free of igneous intrusions and would have potential for extraction by other underground mining techniques such as the mini wall and the Wongawilli methods.

CONCLUSION

Diatremes and basaltic plugs, caps and flows are abundant in the Rylstone area. Drilling to date has not intersected basaltic sills in the Lithgow seam and diatremes have escaped detection in all drilling. An airborne geophysical survey over the Rylstone area was, therefore, carried out to identify these igneous intrusions and assess their impact on the coal resource and its mining potential.

Image analysis of merged Landsat TM and SPOT Pan data have been used to help identify igneous features, particularly in rugged terrain. A selected image was used as a base on which filtered magnetic and radiometric images were superimposed to study the relationship between topography and the magnetic and radiometric anomalies.

ER Mapper was used to filter out the magnetic background noise and anomalies resulting from shallow sills and basalt flows. The residual signal consists of discrete, very sharp, well-defined magnetic anomalies produced by deeply sourced basaltic plugs, feeder pipes and basalt-intruded diatremes. Field investigation validated this technique. ER Mapper was also used to enhance the filtered data and to generate anomaly maps of the diatremes and basaltic plugs and to calculate the cross sectional area of each igneous intrusion and the zone of heat-affected coal.

The survey revealed consistent anomaly character across the survey area. Numerous magnetic anomalies were identified from sources that include basement, sills, dykes, plugs and surface volcanic rocks. Several of the prominent magnetic anomalies correlate with topographic highs associated with plugs and caps and intruded diatremes. Magnetic anomalies that had not previously been mapped have no surface expression because of surface cover. The magnetic expression of feeders is masked by the stronger magnetic anomaly of an overlying thick flow or a sill at or near the surface. The magnetic data confirm the drilling results with regard to areas that contain thick sills in the coal measures.

Mapped features that have no magnetic expression are basalt-free diatremes, some of which produce localised high total radiometric counts. Thorium counts are relatively high and thus have been used to map out diatremes that have escaped detection because of their low magnetic signature.

The magnetic anomaly map superimposed on the resource plan for the Lithgow seam shows that Resource Blocks A and B have the best longwall mining potential because a few basaltic plugs and diatremes affect the coal. The seam in Resource Block C is thicker and better in coal quality, but is affected by numerous large intrusions; however, the area is very large and can accommodate two large longwall mining blocks. Resource Block D has the least longwall mining potential because numerous basaltic plugs disrupt the coal. Small, intrusion-free areas of the Lithgow seam within this resource block may have potential for mining by other methods.

Although the preliminary results of the aeromagnetic survey appeared to have significantly downgraded the coal resource potential of the Rylstone area, the present detailed study has outlined large resource blocks in the Lithgow seam with good potential for mining by longwall methods. This study has demonstrated the use of discriminatory analysis of airborne magnetic data as an effective mine planning tool.

REFERENCES

AGNEW, B. & BAYLY, K. 1989. Report on the Rylstone Stage 3B exploration programme - Authorisation No. 230. New South Wales Department of Mineral Resources - Coal Geology Report 1989-001(unpubl.). New South Wales Geological Survey - Report GS 1989/033 (unpubl.).

BRADLEY, G.M., YOO, E.K. & WEST, P. 1984. Geological mapping of Mesozoic to Tertiary Diatremes and Illawarra Coal Measures east of Rylstone. New South Wales Department of Mineral Resources - Coal Geology Report 1984-037 (unpubl.). New South Wales Geological Survey - Report GS 1984/203 (unpubl.).

CARNE, J.E. 908. Geology and mineral resources of the Western Coalfields. Geological Survey of New South Wales, Memoir 6.

CRAWFORD, E.A., HERBERT, C., TAYLOR, G., HELBY, R. MORGAN, R., & FERGUSON, J. 1980. Diatremes of the Sydney Basin. In a Guide to the Sydney Basin. New South Wales Geological Survey - Bulletin 26, pp. 294-323.

FOSS, C.A. & PRATT, D.A. 1997. Rylstone airborne geophysical survey interpretation report for Coal and Petroleum Geology Branch NSW Department of Mineral

Resources. Encom Technology Pty Limited (unpublished).

LORENZ, V. 1975. Formation of phreatomagmatic maar-diatreme volcanoes and its relevance to kimberlite diatremes. pp. 17-27. In Aherns L.H., eds. Physics and chemistry of the earth. Vol. 9. Pergamon Press, Oxford and New York.

SHIELS, O.J. & KIRBY, B.C. 1977. Geological report on the Joint Drilling Program, Ulan Area. Joint Coal Board Report LR 77/1 (unpublished).

TEMBY, P.A. 1983. Report on EL 1943 (Olinda), EL 1944 (Nullo Mountain) and EL 1945 (Coricudgy), NSW for the six months ending 13th April and 12th October, 1983. CRA Exploration Pty Ltd (unpublished).

TADROS, N.Z. 1999. Utilisation of airborne geophysics in the assessment of the impact of igneous intrusions on the coal resources of the Rylstone area. New South Wales Geological Survey - Report GS 1999/665 (unpubl.).

Geological hazards — The impact to mining 15-16 November 2001, eds Doyle, Moloney, pp 81-88

Mineralogical Analysis in Hazard Assessment

COLIN R. WARD

School of Geology, University of New South Wales

Although long regarded as a tool for mineral identification in a qualitative or at best semi-quantitative sense, X-ray diffraction has recently benefited from developments in computer-based processing that allow its use as a quantitative tool for evaluation of mineral percentages. A particular example is the interactive computer-based SIROQUANT technique, which provides quantitative XRD analysis of powdered rock samples. This technique has been extensively tested on a range of geological materials associated with coal mining, including but not restricted to the minerals in the coal itself, and found to give results consistent with other indicators, such as independent chemical and petrographic data.

The availability of such techniques allows the relationships to be investigated more thoroughly between mineral percentages and other rock or coal properties, including those related to both mining hazards and difficulties with coal quality. Recent studies suggest, for example, that the total percentage of clay minerals indicated by SIROQUANT, and not only the well-known swelling clays such as montmorillonite, has a direct relationship to the slaking characteristics of the materials and to the moisture content. These results have implications in evaluating the long-term stability of rock strata and spoil piles for a range of surface and underground mining operations. The nature and relative proportions of the clay minerals can also affect different types of materials handling activities.

Other studies have shown that the total percentage of quartz, feldspar, clays and carbonates in sandstones and other materials, determined by SIROQUANT, can be related to the potential of the rocks to ignite methane in mine atmospheres by frictional processes. The concentration of particular trace elements in coal can also be related to the proportions of specific minerals in the coals concerned. Such data have significant applications to coal marketing and use, and to the release of elements in leachates from mine waters, stockpiles or refuse emplacements. Other mineralogical hazards include silicosis risk associated with the quartz content of coals and adjacent strata, marketing and utilisation problems associated with particular minerals in mine products, and the impedance of gas drainage from coal seams by epigenetic mineral impregnations.

INTRODUCTION

Many types of geological hazards associated with coal mining are based on, or can be related to, the relative proportions of different minerals in either the coal itself or the non-coal rocks within and around the coal seam. Such hazards include adverse mechanical behaviour of non-coal strata, frictional ignition of methane in mine atmospheres, the inclusion of toxic constituents in mine dusts, and the release of environmentally significant trace elements from stockpiles and refuse emplacements. There are also a number of mineral-related issues that may affect the preparation and quality of the coal product, including the sulphur and phosphorus content, the reaction of dispersive clays in water, and the development of abrasion, slagging or fouling in combustion processes.

A number of these hazards can be identified, predicted, and perhaps ameliorated, based on comprehensive mineralogical analysis of the coal or rock materials in question. To be effective, however, the data from the mineralogical analysis must be provided in a reliable quantitative form. Only with quantitative data can mineralogy be related to other properties of the rock or coal in question, also quantitatively assessed, such as the material's chemical, physical and geotechnical characteristics.

METHODS FOR QUANTITATIVE MINERALOGICAL ANALYSIS

Mineralogical analysis is concerned with determining the nature and, ideally, the relative proportions of the different minerals in a rock, coal or similar material. It differs from chemical analysis, which involves determining the relative proportions of chemical elements. It also differs from petrographic analysis, in which proportions of constituents with visibly different appearance are evaluated, including

components such as rock fragments and matrix in sandstones and macerals in coal samples.

Identification of the minerals in a rock, such as the roof or floor of a coal seam, or even the coal itself, may not be an easy task. A number of different techniques have been developed over the years to identify the minerals in rocks, especially fine-grained materials such as coal, shale and similar strata. The principal methods are based on either observation under the microscope or crystallographic studies through X-ray diffraction techniques.

Optical and Electron Microscopy

Point counting using optical microscopy of thin or polished sections may be useful in quantitative mineralogical studies, but is really only appropriate if the minerals in question are large enough to be seen under the microscope, and if the minerals can be identified on the basis of their optical properties. In many cases the minerals are too fine grained to be adequately identified, or intimately mixed with other components in a way that prevents their separate recognition (e.g. the minerals in the rock fragments or the matrix of sandstones). Many minerals, such as the carbonates or the clay minerals, cannot be readily identified from their optical properties alone. While providing useful information on the form in which minerals occur, such as differentiating rock fragments and matrix constituents in sandstones, optical microscopy of coals or other rocks inherently provides a petrographic rather than a true mineralogical analysis of the material in question.

Electron microscopy provides a greater level of magnification than optical methods, and has the additional capacity to determine the chemical constitution of individual components through accessory X-ray fluorescence analysis of the particles concerned. This capacity can be combined with point-count methods to determine the percentages of different minerals in a rock, coal or ore sample through computer-controlled electron microscopy, including the sophisticated QEM*SEM system (Creelman and Ward, 1996). Such techniques are costly, however, and mineral identification in many cases is still uncertain. Being point-count based methods, they also have the same limitations as other microscope techniques in differentiating minerals intimately admixed with other components, and in the general level of precision associated with the mineral percentage determinations.

Quantitative X-ray Diffraction Techniques

The most definitive basis for mineralogical analysis is X-ray diffraction (XRD), which distinguishes minerals from each other on the basis of their atomic or crystal structure rather than optical properties or chemical composition. This is particularly important for components such as clay minerals, which are difficult to identify by any other means.

X-ray diffraction has long been recognised as an almost unequivocal basis for (qualitative) mineral identification. However, it has suffered from limitations in determining mineral proportions (i.e. as a tool for quantitative analysis) due to factors such as the inherent variability of some crystal structures, preferred orientation effects, and the absorption of X-rays by other minerals in the mixture. Several methods have been developed to counteract some of these effects, but their application is cumbersome and limited to only a small number of minerals in a mixture.

The use of XRD as a quantitative tool has been considerably enhanced in recent years following development of purpose-specific computer processing systems such as the CSIRO-developed SIROQUANT technique (Taylor, 1991). Based on principles developed by Rietveld (1969), these allow diffraction patterns of individual minerals to be systematically adjusted and combined to match the observed XRD profile of the sample under analysis, evaluating in the process the percentages of the different crystalline minerals present.

Operation of SIROQUANT involves generation of a synthetic X-ray diffractogram from the diffraction data of the individual minerals identified in the mixture, and adjusting that pattern interactively, through refinement of key parameters, to match the observed diffractogram of the sample under investigation (Ward et al., 1999b). Up to 25 different minerals can be incorporated in the analysis. Allowance is made in the process for factors such as crystal lattice variations, preferred orientation, and differential absorption of diffracted X-rays by other minerals in the mixture. Because of its ease of operation and the wide range of minerals that can be incorporated, the technique represents a considerable advance on older empirical methods, based on measurement of key peak heights on the diffractogram in relation to peak heights from a known mass of added spiking material. These could only evaluate a very limited number of minerals, and required a complex series of associated calibration experiments.

The validity of the mineral percentages provided by X-ray diffraction and SIROQUANT has been tested for a range of rocks, including coal, against independent information derived from chemical analysis and in some cases petrographic data (Ward et al., 1999a, b; 2001b). The (theoretical) chemical composition of the mineral mixture indicated by SIROQUANT, for example, is usually very close to the (actual) chemical composition of the same material as determined by direct chemical analysis. Where appropriate comparisons can be made, such as with sandstones, the

SIROQUANT results are also compatible with, though not necessarily equivalent to, those obtained from petrographic (point count) data.

USE OF MINERALOGICAL DATA IN HAZARD ASSESSMENT

As indicated above, a number of different hazards related to the mineralogy of rocks, and even the minerals in the coal itself, may occur in coal mining, especially with underground operations. These include hazards associated with the mining process, such as rock strength and slaking behaviour, generation of quartz-rich dusts, and ignition of methane by frictional effects. However, they also include hazards related to the quality of the coal product, which may be very significant to mine profitability. Product-related hazards include the impact of dispersive clays on coal preparation and handling, leaching of toxic elements from stockpiles and refuse emplacements, abrasion by quartz in grinding and combustion, and unfavourable behaviour of particular minerals (e.g. slagging and fouling) in different utilisation processes.

Some aspects that have been investigated in recent years at the University of New South Wales are discussed briefly below, in order to indicate the role that can be played by mineralogical studies in geological hazard assessment. These are not necessarily exhaustive, and additional applications will probably be identified as quantitative mineralogical analysis becomes more widely used in the coal industry.

Breakdown of Coal Mine Rocks in Water

The breakdown of rocks by interaction with water is a significant problem in the stability of roof, floor and overburden strata, with impacts on both underground and open-cut operations. It is also, however, a problem in coal handling (stickiness), coal preparation (dispersion) and refuse disposal. Slaking behaviour is usually attributed to the presence of clay minerals such as montmorillonite, which may take water molecules into their crystal structure and expand their lattice in the process to give them considerable swelling properties.

X-ray diffraction analysis, including detailed study of the clay minerals through artificially swelling and collapsing their crystal lattice, has long been used to identify rocks with significant proportions of swelling clays and to indicate potential problems of this type. Montmorillonite, a member of the smectite group, is not the only mineral involved; a range of interstratified illite/smectite (I/S) minerals may also be present in Australian coal measure strata, with similar but perhaps less intense swelling characteristics.

Quantitative studies using SIROQUANT suggest, at least from preliminary studies, that the total proportion of clay minerals in the rock is significant in determining slaking behaviour, as well as if not instead of the nature of the clay minerals themselves. Figure 1, for example, shows the relation of quartz plus feldspar in a series of coal measure mudstones to the relative resistance to slaking in laboratory tests. The slaking test used is based on the Emerson crumb test (Emerson 1967), and involves immersion of small pieces of the rock under test in water. Rocks are categorised from 1 (total breakdown) to 8 (no reaction), with intermediate stages involving slaking, cracking and swelling behaviour under the water immersion.

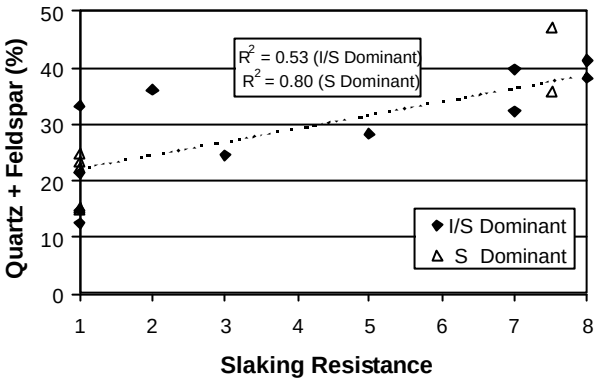

Figure 1 Correlation between percentage of quartz plus feldspar, as determined by SIROQUANT, and a laboratory slaking index for mudrocks from an Australian coal mine.

Quartz and feldspar in these rocks occur as non-reactive particles forming the structural framework of the grain fabric. Carbonates and other components are absent from the rocks tested, and hence in this instance the clay minerals make up the remainder of the material present. A low proportion of quartz plus feldspar therefore implies a high proportion of clay minerals, a fact again borne out by the SIROQUANT analysis data.

Rocks with a low proportion of quartz plus feldspar, and therefore a high clay content, have a lower resistance to slaking (i.e. a lower reaction index in the immersion test) than rocks from the same unit with higher quartz plus feldspar percentages. The same relationship seems to apply in this instance whether the expandable-lattice clay mineral is mainly smectite (S) or interstratified illite/smectite (I/S).

The moisture content of the rocks tested is inversely related to the proportion of quartz plus feldspar minerals, and hence directly related to the total clay content. In this case, however, the nature of the expandable clay does seem to play a significant role. Figure 2 shows that samples rich in smectite have higher proportions of moisture, for equivalent

percentages of quartz plus feldspar, than those in which illite/smectite is the dominant expandable-lattice clay mineral. This feature probably reflects the greater capacity of the smectite minerals to absorb and retain water in their crystal lattice. Prediction of slaking from moisture content alone may therefore be difficult unless complementary mineralogical data are obtained to establish the fundamental relationships involved.

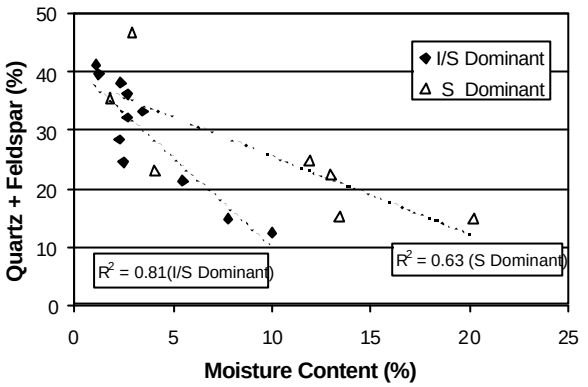

Figure 2 Correlation between percentage of quartz plus feldspar, as determined by SIROQUANT, and moisture content for mudrocks from an Australian coal mine.

A variable proportion of kaolinite and, in some cases, a small proportion of illite is also present in the clay fraction of these materials. This does not, however, seem to significantly affect the inverse relationship between the overall abundance of framework grains and the rocks' slaking or moisture content.

Frictional Ignition of Methane

With the progressive removal of other sources, such as naked flames and unsafe electrical equipment, the generation of heat by friction involving rock materials has become the principal cause of methane ignition in modern underground coal mines. The relationship between the composition of different rocks in Australian coal mines and the potential of those rocks to generate frictional ignitions has been discussed by Ward et al. (1991, 1997). These studies have identified in particular the relative influences of quartz, feldspar and rock fragments in rocks such as sandstone as the prime sources of ignition, and clay matrix and carbonate minerals as suppressors of the ignition process. Pyrite, although rare, can also represent a significant frictional ignition source.

The mineralogy of a range of rocks previously tested for frictional ignition characteristics has recently been re-evaluated at UNSW using X-ray diffraction analysis and SIROQUANT (Ward et al. 2001a). The results (Figure 3) suggest that proportions of quartz, feldspar, clay and carbonate minerals, as determined by SIROQUANT, can be related at least in general terms to the laboratory-determined frictional ignition category (IGCAT value of Ward et al., 1991). The ignition category in this instance is based on laboratory testing on a rock wheel rotating at different speeds in an ignitable methane atmosphere. The categorisation (IGCAT) value increases from 1 (no ignition at any speed) to 5 (ignition at all three test speeds), based on the laboratory test results. Although quantitative XRD does not indicate how the minerals in question actually occur (e.g. quartz in sandstones may form separate grains and may also occur in both the matrix and the rock fragments), the technique does provide a potentially useful alternative to point counting of thin sections for initial categorisation purposes.

Quartz in Coal

Mineralogical studies often show that quartz is much more abundant in the mineral matter of coal than it is in the associated roof and floor strata or intra-seam claystone bands. While some of the quartz may represent detrital fragments washed or blown into the original peat swamp, much of it occurs as pore and cell infillings of probable authigenic origin.

Coarse grained particles or aggregates of quartz may give rise to excessive levels of abrasion when the coal is ground to fine powder for combustion applications, or to erosion of exposed surfaces when the ash of the coal is blown through the furnace system. Siliceous coals, representing horizons of permineralised peat with precipitated quartz filling the cell cavities of the original plant tissues, may also act as sources of frictional ignition when cut by mining equipment (Ward et al., 1997). Even if ignition is not an issue (e.g. in gas-free mines), the quartz content of the dust generated from the coal in underground mining can also provide a silicosis risk for the mine workforce.

Understanding the distribution of quartz in coal can be of assistance in predicting these different hazards, and possibly in developing appropriate mining or preparation methods to ameliorate quartz problems. The quartz content of coal can be evaluated by X-ray diffraction, based either on the mineral matter isolated from the coal by low-temperature oxygen plasma ashing (Standards Australia, 2000) or by XRD of the whole coal or coal dust sample. Little is known of the factors controlling quartz distribution in coal, making this also an area for fundamental geological investigation.

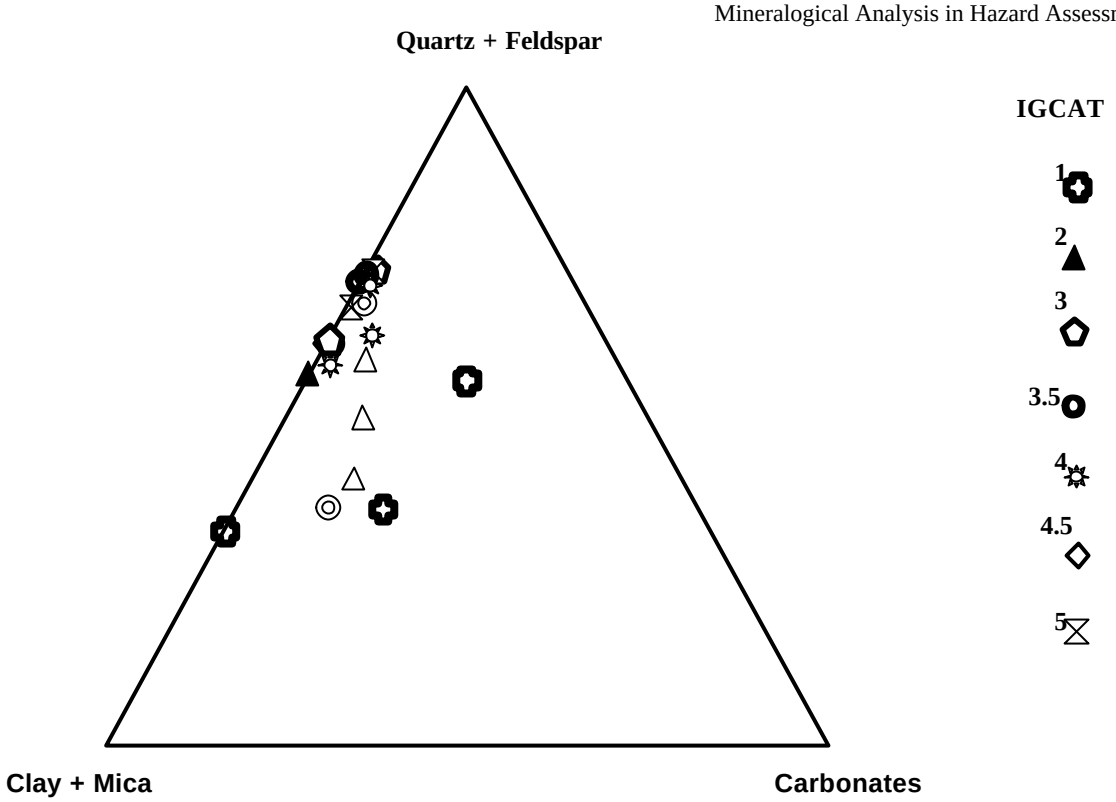

Figure 3 Triangular diagram showing correlation between normalised proportions of key minerals and laboratory-determined frictional ignition category (increasing from 1 to 5) for a range of sandstones and other rocks from Australian coal mines (after Ward et al., 2001a).

Pyrite and Other Sulphides

Pyrite in coal and associated strata is well known as a source of sulphur pollution, through generation of acids on oxidation as well as release of SO_2 during different utilisation processes. Because it burns in air when heated, pyrite can also give rise to frictional ignition of methane in underground mining situations.

Pyrite in and around coal seams is generally formed by bacterial reduction of SO_4 ions in marine waters invading the peat swamp or permeating the peat bed. However, pyrite (and its more easily oxidised polymorph marcasite) can also be introduced as a cleat infilling after deposition, derived from igneous intrusions or from migration of fluids through the sequence generally. Mapping, understanding and predicting the distribution of such sulphides, based on their origin, is a significant issue in some mines for product quality control.

Pyrite and/or marcasite may also be the host for several potentially hazardous trace elements in coal, either within the mineral itself or as separate sulphide phases (e.g. galena or sphalerite) formed by similar processes. Arsenic, for example, appears to occur as a minor element within the pyrite of coals from the Gunnedah Basin, increasing in abundance directly with the proportion of pyrite present (Figure 4).

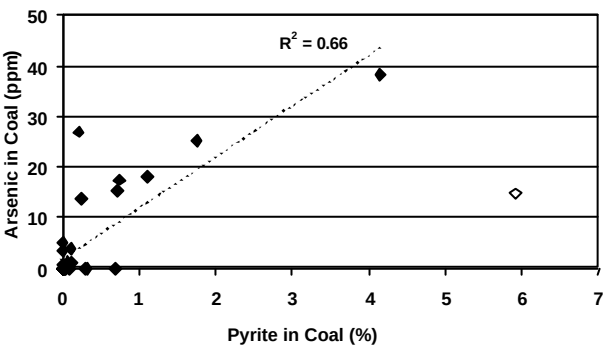

Figure 4 Correlation between percentage of pyrite and proportion of arsenic in coals of the Gunnedah Basin, NSW (after Ward et al., 1999a). The outlier point (open symbol) is not included in the correlation line.

Phosphorus Minerals

Phosphorus is a significant element in coking coals. It is transferred from the coal to the coke and ultimately becomes an undesirable contaminant of the iron and steel produced from the blast furnace, and thus low levels of phosphorus are required for coking coal production.

The phosphorus in coal occurs as small particles of

phosphate minerals, sometimes as veins but usually as pore and cell infillings in the organic matter (Ward et al., 1996). Two different groups of minerals are involved, apatite on the one hand and a range of aluminophosphate minerals such as goyazite and gorceixite on the other. Phosphate minerals are typically abundant only in particular plies of the seam, with a distribution probably determined by the post-depositional chemistry of the water in the original peat deposit; they may also be abundant in the roof and floor strata. Depending on their occurrence, the phosphate minerals may be difficult to remove in conventional coal preparation. However, identification and mapping of phosphate-rich plies may be of assistance in understanding coal quality distribution, and possibly in minimising phosphorus in coal products by selective mining processes.

Carbonate Minerals

Carbonate minerals in coal include material occurring as small nodules of syngenetic origin, intimately admixed with the organic matter, and cleat or fissure infills formed by epigenetic processes. The nodular material usually consists of siderite, while calcite, dolomite and ankerite, and in some cases siderite, constitute the fissure fillings.

The elements in these carbonates may act as fluxing agents, lowering the fusion temperatures of the coal ash and possibly giving rise to slagging problems in combustion applications. Their abundance and distribution may therefore be a factor for consideration in product quality control.

Fissure-filling and other epigenetic carbonates may also impede the flow of water or gas through the coal, and hence be associated with difficulties in drainage of methane and other gases from the seam in underground mining operations (see Gurba et al., this volume). Knowledge of the distribution of epigenetic carbonates, and an understanding of the processes controlling this distribution, may therefore be significant in optimising gas drainage and the associated hazard reduction process.

CONCLUSIONS

A number of different hazards to coal mining and quality control can be related to the minerals in the coal and the associated non-coal strata. Quantitative mineralogical analysis, based on recent developments in XRD technology, together in some cases with optical microscopy and related techniques, can be of benefit in delineating these hazards, and perhaps in providing a basis for their amelioration. The availability of a more quantitative basis for mineralogical studies provides opportunities for a range of relationships to be further investigated, and enables a fundamental branch of geological science to contribute more significantly to the development of safe and efficient coal mining operations.

ACKNOWLEDGEMENTS

Thanks are expressed to a number of mining companies, including Powercoal Pty Limited, Warkworth Mining and Ulan Coal Mines Limited, who have provided samples and identified problems that may be addressed by mineralogical studies. Thanks are also expressed to a number of colleagues, including Bob Creelman, David West, Jim Galvin, Malcolm Ives, Russell Rigby, Anton Crouch, David Cohen, David French, Les Dale, Milan Drazovic, Sorawit Nunt-Jurawong and Lila Gurba, among others, for discussions and input on different applications. John Taylor and Chris Matulis are particularly thanked for detailed instruction in use of the SIROQUANT technique, and for collaboration in some of the key testing programs. Rod Doyle is also thanked for constructive comments on the manuscript.

REFERENCES

CREELMAN, R.A. & WARD, C.R. 1996. A scanning electron microscope method for automated, quantitative analysis of mineral matter in coal. *International Journal of Coal Geology* **31**, pp. 249-269.

EMERSON, W.W. 1967. A classification of soil aggregates based on their cohesion in water. *Australian Journal of Soil Research* **5**, pp. 47-57.

RIETVELD, H.M. 1969. A profile refinement method for nuclear and magnetic structures. *Journal of Applied Crystallography* **2**, pp. 65-71.

STANDARDS AUSTRALIA, 2000. Higher rank coal - mineral matter and water of constitution. *Australian Standard* **1038.22**, 20 pp.

TAYLOR, J.C. 1991. Computer programs for standardless quantitative analysis of minerals using the full powder diffraction profile. *Powder Diffraction* **6**, pp. 2-9.

WARD, C.R., COHEN, D., PANICH, D,. CROUCH, A., SCHALLER, S. & DUTTA, P., 1991. Assessment of methane ignition potential by frictional processes from rocks in Australian coal mines. *Mining Science and Technology* **13**, pp. 183-206.

WARD, C.R., CORCORAN, J.F., SAXBY, J.D. & READ, H.W. 1996. Occurrence of phosphorus minerals in Australian coal seams. *International Journal of Coal Geology* **31**, pp. 185-210.

WARD, C.R., CROUCH, A. & COHEN, D.R. 1997. Identification of frictional ignition potential for rocks in Australian coal mines. *In:* Doyle, R., Moloney, J., Rogis, J. and Sheldon, M. (eds), *Safety in Mines: the Role of*

Geology, Coalfield Geology Council of New South Wales, Newcastle, pp. 169-175.

WARD, C.R., CROUCH, A. & COHEN, D.R., 2001a. Identification of potential for methane ignition by rock friction in Australian coal mines. *International Journal of Coal Geology* **45**, 91-103.

WARD, C.R., MATULIS, C.E., TAYLOR, J.C. & DALE, L.S., 2001b. Quantification of mineral matter in the Argonne Premium Coals using interactive Rietveld-based X-ray diffraction. *International Journal of Coal Geology* **46**, pp. 67-82.

WARD, C.R., SPEARS, D.A., BOOTH, C.A., STATON, I. & GURBA. L.W. 1999a. Mineral matter and trace elements in coals of the Gunnedah Basin, New South Wales, Australia. *International Journal of Coal Geology* **40**, pp. 281-308.

WARD, C.R., TAYLOR, J.C. & COHEN, D.R. 1999B. Quantitative mineralogy of sandstones by X-ray diffractometry and normative analysis. *Journal of Sedimentary Research* **69**, pp. 1050-1062.

Geological hazards — The impact to mining 15-16 November 2001, eds Doyle, Moloney, pp 91-106

Structural sequencing in the Macquarie Syncline

I.D. BLAYDEN

Geological and Management Services Pty Ltd, 19 Debs Parade Dudley, NSW 2290

The Macquarie Syncline is a northerly trending, probably basement controlled, structure affecting Permian and Triassic sediments in the northeastern corner of the Sydney Basin (Figure 1). The structure is about 25km wide and is recognised over a strike length of about 70km. Subsidiary structures affecting the rocks include a complex pattern of joints along with wrench faults, normal faults, reverse faults and dykes. An investigation of the sequencing of these structures has been carried out as a means of understanding the evolution of the syncline, and to assist mine geologists to better evaluate the structural significance of features encountered within individual mines.

Investigation of the structures was by means of surface and underground measurement as well as by means of detailed mapping of coastal rock platforms. The earliest penetrative structure is a set of systematic north westerly trending joints associated with an episode of right lateral shearing. The dynamics of formation is demonstrated by associated systematic second and third order joints as well as by local lateral displacement and associated feather structures. The manifestation of the structures is strongly influenced by lithology and bed thickness.

Coal seams contain similar fracture systems to the clastic rocks but in addition contain an easterly trending fracture set. This fracture set may be an a-c tensional fracture developed during the formation of the Macquarie Syncline and is the only structure, which can be in any way related to the formation of the fold.

Dykes and normal faults of late Cretaceous age with a predominant north-westerly trend are superimposed on and utilise the earlier fracture and fault planes. Postdating the dykes and normal faults are a series bedding plane faults in which the hanging wall blocks have a southwesterly direction of movement. The principal planes of movement for these faults are often claystone bands within coal seams. Listric thrusts and drag folds locally occur in association the bedding plane faults.

Understanding the structural sequencing is critical to evaluating the geological significance of features underground and in assessing areas of potential hazard. Local areas of weakness in roof strata will commonly be associated with shear zones and normal faults, listric thrusts and drag folds, particularly if developed in thinly bedded strata and/or slaky strata. Of particular concern are those areas where bedding plane faults interact with the pre-existing shear zones and/or normal faults.

GEOLOGICAL SETTING

Structure

The Macquarie Syncline is the principal structural feature affecting the rocks of the Newcastle Coalfield and is situated in the northeastern portion of the Sydney Basin (Figure 1). Extending over an area of approximately 1500km^2 the syncline is a broad gentle fold trending in a northerly direction although it is attenuated in the north where the axis kinks to the west. Strata affected by the syncline have dips generally less than 5°. The Buchanan Monocline (Blayden, 1971), a sub-structure of the northerly trending Lochinvar Anticline bounds the Macquarie Syncline to the west. Strata on the steep limb of the Buchanan Monocline near Maitland have a maximum dip of 60° to the east decreasing progressively southwards to less than 20°. Gently southerly dipping strata of Permian and Carboniferous age occur to the north and these strata are disrupted by a series of major northerly trending faults, which predate but probably occur at depth beneath the Macquarie Syncline. The axis of the "Offshore Anticline", identified from seismic data (Boyd, 1996), occurs about 12km seaward of Redhead (5km south of Newcastle) and defines the eastern extent of the Macquarie Syncline.

STRATIGRAPHY

The three principal stratigraphic components of the strata affected by the Syncline are the Tomago Coal Measures and Newcastle Coal Measures of Upper Permian age and the Narrabeen Group of Lower Triassic age (Figure 1). The stratigraphic relationship and principal subdivisions within these groups are shown in Table 1.

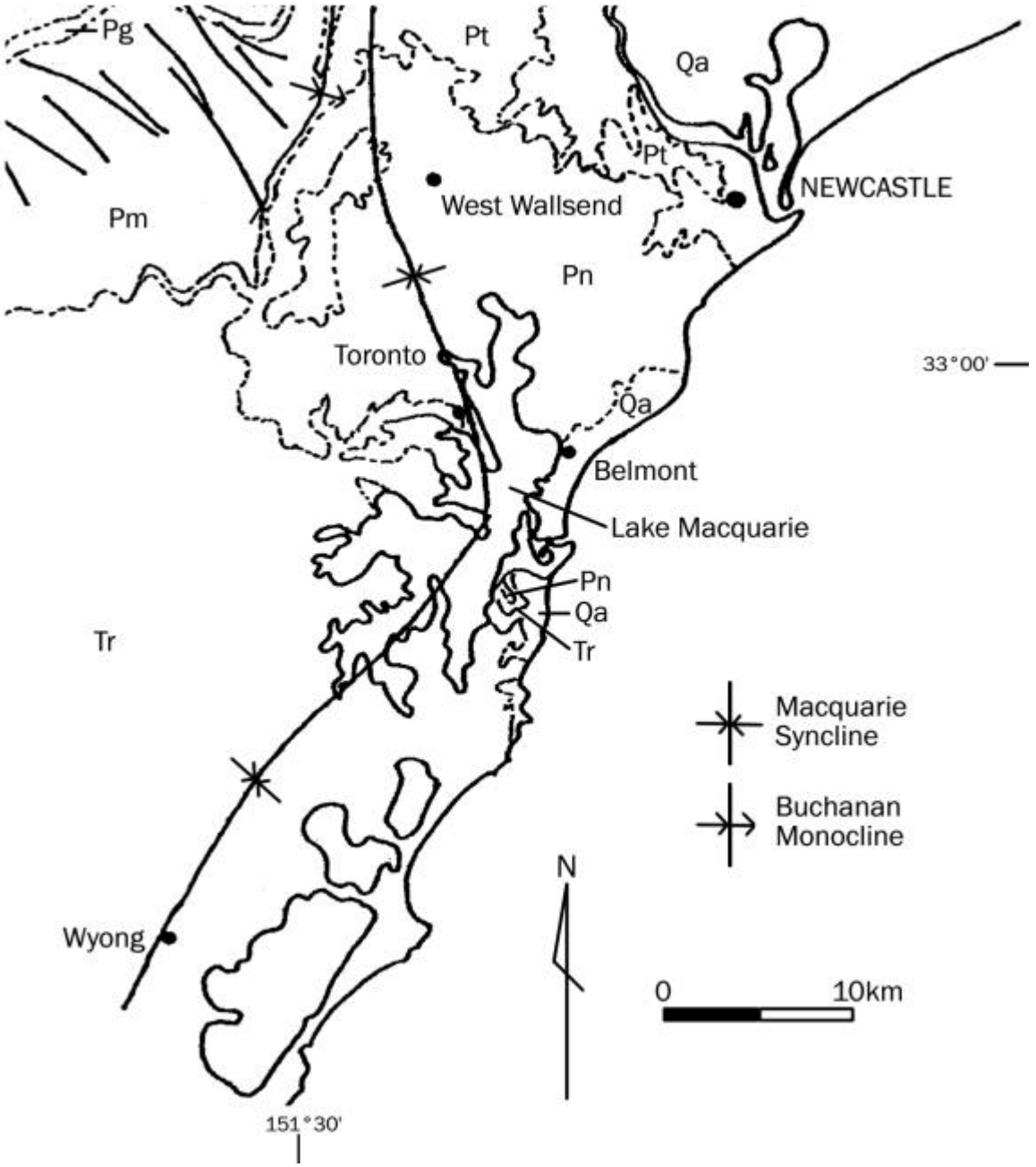

Figure 1 Macquarie Syncline Location Map. **Pg** Greta Coal Measures, **Pm** Maitland Group, **Pt** Tomago Coal Measures, **Pn** Newcastle coal Measures, **Tr** Narrabeen Group, **Qa** Quaternary Alluvium.

The Tomago Coal Measures are about 370m thick and comprise interbedded sandstone, mudstione and coal. Some horizons with tuffaceous affinities also occur. Up to 13 individual seams or seam splits are recognised with the principal economic seams developed within the Four Mile Creek Subgroup.

On the steep limb of the Buchanan Monocline sediments of the Hexam Subgroup rest unconformably on strata of the Wallis Creek Subgroup (Blayden 1971) implying there was uplift of the Lochinvar anticline during Tomago Coal Measures time. To the east of the Buchanan Monocline where the Four Mile Creek Subgroup is developed it is believed there may be a disconformable or, where there minor folding and faulting associated with the Lochinvar anticline uplift, an unconformable relationship between this Subgroup and the overlying Hexam Subgroup.

The Newcastle Coal Measures consists of coal, shale, sandstone, conglomerate and tuff, while the sequence is characterised by rapid lateral lithological variations. Many of the tuff bands may be correlated over wide areas and three of these units are used to divide the sequence into the major subdivisions. On the eastern flank of the Macquarie Syncline the Newcastle Coal Measures may be in excess of 340m thick and contain up to 16 individual seams. On the western flank

of the syncline the sequence is compressed with a thickness of around 220m and perhaps 10 or 11 seams. The number of seams is variable because some have coalesced and others have deteriorated or were not developed in this part of the basin.

The Narrabeen Group of Early Triassic age overlies the Newcastle Coal Measures and has a maximum thickness of 808m. The lower of the two major subdivisions in the Narrabeen Group is the Clifton Subgroup, which has a maximum thickness of 492m and comprises conglomerate, sandstone, siltstone and claystone. The Narrabeen Group rests on the Newcastle Coal Measures with a slight angular unconformity or disconformity.

Epoch	Group	Formation
Triassic	Narrabeen Group	Clifton Subgroup
Permian	Newcastle Coal Measures	Moon Island Beach Formation
		Awaba Tuff
		Boolaroo Formation
		Warners Bay Tuff
		Adamstown Formation
		Nobbys Tuff
		Lambton Subgroup
		Waratah Sandstone
	Tomago Coal Measures	Hexam Subgroup
		Four Mile Creek Subgroup
		Wallis Creek Subgroup

Table 1 Principal stratigraphic components in the Macquarie Syncline.

JOINTING

Initial investigations of the jointing in the Macquarie Syncline were directed towards a regional study of joint orientations and some 5,078 individual measurements were made at 166 separate locations. Some 20 locations were in Narrabeen Group sediments, 114 in the Newcastle Coal Measures and the rest in Tomago Coal Measures or older rocks. Apart from the coastal cliffs and platforms there are very few natural exposures suitable for study so most measurements were obtained in road and rail cuttings or in quarries. As a consequence the distribution of the sample locations is quite irregular with high concentrations in some part of the area and large gaps in other parts.

Synoptic diagrams of the measurements indicated a wide range of fracture orientations but with the most common element being a preponderance of northwesterly oriented fractures. The significant point though was that the joint pattern did not appear to bear any obvious geometric and therefore dynamic relationship with the fold axis of the Macquarie Syncline. In order to better understand the nature of the jointing and the relationship between the various sets it was decided to carry out a programme of detailed mapping on the coastal wave cut platforms. It is these investigations, which provided the key for the understanding the regional pattern.

Joint Trace Data

The joint trace data were collected by superimposing a grid 0.6m square over the area to be surveyed and mapping the joint traces within each grid square. To produce the grid a series of traverse lines 6m apart were surveyed and marked out into 6m segments. Using the marks as corner points the grid was moved progressively across the area to be mapped. The grid was made of reinforced rubber tape 12mm wide and 1.5mm thick joined by a series of brass press-studs. The tape was slightly flexible allowing the grid to accommodate an uneven surface and was non-perishable in salt water.

Seven maps were produced at a scale of 1:50 over areas from 37m^2 up to 4,310m^2 (Table 2). Five of the maps were produced to show intra and inter-set relationships whilst the sixth was designed to investigate jointing associated with a dyke and series of small wrench faults.

Joint Classification

The joint classification adopted in this paper is that proposed by Leith (1923) and accepted by Nevin (1949) and Price (1966) i.e. a fracture in rock on which there has been little or no movement. Hodgson (1961) recognised two basic varieties of joints, which he classifies as "systematic and "non-systematic". The principal characteristics of the systematic joints being that they are planar and occur in parallel or sub-parallel sets. Under Hodgson's definition systematic joints also cross other joints. In the Macquarie Syncline as elsewhere (Nickelsen and Hough, 1967) fractures have been observed which differ from systematic joints only in the fact that they do not transect other fractures and referred to as "truncated joints" by Nickelsen and Hough (1967). For the purposes of this paper the definition of systematic joints has been modified to include truncated joints.

As a result of the joint trace studies in the Macquarie Syncline two principal sub-sets of systematic joints have been recognised and referred to as "intrinsic" and "extrinsic" joints. The term "intrinsic joints" is applied to those systematic joints that do not appear to be directly related to, or are the secondary effect of, the formation of other structures. The relative movement of opposing fracture surfaces is normal to these surfaces.

Locality	Area Mapped (m^2)	Lithology
Fort Scratchley	4310	Sandstone and silty sandstone
Northern end of Bar Beach	150	Sandstone
100m SW of Merewether Baths	37	Sandstone
800m SW of Merewether Baths	1860	Sandstone
400m NE of Dudley Bluff	150	Sandstone
Northern end of Burwood Beach	37	Tuffaceous sandstone
Foot of Jetty, Catherine Hill Bay	37	Coal

Table 2 Platform mapping summary.

The term "extrinsic" is applied to those systematic joints that are related to or the secondary effect of the formation of other structures. Extrinsic joints may be either extension or shear fractures and in the Macquarie Syncline this type of joint is readily observed in association with dykes and faults. The term may be equally applied to joints that are directly related to folds including both tension and conjugate shear fractures.

DESCRIPTIVE TERMINOLOGY

Because of the particular style of jointing in the Macquarie Syncline and the detailed nature of the observations it has been necessary to establish a set of terminology that describes the relationships between and within the various joint sets. This terminology refers to the termination relationships between different joint sets (inter-set relationships), the relationship between individual fractures within a joint set (intra-set relationships) and the areal distribution of individual sets (set classes).

Inter-set terminology

Three inter-set relationships are recognised and referred to as "independent", "dependent and "interdependent" and are illustrated in Figure 2.

Independent joint sets are those not truncated or deflected by joints of other sets. If two or more sets are present in which these relationships occur the sets are referred to as mutually independent. Dependent joint sets are consistently truncated by joints of one or more other sets and Interdependent joint sets are those that have a mutually dependent termination relationship.

No angular relationship is implied by the terms Independent, Dependent or Interdependent in contrast to the terms "truncated joints" (Nickelsen and Hough, 1967) and "cross-joints" (Hodgson, 1961) which refer to sets which are orthogonal to and terminate against other sets. In the proposed classification these joint sets would be referred to as "orthogonal dependent sets".

Intra-set Terminology

The two aspects of intra-set terminology relate to the distribution of the joint planes within each set and the pattern of joint plane termination.

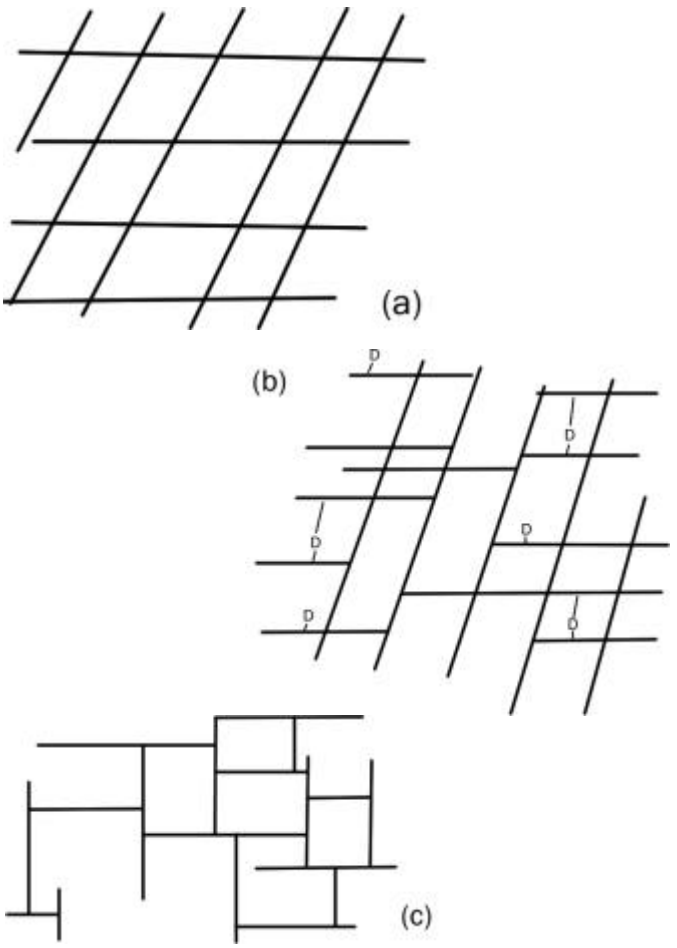

Figure 2 Joint Inter-set relationship terminology (**a**) Independent, (**b**) Dependent, (**c**) Inter-dependent.

Joint Plane Distribution

Three types of joint plane distribution are recognised in the rocks of the Macquarie Syncline, referred to as: "zonal arrangement", "diffuse arrangement" and "interlocking arrangement" (Figure 3).

The distribution of joint sets into a series of joint zones (Figure 3)(Hodgson, 1961) is the most common form of joint plane distribution in the Macquarie Syncline and is the characteristic arrangement for intrinsic joints. The diffuse arrangement is sometimes a form of intrinsic joint distribution but is more commonly seen in extrinsic joint sets adjacent to dykes, probably as cooling joints. The interlocking arrangement has been seen in only one locality in tuffaceous rocks at the northern end of Dudley Beach. This occurrence may be a result of a particularly localised strain regime and/or the lithology of the host rock (Figure 4).

Joint Plane Termination

Joint planes rarely simply die out along strike. In most cases the termination of the joint plane is related to, or determined by other joint planes of the same or different sets. Five types of joint plane termination are recognised (Figure 5) referred to as: simple, overlap, truncation, traverse and en echelon.

Simple Termination - In those cases where the joint plane does terminate without being associated with other joints the end of the fracture may be straight, curved or forked (Hodgson, 1961).

Overlap Termination – Joint planes most commonly terminate when slightly off-set and overlapping another joint plane of the same set. The amount of overlap may vary from a few cm to over one metre and the degree of overlap is usually less than 15cm and most commonly less than 2.5cm. The amount of overlap and width of the overlap is to a large extent influenced by the lithology and thickness of the jointed bed with higher values for the coarser and/or thicker units.

Truncation – A common form of truncation is the termination of one joint plane against another of a different set. In most cases the joint is straight at the point of termination but may also be slightly curved.

Traverse – Joints with a diffuse arrangement and sometimes a zonal arrangement may swing off strike with either a curved or straight trace and terminate against another joint of the same set.

En-echelon – Although rarely observed a zone of en-echelon fractures may occur at the end of a joint trace.

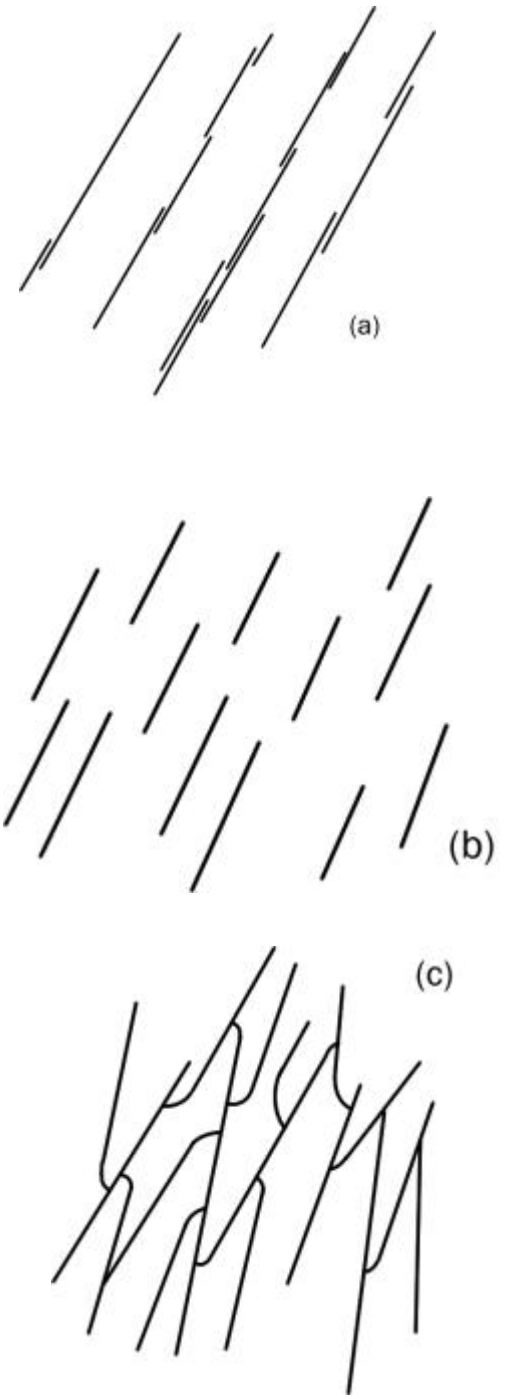

Figure 3 Intra-set trace distribution terminology (**a)** Zonal, (**b**) Diffuse, (**c**) Interlocking.

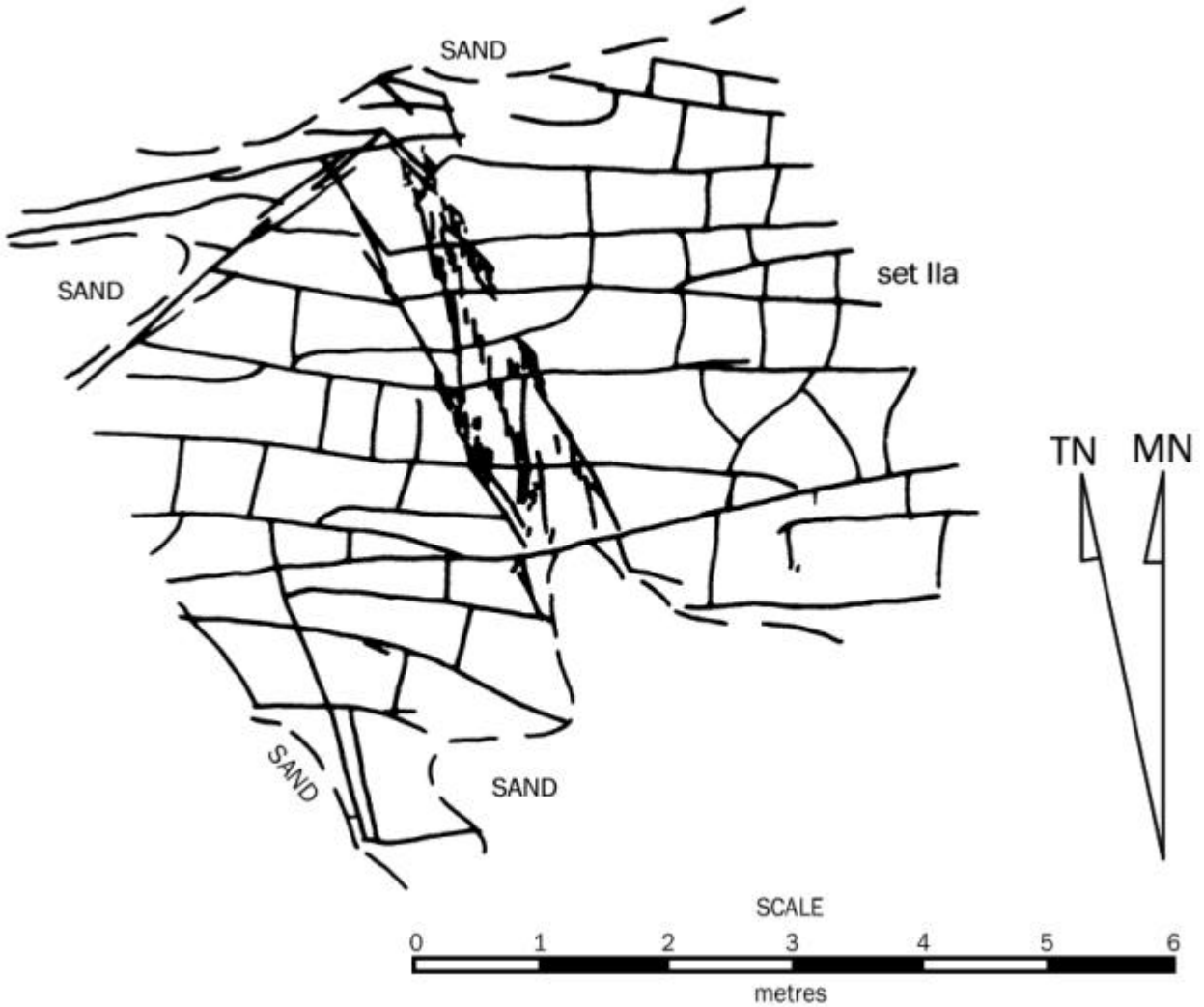

Figure 4 Joint trace map, Burwood Beach North wave cut platform in tuffaceous sandstone of the Nobbys Tuff.

Classification by Areal Distribution

Analysis of the joint trace mapping data and orientation data has shown that the regional intrinsic joint pattern is quite complex but that this complexity can be to some extent deciphered by the recognition of a number of classes of joints based on the areal distribution of each set. Four such classes are recognised as follows:

Class 1 – Those joints that are widely developed both in coal and sediments and may be recognised over the entire area of investigation (aerial extent of many km^2),

Class 2 – Those joints that are widely developed in coal and only sporadically developed in clastic sediments (aerial extent of many km^2),

Class 3 – Those joints that form readily identifiable sets in both clastic sediments and coal, but are of restricted areal development (aerial extent of many hundreds of m^2), and

Class 4 – Those Joints which occur in recognisable sets but which are of very limited lateral development (aerial extent of a few m^2 only).

In terms of regional structural analysis and strata control assessments only the Class 1, 2 and 3 joints are of significance.

MINERALISATION OF JOINT PLANES

As a general rule joint planes in the clastic rocks of the Macquarie Syncline are unmineralised. Exceptions occur where there has been some surface remobilisation of limonite in the zone of weathering and there are occurrences of carbonate infilling of joints. Carbonate mineralisation is, however, commonly developed as a thin film (<1mm) on cleat surfaces in coal seams.

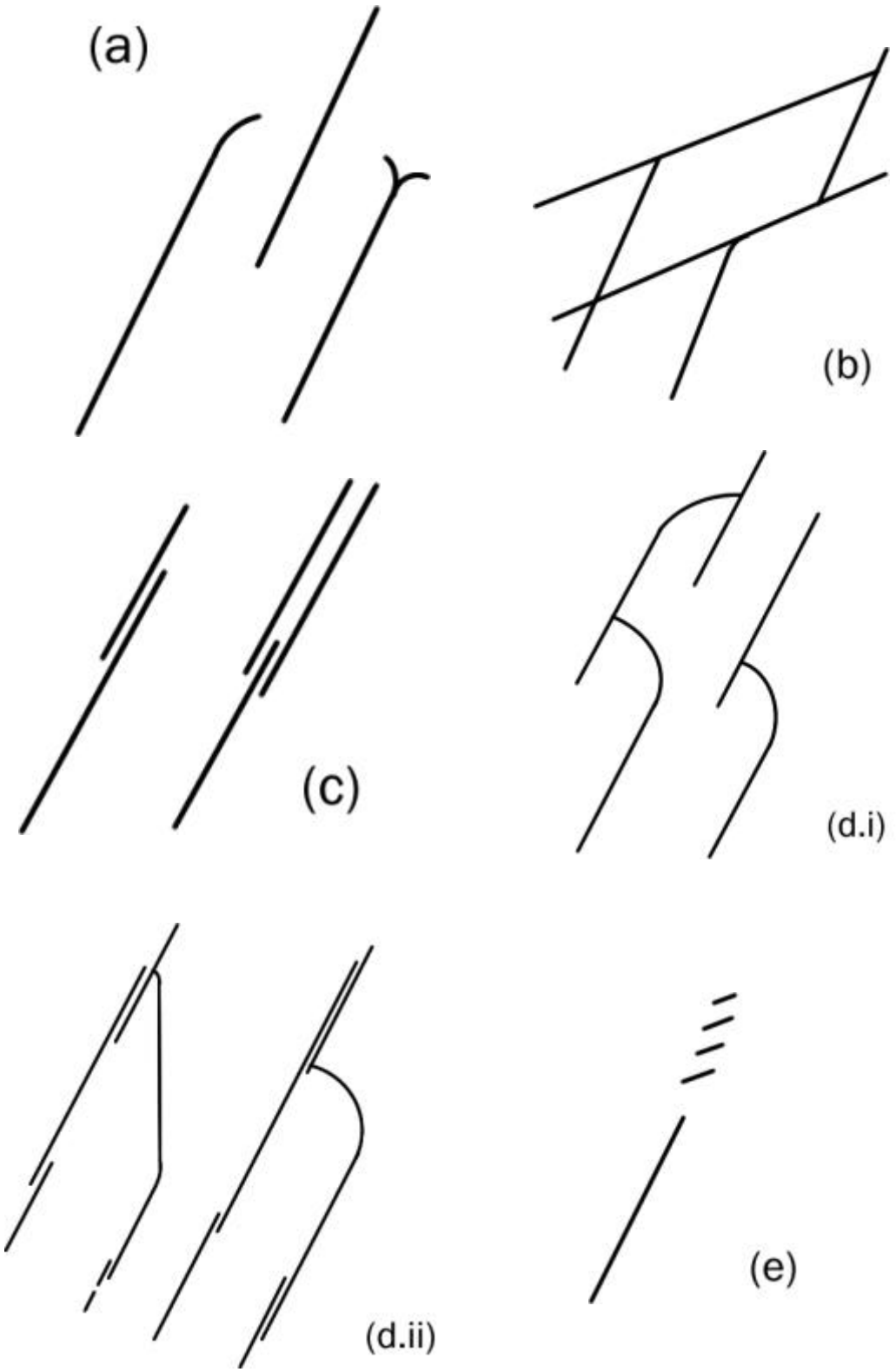

Figure 5 Intra-set termination terminology (**a**) Simple, (**b**) Truncation, (**c**) Overlap, (**d.i**) Traverse (diffuse arrangement), (**d.ii**) Traverse (zonal arrangement), (**e**) En-echelon.

THE OCCURRENCE OF INTRINSIC JOINTS

Class 1 Joints

The joint trace mapping indicate that there is essentially only one set of Class 1 joints and this set controls the development of all other joint sets. A strong north westerly oriented joint set is recognised on virtually all rock platforms (Set 1a). The joints are characteristically vertical to sub-vertical, independent and occur in a zonal arrangement. In some cases, particularly in the coarser grained rocks, it may be the only joint set developed in a given area.

It is considered likely that this one set probably extends inland across the entire Macquarie Syncline, but without the trace information it is not always possible to discern which may be the key set from a pole diagram. The evidence suggests there may be local swings in orientation but in general the orientation ranges between 125° to 140°.

Class 2 Joints

As defined above, the principal characteristic of Class 2 Joints is that they occur primarily in coal. One such set (Set IIa) is recognised in the Macquarie Syncline and is distinguished by three principal characteristics. Firstly, that individual fracture planes rarely penetrate an entire seam, but are restricted to specific plies within a seam. Secondly, that they occur in a diffuse rather than zonal arrangement and thirdly that they maintain a very consistent orientation of around 190°.

There are a few suitable platform exposures where it is possible to study these fractures in detail but it would also appear that this set is also independent (Figure 6).

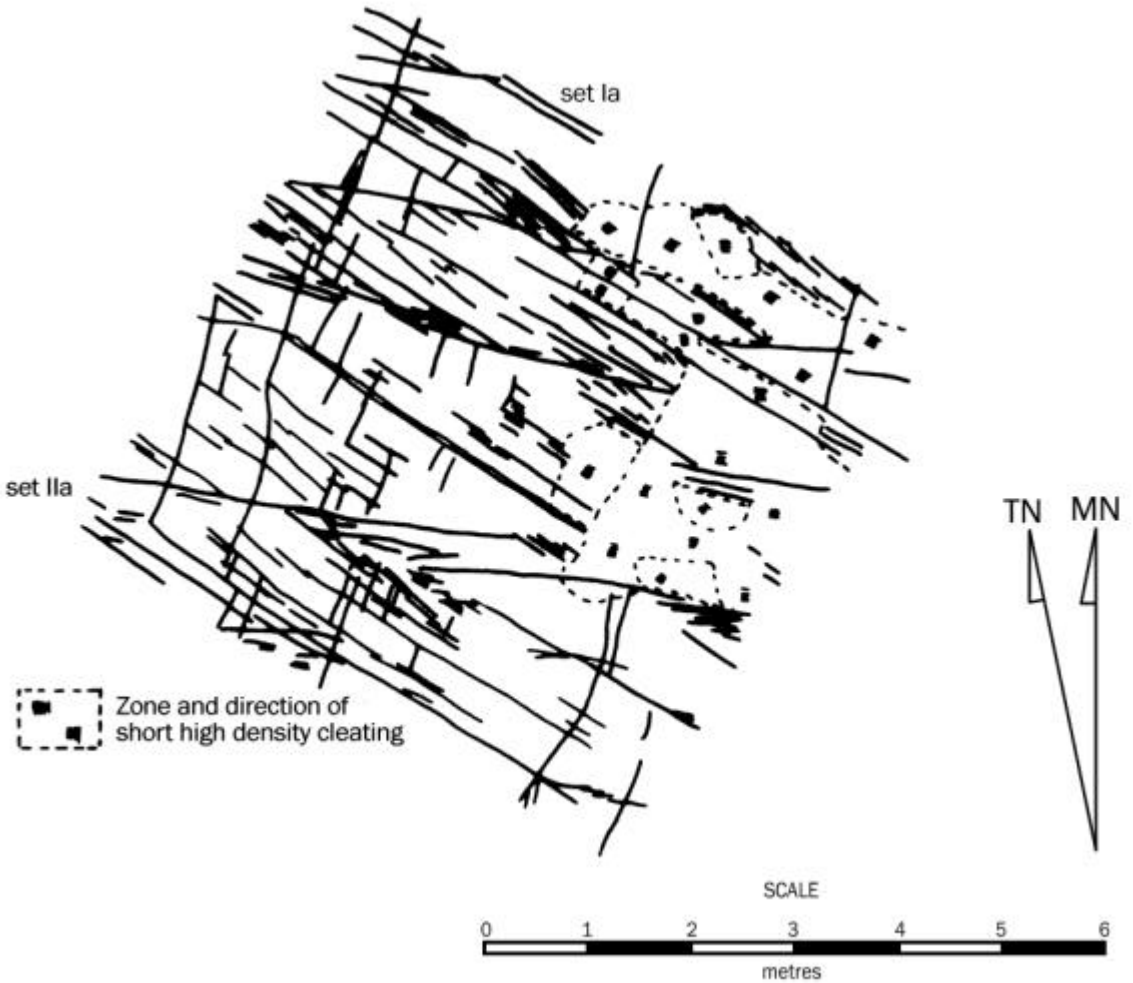

Figure 6 Joint trace map, Catherine Hill Bay wave cut platform in coal of the Great Northern Seam.

Class 3 Joints

As defined above Class 3 joints are of limited areal extent and this is because their occurrence is to a large extent determined by the development of the Class I joints as well as by lithology and the local strain regime. That said, similar patterns of Class 3 joints may occur in different areas. The best example of the development of this class of joint is shown in Figure 7 — a map of the joint traces on a wave cut platform approximately 300m south of the Merewether Baths, Newcastle. The map clearly shows the independent north Class 1 set oriented at 135° traversing the platform in a zonal arrangement and overprinted by two other principal joint sets. One set oriented at 5° in a zonal arrangement but dependent on the Class 1 joints and a second set, oriented at 75°, also in a zonal arrangement but dependent on both the Class 1 set and the 5° Class 3 set.

Figure 7, covers an area of 1858m^2 and it can be seen that the orientation and termination relationships are consistent over the total area. Mapping of other smaller areas illustrates a similar relationship at other locations. Figure 8, is a joint trace map on a platform near Dudley Bluff some 4km south of the Merewether location covering 150m^2. The Class 1 joint set is once again well defined but in this case only one poorly developed Class 3 set oriented at 0° to 10° is present along with a number of non-systematic fractures. Once again though the Class 3 set clearly demonstrates a dependent relationship on the Class 1 set.

Figure 9, also covering 150m^2 is of a wave cut platform at the northern end of Bar Beach, 2km north east of the Merewether Location. In this area two poorly developed Class 3 sets are present, one at about 25° and one at 55°. Once again the dependent relationship on the Class 1 set (about 336°) is clearly evident.

This pattern is not totally consistent though as there are local occurrences of orthogonal, apparently mutually independent joint patterns, as at Merewether Baths (Figure 10), and the interlocking pattern at Burwood Beach (Figure 4).

Recognition of the relationships between the Class 1 and Class 3 joints, and the variability in the orientation development of the Class 3 joints clearly demonstrates the futility of relying solely on geometric data for the structural interpretation of fracture patterns. It also explains why there may be considerable variability in the data acquired.

FAULTS AND DYKES

Wrench faults, normal faults and bedding plane faults occur within the Macquarie Syncline along with a system of teschenite dykes. The distribution of normal faults, bedding plane faults and dykes has been delineated through their occurrence in mine workings. Wrench faults have been largely identified through observations on the wave cut platforms. All structures most commonly strike in a north-westerly direction.

Wrench Faults

Small-scale wrench faults (lateral displacements of <1m) are indicated at a number of locations on the rock platforms of the Lake Macquarie area, through the occurrence of: gouge zones, feather structures, and the lateral displacement of sedimentary features such as fossil logs. Lohe et al 1992, identified a zone of north west trending wrench faults in Myuna Colliery with vertical displacements of up to 3m and estimated horizontal displacement of at least 16m. Structures with substantial lateral displacements probably occur on the rock platforms, but are not exposed as the faulted ones are highly fractured and preferentially eroded by wave action. Some faults classified as normal faults in mine workings may in fact be wrench faults with associated vertical displacement and some structures may also be masked by the fact that the wrench fault zones may have been utilised preferentially by later normal faults. In other words it is believed that wrench faults may be more widespread over the area than current observations would suggest.

One area of wrench faulting has been studied in detail on the wave cut platform at Fort Scratchley (Figure 11). A similar pattern of fractures to the Merewether South location is evident with the independent 312° Class 1 set and two dependent Class 3 sets at about 02° and 52°. In addition, feather fracturing is evident along some of the Class 1 joints and where this is most intense there are breccia zones. The displacement of a fossil log indicates right lateral movement of 3cm on one zone, which is consistent with the sense of movement indicated by the orientation of the feather fractures.

Normal Faults

A number of normal faults are exposed along the coastal cliff faces but most information on these structures has been derived from underground workings. The majority of faults strike in a north-westerly direction with throws of generally less than 4.5m although displacements of up to 22.5m do occur. In the southern part of the area there is also a local but strongly developed north northeast trending set of faults (Lohe et al, 1992).

In the northern part of the Macquarie Syncline the north-west faults are predominantly downthrown to the south-west but there is no evident trend of displacements further to the south.

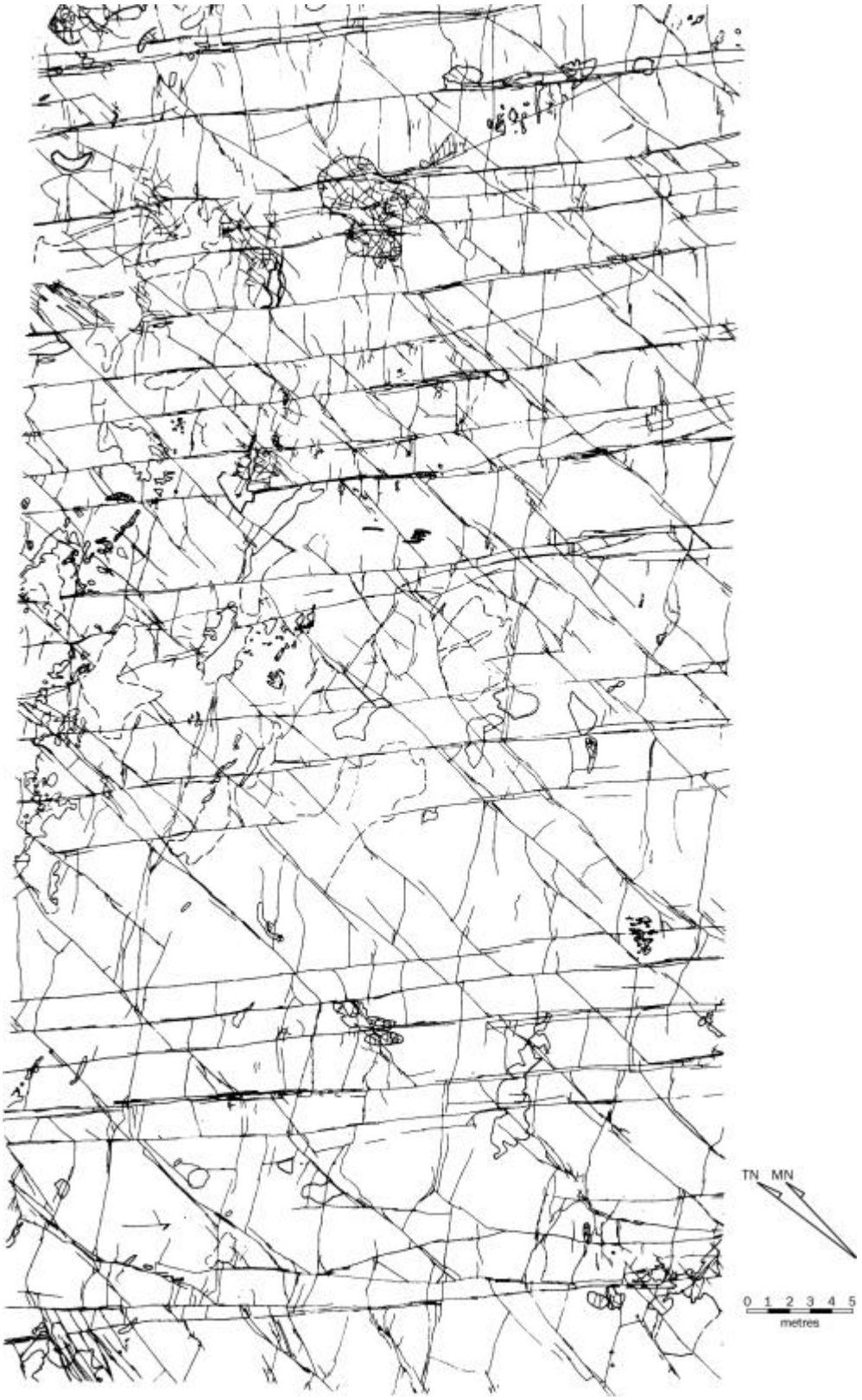

Figure 7 Joint trace map, Merewether South wave cut platform, massive sandstone of the Bogey Hole Formation.

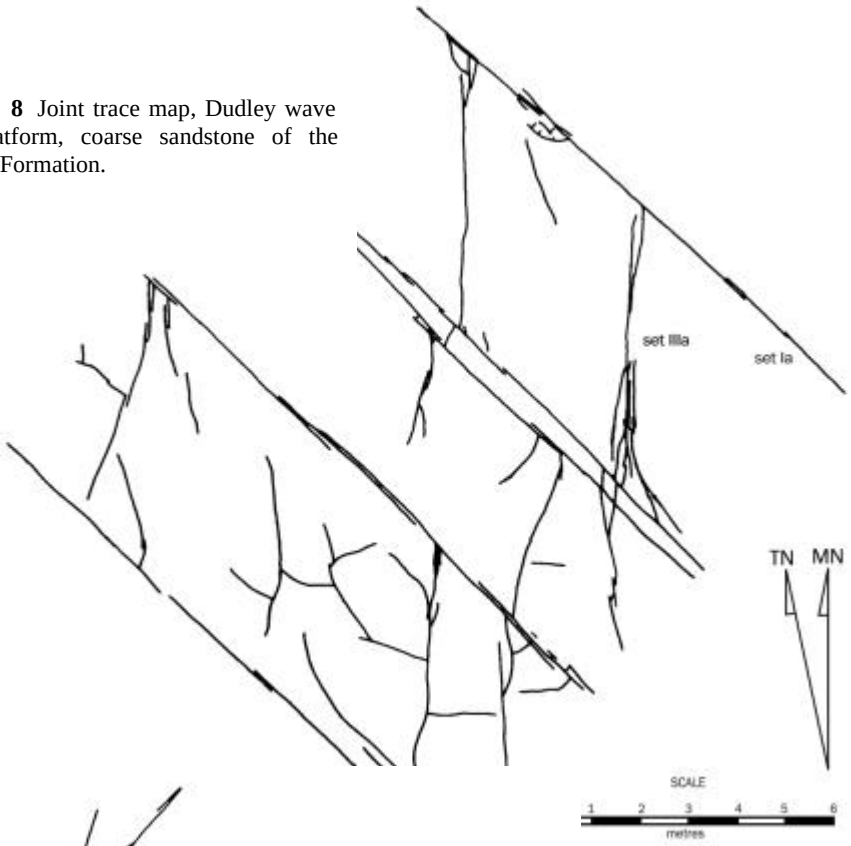

Figure 8 Joint trace map, Dudley wave cut platform, coarse sandstone of the Kotara Formation.

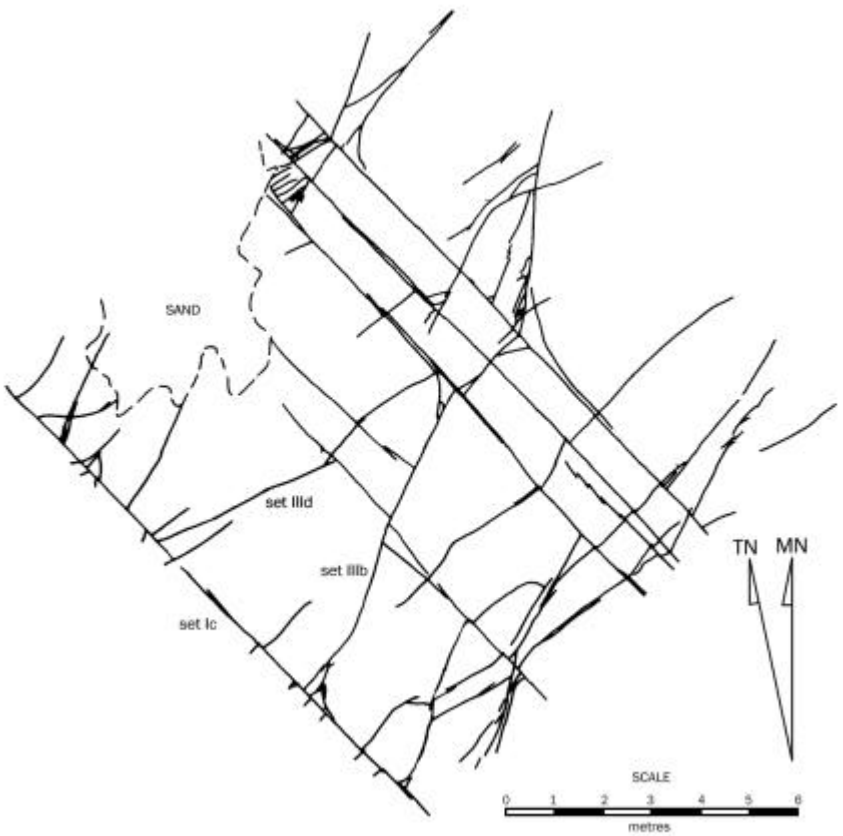

Figure 9 Joint trace map, Bar Beach North wave cut platform in sandstone of the Tighes Hill Formation.

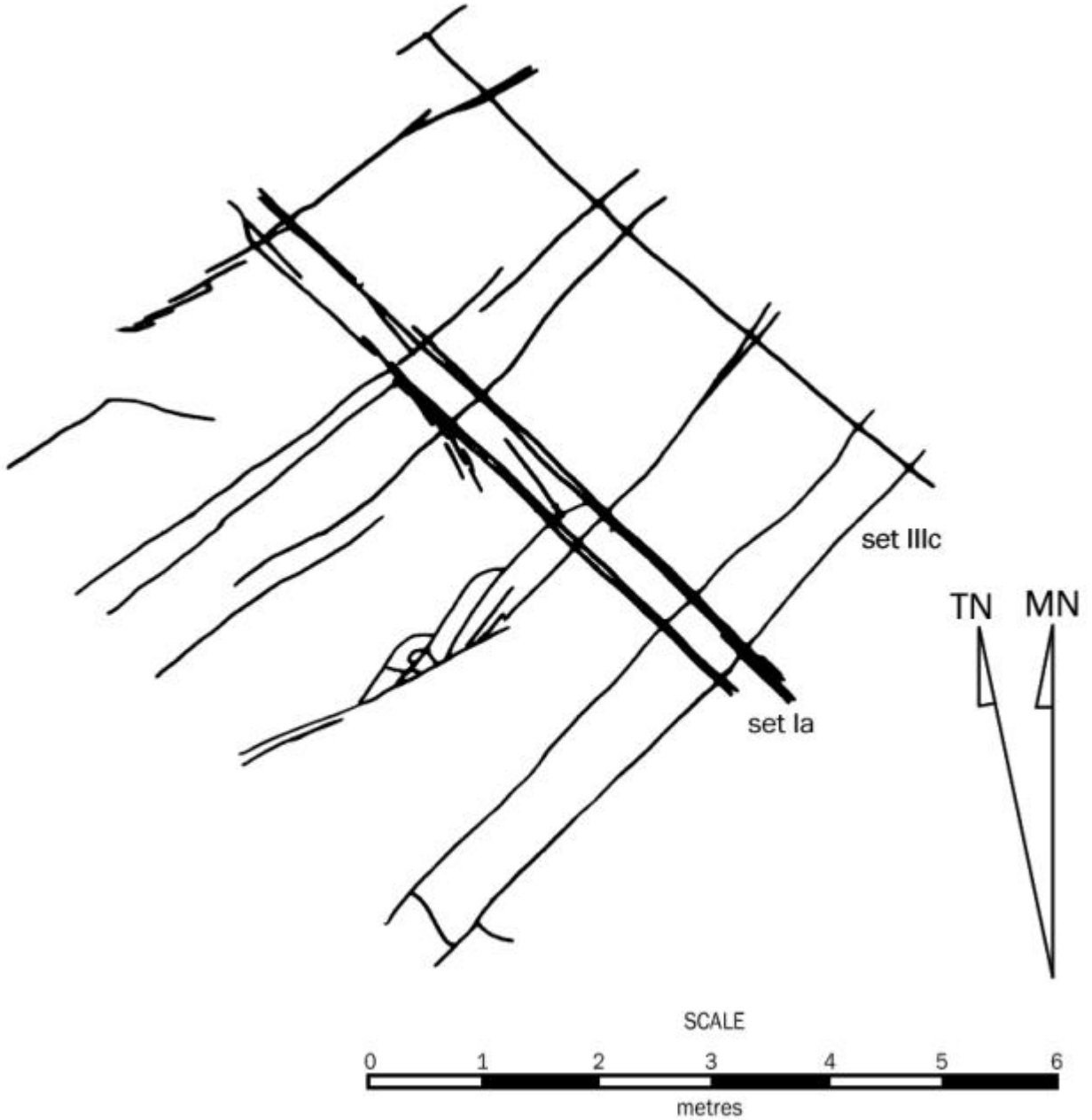

Figure 10 Joint trace map, Merewether Baths wave cut platform in sandstone of the Bogey Hole Formation.

Where the normal faults traverse the rock platforms it is quite evident they are parallel to the Class 1 joint set and have formed along the pre-existing weakness created by the presence of these fractures.

Dykes

The distribution and orientation of dykes reflect those of the normal faults in almost every respect. They most commonly strike in a north-westerly direction and also occur in association with the north northeast fault zone in the southern part of the area. Some westerly and north-easterly trending dykes also occur locally in the north (Lohe et al, 1992). In clastic sediments the dykes vary in width from <1m to over 3m and are composed of teschenite. Recent K-Ar dating of plagioclase and whole of rock samples from the dyke on the Fort Scratchley wave cut platform are 79.6±1.8Ma and 77.98±2.22Ma respectively (Upper Cretaceous)(R. Offler, pers com).

Although dykes are relatively common in the area there are few locations where they can be observed on the rock platforms. There is little doubt that, as with the faults, the dykes for the most part have been injected along pre-existing fracture systems, primarily the Class 1 set but also locally along Class 3 fractures (Figure 12).

In the cliff behind Newcastle's South Beach a dyke occurs 3m from, and on the downthrow side of, a normal fault (Figure 13). The normal fault displaces the Yard

Seam and on the upthrown side the seam is cindered. Cindered coal bonds and partially encloses rock fragments in the fault breccia on the fault plane indicating that the fault displaced the coal while it was in a plastic state. It is concluded from this that the formation of the fault and intrusion of the dyke were essentially synchronous.

Bedding Plane Faults & Reverse Faults

Blayden (1971), recognised bedding plane faults in claystone bands of the Borehole seam extending over the entire area of the Burwood and John Darling Collieries and probably extending outside these areas. The faulting was evident from brecciation of the claystone and slickensides in the roof of the workings. The slickensides have a consistent 50° orientation. The pervasive nature of the structures and the consistency of the slickensides orientations indicate that they were part of a widespread system of such structures and that they probably occur at a number of levels in the sequence, particularly in claystones. Horizontal displacements of up to 1.5m of both faults and dykes were observed in John Darling Colliery with the hanging wall moving to the south-west relative to the footwall. These observations not only establish the direction of the bedding plane movements but also determine the relative age relationships between the bedding plane faults and the normal faults/dyke intrusions. North-west trending reverse faults also override normal faults in the Wyee State Coal Mine (Lohe et al, 1992). These authors indicated that it was not possible to establish the relative age relationship between the north west trending reverse faults and northerly trending reverse faults. Reverse faults with a north-westerly strike occur at South Newcastle (Figure 13) and in John Darling Colliery.

The structure in John Darling colliery has a strike length of 5km (Lohe et al, 1992) and a vertical displacement of up to 8.1m. Lohe et al (1992) also reports the occurrence of other structures in Gretley Colliery to the north-west and in mine workings in the southern Macquarie Syncline. In these areas both north-westerly and northerly trending reverse faults were recognised.

Blayden (1971), concluded that given the bedding plane slip movement was orthogonal to the north westerly trending reverse faults the two structural types are related in that the reverse faults are probably listric thrusts developed off the system of bedding plane structures.

STRUCTURAL SEQUENCING

The termination relationships between the Class 1 and Class 3 extrinsic joints clearly demonstrate that the Class 1 joints originated first. The relationship is such that the Class 3 joints appear to be second order effects of the stress which initiated the Class 1 set and probably developed soon after the Class 1 set. Such a pattern is not unlike that expected for a simple right lateral shear couple stress regime and the formation of the joints may in fact be the result a "stored strain release" (Price, 1959) mechanism associated with such a shear system

The measurable displacement and structures associated with the shear zone at Fort Scratchley demonstrate that a right lateral simple shear couple also generates these structures. It is considered therefore that the regional Class 1 set, Class 3 sets and the wrench faults are genetically related. These structures were the first to be developed in the rocks of the Macquarie Syncline and defined the structural fabric of the area. Shear structures of this type do not appear to have been recognised elsewhere in the northern Sydney Basin and it is not possible to relate them to any specific tectonic event and the absolute age of their formation is not known.

The Class 2 joints occur primarily in coal seams. There is insufficient trace mapping data to establish the relationship between this set and the other joints in the area. Nor is there an obvious relationship between these structures and the faults or dyke intrusions. They are however generally orthogonal to the regional axial trend of the Macquarie Syncline and it is possible they may be a-c tensional fractures associated with the formation of this structure. Why they occur primarily in the coal may be related to the brittle nature of the coal and the stress field involved. Their time of formation, if related to the folding, is also unclear, as estimates for the time of formation of the Macquarie Syncline vary from the early Triassic through to some time in the Tertiary.

No doubt there were several episodes of normal faulting due to minor basin adjustments. However, there is some evidence of synchronicity in the formation of some normal faults and dyke intrusion. This together with strong geometric and spatial relationship between the two structures suggests that the bulk of the normal faults may have occurred at the same time of dyke intrusion. K-Ar dating suggest the formation of the structures occurred during the late Cretaceous.

Bedding plane faults with south-westerly directed hanging walls and associated listric thrusts occurred subsequent to the formation of the faults and dykes. There is a second set of thrusts related to east west compression but the relative time relationship for their formation is not yet clear.

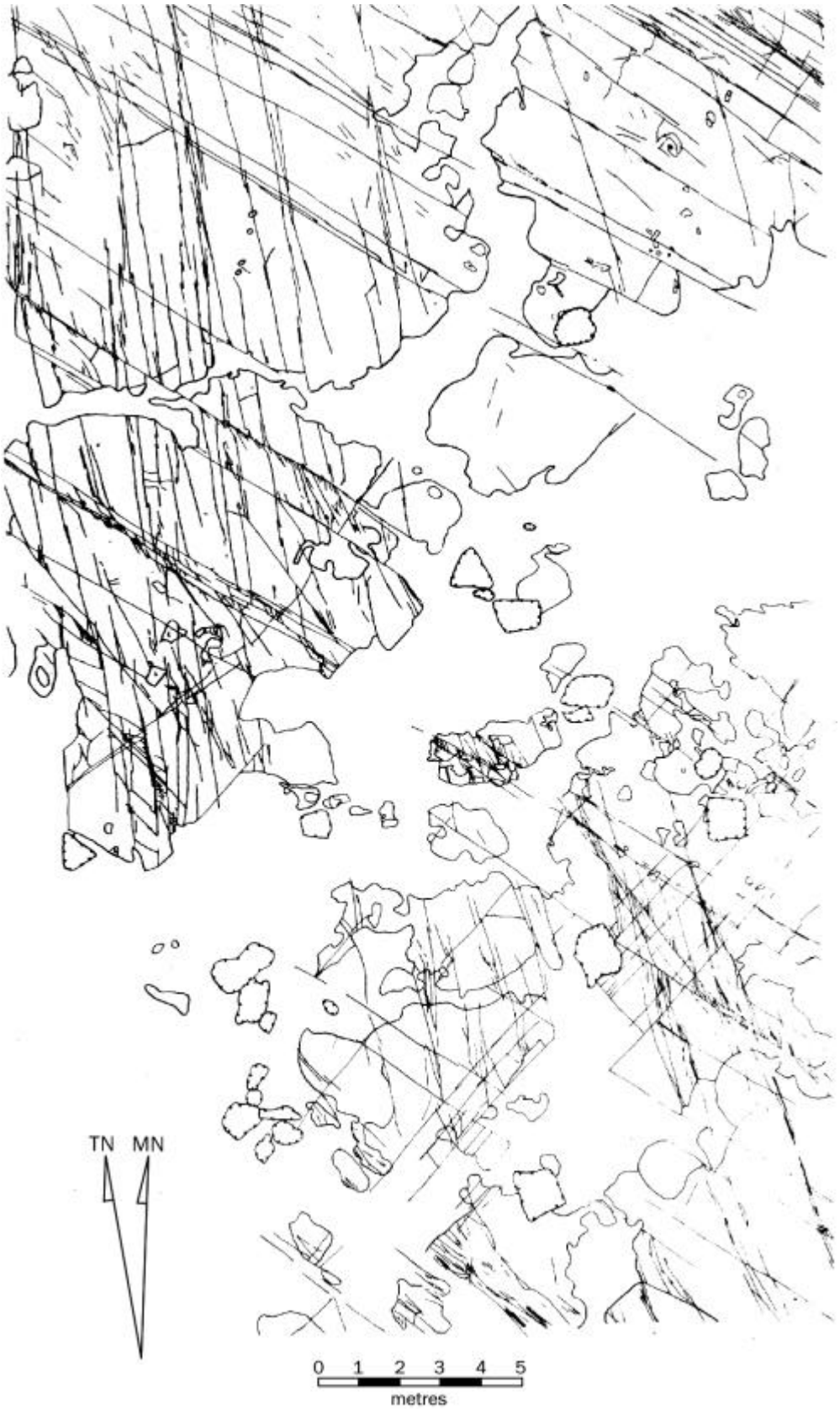

Figure 11 Joint trace map, Fort Scratchley wave cut platform area A in silty sandstone of Shepherds Hill Formation.

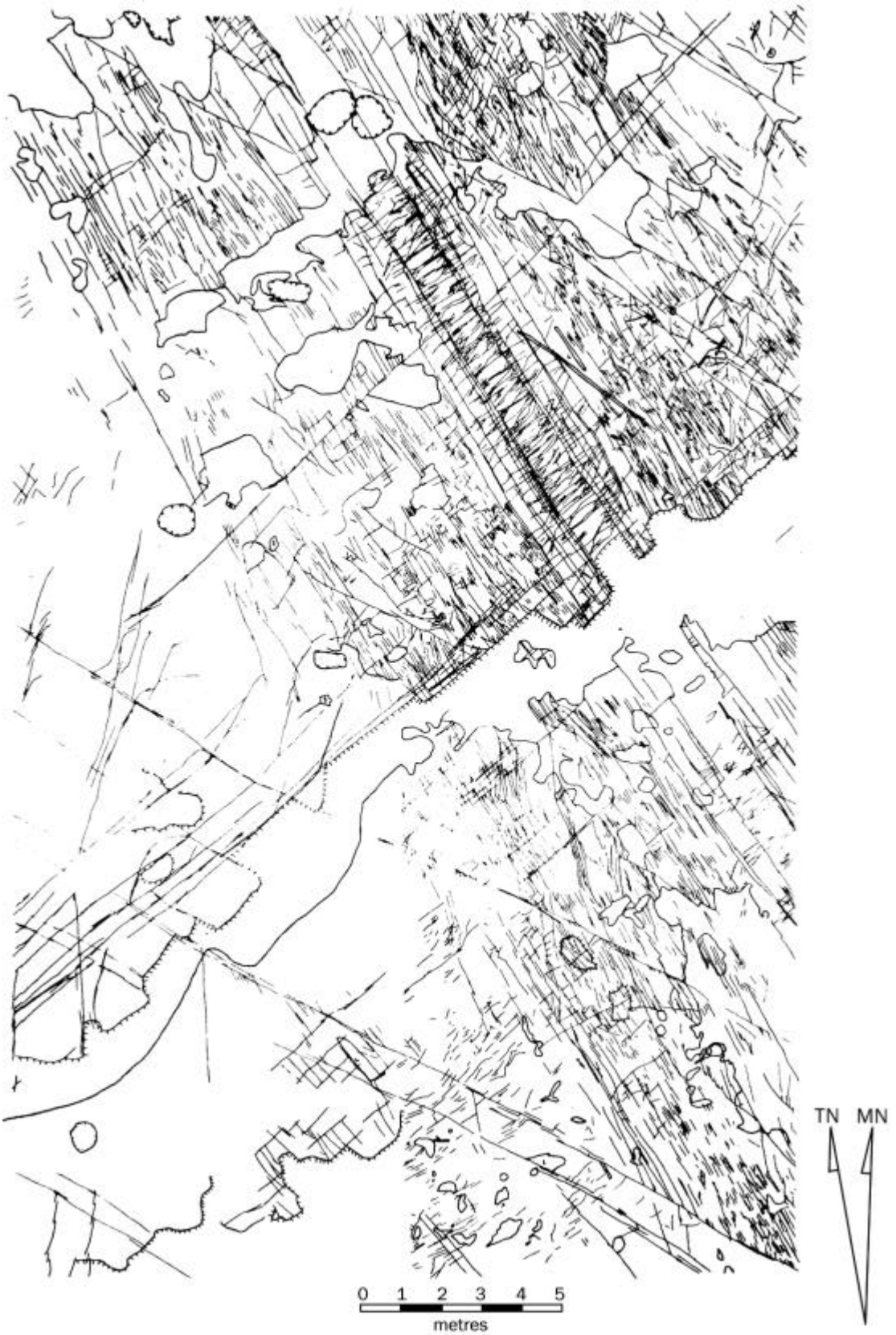

Figure 12 Joint trace map, Fort Scratchley wave cut platform Area B in sandstone of the Shepherds Hill Formation.

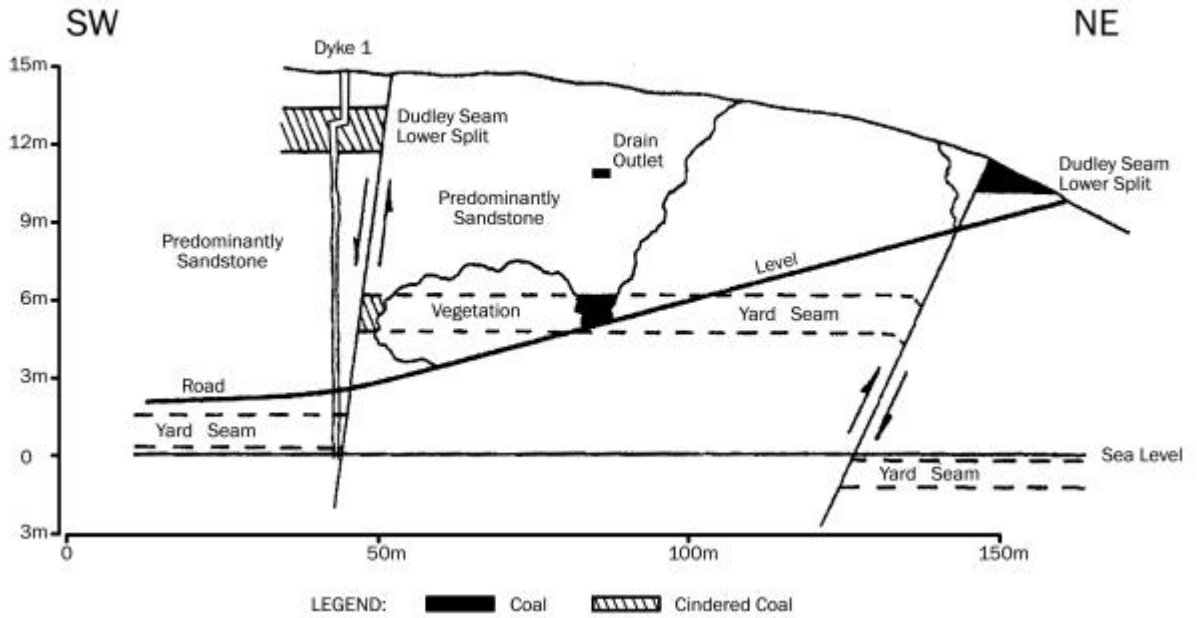

Figure 13 Normal fault, dyke and reverse fault in cliff at Newcastle South Beach in Lambton Subgroup sediments.

OBSERVATIONS RELEVANT TO MINING

The Macquarie Syncline is relatively undeformed compared to elsewhere in the northern Sydney Basin, but nonetheless there is evidence of a complex, though subtle structural history. In particular there is evidence of a widespread right lateral wrench regime, an event not recognised from macroscopic data elsewhere in the region.

Understanding the distribution and relationships between the differing structural types is of considerable benefit to mine geologists in the interpretation and prediction of structures within individual colliery holdings. In particular the dependent relationship of the Class 3 joints on the Class 1 joints may well have significant geomechanical implications for the behaviour of roof strata and it is important that such relationships are recognised during structural studies of colliery holdings.

The structural regime affecting the Macquarie Syncline with the resultant joint patterns, faults and dykes is, in all probability, superimposed on the rocks of the Hunter Coalfield as well. As the structural history of the Hunter Coalfield is more complex than that of the Newcastle Coalfield recognition of structural features evident in the Macquarie Syncline in the rocks of the Hunter Coalfield should greatly assist in the unravelling of the structural evolution of this part of the Sydney Basin. The ultimate outcome should be a greater understanding the mining conditions, which have been and will be encountered.

REFERENCES

BLAYDEN, I.D. 1971. On the structural Evolution of the Macquarie Syncline. *PhD Thesis, University of Newcastle (unpubl.)*

BOYD, R.L. 1996 Sydney Basin Offshore from Newcastle – New structural & stratigraphic insights from high-resolution seismic stratigraphy. *Proceedings of the Thirtieth Newcastle Symposium on Advances in the Study of the Sydney Basin.* pp. 85-88.

HODGSON, R.A. 1961. Regional study of jointing in the Comb Ridge-Navajo Mountain area, Arizona and Utah. *Bull.Am.Assoc.Petrol.Geol., 45* pp. 1-38.

LEITH, C.K. 1923. *Structural Geology*. Henry Holt, New York.

LOHE, E.M, McLENNAN, T.P.T, SULLIVAN, T.D, SOOLE, K.P. & MALLET, C.W. 1992. Sydney Basin – Geological structure and mining conditions, assessment for mine planning. NERDDC Project No.1239. *CSIRO Division of Geomechanics. External Report (New Series)* **20.**

NEVIN, C.M. 1949 *Principles of Structural Geology* Wiley, New York.

NICHELSEN, R.P. & HOUGH, V.N.D. 1967 Jointing in the Appalachian Plateau of Pennsylvania. *Bull.geol.soc.Am.*, **78** pp. 609-630.

PRICE, N.J, 1959 Mechanics of jointing in rocks *Geol.Mag* **96** pp. 149-167.

PRICE, N.J. 1966 *Fault and Joint Development in Brittle and Semi-brittle Rocks* Pergamon, Oxford.

Geological hazards — The impact to mining 15-16 November 2001, eds Doyle, Moloney, pp 107-116

Structural model for Springvale Coal: A hazard prediction tool

S. M. MUNROE[1], A. KNIGHT[2] AND J. TEASDALE[3]

[1] *SRK Consulting, Level 9, 1 York Street, Sydney, NSW 2000*
[2] *Springvale Coal Pty Ltd, Mudgee Road, Lidsdale, NSW 2790*
[3] *SRK Consulting, Suite 7, Deakin House, 50 Geils Court, Deakin West, NSW 2600*

Springvale Colliery, lying west of Lithgow in the Western Coalfields has been the subject of a number of phases of forward structural interpretation (ahead of development) and identification of structurally complex zones that have in the past provided a risk to mining. This paper outlines the techniques used in the work that has been done and the techniques used to identify structurally complex zones that may be linked to unstable ground or zones of high stress.

The structural framework and structural model is derived from an interpretation of integrated data sets, including magnetic data, gravity data, elevation data, bore hole data and mine mapping but may also include Landsat, aerial photographs and seismic data. The structural interpretation derived from the integration of these data sets has been used to qualitatively analyse the risk of intersecting poor ground conditions in the Colliery, similar to those that have been intersected in previous development. The analysis does not take into consideration the change in stress created by longwall mining or development roads, but considers the orientation and intersections of the structures. To this end it can be used as a guide to the ground conditions ahead of development and can be used as a mine planning tool.

Within the mine, underground observations are regularly reviewed against the interpreted structural zones to assess the effectiveness of the structural model and structural risk domains that had previously been predicted. To date the success rate encountering mappable structures within the predicted structural zones lies at approximately 75%. This is a far higher success rate than Springvale Coal ever had in the past and permits far more accurate prediction of zones of structural complexity. Prediction of future hazard areas likely to be encountered in development and/or longwall panels can be undertaken with a high degree of confidence and prior warnings provided to the operational crews. In this way, if a predicted structure is intersected, or the general conditions (roof, ribs etc) change in any way, the mining operators are far more comfortable than they were with the old system when unexpected structures were intersected, often with disastrous results.

The ability to predict structures ahead of development has resulted in Springvale Coal adopting a "Proactive" mining and support regime rather then a "Reactive" one as was the original situation. Overall the Springvale structural model has proven to be a highly successful hazard prediction tool and is contributing to the ongoing fortunes of Springvale Coal.

BACKGROUND

Springvale Coal technical personnel in conjunction with SRK Consulting have undertaken a program of integrated structural mapping, remote sensing interpretation and testing of structural models for Springvale Colliery and its surrounds. This work was done in order to predict and understand the geological controls on areas of poor ground conditions in the Colliery.

Some of the work that has been done over the last two years consists of:

- on-going structural mapping of the seam and roof of the Lithgow Seam in the development areas ahead of mining,
- development of a model of the structural framework of the Springvale Coal area from regional aeromagnetic, gravity and remote sensing data,
- trial testing of closely spaced helicopter-borne magnetic data (heli-mag) to identify the value added by acquiring this data for more detailed interpretation,
- more detailed interpretation of magnetic data to identify the second order structural features and interpret the structural elements that would impact on the seam,
- testing of structural models with in-seam drilling, and
- analysis of interpretation and structure from mapping during longwall mining, with implications for future development areas.

The first order interpretation relies on an

understanding of the basement geological evolution from regional to local scales. This approach is relatively new to the coal industry, but has been used successfully in petroleum and minerals exploration and mining as a technique to identify structural and geological risk.

STRUCTURAL FRAMEWORK

SRK Consulting was contracted by Springvale Coal in mid-1999 to develop an integrated structural interpretation of the Springvale lease area utilising available aeromagnetic data in conjunction with other geophysical datasets (gravity, surface remote sensing) together with the geological mapping from the Colliery.

The principal objective of the structural study was the development of a preliminary structural risk map, which predicted areas of high structural risk.

Regional Tectonic Setting

The basement to the western Sydney Basin is the Lachlan Fold Belt, which is composed of Early Cambrian to Early Carboniferous low-grade metamorphics, volcanics and granitic intrusives. The Lachlan Fold Belt is a complex N-S trending belt that is partitioned by major N-S trending fault zones and WNW to NW trending transfer zones. A major transfer zone in the Springvale area is the WNW striking Lachlan Transfer Zone, which underlies the Colliery. The Lachlan Transfer Zone was intruded by the Bathurst Granite in the early Carboniferous.

At the end of the Carboniferous, NW-SE extension began to affect the eastern margin of Gondwana. Some Fold Belt structures were reactivated at this time, which created a continental rift into which the Sydney-Bowen Basin was deposited.

During the Early-Mid Triassic, E-W directed Hunter-Bowen Compression caused thrusting along the eastern margin of the basin, and large volumes of material were eroded from the New England Fold belt highlands to the east and were deposited in the Sydney Basin as coarse clastics. In the Western Coalfields, E-W compression caused minor reactivation of N-S trending basement faults, which propagated into the overlying sediments, including the coal. Minor thin-skinned thrusting also occurred within the Permo-Triassic sediments.

Since the Triassic, there have been at least three tectonic episodes that have affected the area. These events are caused by changes in the plate tectonic configuration, and potentially caused minor reactivation of basement structures in the Western Coalfields. The episodes that are likely to have affected the Springvale area are:

- Late Cretaceous NNE-SSW extension, which was caused by opening of the Tasman Sea and Bass Strait rift,
- Mid-Eocene N-S compression, which is likely to have been a very minor event in the coalfields, and
- Miocene – Recent NNW-SSE compression caused by the collision at the northern margin of the continent. These stresses continue to operate on the Australian Plate cause high horizontal stress conditions over most of the continent and some readjustment of crustal boundaries, which manifest as earthquakes.

The Triassic to Recent tectonic episodes may have caused minor reactivation of the basement structures. The likelihood and direction of reactivation is strongly controlled by the orientation and geometry of the structures with respect to the applied stresses.

Basement Geology

As shown in Figure 1, two broad lithological associations dominate the basement geology of the Western Coalfields: (i) sinuous N-S trending belts of deformed metasedimentary and metavolcanic units of Devonian age and (ii) relatively undeformed batholiths of Early Carboniferous granite (including the Bathurst Granite).

The granite (part of the Bathurst Batholith) that underlies Springvale Coal postdates the formation of many of the basement faults. Reactivation of the faults adjacent to or beneath the granite will cause the faults to propagate into the granite, and the overlying Sydney Basin sequence where basement faults are shown to crosscut the granites.

Geometric anomalies in and intersections of the basement structures are likely to manifest as stopovers, splays and complex accommodation zones in the granite and overlying sediments. During subsequent reactivation stepovers, splays and complex accommodation zones will localize stresses, particularly during strike-slip reactivation, when complex “lock-up” zones may develop. As a result, stepovers, splays and intersections of structures affecting the coal seam represent the zones of highest structural risk at Springvale Coal.

STRUCTURAL INTERPRETATION OF SPRINGVALE COAL – STAGE I

An integrated structural interpretation of the Springvale Colliery lease was undertaken at 1:25,000 scale using available remote sensing and mine mapping data. The main remote sensing datasets used were the 1995 Wallerawang Airborne Magnetic Survey and 10m digital elevation data (DEM).

The aeromagnetic data was acquired by World

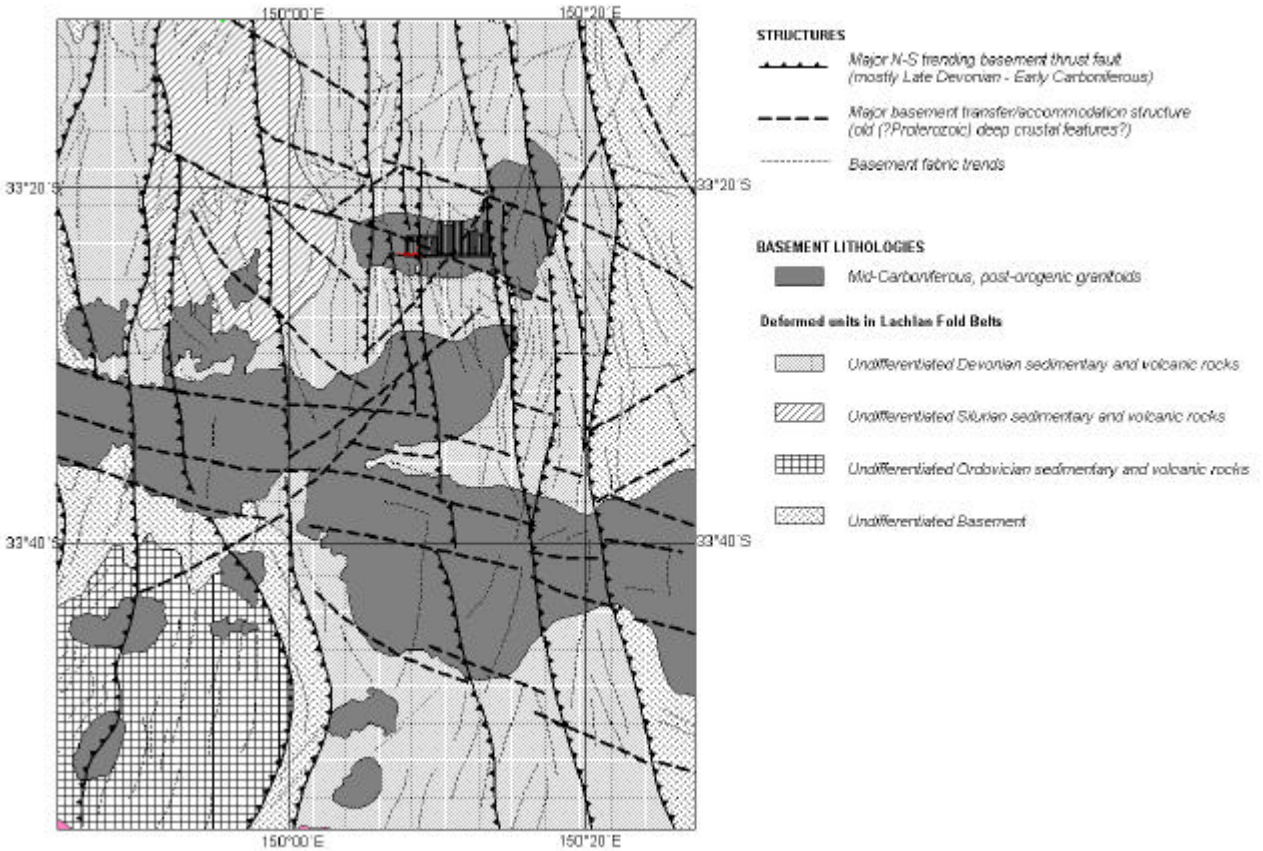

Figure 1 Regional geological interpretation of the basement in the Lachlan Fold Belt, including the Springvale region. The Springvale workings are shown in the map above a Mid-Carboniferous, post-orogenic granitoid, which is controlled by WNW trending transfer zones of the Lachlan Fold Belt.

Geoscience by fixed wing aircraft flown in a west-east path at 100m line spacing approximately 80m above the ground and grided to 20m. The data was then enhanced to highlight structures affecting the sedimentary cover as a guide to the structure in the basement and coal seam. Faults appear as subtle pattern breaks and discontinuities.

Results

A region showing the results of this work is illustrated in Figure 2. Integrated interpretation of the datasets showed reasonable correlation. Many faults were supported by both the aeromagnetic and DEM and most mapped faults or fault zones were expressed in at least one of the geophysical datasets, which enabled good calibration of the interpretation in unmined areas with that in mined areas. The interpreted faults closely match the regional scale basement structural pattern described above, where N-S trending faults dominate.

The 100m data was important for recognising the structural patterns of the basement and cover but is inadequate for mapping individual structures at the scale of longwall mining. The structures identified are likely to represent zones rather than individual faults. Some of the smaller scale faults that may have been important in the mine could not have been detected using this data.

The most significant post-Triassic reactivation event is the on-going Miocene-Recent compression that causes NNW-SSE compressional stress in SE Australia. In the Springvale area, NNW-SSE compression caused sinistral strike-slip reactivation of N-S faults. Stepovers, splays and intersections can prevent fault movement, resulting in stress build-ups, which exhibit great structural complexity, but occur in relatively isolated and discontinuous patches. At Springvale, intersections between N-S and WNW faults are the principal causes of these zones of structural complexity and assist in the localization of zones of high stress.

Risk Analysis

The structural framework and interpretation discussed above has been used to qualitatively analyse the risk of intersecting poor ground conditions in the Colliery. This analysis is independent of the change in

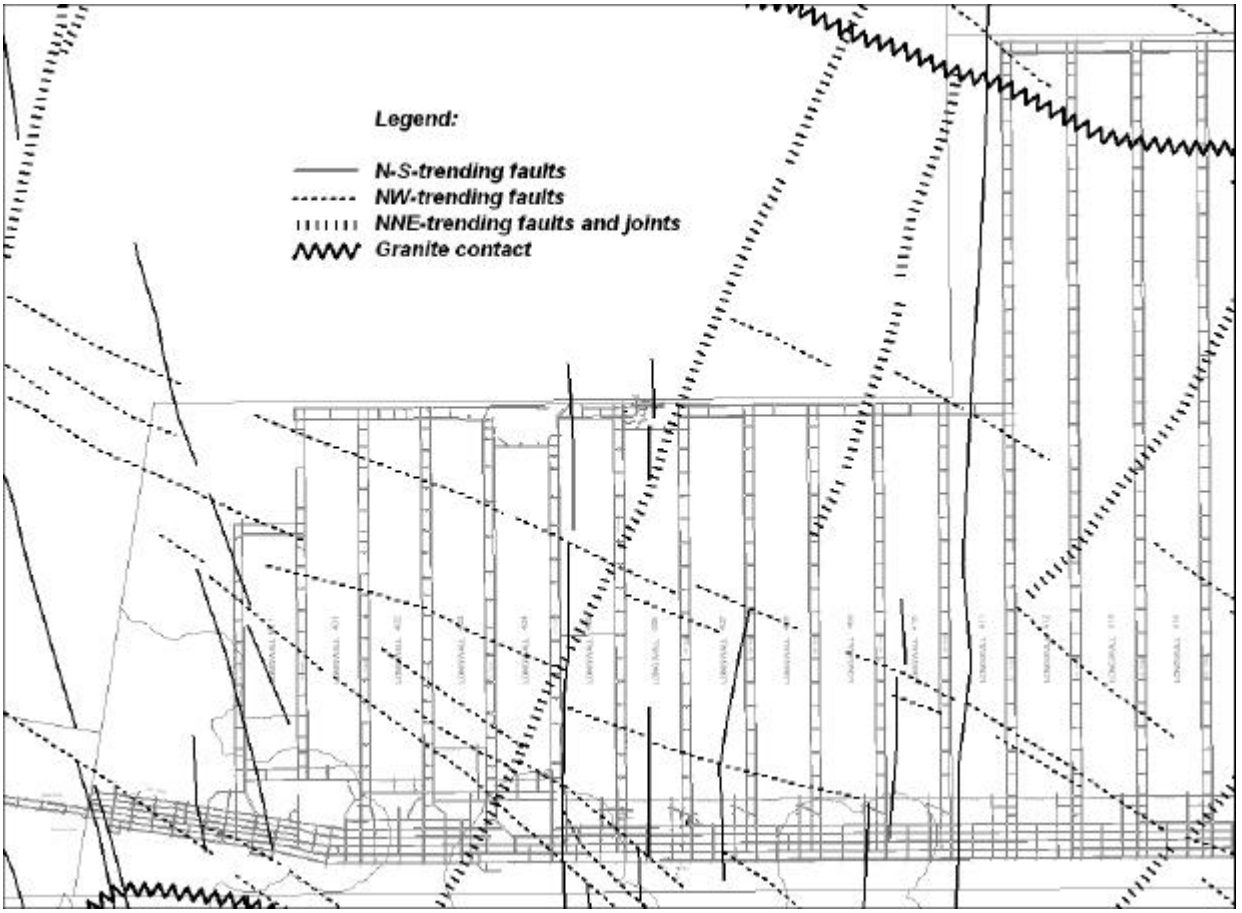

Figure 2 Stage I of the structural interpretation of the Springvale Colliery from regional synthesis and integration of magnetic, gravity and digital elevation data. The NNE trending faults are parallel to the Wolgon River linears and are strong surface features that are not common in the Seam.

stress created by the creation of the longwall or development roads, but takes into consideration the orientation of the structures only. To this end it can be used as a guide only to the ground conditions ahead of development.

Uncertainties in the location and dip of the interpreted faults have been accounted for by allowing a ±100m zone around the interpreted faults. This zone represents a locational uncertainty as a result of the resolution of the data used and the source depth of the faults that have been interpreted.

Historically, the N-S faults had the greatest risk of being associated with poor ground conditions at Springvale. The interpretation indicated that these faults were most likely to intersect WNW and NW striking faults where ground conditions deteriorated. This is consistent with the regional sinistral strike-slip movement on the N-S faults as a result of NNW compression in the Miocene to Recent.

The following risk classification scheme was adopted for Springvale.

- Areas of **highest structural risk** - (intersections and stepovers of N-S and WNW trending faults, other splays and geometric complexities on N-S faults). These areas appear to be the main cause of high stress concentrations and complex "lock-up" structures during strike-slip reactivation of the N-S faults.
- Areas of **high structural risk —** (intersections of N-S and NE trending faults, intersections of N-S faults and margin of basement granite). These areas were also thought to cause high stress concentrations and complex lock-up on a lesser scale than those caused by the WNW fault intersections.
- Areas of **moderate to high structural risk —** (intersections of WNW and NE trending faults, geometrically simple N-S trending faults, intersections of NE, WNW and the margin of basement granite). These areas are likely to represent zones of structural complexity during fault reactivation, but there was no information from pit mapping as a control.
- Areas of **moderate structural risk** - (NE trending faults). These zones are linear but were thought to represent some risk.
- Areas of **low to moderate structural risk** (WNW fault zones and margin of basement granite). Structures may be present but are unlikely to represent a high structural risk.
- All other areas were thought to have represented a **low structural risk**.

The main limitation of the interpretation and risk

analysis was the resolution of the magnetic data used in the interpretation. It was decided that the acquisition of higher resolution magnetic data was critical. This was achieved by a helicopter survey that could get closer to the source of the anomalies by flying lower and draping the irregular terrain.

TRIAL HELICOPTER-BORNE MAGNETIC SURVEY

To test the effectiveness of more detailed magnetic data, Geo Instruments were contracted to conduct the trial survey which was flown by helicopter at 50m line spacing for a selected portion of the lease area and at 25m over a smaller portion of the workings within the trial area. A number of enhancements of the data were attempted by Encom Technology and compared with the results from the 100m Wallerawang survey.

The improvement in frequency content and resolution was apparent from the new data, which was particularly apparent in the residual enhancements. The improvements achieved by the helimagnetic survey reflect both the lower flying height and the closer line spacing, however the 25m line-spaced data offered little improvement on the 50m data, largely as a result of microleveling errors apparent on the closer spaced lines.

The heli-mag survey introduced some terrain artefacts as a result of flying into deeper gullies and being significantly closer to the magnetic basement in the valleys or detrital magnetic material in the major drainage channels. These anomalies can be matched with the creeks in the digital terrain data and eliminated during the interpretation stage.

As a result of the trial survey it was concluded:

- helicopter-borne data would be effective in improving the structural interpretation, and that
- the optimum line spacing for Springvale would be 0-50m at a flying height that was considered safe by the pilot for that area (approximately 30m above the ground).

STRUCTURAL INTERPRETATION OF SPRINGVALE COAL – STAGE II

An interpretation at higher resolution was done by using the results of the Stage I interpretation and combining them with newly acquired 50m heli-magnetic data, which was flown E-W over the Springvale lease. An area of the interpretation is shown in Figure 3. The data acquisition and reduction was done by Geo Instruments. Quality control of the data and enhancement processing was done by Encom Technology. The data was put through a number of algorithms to remove the effects of regional gradients, remove the effects of larger basement features that have already been accounted for in the Wallerawang survey and enhance basement and surface magnetic features. SRK Consulting did image processing of the data to produce plans at 1:10,000 scale, the interpretation and risk analysis.

Because of the enhanced frequency information in the magnetic data, it was possible to differentiate between basement and surface signals with a higher degree of precision.

The objectives of this phase are to:

- build on previously completed geophysical interpretations to validate and further define the data,
- interpret structure zones within the basement, identify the surface and joint orientations and predict which of the faults were likely to intersect the Lithgow Seam within the Springvale Coal workings, and
- evaluate the factors that result in structural complexity and identify the structurally complex zones in the proposed Colliery plan that may contribute to geotechnical instability.

Calibration

Some calibration of the structure in the newer areas of development was done to correlate known structure with the magnetic data. The faults that penetrate the Lithgow Seam at Springvale commonly have only minor vertical displacement of the seam (of the order of 10's of centimetres), however the gouge zone that defines the fault may be up to 2m wide. The fault gouge is generally unwelded and locally contributes to poor ground conditions, however the faults more commonly mark boundaries to zones of higher horizontal stress. Wider zones of gouge and greater structural complexity occur where there are a number of parallel faults or where faults intersect and splay, particularly at the intersections of N-S and NW trending faults.

The small vertical displacements and relatively thick fault gouge present on the faults indicates considerable strike-slip movement on the faults in the seam. Early periods of normal and later reverse movement are likely to have been very minor compared to the strike-slip movement.

The well developed gouge zones at the intersections indicate likely dextral movement accompanied much of the gouge formation. Dextral fault movement on the N-S faults is consistent with approximately NE compression, which is most likely to have occurred during the Early-Mid Triassic Hunter-Bowen compression that inverted the Basin.

Intersections of N striking faults with NE striking faults would have been associated with less destruction since dextral movement would have assisted dilation on the NE striking faults rather than compression or crushing.

Interpretation of Magnetic Data

The magnetic data that is used for the interpretation

is sourced from:

- the magnetic basement or lower volcanic sequence of the Sydney Basin, and
- the near surface features (magnetic iron oxides in the weathered horizon).

The Illawarra Coal Measures and overlying sandstones have a very subdued magnetic signal that is not discernable against the basement and surface signals.

The interpretation identifies surface magnetic features and basement magnetic features and extrapolates to the (non-magnetic) Lithgow Seam. For any one fault system, a number of surface fault signals may be related to a single basement fault system (Figure 4).

-

Unless the faults are vertical, the basement signal will not overlap with the surface signal. The N-S faults at Springvale generally have a dip of 30-60° (both east and west), however the NW striking faults and NE striking faults are sub-vertical. The dip of the faults in the coal seam may be different to the overall dip due to refraction. It would be expected that a fault in a coal seam would have a shallower dip than in shale or sandstone.

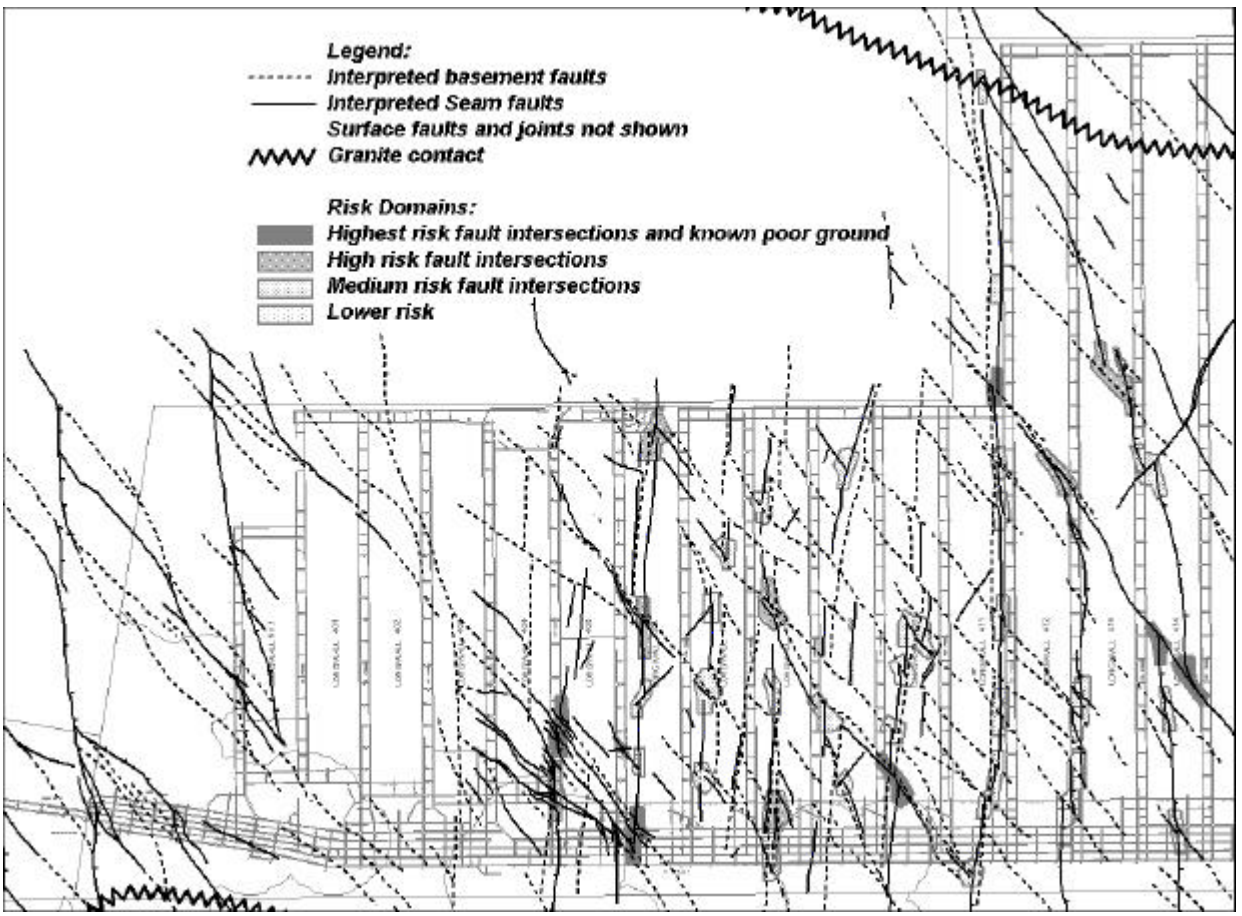

Figure 3 Stage II of the structural interpretation following acquisition of more detailed heli-magnetic data (E-W 50 metre line spacing). Note that the faults and joints interpreted to be at surface are not shown here. The faults that are shown here are interpreted to be in the basement and in the Seam (40–80 metres above the basement). Also shown are the fault intersections that are at risk of creating structural complexity that may lead to stress lock-up. Individual faults create few problems in the current mine. The individual N-S faults may form large zones of gouge that may be inherently unstable, but will not normally attract a stress anomaly.

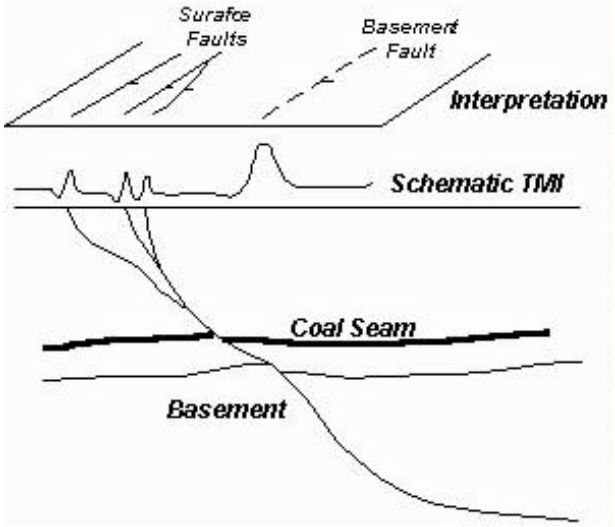

Figure 4 Schematic diagram illustrating the relationship between magnetic intensity (TMI) and the interpreted surface and basement fault zones. Faults will change dip across more or less competent beds and may splay and change strike with depth. The location of the faults that intersect the Lithgow Seam will be between that for the surface faults and the basement fault zone.

Main Findings of the Interpretation

The structural risk interpretation is based on a structural interpretation of the basement and a structural interpretation of the surface fault and joint features. From these layers, an interpretation is made for the Lithgow Seam, which is thought to lie approximately 100m above the basement and 200–400m below the surface.

The structural interpretation presented here has been separated into:

- an interpretation of the faults that are present in the basement and lower Sydney Basin sequence,
- an interpretation of the faults and joints that are present near surface (within the weathered horizon), and
- an interpretation (based on the above layers) of the basement faults that are likely to have penetrated the Lithgow Seam.

The penetrative fault directions interpreted for the Lithgow Seam are:

- N-S striking. May have formed initially as normal and then reverse faults but have subsequently been strike-slip reactivated (dextral),
- NW striking faults at the intersection with the N-S striking faults, where they would have produced compressional "crush zones" during dextral strike-slip movement, and
- NE striking faults (mostly east of current workings shown above), where they would have produced dilational "opening zones" during dextral strike-slip movement, which may have facilitated dyke emplacement in some areas.

The structural risk interpretation is used as a base model that is annually reviewed and recalibrated against further information derived from detailed pit mapping and in-seam drilling. Some aspects of the geotechnical risks cannot be addressed by this interpretation of the magnetic data. In particular, sub-horizontal faults in clay bands, roof lamination and floor lamination will not be resolved by this work. Other methods such as underground seismic refraction may need to be applied.

UNDERGROUND MAPPING

Detailed underground mapping, by Springvale geologists, has identified many geological structures (particularly small-scale faults) that can be correlated with zones of poor ground conditions. Prior to initiation of the forward modelling techniques, there was no effective technique for prediction of geological structure at Springvale, resulting in high roof support costs and lower production when zones of structural complexity interfere with development and mining schedules.

Springvale Coal has implemented a Strata Management Plan that prescribes the mechanisms for gathering details on, and monitoring of, the geological and geotechnical conditions encountered in the workings. Repetition of structural patterns in areas with similar basement terranes is likely given the similar geology and geological history of an area within the mine-scale. Therefore, mapping of structural features and correlation with ground conditions in development areas is essential to identify structure that can be used as a guide to future ground conditions and later mining conditions.

Geological and geotechnical mapping of development gateroads and the longwall face are undertaken on a routine basis. Geological structures that are regularly mapped are:

- penetrative faults (60 - 90° dip and up to 2 metres of gouge on faults that usually have only minor vertical displacement),
- non-penetrative faults (usually occur in claystone bands near the top of the seam and may locally concentrate areas of high horizontal stress) - locally referred to as "Greasyback faults",
- areas of intense jointing and joint swarms,
- swillies, and
- seam or ply thickness variations.

In addition, geotechnical ground conditions are monitored using observations of:

- roof conditions such as gutters, potholes, flaking and roof bolt conditions,
- rib conditions such as spall, soft patches, and
- floor heave.

All of which can be used to derive the direction of the primary and secondary horizontal stress directions.

Using the mapped geological and geotechnical

information from previous panels in conjunction with the predicted structures from the model, Springvale technical personal review the potential conditions of future development areas and assign Structural Risk Domains. These domains are then incorporated into the mine schedules so that development rates can be adjusted to accommodate any additional roof support that may be required.

STRUCTURAL RISK DOMAINS

The structural risk is based on intersections of fault zones that are known to contribute to high stress domains in the current and past mining areas. The structural model needs to be applied to development and mining design to establish geotechnical risk as distinct from structural risk.

Under the present day stress conditions (ENE directed maximum principal stress), the N trending and NE trending fault intersections are zones of lock-up.

Structural risk has been divided into four risk domains based on the intensity of the faulting reflected in the magnetic data and the intersection of the faults.

The **highest structural risk zones** identified are located at the intersection of the NS striking faults with the major NW striking faults. The individual faults on their own, although they may deform the coal seam, are thought to affect the mining conditions enough to slow the development rates.

Slightly **lower structural risk** is identified for second order NW-NS fault intersection. **Medium structural risk** is identified for third order NW-NS fault intersections. **Low structural risk** has been interpreted for:

- intersections of NW trending faults with NE trending faults,
- individual N-S trending fault zones,
- individual NE trending or NW trending fault zones,
- basement fault zones, and
- intersections between faults and joints.

All these structures and structural intersections have some risk associated with the presence of the structure, however many of these faults occur in the mine and have had no major adverse effects on

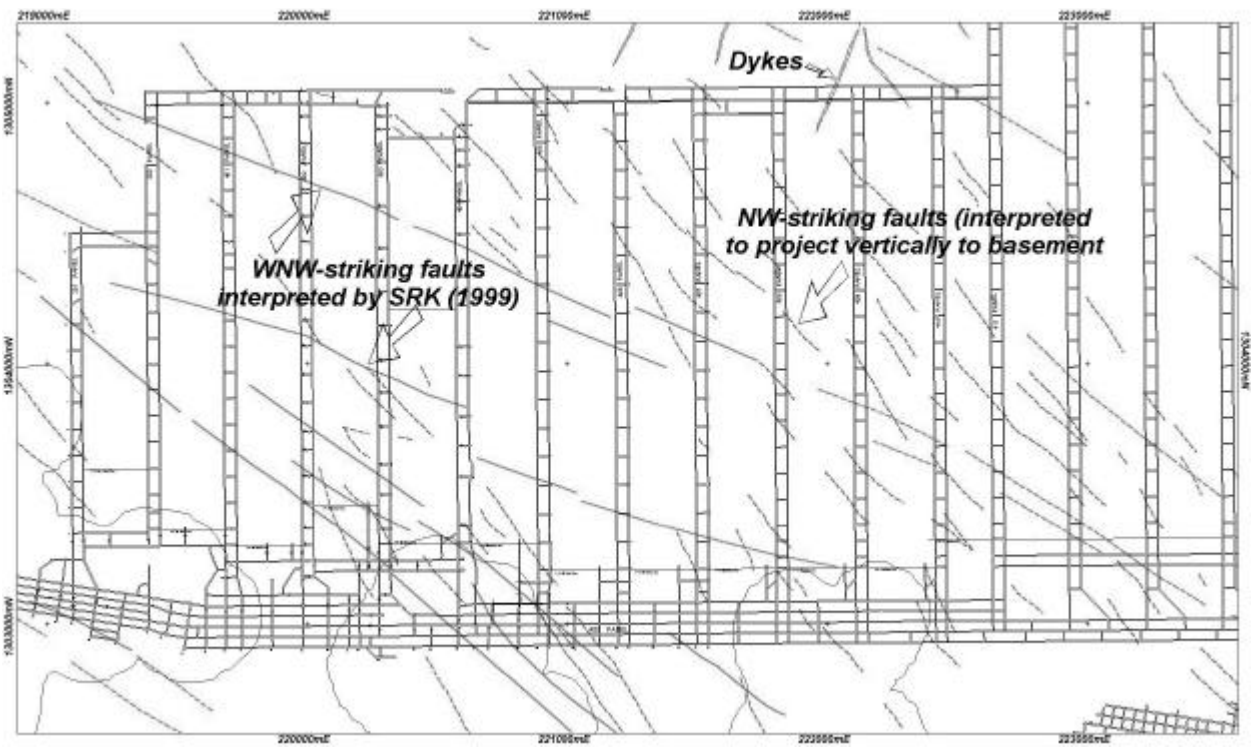

Figure 5 Integration of the interpretations done from different magnetic data sets. The WNW trending faults from the Stage I interpretation mark the boundaries of shorter strike-length NW trending basement faults.

development or production.

An important implication of this is that the interpretation from magnetic data has produced many fault and joint directions that are likely to create no major problem for development and a few fault intersections that need to be treated with caution.

COMBINING THE RESULTS OF ALL INTERPRETATIONS

Figure 5 illustrates the combined use of both the regional and detailed surveys in identifying the basement structure. The Wallerawang survey and interpretation (done at 1:25,000 scale) is most useful for identifying regionally extensive basement features. The detailed survey also picks up these features, however they are less readily discernible at the finer scale of the interpretation (1:10,000 scale).

The NW striking faults identified in this study are interpreted from surface and basement signatures to be steeply dipping.

The WNW striking basement faults have a stronger basement magnetic response than the NW striking faults. The WNW striking faults also tend to bound domains of NW striking faults. This indicates the NW striking faults may be slightly later, smaller scale faults that may have formed by dextral strike slip movement on the WNW faults. This would indicate a period of NW-SE or N-S directed compression prior to deposition of the Lithgow Seam. Subsequent reactivation of these basement faults and propagation into the Lithgow Seam would have occurred during a later event.

The regional interpretation and Stage I interpretation from the Wallerawang survey was important for identifying the setting of the Springvale area and identifying the major crustal breaks. Importantly, the interpretation identified N-S trending and NW trending faults as important features, which supported the pit mapping. The Stage II interpretation focused on the Colliery and had the advantage of being able to better identify the surface features from the basement features and make an interpretation of the structure in the Seam. The same fault intersections are considered high risk, ie. intersections of N-S faults and NW faults, however the more detailed magnetic data allowed better definition of the likely position of these intersections.

CONCLUSIONS

Routine geological and geotechnical mapping is undertaken at Springvale Coal as an integral part of the mine's Strata Management Plan. The results of the underground observations are regularly reviewed against the modelled structural zones to assess the effectiveness of the structural model and thus the Structural Risk Domains that had previously been predicted. To date the success rate encountering mappable structures within the predicted structural zones lies at approximately 75%. (Not all structures encountered have caused development problems, many have been small-scale fault zones that may have had a couple of additional roof bolts installed by the development crews. These structures have largely been intersected within the error margin of the model, approximately 20m each side of the predicted structure on the plans.) This is a far higher success rate than Springvale Coal ever had in the past and permits far more accurate prediction of zones of structural complexity.

Prediction of future hazard areas likely to be encountered in development and/or longwall panels can be undertaken with a high degree of confidence and prior warnings provided to the operational crews. In this way, if a predicted structure is actually intersected, or the general conditions (roof, ribs etc) change in any way, the mining operators are far more comfortable than they were with the old system when unexpected structures were intersected, often with disastrous results.

The ability to predict structures before actually intersecting them has resulted in Springvale Coal adopting a "Proactive" mining and support regime rather then a "Reactive" one as was the original situation. Overall the Structural Model has proven to be a highly successful hazard prediction tool and is contributing to the ongoing fortunes of Springvale Coal.

ACKNOWLEDGEMENT

The authors wish to thank the management of Springvale Coal for permission to publish the results of this study.

Geological hazards — The impact to mining 15-16 November 2001, eds Doyle, Moloney, pp 117-123

Geological Hazard Detection at Newstan Colliery – Methodologies and Outcomes

JOHN SHEEHAN[1] AND SCOTT THOMSON[2]

1 Geologist, Newstan Colliery, Powercoal Pty Ltd., 2 Principal, CoalBed Concepts Pty. Ltd.

Newstan Colliery is located approximately 30km southwest of Newcastle on the western side of Lake Macquarie (Figure 1). It is currently operating three development units and one longwall in the three to five metres thick West Borehole Seam. The seam occurs at the base of the late Permian Newcastle Coal Measures. Recent workings are shown in Figure 2. The mine has been affected by geological hazards, mainly dykes and faults, which tend to trend NW-SE, although other strike directions do occur. Dykes can vary in thickness both laterally and vertically, and faults commonly vary in throw over short distances along strike. The variability of the geology at the mine constitutes a risk to mining. Consequently, a range of geological and geophysical exploration methods have been tried to help manage that risk, with varying levels of success. This paper attempts to describe the application of the various methodologies and provide suggestions for improved future outcomes.

LOCAL STRATIGRAPHY

The West Borehole Seam represents the coalescence of the Nobbys, Dudley, Yard and Borehole Seams of the Lambton Formation at the base of the Upper Permian Newcastle Coal Measures. The seam thins from around 5m near pit bottom to around 3m in the southwest of the Newstan Colliery Holding.

Above the West Borehole Seam is a sequence of interbedded coal, shaly coal, coaly shale, tuff and claystone with intervening clastic channels up to 60m thick. These channels tend to thin to zero thickness towards the southwest such that the entire sequence from the top of the Hartley Hill Seam to the base of the West Borehole Seam consists of 30 to 40m of coal, shaly coal, coaly shale, tuff and claystone.

CURRENT EXPLORATION PRACTICE

Cored surface exploration boreholes are being drilled ahead of development on a nominal 500m by 500m grid. These boreholes enable the:

- calculation of resources and reserves,
- modelling of stratigraphy and coal quality,
- approximate definition of the boundary of the sill which intrudes the West Borehole Seam in the southwest of the Colliery Holding, and
- assessment of the geotechnical environment for mine planning, including:

– the nature and frequency of bedding plane partings,
– rock strength,
– groundwater quantities,
– in situ stress regime,
– in situ gas quantity and composition, and
– spontaneous combustion potential.

These holes have little chance of detecting steeply dipping faults with throw less than 10m and steeply dipping dykes. An evaluation follows of methods used in an attempt to detect these hazards ahead of development.

ADDITIONAL SURFACE DRILLING AND BOREHOLE-TO-BOREHOLE GEOPHYSICS

Non-cored, nominally vertical and coplanar surface exploration boreholes are now being drilled at 50 to 100m centres ahead of development along easements 500m to 1000m apart. These holes are routinely logged by geophysical methods to enable sufficiently accurate determination of apparent dips between boreholes. Fortuitously, the easements are approximately parallel with strike so faulting can be readily indicated by a change in apparent dip, although not all changes in apparent dip are necessarily due to faulting.

This approach will not detect dykes, or symmetrical horsts or grabens unless they are wider than borehole spacing (and not parallel to the easements). To explore for these hazards the holes have been left open for borehole-to-borehole geophysics (RIM or in-seam transmission seismic).

A change in apparent dip between NDB90 and NDB91 accompanied by an anomaly on the RIM tomogram between these holes was interpreted to be due to faulting. Faulting has now been intersected in Maingate 18 (net throw 1.3m) and Maingate 19 (net

throw 3.1m) and interpolated across the Longwall 19 block between NDB90 and NDB91.

This approach is only useful for the detection of hazards that intersect the plane(s) of boreholes. The likelihood of a hazard being detected is directly proportional to its strike length and to the angle with which its strike direction intersects the easements along which the holes are collared. The easements run at high angles to both the primary and secondary structural directions. As strike length appears to be directly proportional to throw this makes the larger hazards more likely to be detected, at least as far as faults are concerned.

Borehole-to-borehole geophysics is relatively useful for providing "yes/no" answers as to the presence of structures between individual boreholes. RIM relies on the seam wave propagation mode which assumes that the radio wave will decay in an even, consistent manner over a given distance for a given seam electrical characteristic. In principle, the RIM wave should be measured as a consistent strong signal between equally spaced boreholes. Any change to this implies that a seam anomaly exists. The down side to this is that even if an anomaly is detected RIM will not be able to determine exactly: where the anomaly exists between the boreholes, its magnitude, or what it is. The method will respond to faults, dykes, seam thinning, changes in roof/floor conditions, sedimentary changes in the coal and in-seam moisture variation. Cross-well tomography is not an option in a sedimentary sequence due to the mixing of propagation spreading factors (cylindrical in coal, and spherical in rock).

Cross-borehole and borehole-to-borehole seismic suffers from the same limitations as RIM in this configuration, but (in principle at least) should provide a theoretically sound cross-borehole tomography image.

From the application of downhole geophysics, borehole-to-borehole RIM and seismic at Newstan generally give a better understanding of the distribution of structure in the lease has been achieved, however definitive answers have proved elusive with either of the transmission geophysics methodologies.

EXTRAPOLATION FROM EXISTING WEST BOREHOLE SEAM WORKINGS

Faults

The strike length of most faults mapped in the workings is somewhere between one hundred and three hundred times their inferred maximum throw. This limits the confidence with which faults (or their absence) can be extrapolated. It is possible for a fault to be absent from Tailgate X and have a throw of more than 1m in Maingate X. For example:

- a fault of vertical displacement 1.3m in the Longwall 18 Installation Road and 1.7m in the sub-parallel "bleeder" had ceased to exist within 50m of longwall retreat, and
- a number of smaller faults do not extend further than two to four pillar widths (60 to 120m) within the South-West Headings main development panel.

Dykes

As can be seen from Figure 2, the dyke parallel with Longwalls 15 to 18 changes position at West Borehole Seam level by approximately 30m within the Longwall 11 block and within the Longwall 14 block. (This behaviour is fault controlled: the dyke appears to preferentially intrude one of two parallel fault swarms, presumably the better developed of the two at any given location). This makes extrapolation and even interpolation uncertain.

Elsewhere in the Newcastle Coal Measures and in neighbouring leases variable thickness dykes have proven a hazard to mining. Dykes that sill from 1-2m to >10m are a particularly major problem for longwall extraction.

EXTRAPOLATION FROM GREAT NORTHERN SEAM WORKINGS

Faults

Great Northern Seam to West Borehole Seam interburden thickness ranges from 100 to 200m. Where faults have been mapped in Great Northern Seam workings, it is possible to project them downward to West Borehole Seam level. This requires an average dip to be assumed and therefore is prone to error in position of the fault. Throw at West Borehole Seam level may or may not be similar to that at Great Northern Seam level.

Dykes

No dykes have been mapped in the Great Northern Seam workings, but this may only mean that they have not penetrated to this level. Therefore, it cannot be assumed that no dykes intrude the West Borehole Seam.

SURFACE GEOPHYSICAL METHODS

The surface in the Newstan area is dominated by either urban development or by moderately to heavily timbered bushland with localised slopes as steep as 1:1. Neither of these surface landscapes provides cheap or easy access for surface exploration. Other factors are the environmental sensitivity of the area, the presence of power lines and the presence of the Awaba State Forest (an Exempted Area under the Mining Act requiring Ministerial consent for exploration).

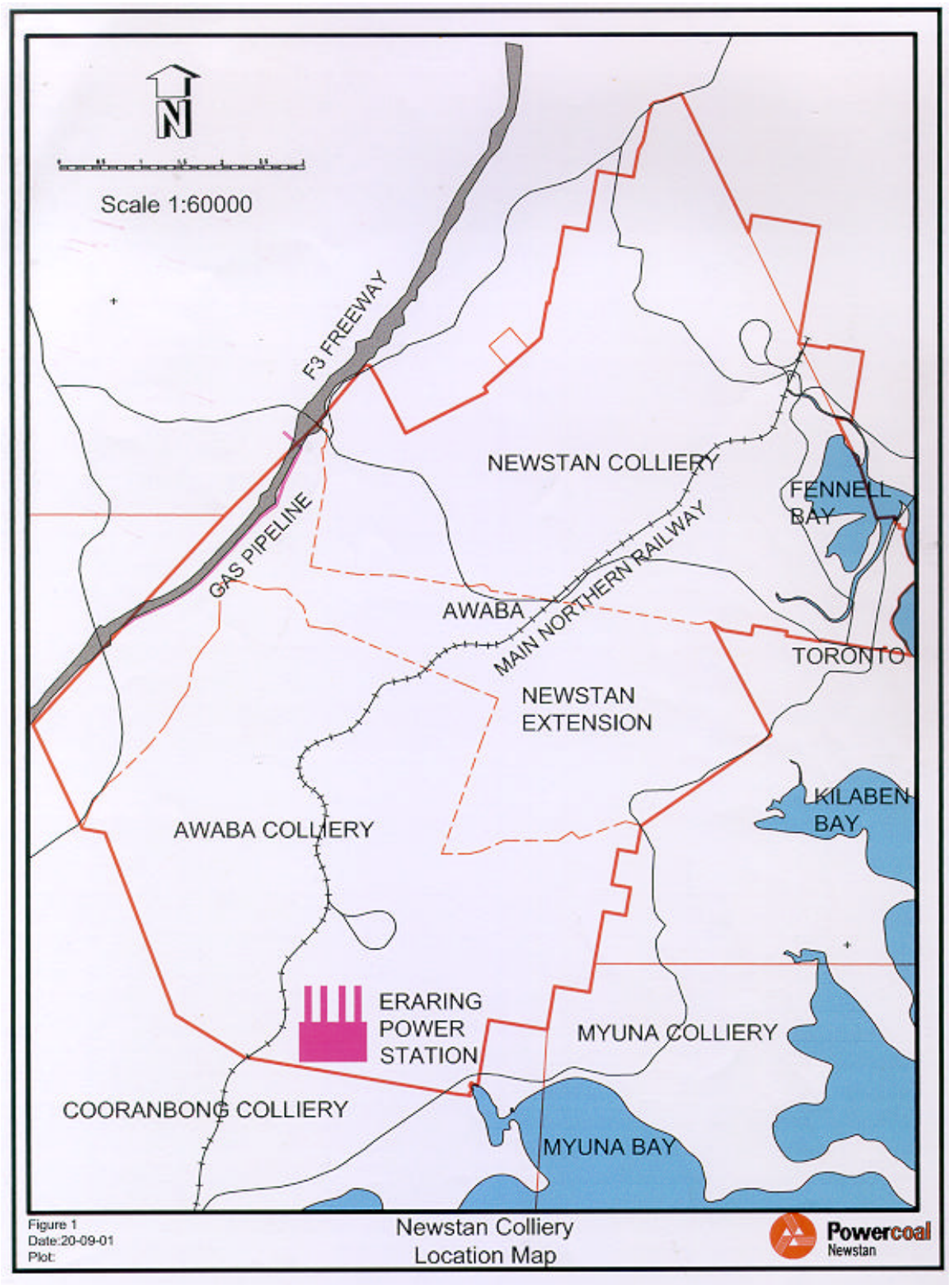

Figure 1 Location 9 Newstan Colliery adjacent to Lake Macquarie.

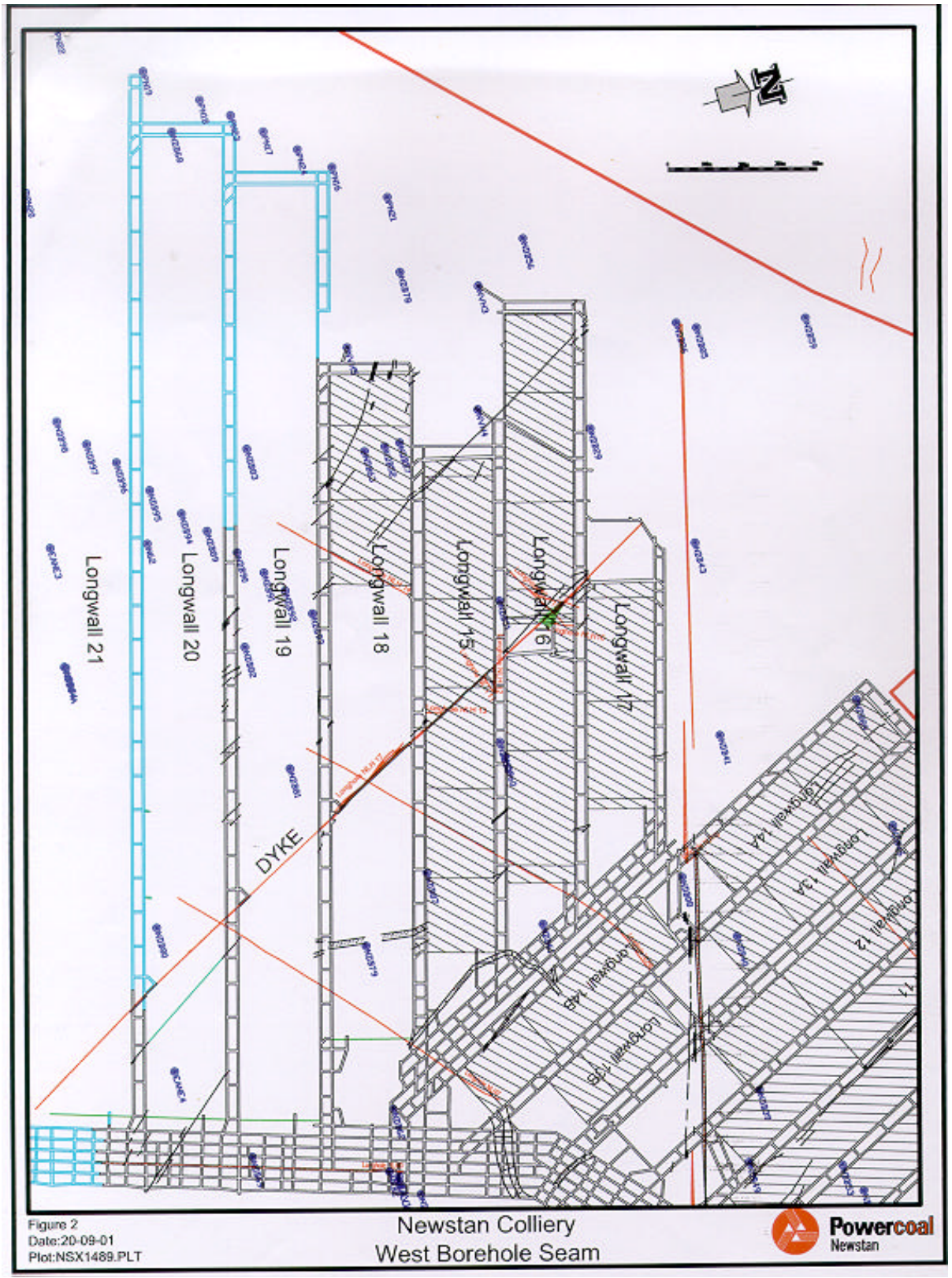

Figure 2 Newstan Colliery main working showing faults on in seam boreholes.

Stratigraphy and surface features are not conducive to the detection of faults and dykes by surface geophysics, particularly seismic. The West Borehole Seam overburden contains multiple energy reflectors, which make processing and interpretation of geophysical data difficult.

Surface magnetics is the traditional exploration method in the Australian black coal industry for the detection of igneous intrusions ahead of development. The dyke parallel with Longwalls 15 to 18 (secondary structural direction) is evident from airborne magnetics (Geoterrex Pty Ltd, job 1-334,1987 and reprocessed by SRK Consulting, 6/9/1999). The dyke parallel with Longwalls 9 to 14 (primary structural direction) is transparent even to ground magnetics (Ultramag Geophysics Pty Ltd, job 5001, 14/4/1999). This is despite the fact that high magnetic intensities (average $2{,}500 \times 10^{-5}$ SI) were measured on lump samples of this dyke. The transparency of this dyke to magnetics can be attributed to any combination of the following: noise from magnetically susceptible pebbles in near surface conglomerate, deep magnetic weathering, and/or failure of the dyke to penetrate close to the surface. Under more favourable conditions ground magnetics is capable of detecting dolerite dykes thicker than 1m at depths of up to 20m (Philip McClelland, Ultramag Geophysics, personal communication).

IN-SEAM DIRECTIONAL DRILLING (LONGHOLES)

Twelve longholes have been drilled at Newstan Colliery. The first four of these were drilled by ACIRL, two were drilled by Valley Longwall Drilling and the remainder by ACDrill. The methods and the equipment were essentially the same, whoever drilled the borehole.

The main limitation on this method of exploration is its effective range. Effective range can be defined as the in-seam distance from the collar within which coal/non-coal contacts can be plotted with sufficient accuracy to detect hazards deemed to be significant for mining. This in turn depends on four main factors:

- nature and magnitude of hazards deemed to be significant for mining (ease of detection is directly proportional to magnitude and for faults is dramatically reduced for throws less than seam thickness),
- identification of lithology (coal or non-coal) being drilled as determined from rig behaviour and cuttings return,
- survey accuracy, and
- number of deliberate roof/floor marker band intersections.

The effective range may be less than half the rated range of the drilling rig, depending on the above factors.

In-seam borehole NLH14 failed to detect the fault zone of throw one to two metres shown intersecting it in Longwall 18. This fault zone has been interpolated to intersect NLH14 approximately 360m from its collar. Roof/floor contacts were on average 70m apart, too far to enable the detection of a fault of 1-2m in a 4m seam.

In-seam borehole NLH8 failed to detect the one to two metre thick hard white igneous dyke shown intersecting it in Longwall 18. This has been attributed to the longhole passing over the top of the dyke in an area where the dyke did not penetrate to the roof of the seam. In-seam borehole NLH7 did not detect this dyke either. NLH7 intersects the projection of the dyke in the proposed Longwall 20. As this is yet to be mined the geometry and nature of the dyke is unknown here.

In-seam borehole NLH15 failed to detect the stockwork mineralisation associated with this same dyke in Longwall 16. This can be attributed in hindsight to the failure to drill more branches and take more cores. Data from NLH15 was taken into account when a decision was made to cut the dyke with the shearer rather than pre-mine it as in Longwall 15. The shearer was able to efficiently cut the dyke itself, but was unable to efficiently cut the surrounding zone of stockwork veins and mineralisation. This led to a decision to move the longwall outbye of this zone. This involved driving another installation road to intersect the tailgate outbye of the dyke and then mining out the mineralised zone in front of the longwall supports with a roadheader to enable the supports on the tailgate side of the zone to be relocated to the new installation road. The shortened face (on the maingate side of the zone) was then retreated to link up with the supports and AFC already installed on the new installation road. Clearly, this was a more expensive exercise than a pre-planned relocation around a previously known hazard.

Longhole drilling is a relatively expensive technique, and in the case of exploration drilling, multiple branches (and cores) are required to enhance the flow of information (which all adds to the cost). In addition, the different skill level of individual drillers introduces an unwanted variable in the process. Whilst the technique does in general deliver useful exploration data, the kind of problems experienced at Newstan may be repeated until seam roof and floor levels can be surveyed at an accuracy approaching that achieved in surface boreholes. This may be achievable in the future by quantitative continuous drill rig monitoring similar to open cut blast hole drilling or by the application of downhole geophysics or by a combination of the two.

Contract drilling companies are also essentially experienced in gas drainage drilling, and the different requirements of exploration drilling are not always met with enthusiasm. The price per metre is essentially the same whether drilling for gas drainage or exploration yet the care and attention to detail required is markedly different. This suggests that exploration drilling requires specialist skills and equipment, and a different pricing structure in order for real improvements to be made.

ROADWAY TO ROADWAY RADIO IMAGING METHOD (RIM)

A RIM survey of the Longwall 16 block or at least that part of it containing the dyke may or may not have alerted the mine to the abnormal nature of the dyke in this block. Although the dyke was to be (and now has been) pre-mined in the Longwall 18 block it was decided to conduct a RIM survey of the part of this block containing the dyke. It was hoped that a RIM signature could be matched with the geometry and nature of the dyke as mined and any variation from this RIM signature in the future would signify a variation in the geometry and nature of the dyke from that in Longwall 18. Although the survey successfully detected an anomaly in the part of the block containing the dyke there was no signature specific enough for the purpose intended (Geophysics Australia Pty Ltd reference PC661, 15/12/2000). This exercise was repeated for Longwall 19 using different fan angles. Results were similar (Sub-surface Imaging reference PC771, 2/9/01). Whether a sufficiently different tomogram would have been generated from Longwall 16 will never be known.

The RIM technology used in the Longwall 18 and 19 surveys is essentially 10-year old ("RIM II"). Whilst the results of the surveys are valid, there is clearly a need for improved resolution and improved imaging techniques. Development is currently underway of a RIM IV system in the USA, and prototype trials have been carried out. Essential to the improved system is phase coherence, a means of ensuring greater range for any given frequency and higher resolution. In addition, imaging methods have improved from the 'straight ray assumption' used in ART and SIRT based algorithms, to algorithms that take into account the refraction and reflection of RIM rays. The result is improved resolution, and the real possibility that the objectives discussed above can be met. The RIM IV system is due to be submitted for Department of Mineral Resources approval early in 2002.

FINANCIAL DISCUSSION

The potential financial impact of a geological hazard is generally directly proportional to its size.

The cost of detection of a geological hazard before mining is generally inversely proportional to its size. Therefore, the bigger the hazard the greater its financial impact, but the cheaper it is to detect before mining.

There must be some lower limit to the size of a hazard worth detecting before mining. This limit would be a financial cut-off which can be expressed as follows:

A = cost to mining if hazard Z known before mining,

B = cost to mining if hazard Z unknown before mining (a "surprise"), and

C = (B minus A) is the maximum justifiable expenditure for detection of hazards like Z.

In the case of Longwall 16:

A = cost of relocating longwall around known dyke eg Longwalls (13 and 14) including drivage of second installation road, and

B = actual cost of relocating Longwall 16 around dyke including drivage of access roadways, second installation road, and roadheader drivage.

For small hazards B is unlikely to be much greater than A so C is likely to be small. While A and B may be difficult to estimate it can be said with some confidence that the cost of detecting isolated faults of throw 0.1m would exceed C. Conversely, it can be said with confidence that the cost of detecting isolated faults of throw greater than working height would not exceed C. Finding an optimum level of exploration expenditure somewhere between the extremes illustrated by this example is the challenge facing many coal mining geologists.

Of course the potential impact on safety of geological hazards must also be taken into account, but this is even more difficult to quantify than financial impact.

Powercoal is continuing to reduce the amount of uncertainty in mine planning at Newstan Colliery by using traditional methods within the limitations imposed by the geological, geographical and human environment. The company is also supportive of innovative technologies with the potential to improve this process. If surface access was easier and cheaper the spacing between planes of surface boreholes with borehole to borehole geophysics could be reduced to decrease the interpolation distance between planes and therefore increase the confidence in the interpretation.

CONCLUSIONS

Identifying geological structure in the West Borehole Seam for improved longwall mine planning is clearly a difficult task. Many of the established geological and geophysical techniques have been tried with mixed results. There is no easy 'magic bullet' solution and it is certain that geological 'surprises' will continue to occur in the future. The challenge is to limit the magnitude of these surprises and therefore their impact on mining.

The best prospects for improved hazard detection in the future include enhanced RIM developments (RIM IV) and geophysics in horizontal boreholes. However, these techniques still require considerable time for development and approval.

ACKNOWLEDGMENTS

Information on the RIM IV developments in the USA has been provided by the inventor and founder of the technology, Dr. Larry Stolarczyk. Powercoal has kindly provided permission to discuss the specific geologic features of Newstan Colliery, and the author's are grateful for the opportunity to do so.

REFERENCES

GEOTERREX PTY LTD. Job 1-334,1987 and reprocessed by SRK CONSULTING, 6/9/1999.

ULTRAMAG GEOPHYSICS PTY LTD. Job 5001, 14/4/1999.

GEOPHYSICS AUSTRALIA PTY LTD. Reference PC661, 15/12/2000.

SUB-SURFACE IMAGING. Reference PC771, 2/9/01.

Geological hazards — The impact to mining 15-16 November 2001, eds Doyle, Moloney, pp 127-140

Lessons learnt from highwall mining instabilities

BAOTANG SHEN AND MARY E. DUNCAN FAMA

CSIRO Exploration and Mining, PO Box 883, Kenmore, QLD 4069

Highwall mining methods have been used in Australia for 10 years. Apart from the significant success of using this method to mine millions of tonnes of coal in 15 mines, a number of major roof/panel failures have been experienced, caused by various reasons, including the lack of comprehensive understanding of the mine geology in the mining reserve. This paper summarises the major highwall mining instabilities experienced in the past and the lessons learnt from these instabilities. A detailed case study on a panel failure at Yarrabee Mine is presented.

INTRODUCTION

Highwall mining is a remotely controlled mining method that extracts coal from the base of an exposed highwall, typically via a series of parallel entries driven to a significant depth within the seam horizon. The method has the advantage of low capital cost and less lead time compared with a full underground mine, while being capable of producing in excess of 1 million tonnes per system per year.

The highwall mining method is sensitive to the geological and geotechnical conditions in the mining reserve. The success of a highwall mining operation relies upon the stability of individual entries (span and pillar) and the stability of the mining panel. The common problems encountered during highwall mining operations include:

- Roof falls,
- Soft and muddy floor,
- Major geological structures, such as fracture zones, fault etc,
- Seam discontinuity,
- Pillar instability,
- Panel failure, and
- Highwall/lowwall instability.

All the above problems are associated with local and regional geology in the mining reserve. For instance, roof falls are often a result of weak roof material and intensive jointing in the immediate roof. Seam discontinuity is primarily caused by faulting in the mining reserve.

During the past 10 years, several major instabilities occurred during or after highwall mining (Shen and Duncan Fama, 1999). The instabilities caused burial of continuous miners, sterilisation of mining resource and/or damage to environment.

This paper presents a summary of the major highwall mining instabilities in Australia and a recent case study of Yarrabee highwall mining panel instability.

MAJOR HIGHWALL MINING INSTABILITIES IN AUSTRALIA

During the last 10 years of highwall mining operations in Australia, there have been at least 8 major panel failures and 3 major roof collapses in different mines during or after highwall mining, which have caused loss of time, mining equipment, and/or mining resource. The major roof or panel failures are summarised in Table 1.

At least 4 of these failures were a direct result of insufficient understanding of the geological and geotechnical conditions in the mining reserve. They were: panel failures of Pit P South and Pit C at German Creek Mine, panel failure of the Trench Pit at Ulan Mine, and localised panel failure of Pit B at Yarrabee Mine. A brief description of the first three failures is given below. The failure at Yarrabee Mine is discussed in details in the next section.

Panel failure at Pit P South, German Creek Mine

Pit P South was mined initially using a radial layout with 1 degree separation angle between entries. The size of the pillars at the highwall was initially set to be 2.0m and 5 entries were mined using this pillar size. Because of signs of pillar stressing, a 5.5m barrier pillar was left between Entries 5 and 6, and from Entry 6 onward the pillar size was increased to 3.5m. When Entry 16 was being mined, a panel collapse occurred over the whole mined area and consequently buried the continuous miner. Pit P South highwall was benched. Surface cracks and subsidence extended back a distance of about 50m from the highwall. It appeared that the failure initiated at a penetration depth of 20-30m.

Back-analyses conducted for this failure (Shen and Duncan Fama, 1999) suggest that the collapse of the panel was due to three factors:

Mine/Pit	Description of failure	Consequence	Main causes
Oaky Creek Pit G6 (Auger)	Highwall failure of a length of 10-15m.	Auger was damaged	Pillar failure due to misalignment of auger holes. (Adie, 1993)
Oaky Creek Pit G5 East	Roof collapse to a height >2m at 100m inbye	Continuous miner was buried.	Collapse of two narrow pillars (width=1.0-1.5m) between three entries; weak laminated roof. (Shen and Duncan Fama, 1999)
Moura Pit 17DU South	Roof collapse to a height of 2-3m at 180m inbye	Continuous miner was buried.	Converge of three entries results in an unsupported span of 10-11m. (Shen and Duncan Fama, 1999)
Moura Pit 16BL	Panel failure of 20 entries during mining	Continuous miner was buried.	Pillars were heightened due to coal falls from roof; stress concentration beneath benched highwall. (Kelly et al, 1998)
Moura Pit 17DU Central	Panel failure of 40 entries after mining	No damage	Undersized pillar in the radial layout (Shen and Duncan Fama, 1999)
German Creek Pit A	Panel failure of 12 entries during mining	No damage	Cut-throughs and reduced barrier pillar size (Follington et al., 1996).
German Creek Pit P South	Panel failure of 16 entries during mining	Continuous miner was buried.	Weak floor and stress concentration beneath benched highwall (Shen and Duncan Fama, 1999)
German Creek Pit C	Panel failure of 10 entries during mining	No damage.	Intensive inclined coal joints weakened the pillar (Highwall Mining Services, 1997b).
Ulan North-West Pit	1. Major roof falls at 200m inbye during mining; 2. Panel failure of 50 entries a year after mining	1. Temporarily trapped continuous miner; 2. No damage	1. Stress release near free wall; blast damage; (Shen and Duncan Fama, 1999) 2. Entries filled with water, time effect. (Highwall Mining Services, 1999)
Ulan Trench Pit	Panel failure of 130 entries 6 months after mining	No damage	Coal strength was overestimated; Presence of a regional lineament in the mining reserve; Time effect. (Shen et al., 2000)
Yarrabee Pit B	Panel and highwall failure over 12 entries after mining	No damage	Alteration of local roof bedding, time and water effect. (This study)

Table 1 Summary of recorded major highwall mining instabilities in Australia

- Weak floor. Weak claystone was found in the seam floor in two boreholes near the southern endwall.
- Stress concentration beneath the benched highwall. Due to stress redistribution after highwall excavation and possibly blast damage, particularly in part of the lower bench, the vertical stress in the coal seam under the bench was elevated. Modelling indicated the vertical stress to be significantly higher (approximately 15%) than it would be as calculated using overburden depth. This stress elevation was not considered in the design.
- Weak roof. The roof of the seam was found from some boreholes to be very weak and possibly sheared. When drilling the seam after the failure, no roof core could be recovered.

Panel collapse in Pit C South, German Creek Mine

Pit C South was mined using a radial layout with 0.7° separation angle between entries. The designed pillar width was 2.3m. The pit highwall was benched. On December 7, 1997, after 10 entries had been mined, a collapse of pillars between Entries 1-10 occurred. As a result, the overburden sandstone subsided over a length of approximately 60m of the highwall face.

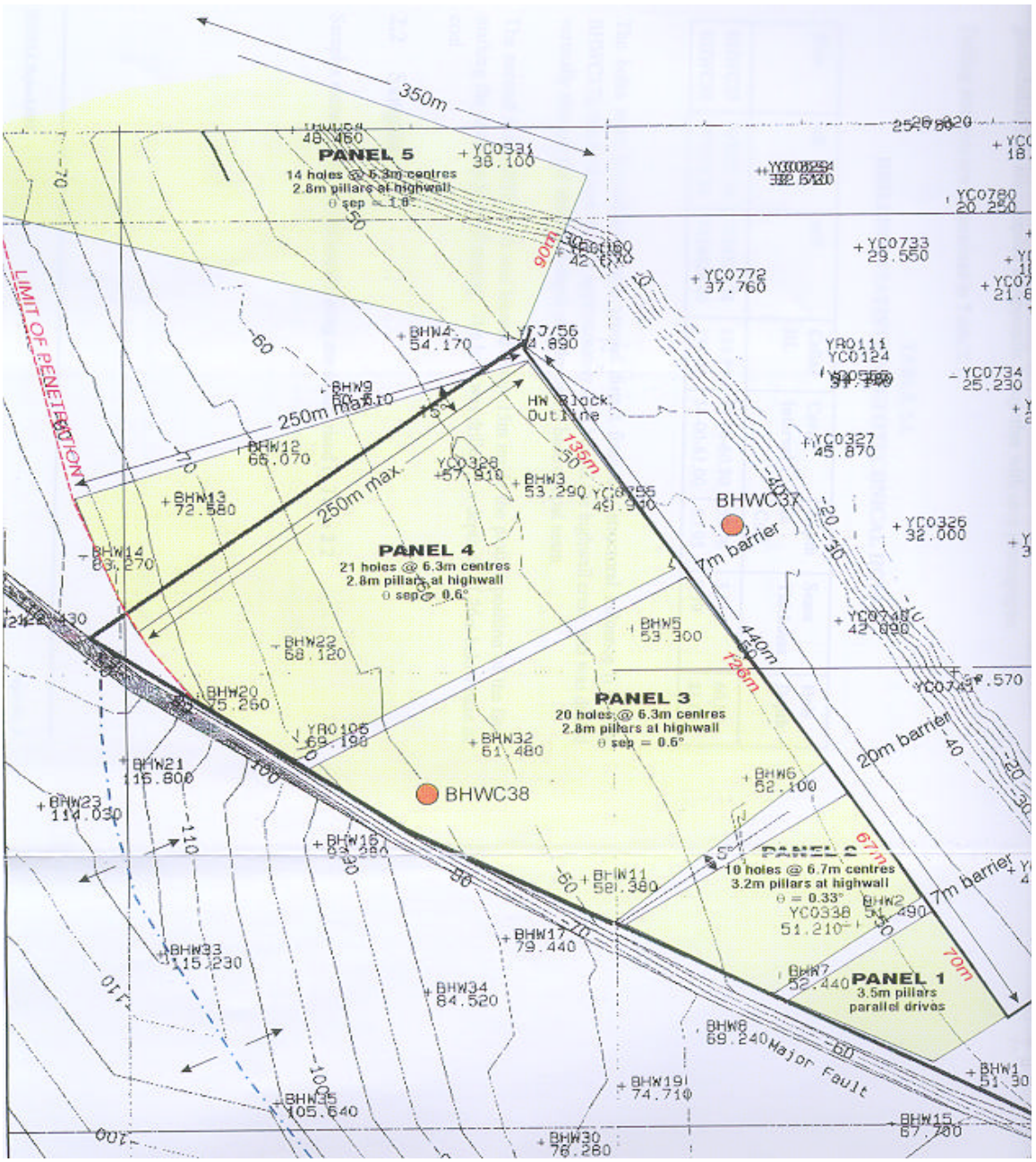

Figure 1 Highwall mining panels and design specifications, Pit B, Yarrabee. (After Highwall Mining Services, 1997a)

A study conducted by Highwall Mining Services (1997a) suggests that the failure was mainly due to the presence of intensive joints in the coal seam. Numerical analyses conducted during that study show that the strength of coal pillars would have been reduced by 50% because of the intensive coal joints. The original design did not consider the effect of the joints, and hence appeared to have resulted in undersized pillars. In addition, the failure line coincided with a dyke in the pit reserve, suggesting that major rock structure may have contributed to failure.

Panel collapse in the Trench Pit, Ulan Mine

A highwall mining panel failure encompassing up to an estimated 119 entries occurred in HW3 Trench of Ulan Mine on the 18th of March 2000. The event occurred about 6 months after the last entry of the panel was mined. The panel covered a total of 119 entries along a length of 700m of highwall. Based on the survey of the surface cracks, it is believed that the failure initiated between Entries 40-70 at a penetration depth of approximately 240m.

Mining difficulties due to roof falls and water were encountered in Entries 20-40. The locations of the entry termination due to roof falls etc. coincide with a regional lineament.

A study conducted by CSIRO (Shen et al., 2000) suggests that the panel failure in HW3 Trench was a result of a combination of the following factors.

- The actual mass coal strength was lower than the value used in design. A mass coal strength of 5.9MPa was estimated for the DWS seam (10MPa was used in design). In the vicinity of the lineament the strength could be further reduced.
- Variation in pillar width during actual mining. Actual pillar sizes varied significantly and this was found to reduce the panel Factor of Safety (FOS) by 14% from the design FOS.
- Effect of time and water inflow on pillar strength. The time dependent deterioration of pillar strength is believed to have been accelerated by water in the entries. The time dependent strength reduction may have been sufficient to trigger the panel failure. Coal roof falls resulting in heightened pillars.
- Increased mining cut height. It is likely that the mining height was higher than the designed mining height due to the limited horizon control of the highwall mining system. The increased mining height could have reduced the FOS.
- Possible existence of areas of intensive jointing in the coal seam.

CASE STUDY OF PANEL FAILURE AT YARRABEE MINE

Description of the failure

A highwall mining trial was conducted in Pit B at Yarrabee Mine in late 1997 to assess possible fullscale deployment of highwall mining in the mine.

Pit B is a highwall block bounded to the south and west by regional faults. A total highwall length of about 550m is available for mining, including an angled end forming the northern pit boundary (Figure 1). The mining operations in Pit B were conducted by MTA Pty. Ltd. using a Continuous Highwall Mining system (CHM). A total of 67 entries were mined in this pit in a time span of about 6 weeks. The penetration distance achieved was on average about 100m, far shorter than the planned maximum penetration depth of 350m. Various problems including roof falls, soft floor, and gas problems contributed to the poor performance. Despite these problems, the highwall mining panels were observed to be stable during mining.

The mining operations stopped after completion of Entry 67. The pit gradually filled with water after the pit was closed, and by August 1998, all mined entries were submerged in water.

On the 12th of January 1999, a localised panel failure occurred in the middle section of the pit (Figure 2). The failure extended about 80m along the highwall and 50m into the highwall. The whole process of failure was observed by Mr. Matthew McCauley, Operations Superintendent at Yarrabee Mine. Based on his description, the initial failure occurred in a time span of about 5 minutes. The subsidence was fully developed in a period of two weeks.

Pit Geology and mining record

Pit B highwall has a SE-NW orientation, and it extends about 455m in total. The height of the highwall is about 50m. There is a bench about 15m wide 10m below the top of the highwall.

The overburden stratigraphy is typical Rangal Coal Measure sedimentary sequence comprising clayey siltstones, massive to well-bedded, with sub-dominant labile fine-grained sandstones and claystone. A simplified core log is shown in Figure 3, based on the core log from Borehole BHWC37 (Highwall Mining Services, 1997a).

The immediate roof comprises a 0.8m thick claystone, silty, weak to moderately strong, and is gradational with coal at the fused roof contact. Bedding planes in the roof strata are planar and rough. Bed thickness in the roof is 10cm to 35cm. In the area of failure, roof bedding planes are observed to dip toward the seam at an angle of approximately 15° (Figure 2). This feature however, was not reported in the design report (Highwall Mining Services, 1997a)

The seam has an average thickness of about 4m. It

dips to SE with an average dip angle of 8°. The seam comprises dull, to dull and bright banded compositions in roof and floor plies for a thickness of about 0.8m. The central seam is bright banded. A weak, carbonaceous mudstone band, about 0.02m in thickness, occurs about 0.4m below the seam roof.

The most significant structural feature in this pit is the relatively frequently occurring planar slickensided joints observed in the upper to mid plies of the coal seam. The joints dip about 35° to the south along the highwall. The intensive coal joints are persistent within the seam and most of them extend to the roof and floor.

Highwall mining operations started from the southern end of the pit and progressed to the north. The whole reserve was mined in four panels (see Figure 4). Panel 5 shown in Figure 1 was not mined. The pillar size and layout as designed and used in each panel are listed in Table below.

Panel No.	Layout	Pillar width at highwall	Entry No.s
1	Panel entries	3.5m	1-10
2	Fanned Layout with a radial angle of 0.33°	3.0m	11-20
3	Fanned layout with a radial angle of 0.58°	2.8m	21-40
4	Fanned layout with a radial angle of 0.58°	2.8m	41-67

Barrier pillars were left between panels. The size of the barrier pillar at the highwall was 7m, 13m and respectively between panels 1, 2, 3 and 4.

A total of 67 entries were mined. The penetration depths of the entries are shown in Figure 4. Frequent roof falls occurred in Entry 43 and the subsequent entries. As mining advanced the roof falls occurred closer to the highwall. The roof fall problem appeared to have been associated with the change in bedding planes from parallel to the seam to dipping down onto the seam, as indicated in Figure 2.

It should be emphasized that major roof falls occurred in entries from #43 onward. The subsided area appears to be right behind the area where major roof falls occurred during mining.

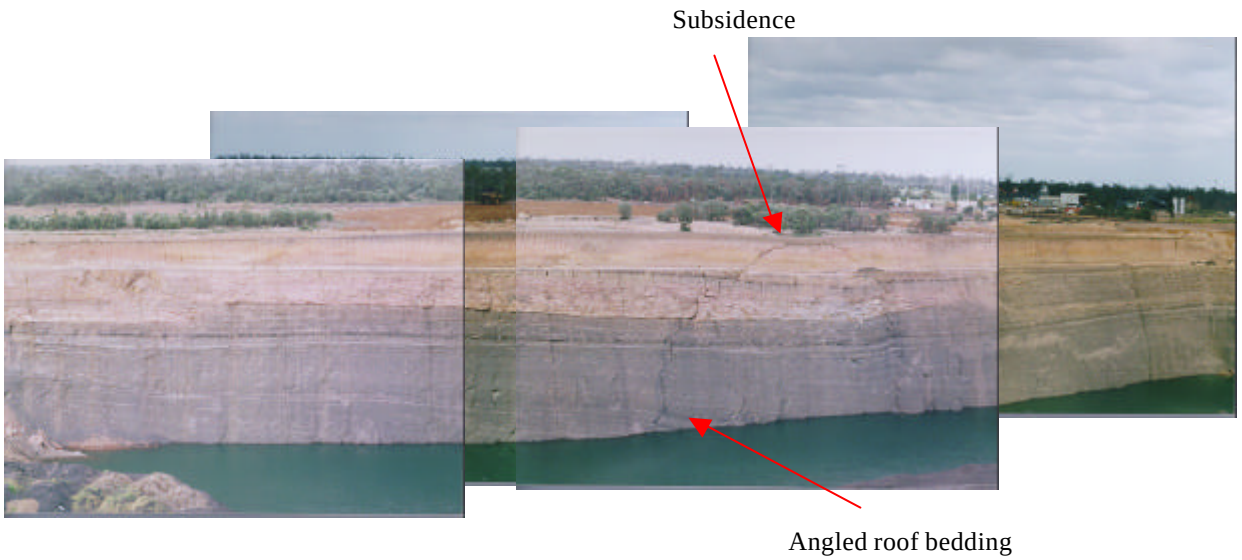

Figure 2 Highwall face and a panel failure at the mid-section of the highwall, Pit B, Yarrabee Mine. Angled roof bedding planes are noticed at the area of failure.

Back-analysis of the observed panel failure

The subsidence extended about 80m along the base of the highwall between Entries 33-43 and 50m into the highwall (Figure 4). The area covered nearly half of Panel 3, three entries in Panel 4, and a barrier pillar between the two panels. The barrier pillar had an initial width of 7m at the highwall but narrowed to 3.9m at a penetration depth of 50m due to the radial entry pattern in both Panels 3 and 4.

It is surprising that the subsidence occurred right above a barrier pillar, although this barrier pillar narrowed to close to the normal pillar width at about 50m inbye.

Limit Equilibrium Method and numerical tool UDEC (Itasca, 1996) analysis were used in the back-analysis. UDEC models were used to investigate the stresses under the highwall, span stability, and the strength of pillars of different widths. Limit Equilibrium Method was used to evaluate the FOS of the panel. In the numerical models, the simplified geology shown in Figure 3 was used, except that the thin mudstone floor was modelled as a weak interface.

COAL STRENGTH, ROCK PROPERTIES AND IN SITU STRESSES

Coal strength

Seven core samples from Pit B had been tested for the uniaxial compressive strength (UCS) and elastic modulus (Highwall Mining Services, 1997a). Results are summarized in Table 2.

It is known that the in situ pillar strength on mass is much less than that of samples in laboratory size due to size effect. The mass coal strength for the Yarrabee seam is estimated using the CSIRO's method to be 3.0MPa. This is compared with a mass UCS of 3.6MPa used in the design (Highwall Mining Services, 1997a). Note that a mass coal UCS is the uniaxial compressive strength of a cylindrical coal mass. It differs from the cubic mass coal strength, which is more widely used in literature. It has also been reported that the mass coal UCS is typically 20-30% less than the cubic strength (Townsend, et al 1977).

The intensive and inclined coal joints in the seam may have had a significant effect on pillar strength. They were considered in the original design and have been considered in this study as well.

Rock properties

The strength and elastic properties of roof and floor rocks have not been tested, nor were any interface or joint properties available. For the purpose of numerical modelling, these material properties have been estimated mainly based on geological descriptions and previous modelling experience. The material properties used in this study are listed in Table 3.

In situ stresses

Stress measurements were not carried out at Yarrabee Mine. Low horizontal stresses were suggested by Highwall Mining Services (1997a). In this study, it was assumed that the ratio of principal horizontal stress to vertical stress was $\sigma_h/\sigma_v = 0.33$ in the direction parallel to the highwall, and $\sigma_H/\sigma_v = 1.0$ perpendicular to the highwall, as it is close to the normal direction of the regional fault. These stress ratios were assumed to be the same in both coal and other rocks, prior to the excavation of the highwall.

Stresses in the vicinity of the highwall

Previous studies (Kelly et al., 1998, Duncan Fama et al., 1999) suggest that stress concentration could occur near the highwall face due to the effect of an overlaying bench, and could lead to elevated stress in the coal seam beneath the bench. The possibility of a high stress in Pit B at Yarrabee Mine was investigated. A 2D numerical model simulated a cross section perpendicular to the highwall prior to highwall mining extraction. The highwall profile in the area of subsidence was used. In this model, intact rocks and coal were modelled as elastic materials, and their properties are listed in Table 3. All interfaces and joints except for the coal/roof and coal/floor interface were assumed to have a friction angle of 30° and cohesion of 0.5MPa. The roof and floor interface was assigned a friction angle of 16° and cohesion of 0.012MPa. The Pit B highwall appears to be smooth and free from major fractures. Therefore no blast damage was included in the model.

The stress model is shown in Figure 5. The predicted vertical stress at the mid-height of the seam is plotted in Figure 6. The maximum principal stress is also plotted in the figure. At the toe of the highwall, a vertical stress of 0.87MPa and a maximum principal stress of 1.05MPa are predicted. The maximum principal stress is predicted to be higher than the vertical stress

Sample No.	Sample depth (m)	Diameter (mm)	Length (mm)	Density (Kg/m^3)	UCS (MPa)	Young's modulus (MPa)	Poisson's ratio
BHWC37-3	54.11-54.32	62.8	83.0	1400	13.9	3734	0.51
BHWC37-4	54.32-54.69	62.9	161.3	1391	2.9	2461	0.28
BHWC37-5	55.13-55.43	62.5	162.5	1378	5.9	2901	0.39
BHWC37-6	56.13-56.43	62.8	161.4	1384	11.6	3591	0.44
BHWC38-3	66.04-66.28	62.5	89.0	1608	7.4	3739	
BHWC38-4	66.94-67.16	62.7	110.6	1391	6.5	1760	0.30
BHWC38-5	68.35-68.61	63.0	120.1	1325	7.0	1887	0.30

Table 2 Laboratory test results of 7 coal samples from Pit B of Yarrabee Mine.

	E (GPa)	ν	Cohesion (MPa)	ϕ (°)	σ_t (MPa)	Mass UCS (MPa)
Coal	2.0	0.37	Hoek-Brown m = 2.93, s = 0.075, σ_c =16.2 MPa, a = 0.65			3.0
Siltstone	4.0	0.25	1.3	35	0.5	5.0
Claystone	2.5	0.25	1.04	35	0.4	4.0
Coal/roof/floor interfaces			0.012	16	0	
Other interfaces			0.5	30	0	
Coal joints			0.1	33	0	
Rock joints			0	30	0	

Table 3 Geomechanical input parameters for numerical modelling.

within a penetration distance of 70m. The vertical stress appears to be increasing gradually with the penetration distance, whereas the maximum principal stress reaches a local peak of 1.5MPa at 40m, where the vertical stress is 1.25MPa. At penetration depths greater than 70m, the two stresses are generally the same, indicating that the disturbance to stress field due to the highwall excavation diminishes away from the highwall.

Because the maximum principal stress is not in the 2D vertical cross section, its effects on the results obtained by a 2D study are uncertain. To consider the unknown effect from the out-of-plane principal stress on the results of a 2D analysis, both the vertical stress and the maximum principal stress as obtained in this 2D section were used.

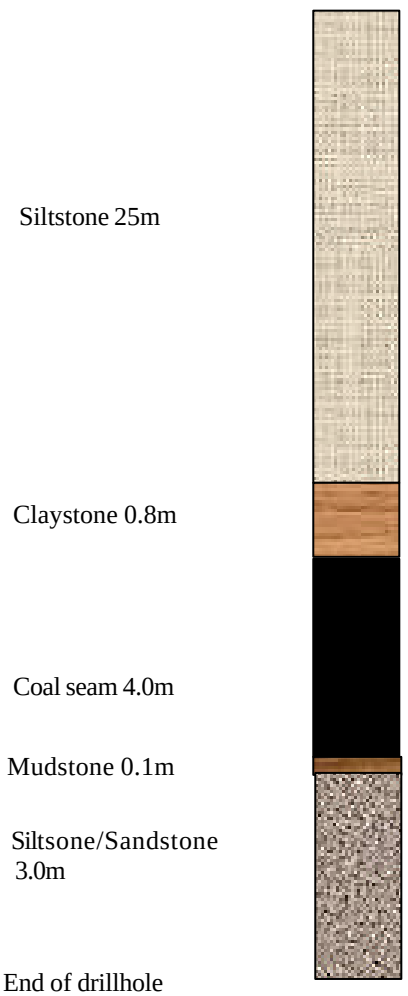

Figure 3 A simplified core log of the roof and floor geology in Pit B, Yarrabee.

Span stability

The stability of a highwall mining entry span at Yarrabee was investigated using a UDEC model. Two cases were studied and compared: (1) when the bedding partings in the roof claystone were horizontal, and (2) when the roof bedding partings dipped at 15° toward the seam. In both cases the mining section was assumed to be the full seam height, exposing the bedded claystone at the immediate roof. Vertical joints in the claystone layer were modelled at a spacing of 3.5m.

Figure 7 shows a comparison of modelled roof stability for the two cases. When the bedding planes are parallel to the seam, the layers act as fixed-end or simply supported beams after delamination. The beams mainly under their self-weight are predicted to be stable, and hence the span is predicted to be stable. When the bedding dips toward the seam at an angle, the layers behave as cantilever beams, and in this case the span is predicted to be unstable.

Roof falls are expected to be more severe at a shallow penetration depth near the highwall. This is because (1) the rock mass near the highwall often suffers disturbance, and (2) the confining stress in the direction perpendicular to the highwall is low. No evidence of more frequent roof falls, close to highwall has been recorded in this pit during mining. However, most of the roof falls are expected to occur after mining, particularly after the entries have been filled with water.

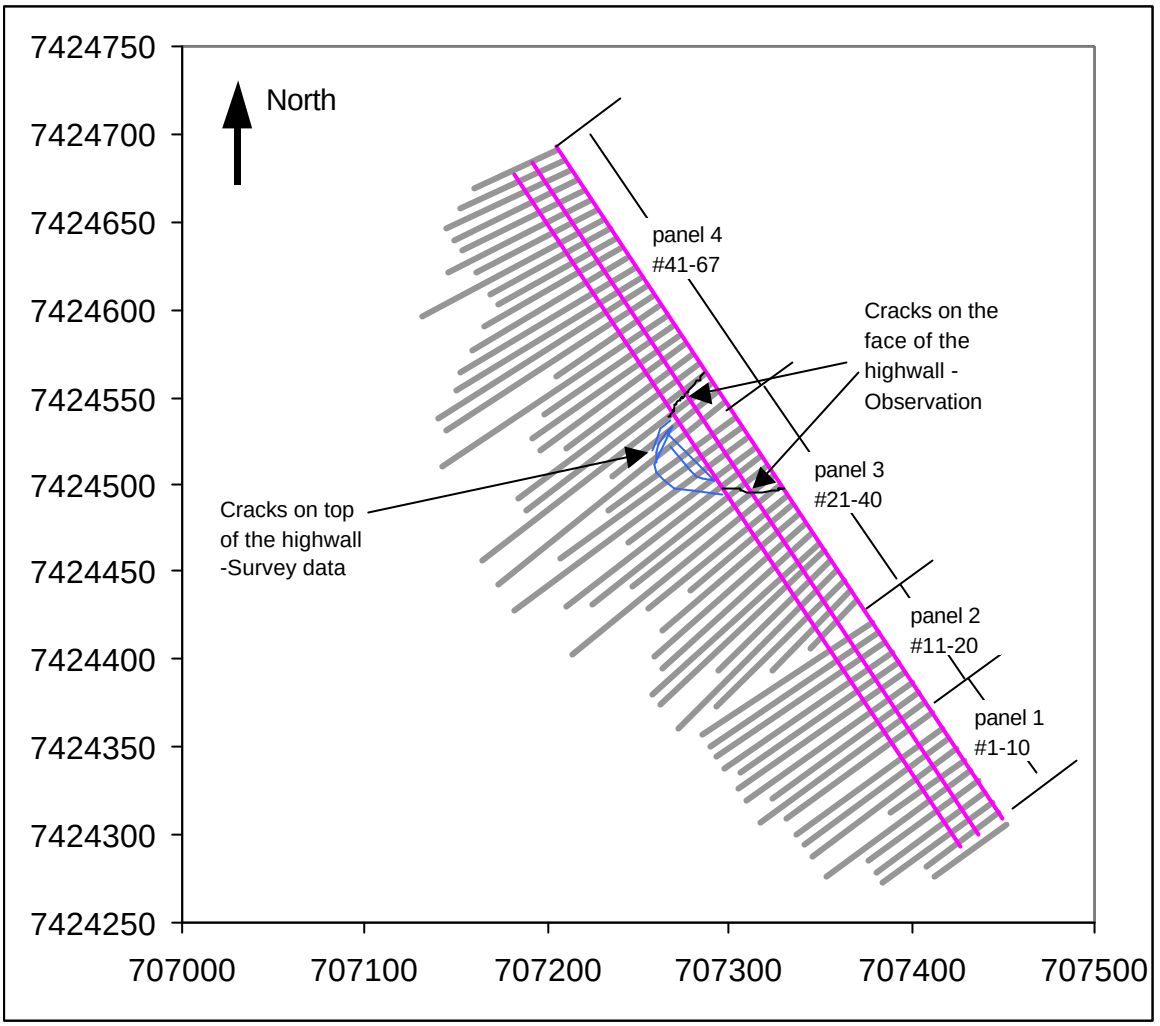

Figure 4 Highwall mined entries, and the surface cracks after subsidence based on survey and observation.

Pillar strength

Within the subsided region (Figure 4) there were both the regular pillars and a barrier pillar. The barrier pillar had a width of 7m at the highwall and narrowed to 3.9m at a penetration depth of 50m, based on the design. The regular pillars ranged from 2.8m wide at the highwall to 3.3m wide at a penetration depth of 50m.

The subsidence was apparently caused by the failure of 12 pillars, which had widths ranging from 2.8m to 7m. To analyse the instability, it was necessary to investigate the strength of a pillar of various widths.

The pillar strength was investigated numerically using UDEC. The mechanical properties listed in Table3 were used as the base case for this study. The following variations from the base case were investigated:

Case 1. Designed entry geometry. Pillar/entry height = 2.8m, and coal layer of 0.6m was left in the roof and floor. This is an ideal case configuration, which the mining operators tried to achieve. It is uncertain how well this was achieved during actual mining. Coal falls and cutting into the high ash floor were reported in the mining record.

Case 2: Entry geometry after roof falls. Pillar/entry height = 4.8 m. An entry this high could have resulted from mining too close to the floor combined with extensive falls of roof coal and roof claystone. This was likely in the region of subsidence due to the angled roof bedding. Mining records reported regular coal falls during mining in this region. The claystone roof with inclined bedding was shown in Section 0 to be unstable once exposed. Time and water in the entries would have worsened the roof falls.

Case 3: Entry geometry after roof falls and time effect. Pillar/entry height = 4.8m, and the strength of the intensive coal joints was reduced due to time and water effect. It is considered that this case represents the most likely scenario. A cohesion of 0.1MPa and friction angle of 33° were estimated in the design report for the inclined coal joints through the seam. This estimate may reflect the in situ strength conditions. More than one year after mining, particularly after the entries were flooded, the coal joints would be expected to have lost their cohesion and their friction angle might have been reduced. A zero cohesion value and a friction angle of 30° were used in Case 3.

A number of pillar sizes were modelled for all the three cases. The results are summarised in Table 4 and

plotted in Figure 8.

As expected, the pillar strength in Case 1 is the highest among all the three cases. When the pillar height increases from 2.8m for Case 1 to 4.8m in Cases 2 and 3, the pillar strength for a given pillar width (>3.0m) is found to reduce significantly (compare the three curves in Figure 8.)

In Case 2, a pillar strength of 3MPa is obtained for pillars ≤ 3.7m wide. This strength is equal to the mass coal UCS used in the modelling. This result suggests that the effect of the coal joints with the particular strengths that were assigned have only a minor effect on pillar strength.

In Case 3, which was formulated to simulate the effects of time and water, the calculated pillar strength is found to reduce by up to 30%, based on the assumed reduction of the strength of the intensive coal joint. This reduction is significant and based on purely theoretical considerations requires a minimum design FOS of 1.4 to achieve a medium term pillar stability.

Panel stability

Having evaluated individual pillar strength under various mining scenarios the next phase of the investigation was to evaluate overall panel strength. The Limit Equilibrium Method was used. The average strength of the panel in the subsided area can be calculated from the individual pillar strengths obtained above in Case 3. The average panel strength is calculated in a number of 2D vertical sections parallel to the highwall and at various penetration depths, using the following formula.

$$AveragePanelStrength = \frac{\sum(PillarWidth \times PillarStrength)}{PanelWidth}$$

After calculating the average panel strength, the FOS at a specific penetration depth can then be obtained by using the loading stress. Here both the vertical stress and the maximum principal stress have been used.

$$FoS = \frac{AveragePanelStrength}{ActualStress}$$

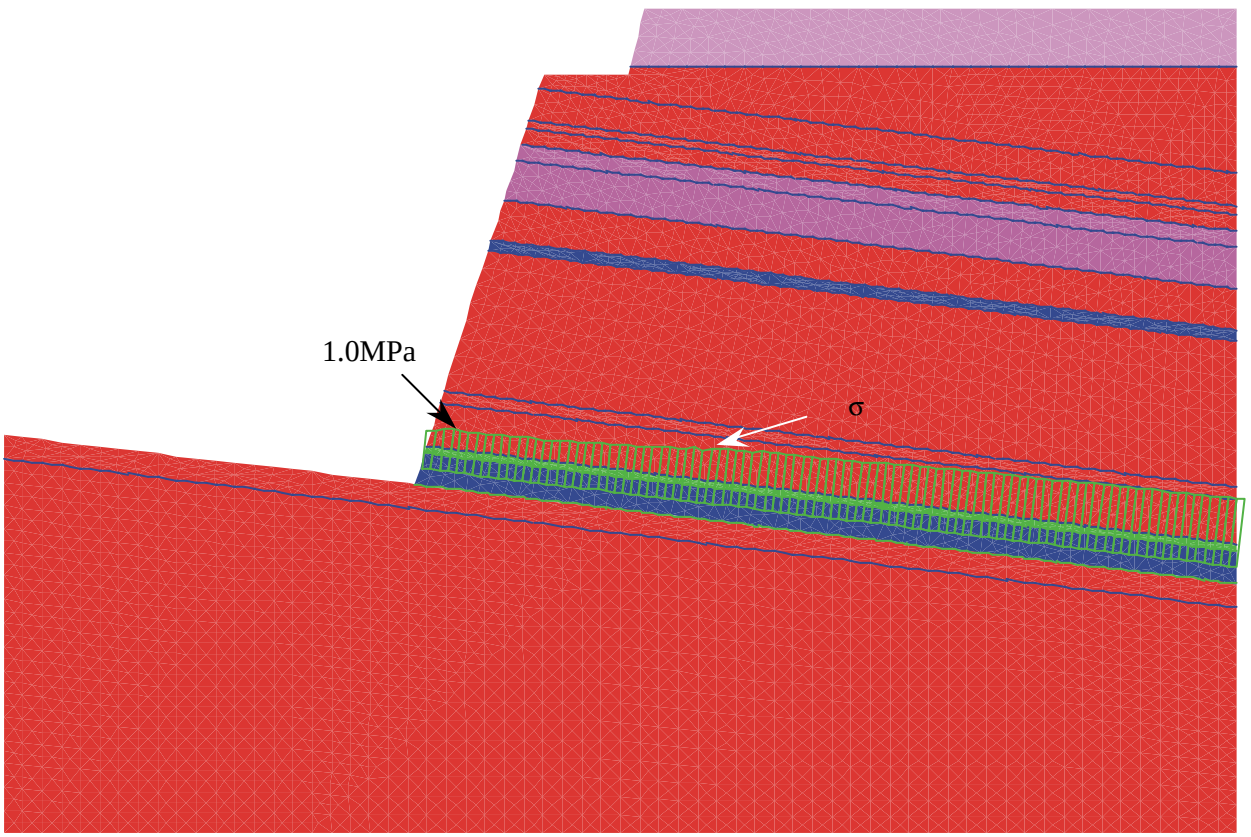

Figure 5 A 2D model to study the stresses near the highwall. The vertical stress is plotted.

Pillar width (m)	Pillar strength (MPa)		
	Case 1 (height =2.8m)	Case 2 (height=4.8m)	Case 3 (height=4.8m, weaker coal joints)
2.8	3.2	3	2.2
3.2			2.2
3.7	4.8	3	2.6
4.4	6.1	4.2	3.3
7.0		5.2	4.1

Table 4 Pillar strengths for various conditions, redicted by numerical modelling.

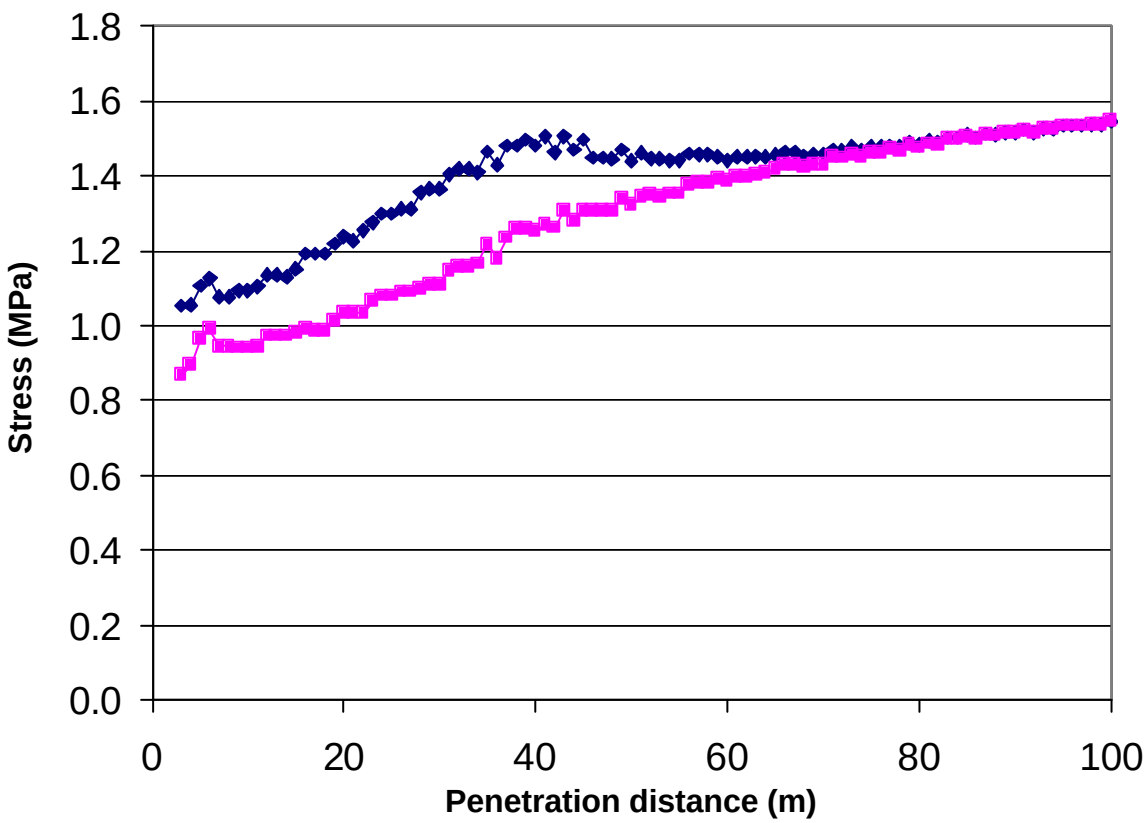

Figure 6 Numerically predicted vertical stress and maximum principal stress in the coal seam in the vicinity of the highwall.

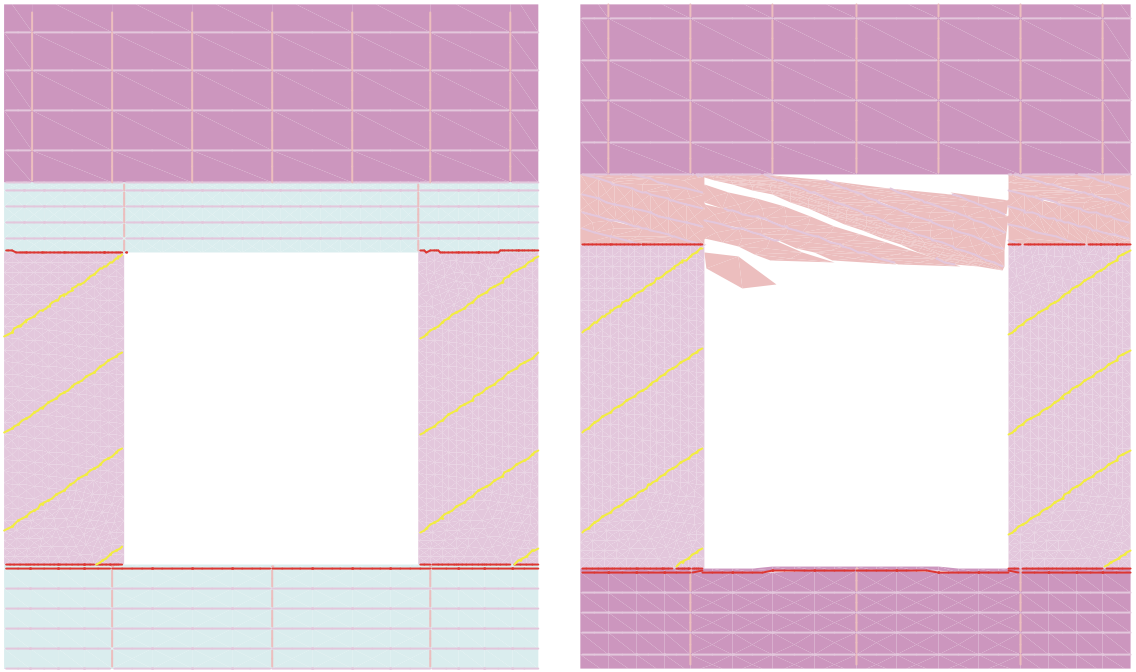

(a) Horizontal roof bedding (b) Inclined roof bedding

Figure 7 Stable and unstable spans for horizontal and angle roof bedding, numerical predictions.

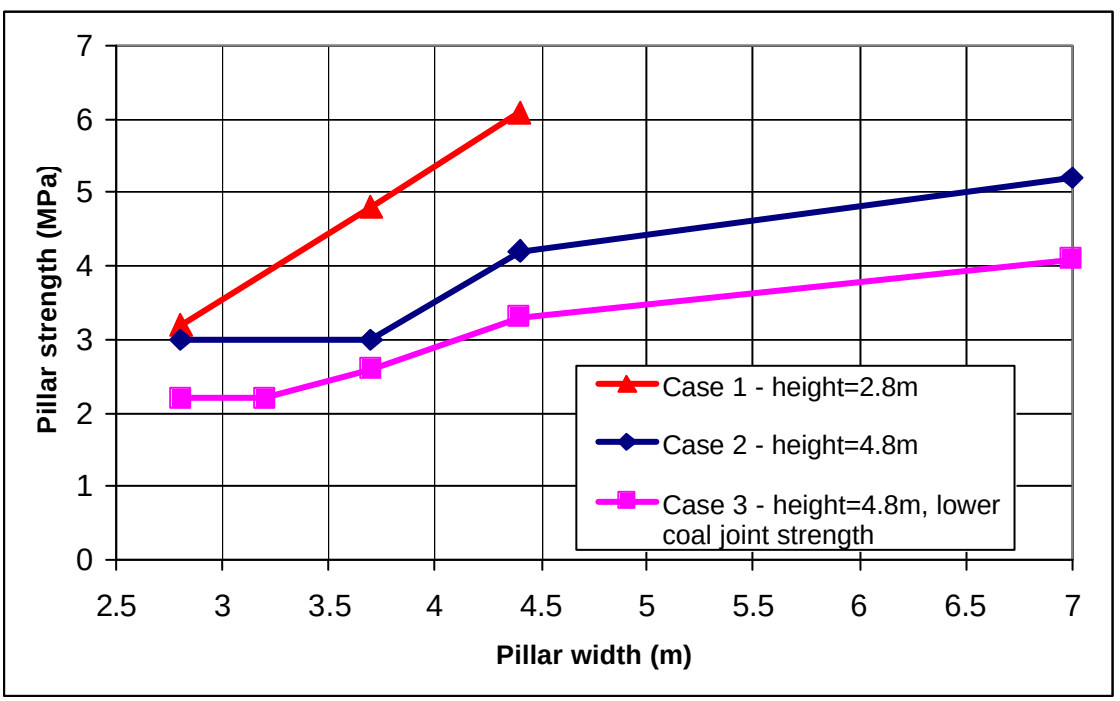

Figure 8 Variations of pillar strength with pillar width for three different cases.

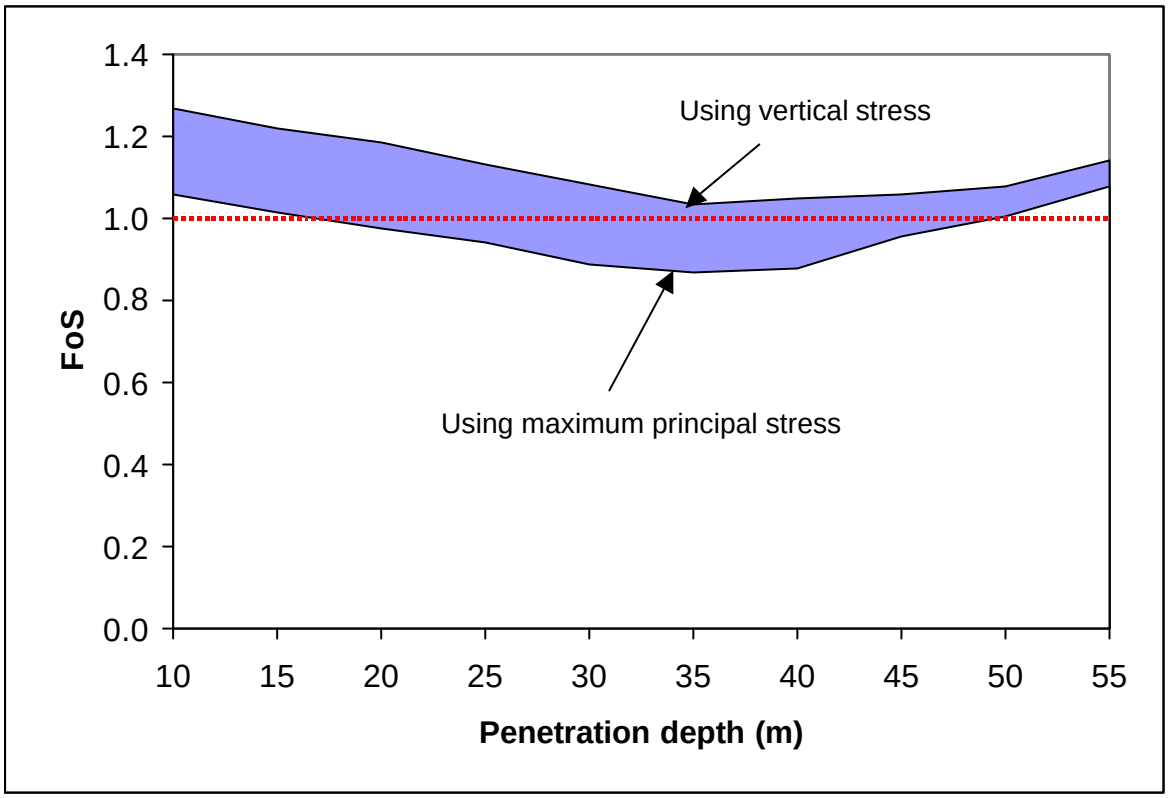

Figure 9 Variations of Factor of Safety (FOS) with penetration depth in the subsided area.

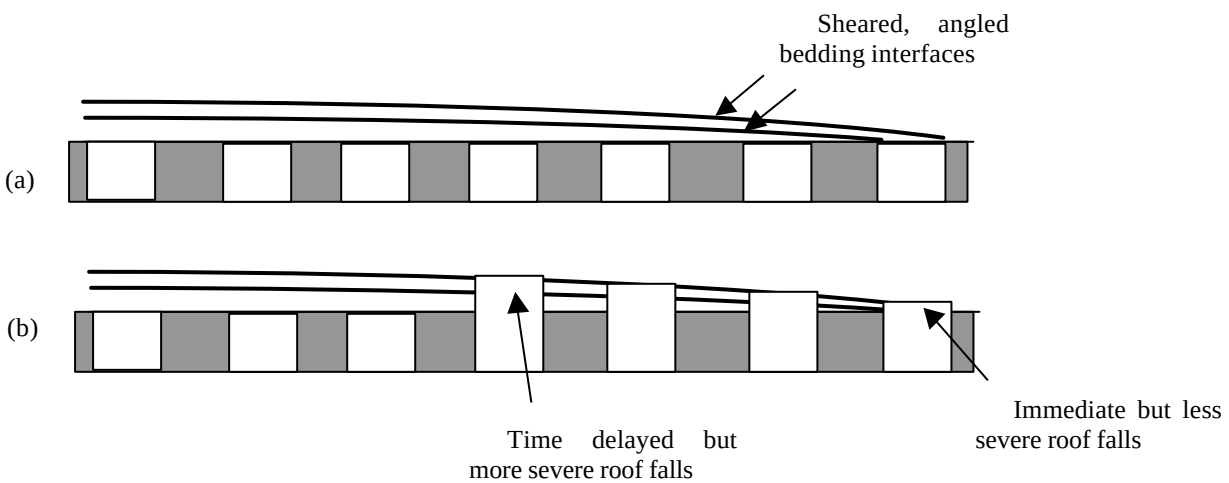

Figure 10 A sketch drawing of roof fall mechanism. Roof falls of different sizes occur at different locations due to angled roof bedding

Penetration (m)	In-panel pillar width (m)	Barrier pillar width (m)	Failed panel width (m)	Average panel strength (MPa)	Actual stress (MPa) (σ_v, σ_1)	**FOS**
0.00	Penetration depth less than 10m is excluded in this calculation because the plane strain assumption used in the study is no longer valid.					
5.00						
10.00	2.90	6.39	70.0	1.19	0.94-1.13	**1.06-1.27**
15.00	2.95	6.08	63.7	1.20	0.99-1.15	**1.01-1.22**
20.00	3.00	5.78	57.4	1.22	1.03-1.29	**0.98-1.18**
25.00	3.05	5.47	51.0	1.24	1.09-1.31	**0.94-1.13**
30.00	3.10	5.17	44.4	1.26	1.16-1.42	**0.88-1.08**
35.00	3.15	4.86	37.8	1.28	1.24-1.48	**0.87-1.03**
40.00	3.20	4.55	31.1	1.32	1.26-1.51	**0.88-1.05**
45.00	3.26	4.25	24.3	1.38	1.31-1.45	**0.95-1.06**
50.00	3.31	3.94	17.4	1.45	1.35-1.45	**1.00-1.08**
55.00	3.36	3.64	10.4	1.57	1.38-1.46	**1.08-1.14**

Table 5 Calculated average panel strength and Factor of Safety (FOS) in the subsided area.

The results are summarized in Table 5 and plotted in Figure 9.

Table 5 provides ranges of actual stress values that were used in the calculation of FOS. The upper bound of the range is the maximum principal stress and the lower bound is the vertical stress. These values were taken from the numerical modelling results reported in Section. As a result, a range of FOS was obtained and is given in Table 5. The true FOS should lie within the given range.

Figure 9 presents the FOS variation with penetration distance for the failed panel for Case 3 conditions. It shows that the FOS reaches a minimum at a penetration distance of 35m, and the minimum FOS is predicted to be in the range 0.87-1.03. At a penetration distance of 15-50m, if the maximum principal stress is used, the FOS is predicted to have fallen below 1.0.

Judging from the plot of FOS presented in Figure 9, it is believed that the subsidence started at about 30-40m inbye, which is just behind the top bench of the highwall. The failure propagated both toward the highwall and deeper into the panel. But due to stronger confinement deeper in the reserve, the extent of the subsidence was further toward the highwall than into the panel.

For the analyses of Case 3, a pillar height of 4.8m was used. It is believed that the maximum increase in height of the pillars occurred only in the subsided area due to extensive roof falls. In the subsided area, the steeply dipping bedding planes led to the roof falls. The mining records reported that the worst roof falls experienced during mining occurred in Entry 43, towards the northern end of the subsidence zone. The locations of roof falls experienced during mining may reflect the intersection between the angled roof layers and the seam. It is possible that more severe roof falls may have occurred in the area behind the intersection after mining, given that the immediate roof is sheared. It is postulated that some form of progressive failure took place. This mechanism is demonstrated in Figure 10. In Entries 33-42 where the subsidence occurred, although no major roof falls were reported during mining, it is possible that extensive roof falls occurred after mining, which eventually caused the failure.

Progressive panel failure

Previous experience has shown that highwall mining panel failures can occur rapidly, sometimes violently, and often extends throughout the mined panel. The subsidence at Pit B showed the opposite

characteristics. It occurred rather slowly (the full subsidence developed over two weeks) and was confined to a limited area. The wide barrier pillar (7.0m) is believed to be the key factor for the slow panel failure.

It is known that a wide "fat" barrier pillar behaves quite differently compared with a narrow and "skinny" web pillar. While a skinny pillar often collapses quickly, a fat pillar may fail progressively. This is because the confinement from the roof and floor contact often restricts the volume expansion associated with coal failure, and hence increases the confining stress in the centre of the wide pillar.

It is believed that the failure of the 7.0m barrier pillar in Pit B at Yarrabee occurred progressively, which in turn led to a progressive panel failure as observed.

Summary of the case study

The back-analysis results presented above suggested that the subsidence in Pit B might have been caused by three major factors.

- Angled roof bedding over a limited area led to severe roof falls, which heightened the pillars and reduced the pillar strength,
- Water infill into the mined entries contributed to the roof falls and weakened the pillars, mainly by weakening the coal joints, and
- Time effects also led to progressive roof falls and pillar weakening, as observed in other highwall failures.

CONCLUSIONS

A number of lessons have been learnt from the previous highwall mining instabilities. They have highlighted that a successful highwall mining operation relies on accurate and comprehensive understanding of the geology in the mining reserve. Detailed and comprehensive roof/coal/floor geological information should be the basis for a highwall mining layout design. Where geological features or rock strengths are not fully represented in the model used in design, the margin of safety predicted for the design will not be accurate. It was this factor that led to at least four panel failures at Yarrabee, German Creek and Ulan Mine.

Highwall mining operators must consider the lessons learnt from past highwall mining failures:

- assessment of span stability in advance,
- adequate layout designs,
- guidance of the CHM system to preserve pillar and span integrity,
- critical panel width, with barriers considered if problems need to be isolated,
- constant monitoring of mining conditions during operations,
- in situ stress and stress concentration near the highwall, and
- time dependent reduction of pillar strength.

ACKNOWLEDGEMENTS

This study is funded by ACARP, CSIRO and Yarrabee Mine. We would like to thank Mr. Matthew McCauley of Yarrabee Mine for providing site data. We also thank our colleagues Hua Guo, Deepak Adhikary, and Michael Kelly for reviewing the paper.

REFERENCES

ADIE, R 1993. G6 Highwall Collapse Report, 3rd March 1993. Oaky Creek Mine Report.

DUNCAN FAMA, M.E. SHEN, B. CRAIG, M.S. KELLY, M. FOLLINGTON, I.L. & LEISEMANN, B.E. 1999. Layout Design and Case Study for Highwall Mining of Coal. Proc. 9th Int. Congr. Rock Mech., Balkema, Rotterdam.

FOLLINGTON, I.L. LEISEMANN, B.E. DUNCAN FAMA, M.E. & SHEN, B. 1996. Geotechnical Monitoring for Safety in Highwall Mining, German Creek Mine. ACARP Report C3053.1.

HIGHWALL MINING SERVICES, 1997a. CHM Panel Design, Pit B, Yarrabee Mine. Report prepared for Yarrabee Coal Company Limited. May 1997.

HIGHWALL MINING SERVICES, 1997b. Back-analysis of Pillar Failure, German Creek – Pit C South. Report for Mining Technologies Australia Pty. Ltd.

HIGHWALL MINING SERVICES, 1999. Analysis of Telecom Hill Subsidence. Report for Ulan Coal Mines Limited.

ITASCA, 1996. UDEC – Universal Distinct Element Code, Version 3.0. User's Manual. Itasca Consulting Group, Inc. Minneapolis, Minnesota, 55415 USA.

KELLY, M. DUNCAN FAMA, M.E. SHEN, B. FOLLINGTON, I.L. & LEISEMANN, B.E. 1998. Investigation of Highwall Mining Instability, Pit 16BL South, Moura Mine, QLD. CSIRO Exploration and Mining Report No. 467C (Confidential).

SHEN, B. & DUNCAN FAMA, M.E. 1999. Review of highwall mining experience in Australia and case studies. CSIRO Exploration and Mining Report No. 316F.

SHEN, B. MACONOCHIE, A.P. & DUNCAN FAMA, M.E. 2000. Review and Back-analysis of Highwall Mining Panel Failure in Pit HW3 Trench, Ulan Mine. CSIRO Exploration and Mining Report No. 722C.

TOWNSEND, J.M. JENNINGS, W.C. HAYCOCKS, C. NEALL, G.M. & JOHNSON, L.P. 1977. A Relationship Between the Ultimate Compressive Strength of Cubes and Cylinders for Coal Specimens. Proc. 18th U.S. Symp. On Rock Mech., ed. F. Wang and G.B. Clark, 4A6-1-4A6-6. Golden: Colorado School of Mines Press.

Geological hazards — The impact to mining 15-16 November 2001, eds Doyle, Moloney, pp 141-150

Slope stability radar for monitoring mine walls

BRYAN REEVES, DAVID NOON, GLEN STICKLEY AND DENNIS LONGSTAFF

Cooperative Research Centre for Sensor Signal and Information Processing (CSSIP),The University of Queensland; Australia

Slope stability is a critical safety and production issue for coal mines. A common technique to determine slope stability is to monitor the small precursory movements, which occur prior to collapse. The "slope stability radar" has been developed to remotely scan a rock slope to continuously monitor the spatial deformation of the face. Using differential radar interferometry, the system can detect deformation movements of a rough wall with sub-millimetre accuracy together with high spatial and temporal resolution. The effects of atmospheric variations and spurious signals can be reduced via signal processing means. The advantage of the slope stability radar over other monitoring techniques is that it provides complete slope coverage without the need for mounted reflectors or equipment on the wall. In addition, the radar waves adequately penetrate through rain, dust and smoke to give reliable measurements, twenty-four hours a day. The system has been trialed at Drayton, Moura and Callide mines, which demonstrated the potential for real-time monitoring of slope stability during active mining operations. These trials showed that outward deformation movements of a rock face could be detected with accuracy around 1mm. It overcomes the shortcomings of conventional monitoring systems by providing greater coverage of the rock face, hence giving a better understanding of the geodynamics, which should in turn lead to extra warning time. This translates to greater productivity in the sense of lower risk associated with recovery of coal. It would enable direct recovery, where under conventional monitoring conditions the area would be quarantined on grounds of excessive risk.

INTRODUCTION

Monitoring slope stability is a critical safety issue in coal mines. Major wall failures can occur seemingly without warning, causing loss of lives, damage to equipment and disruption to the mining process. US Mining Safety and Health Administration reports indicate that highwall fatalities account for around 10% of surface fatalities in US coal mines (US MSHA, 1998).

Tell-tale signs of slope instability include: the opening of cracks on the wall surface and crest, audible creaking, and increased rilling of spoil from the rock face. It is difficult to predict the progression of such signs to slope instability. With highwalls and in-pit benches in particular, movements may accelerate with little or no warning. Hence, mines take a conservative approach when deciding whether to expose personnel and equipment near a potentially unstable slope. Over-cautious decisions impact on mine productivity, while the reverse emphasis places lives at higher risk.

A more reliable determinant of slope instability is the measurement of outward movement and acceleration of material as an instability mechanism develops. There is strong evidence that small precursor movements of the rock wall occur for an extended period (weeks to months) prior to collapsing (Hoek and Bray, 1981). The acceleration of movement and the point of failure vary for different slopes depending on the site specific failure mechanisms (Figure 1). The type of failure mechanism depends on the rock mass and underlying geology. For example, wedge and plane-type failures occur where highly faulted/jointed rock masses and steeply dipping layers are prevalent. Another example is circular-type failures of mine spoil piles, where mining destabilizes the pit floor below the spoil pile.

There are various monitoring systems that can measure the movement of the rock face (Bell, 1994). Geotechnical specialists can interpret the pattern and history of movement to improve prediction of the failure process and advise appropriate and timely stabilisation, or alternatively implement safety management actions. Mines can use such information to more reliably assess risk and maintain records for due diligence purposes. In addition, monitoring systems can sound an alarm to warn workers when the movement or acceleration of the rock face exceeds a set threshold.

A review of the literature and discussions with geotechnical specialists identified the following desired requirements for the slope monitoring system:

- monitoring coverage should be sufficiently broad and uniform to determine the slope failure mechanism, Deformation measurement accuracy should be at least 10 mm, preferably 1 mm,
- operation should be reliable in a dusty and smoke filled mining environment,

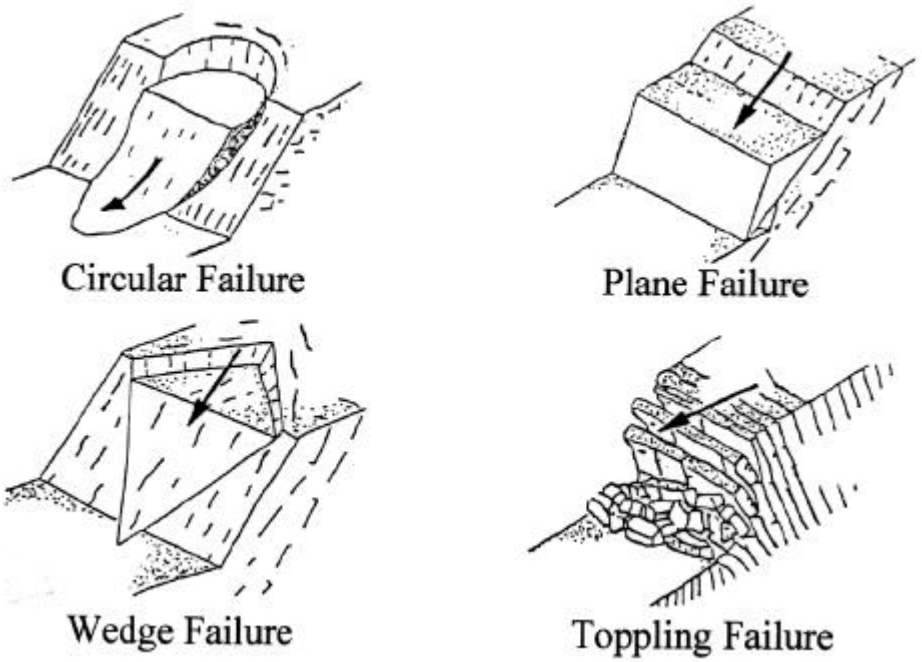

Figure 1 Main types of slope failure mechanisms. The type and rate of failure depends on the nature of the rock mass

- mining personnel should easily interpret data obtained,
- system should be safe to use around mining personnel,
- system should not hinder the mining process (this includes a low false alarm rate), and
- system should function economically (this includes installation and running costs).

Current monitoring methods at some mines use extensometers and laser EDM (Electronic Distance Measurement) to measure the dilation of cracks appearing on the crest or face of the rock slope. These methods monitor points or lines on the wall rather than the area of the wall face, which makes interpretation of failure mechanisms very difficult (Sullivan, 1993). In addition, these methods are costly and time consuming to set up and relocate because they usually require the careful placement of sensors or reference reflectors on unstable or inaccessible ground. While other researchers have suggested the use of reflector-less laser EDM, currently available systems are extremely expensive to purchase, and they do not have the desired accuracy (errors of ±5 to ±10mm when measuring to a light-colored, perpendicular, flat surface; Leica, 1998).

The slope stability radar is a new technique for monitoring mine walls and general slopes. The concept is based on the considerable success achieved by differential interferometry obtained with synthetic aperture radar. Which can measure small movements of land masses from satellites, for example: along-fault slippage associated with earthquakes, ground subsidence associated with underground mining, and velocity of slowly moving ice masses, (Goldstein *et al*., 1993). Instead of using synthetic aperture radar from a moving radar platform, the slope stability radar uses a real-aperture on a stationary platform positioned 50 to 400 metres back from the foot of the wall (Figure 2). The system scans a region of the wall and compares the phase measurement in each footprint (pixel) with the first scan to determine the stability of the slope and the nature of the movement (Figure 3). The advantage of radar over other slope monitoring techniques is that it provides full area coverage of a rock slope without the need for reflectors mounted on the rock face. The radar wave adequately penetrates through rain, dust and smoke to give reliable measurements, although reduced accuracy occurs in pixels where there is low phase correlation between scans (e.g. vegetation on the slope).

SYSTEM

The most critical performance requirement for a slope monitoring system is the outward movement accuracy of 1mm or less. Although the outward movement accuracy of the interferometric technique is independent of range, a maximum range of 500 metres is specified for the slope stability radar, so that enough reflected signal from the rock slope would be received.

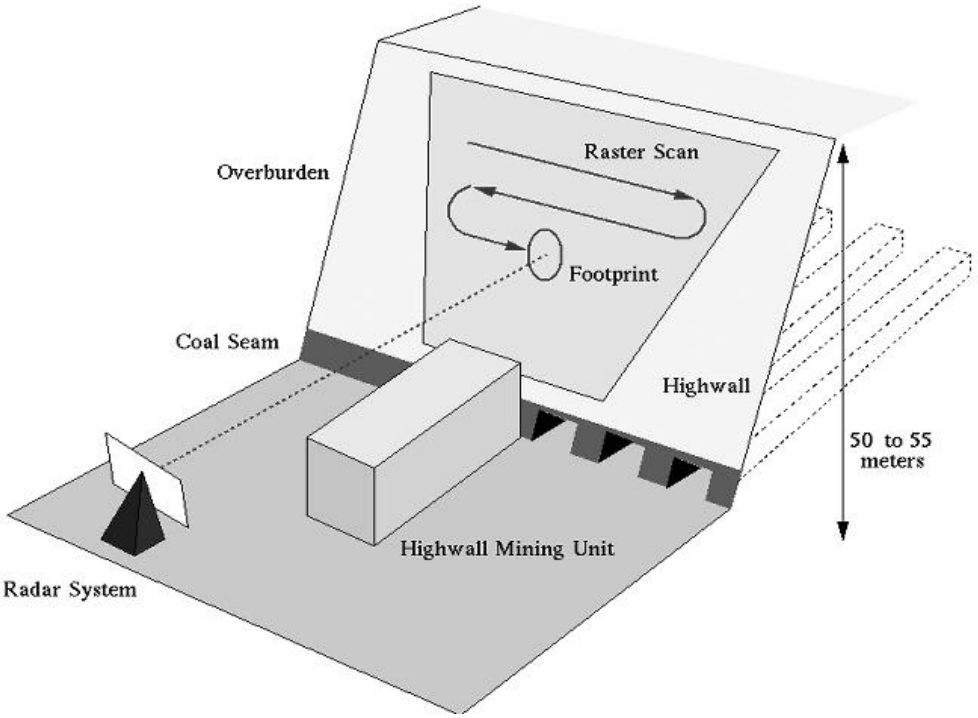

Figure 2 Configuration of the radar sensor for mining under a highwall. The radar scans the wall producing a two dimensional image of the deformation in the monitored region, without the need of artificial reflectors on the wall.

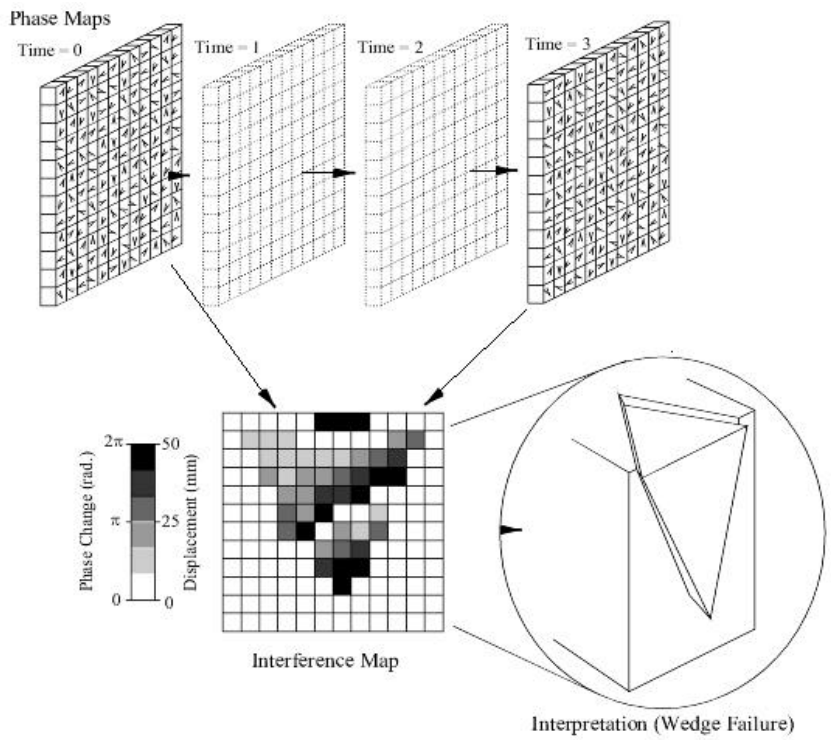

Figure 3 Differencing the phase of each pixel from two separate scans creates the deformation image.

Typically though, the system would operate closer to the rock slope to improve the spatial resolution of the measurements. Operating the system closer to the rock slope will improve the spatial resolution of measurements.

The outward movement accuracy of the system is determined by the inherent stabilities of the electrical system, the mechanical structure, and the atmospheric conditions. The electrical and mechanical specifications were set such to be below the errors expected due to atmospheric disturbances in the path. These can be corrected to 3ppm using atmospheric measurements, although 1ppm can be achieved using special techniques (Reuger, 1996). This higher accuracy corresponds to 0.1mm for a radar range of 100m. Setting the system accuracy for the electrical and mechanical specifications to this value allowed the true limits in monitoring deformations using radar interferometry to be determined. With a lower accuracy, the equipment would limit the performance, rather than letting the unavoidable environmental effects define the accuracy. Setting a high system accuracy does not mean that an outward movement accuracy of 0.1 mm will be achieved. Instead, other effects such as changes in the rock surface from atmospheric effects (e.g. rain) will limit the measurement accuracy.

The system consists of two main parts, the scanning antenna and the radar electronics box connected via an umbilical cable (Figure 4). The scanning antenna consists of a 0.92m diameter parabolic dish mounted on a sturdy tripod and controlled by separate motors and gears for azimuth and elevation movement. The beam width of the antenna is approximately 2°. The mechanical pointing accuracy and tripod stability requirements were designed to be within the system accuracy specification. A computer in the radar electronics box can position the parabolic dish to anywhere between -15° and 165° in elevation from the horizontal, and between -170° and 170° in azimuth. The 2D-scan region is set manually for the application. The scan speed is approximately 25 minutes for 4000 pixels on the wall. The pixel size on the 2D image is determined by the range extent of a 1° angle increment. For a rock slope at 100 metres range, the pixel size will be approximately 2m x 2m. Two-by-two pixels constitute one spatial resolution cell provided by the 2° beam divergence of the antenna.

The umbilical cable between the scanning antenna and radar electronics box transfers power, control signals and intermediate frequency signals. The radar electronics box houses the computer, radar source and power supply modules in an air-conditioned and shock-mounted environment. A diesel generator that has extended fuel tanks for 3 days continuous operation powers the equipment. An earth leakage breaker and high-temperature thermocouple are installed for protection.

The radar source in the radar electronics box produces an intermediate frequency signal that is transmitted via the umbilical and up-converted to an X-band (9.4-9.5GHz) carrier frequency at the feed of the scanning antenna. Range resolution of 1.5 metres is provided by a stepped-frequency waveform with 100MHz of bandwidth. The maximum transmitted power from the feed antenna is 30mW. The received signals are down-converted to the intermediate frequency and sent via the umbilical to the radar electronics box and recorded by the computer. The specifications for: electrical stability, signal phase stability and signal-to-noise ratio were set to be within the system accuracy

Figure 4 Radar electronics and scanning antenna joined by umbilical cable.

specification of 0.1mm.

Atmospheric disturbances caused by local changes in temperature, pressure and humidity are automatically compensated using the radar data for changes in the propagation velocity. Phase ambiguities occur in the measurements if outward wall movements are greater than $\lambda/4$. As the system has a high repeat rate compared with the time mechanics of slope deformation, phase unwrapping can be performed on a pixel-by-pixel basis through tracking the change over time. A spatial filter is then used to smooth the interferogram, and reduce phase errors caused by signal fades to pixels with a low signal-to-noise ratio.

Because there is no reflection target in the sky, the interferometric phase variation is random, and hence is masked in the interferogram. In addition, incoherent phase signals caused by fluctuating vegetation on the slope are masked. Spurious targets caused by moving vehicles that briefly block the view of the radar affect a small region of pixels. These localized effects recover with the subsequent scan and are easily ignored by the software.

A time series of interferograms are combined to make a movie, thereby conveniently displaying the temporal and spatial movement characteristics of the wall surface. The amount of outward or inward movement of each pixel relative to the radar position is indicated by a colour change. The displacement history of selected regions can be displayed by spatially averaging over an unstable region and compared with a stable region. A polynomial regression fit to the data points can be made to measure the outward acceleration of the rock mass. A graphical user interface (GUI) has been developed to display and compare the interferograms with co-registered images of the reflection amplitude, reflection range, or photographed scene. It also allows regions to be selected for continuous tracking and an adjustment of the various parameters used in the image reconstruction tools. A typical display of the GUI is shown in Figure 5.

FIELD RESULTS

The slope stability radar first monitored an unstable slope at Drayton Coal Mine in the Hunter Valley in late 1999. Extensometers on the brow of the slope had shown significant stick-slip movement of cracks (0-200mm dilation) over the six months prior to the trial. However, the slope was relatively stable during the period the radar was monitoring. Figure 6 contains a photograph view from the radar position. The plane of weakness, on which the rock was slipping, could be clearly seen by its surface expression on the rock face. Extensive cracking was evident to the left, indicating the extent of the unstable region. This unstable section was

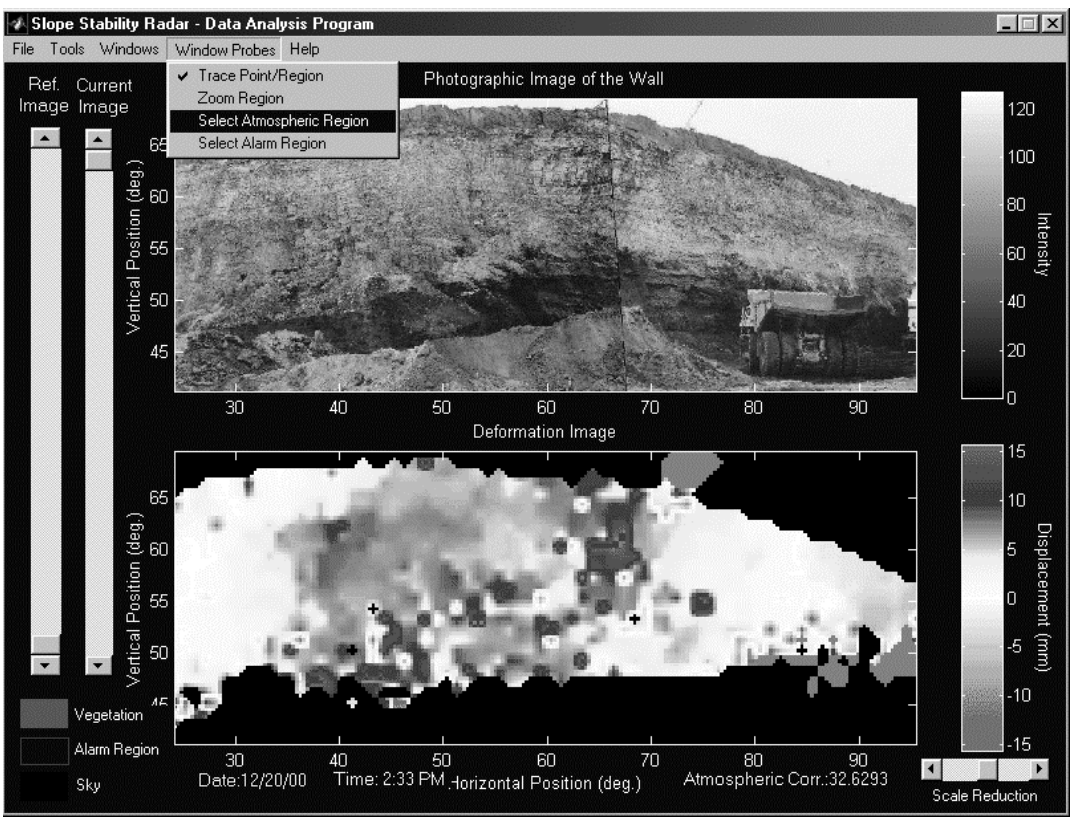

Figure 5 Typical GUI display with photograph image of the slope in the top view and radar deformation image in the bottom view (a color scale is used to indicate displacement in millimetres).

expected to initially move out and then down to the right, if it failed. The radar was placed at a safe location some 100m from the face, and scanned the scene containing both stable and unstable areas. The radar acquired deformation measurements across 3870 pixels in the scene, with each pixel measuring approximately 2 metres wide by 2 metres high. One complete scan of the scene took approximately 25 minutes. The radar continuously scanned the scene across the twelve-day period.

Figure 6 also contains an interferogram produced by the radar after 6 days of monitoring. A test was performed where a spoil pile located in front of the rock slope was manually disturbed. This induced change is clearly seen in the circled region of the interferometric image.

After the trial was completed, further analysis of the data showed that the unstable section of the wall had moved 2mm over the twelve days of monitoring. Measurements from a region in the unstable section were averaged and compared with an averaged region in the stable section. The result is shown as Figure 7. The curve is a polynomial regression fit to the data points indicating an outward acceleration of the rock mass. This result is broadly consistent with the wire extensometer readings during the trial period.

The slope stability radar was further tested at Moura Mine in Queensland in early 2000. For the first five days, the radar monitored the highwall face above an active highwall mining operation. The radar was positioned 75 metres back from the highwall, and scanned a 120m wide by 50m high region of the face every 25 minutes. The progression of the launch vehicle along the highwall could be seen in the time-elapse images produced by the radar. Haul trucks operated directly in front of the radar, and sometimes blocked the view.

Figure 8 shows a photograph image of the view, and a radar image after 2 days of monitoring. The highwall area immediately above the launch vehicle had moved 2mm outwards relative to the stable sections to the left and right of the scene. The highwall mining unit and machinery operating around the base of the highwall exhibit random phase measurements in the interferogram.

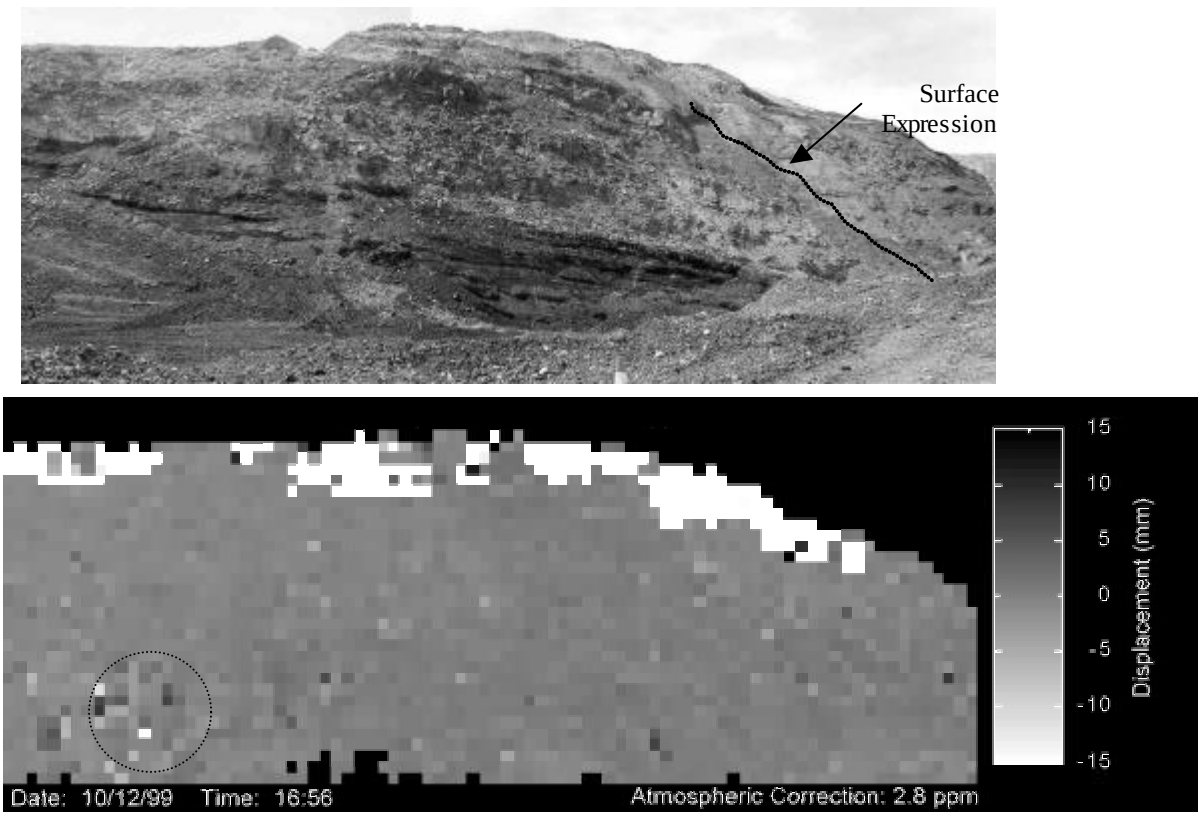

Figure 6 Photograph and interferogram of slope over six day period. The sky has been masked out. The grassed areas at the top of the slope have been whitened out. Dark pixels on the wall are due to weakly reflected signals. The circled region is movement caused by manual disturbance. Otherwise, the slope appears to be stable.

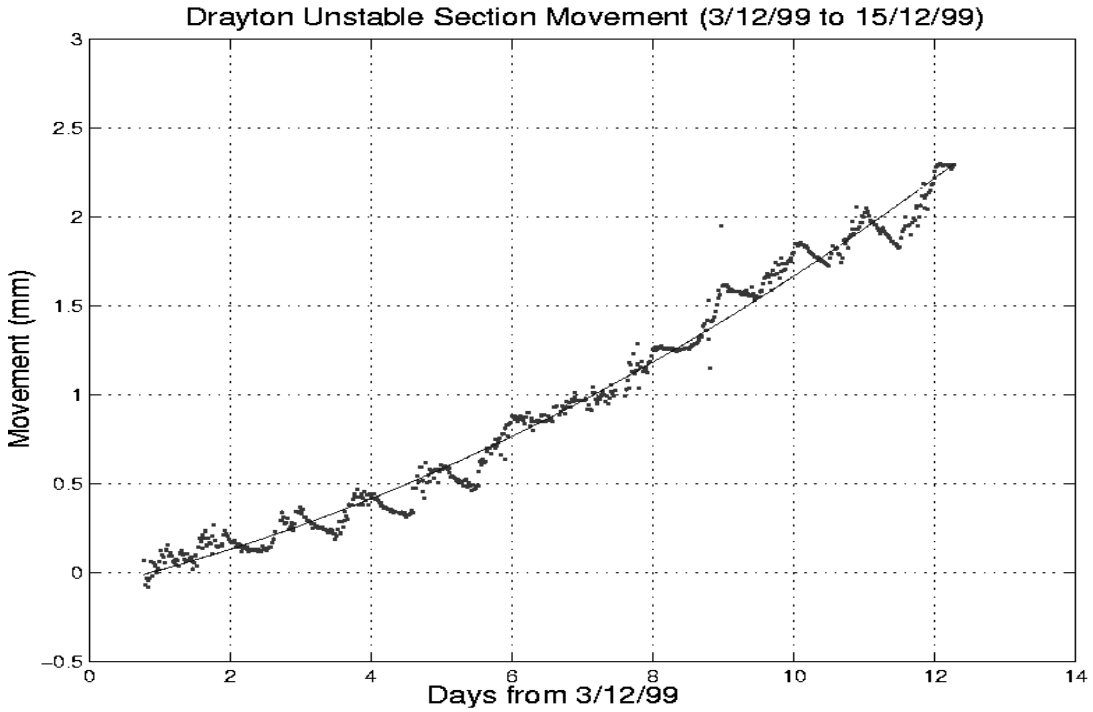

Figure 7 Movement of unstable section of slope relative to stable section as measured by the radar.

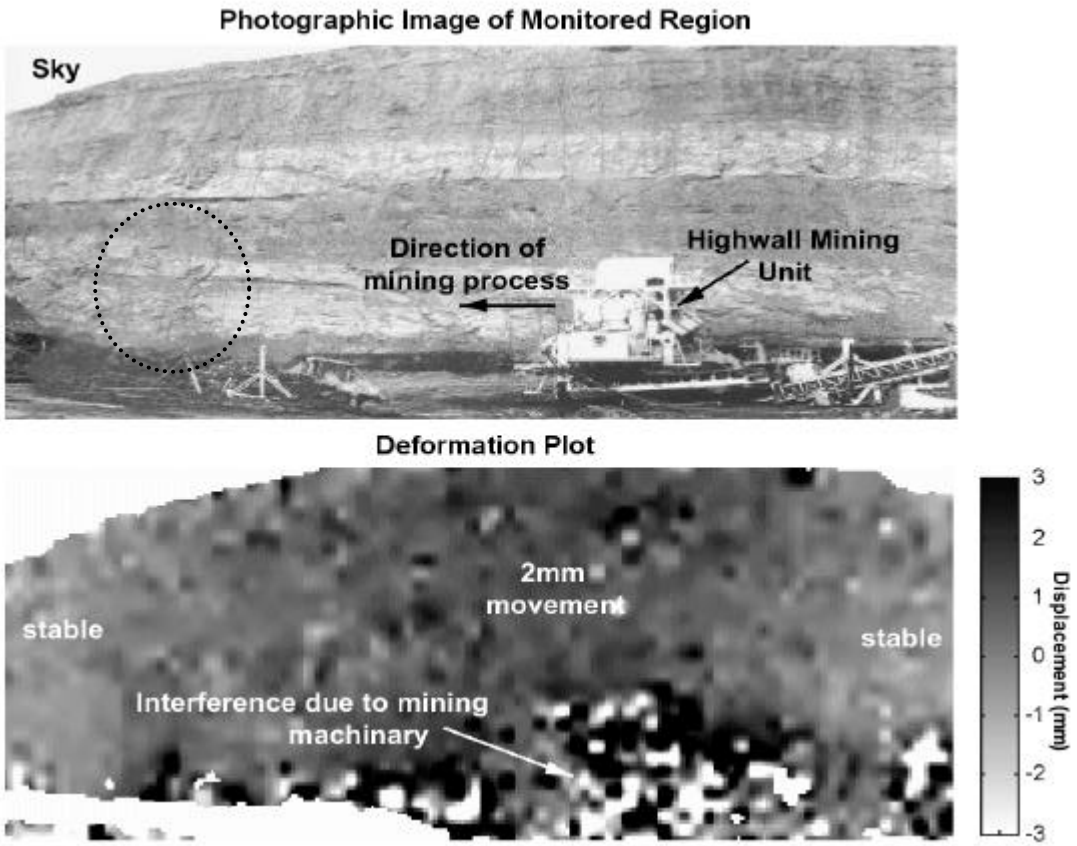

Figure 8 Photograph and interferogram of highwall site at Moura.

About one week after the radar left Moura, a 25m wide by 30m high section of the highwall collapsed alongside the launch vehicle. A dotted circle in the photograph of Figure 8 marks this region. There may be early signs of movement in the interferometric image, but it is unknown if these were a pre-cursor to failure because the radar did not monitor this region for the days leading up to the failure.

Figure 9 is a graph showing the outward movement of the wall above the launch vehicle over the elapsed time. A total movement of 6mm occurred during a 6 day period. It is interesting to note that movement of the highwall occurred only during mining. No movement was detected while the launch vehicle was being moved to the next drive, nor during the maintenance downtime (between hours 58 and 88). During these times of total wall stability, the standard deviation error of the system was measured at 0.1mm.

A short period of rain occurred at the 90 hour stage of the trial. Rain affects the deformation measurement by randomly changing the rock slope surface characteristics. This induces an error in the measurement, which was either averaged out over a region of the wall, or removed for subsequent scans by initializing the phase reference image. Figure 9 shows that the actual wall movement appeared to increase after the rain period (at 90 hours).

For the last two days of the Moura trial, the radar was positioned at another site where a highwall had failed several weeks prior (Figure 10). The radar detected the fall of an overhanging rock near the top of the highwall to the spoil pile below. No other highwall movements at this site were apparent.

An operational test of the slope stability radar was conducted at Callide Mine in Queensland over a 3 month period in 2000/2001. The system was employed by the mine personnel to assess the stability of a highwall below an active mining operation. The previous Figure 5 shows an example of the data collected during this extended field trial. Total wall movement of 30mm was recorded by the system over the unstable section. The system provided the mine personnel with an increased level of confidence in assessing the stability of the highwall.

CONCLUSIONS

The slope stability radar has been developed to remotely scan a large section of a wall or rock slope, thereby allowing continuous monitoring of the face deformation. Such deformations are expected to give

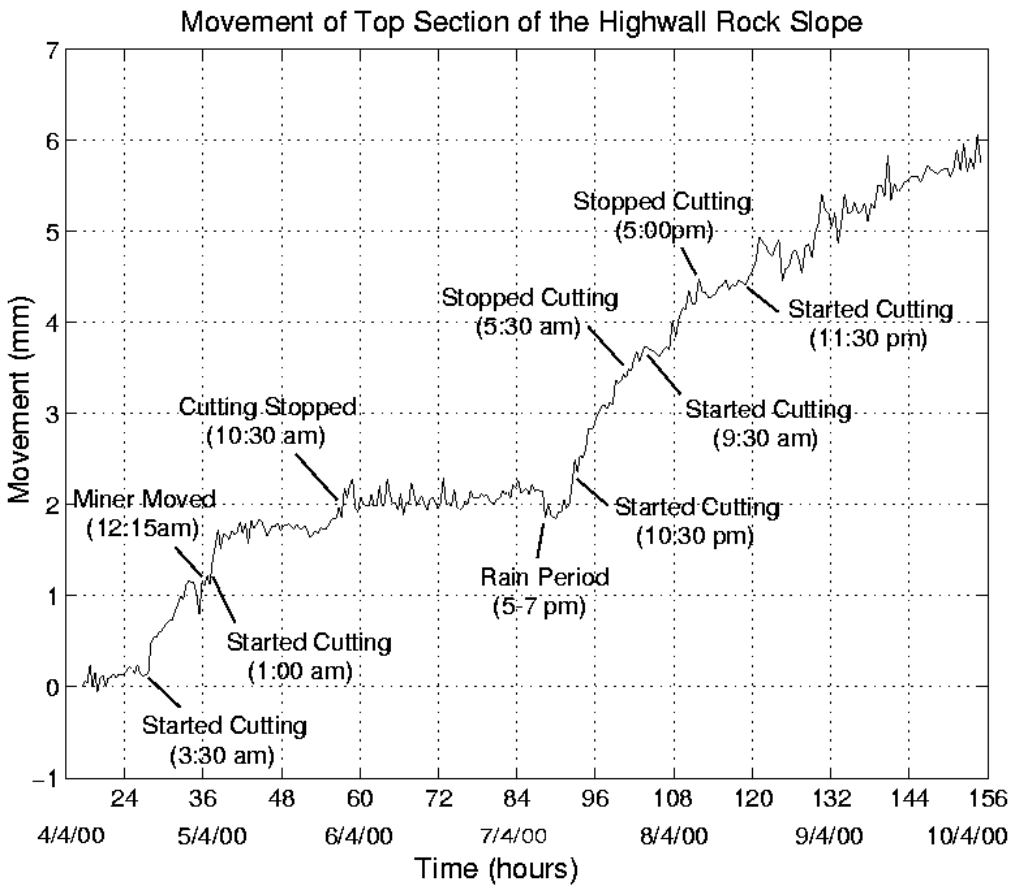

Figure 9 Movement of the wall immediately above the launch vehicle and relative to the stable sections.

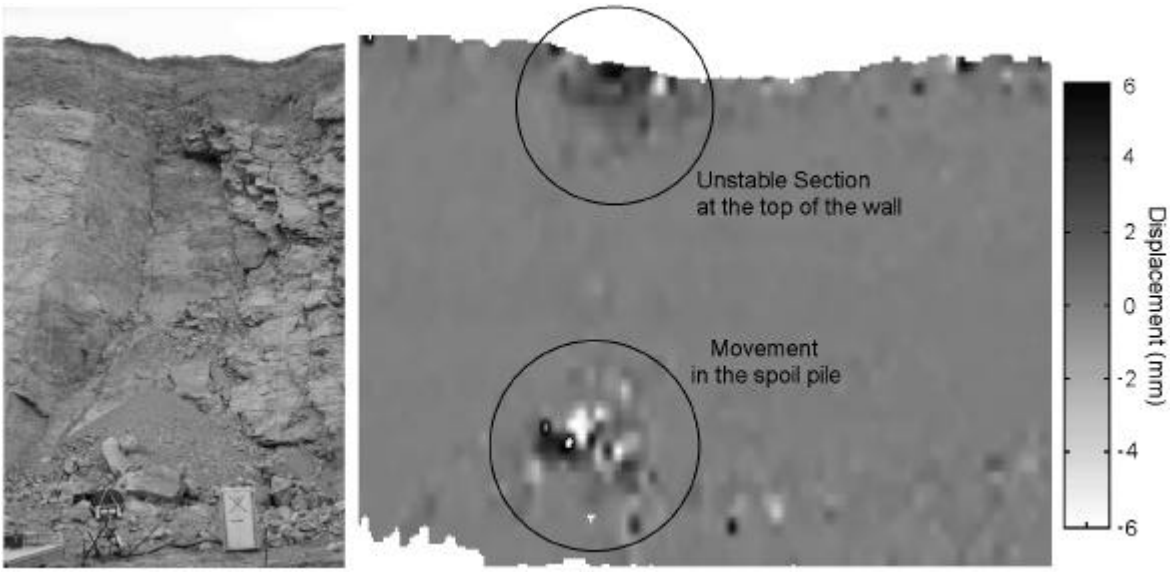

Figure 10 Photograph and deformation image of unstable wall section at Moura.

an early indication of wall instability. The system the directly measures the outward displacement of the wall using radar differential interferometry. This technique overcomes the need of a highly stable footing that is required by other electronic-distance-measuring systems.

The system has been tested at three open-cut coal mines that exhibited slope movements. Outward movements of rock slopes were measured by the system with accuracies better than 1 mm in these typical mining environments. The accuracy limitation is primarily due to atmospheric changes that, either affect the surface conditions of the rock slope (caused by rain), or change the propagation characteristics of the radar waves. Averaging the measurement over a spatial region can minimize surface condition changes. Comparing the movement of an unstable region with a stable region can compensate for propagation changes. The spatial resolution and update rate of the prototype system are adequate for monitoring pre-cursor movements of a rock slope at close range (i.e. less than 500 metres).

It is apparent that the Slope Stability Radar has broad application in coal mines.

- General highwall stability — There are areas in general open-cut mining where highly faulted/jointed rock masses and steeply dipping coal seams pose serious concerns for highwall stability. This is particularly important when coal recovery operations take place adjacent to highwalls, since there is believed to be a strong correlation between coal removal and wall movement.
- Lowwall or spoil-slope stability — Destabilising influences on spoil slopes are often located at or within the floor of the pit that is being mined. Early warning of movements allows in-pit operations to be modified to maximise safety while minimising disruption.
- In-pit bench stability — For in-pit bench dragline operations, there is the potential for failure of the extended bench, due to shears and weak bands associated with the coal seam or shot overburden. Early warning of movements allows remedial action to be taken with minimal disruption to productivity.

Further development is currently underway to make the system suitable for use in a production mining environment. The practical benefits to coal producers of a fully developed Slope Stability Radar will include the following aspects.

- Easy and quick setup time — The system will be housed in a self-contained trailer (similar to a lighting plant) or sled that can be easily and quickly moved around the mine.
- Remote monitoring without the need for instruments or wires on the unstable slope — the system provides full area coverage of a rock slope without the need for mounted reflectors and wires, and can be moved easily to focus on areas of particular concern.
- Ability to operate continuously and obtain real-time, immediate response of unstable slope movements — The system provides immediate monitoring of slope movement without calibration and prior history.
- Improved geotechnical interpretation of slopestability — The radar allows for the first time to detect movements over the entire wall face. This gives a better understanding on how rock slopes move and when they may fail. This information is important in the prediction of failure. It may also be extremely valuable in testing the validity of

geotechnical models of movement behaviour of slopes.

ACKNOWLEDGMENTS

This paper reports work predominately funded by the Australian Coal Association Research Program (ACARP) for Project C6015, with subsequent funding assistance provided by Anglo-Coal (Callide). The Cooperative Research Centre for Mining Technology and Equipment (CMTE) is acknowledged for their initial assistance with project C6015. We would also like to thank Drayton Coal, Moura Coal and Callide Coalfields for their cooperation with the field tests.

REFERENCES

BELL, F. G. 1994. Engineering in Rock Masses. Chapter 10: Instrumentation and monitoring in rock masses, Oxford.

GOLDSTEIN, R. M., ENGELHARDT, H., KAMB, B. & FROLICH, R. M. 1993. Satellite radar inter-ferometry for monitoring ice sheet motion: application to an Antarctic ice stream. *Science*, **262**, pp. 1525-1530.

HOEK, E. & BRAY, J. W. 1981. Rock Slope Eng-ineering. The Institute of Mining and Metallurgy.

LEICA. 1998. WILD DI3000S Series Brochure. Leica AG, Switzerland.

REUGER, J. M. 1996. Electronic Distance Measure-ment: An Introduction. Fourth edition, Springer.

SULLIVAN, T. D. 1993. Understanding pit slope movements. Geotechnical Instrumentation and Monitoring in Open Pit and Underground Mining, pp. 435-445.

US MINING SAFETY AND HEALTH ADMINISTRATION. 1998. Fatal alert bulletins and fatal investigation reports. http://www.msha.gov/FATALS/FABC.HTM

Geological hazards — The impact to mining 15-16 November 2001, eds Doyle, Moloney, pp 151-171

Application of slope stability risk design process to open cut mines

NORBERT BACZYNSKI[1], ROSS MARPLES[2], SHAUN TAMPLIN[3], EDEK CHOROS[4]

Douglas Partners Pty Ltd, Brisbane[1], Thiess Pty Ltd, Singleton[2], Tamplin Resources Pty Ltd, Singleton[3], Polchor Pty Ltd, Singleton[4]

Geological hazards exist because, under a particular external environment, a geological system is close to its limit equilibrium. Small changes in the external environment may render this system unstable. Mining is a process that alters the external environment. It often reduces the equilibrium of the geological system. Mining typically involves the creation of temporary openings with a limited design life in the ground. These openings must be suitably engineered for stability and safety reasons. Adequate appreciation and statistical quantification of the various factors impacting on stability are the basis to risk-based design and slope optimization in open cut mines. Basic data inputs and their statistical processing, stability and risk assessment methodology, ensuing analysis outputs and the typical slope design approach at several mines are presented in this paper. The focus is on the background logic and statistical assessment of the shear strength likely to develop along critical 'step-paths' through mine slopes, calculations involved in determining stability risks and general application of this approach to pit slope design.

WHAT ARE GEOLOGICAL HAZARDS?

There are obviously hazardous geological materials and situations in the natural environment. Under various circumstances, some minerals are poisonous, toxic or otherwise harmful to health (e.g., arsenic, uranium, asbestos, mercury, lead, etc.). Likewise, natural geological events such as volcanic activity, earthquakes, etc. may also be deemed as hazardous situations. However, this is a rather narrow perspective of geological hazards, especially when viewed in the context of mining.

A hazard only exists because, under a particular external environment, a geological system is close to limit equilibrium. Small changes in the external environment may render this system unstable.

Mining activity invariably changes the external environment and often reduces the equilibrium of the geological system. Hence, geological systems that were perfectly stable prior to mining may become geological hazards as a result of mining. This broader definition of geological hazards is required in assessing the risk to mining.

As an example, a rock mass is a system comprising intact rock and geological discontinuities. This system exists in an earth stress environment that may be gravitationally or tectonically induced and may be associated with a particular groundwater regime. On a flat ground surface, this rock mass system is inherently stable. It does not constitute a geological hazard. However, by excavating an opening within the rock mass, the pre-existing external environment is altered where, hypothetically, some of the geological defect sets are undercut by the walls of the opening (i.e., defects dip into the excavation) and ground stresses have been concentrated two to three-fold in close proximity to the excavated face. This new environment imposes a "potentially" hazardous situation on what was previously a stable geological system. Nevertheless, the opening may still be well above its limit equilibrium, with instability prevented by the inherent friction and cohesion of the rock mass system. However, further changes in the external environment such as, for example, excavating the face(s) at a steeper angle, rapid weathering of the rock, blasting disturbance of the rock mass (i.e., loss of cohesion), increase in groundwater pressures and earthquake activity may render this system "potentially" unstable and, by definition, a hazardous geological situation.

WHAT ARE MINING RISKS?

Mines are temporary openings in the ground. Their design life is often limited to only a few years. Mines are designed accordingly. An overly conservative design is not in the financial interests of a mining operation.

Figure 1 reinforces the notion that mining activity may potentially create geologically hazardous situations

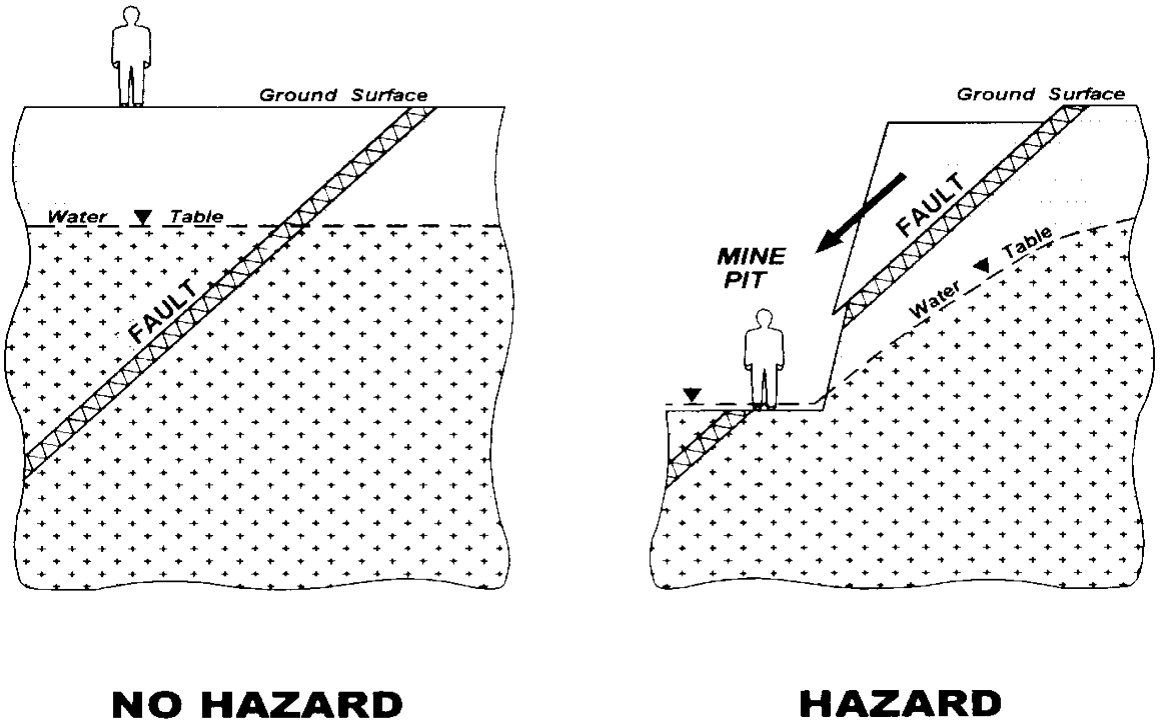

Figure 1 Example of Mining-Induced geological hazard.

where none may have existed prior to mining.

"Good" mine design is to understand the risks involved and to minimize their impact on the mining operation. Because mines are temporary openings, some form of ground failure is inevitable at some time after mining operations cease. Even in operating mines, not all ground failure, per se, is necessarily a hazard – provided that it is anticipated, occurs in a controlled manner and/or does not unduly impact on mining operations. Unpredicted and uncontrolled failure is a hazard and a risk to mining.

There are several types of risks associated with ground failure. The severity of the impact, whether minor, significant or critical, will depend on the location, magnitude and timing of a failure.

Instabilities may have the following impacts:

- impinge on safety — cause injury or worse to mine personnel,
- damage in-pit mine plant — haul trucks, shovels, excavators, etc,
- incur clean up costs — removal of the failed ground or re-establishing mining operations around this area,
- incur stand down / production loss cost — disruption to the mining cycle during the clean up,
- result in loss of ore reserves — i.e. unable to recover the deposit beneath the failed ground,
- increase stability risks to infrastructure — pit workings undermine or encroach upon mine or civil facilities above the failed area, and
- force mine closure — i.e., worst case scenario, where the cost of recovery exceeds the value of remaining reserves or residual safety risks are unacceptable.

PRACTICAL APPLICATION

To be of practical assistance in mine design, the geological hazards must be anticipated, the levels of associated risk must be quantified, the situation must be monitored during mining and appropriate preventative / remedial contingency plans must be formulated to avoid or recover from the instability should it develop.

To anticipate potential geological hazards, the mine designer must have a broad appreciation of the key geological factors likely to impact on design at the mine location. Then undertake a sufficient intensity of geotechnical investigations to either confirm or disprove the existence of the hazards, and if adverse conditions are confirmed to exist, to assess the geotechnical characteristics of each key hazard and compute their stability impact and likely risks for mine operations. Experience at other nearby mines, and to a lesser extent, at more distant mines but insimilar geological settings are also valuable sources of geotechnical information.

Whilst the above investigative approach should in most instances provide the appropriate pit slope design solution, the designer should always remain alert for what Dr Barry MacMahon once described as the "unknown unknown" — a totally unanticipated geological hazard or the "known unknown" — total confidence that a particular hazard cannot possibly exist, but a belief proven otherwise during mining.

TYPICAL DESIGN CYCLE

Mine design is an iterative process generally comprising the following elements:

- review existing data,
- undertake new investigations,
- develop conceptual models,
- stability and risk assess the proposed workings,
- design workings and predict likely ground responses during mining,
- monitor ground behaviour during mining and compare with predictions, and
- repeat cycle, as required.

Figure 2 Typical Design Cycle.

Focus on overriding issues impacting on overall slope design (e.g., faults, shear zones, intrusive dykes, bedding plane 'weak seams', zones of master joint sets, groundwater, seismicity, poor blasting practices, etc.) and progressively 'focus down' to lower order issues (e.g. lower continuity joints, intact rock and rock mass strength, stress, etc).

GENERAL GEOTECHNICAL CONSIDERATIONS AT MINE SITES

Site-specific factors characterize each mine. The inherent attributes impacting on mine design include:

- topography, landform characteristics and development history, surface drainage,
- regional and local geological and structural setting of the deposit and adjacent ground,
- three-dimensional shape and depth of the target deposit,
- hydrogeology: surface and subsurface water conditions, rainfall and recharge,
- tectonic stress regime, and
- Regional and local seismic activity.

The 'local' conditions at the mine are a subset of the 'regional' conditions.

The ground to be mined is rarely, if ever, homogeneous. More often than not, mine geology and structure are complex and considerable geological effort is needed to satisfactorily unravel the situation. The materials may range from soil to rock. A wide spectrum of ground conditions typically exists at most mines.

Where the ground predominantly comprises rock, it is rock mass rather than the intact rock that may best characterize the conditions. A rock mass is a system comprising intact rock and geological discontinuities. All rock masses are characterized by the presence of one or more sets of discontinuities. Members of each discontinuity set are rarely, if ever, uniformly distributed throughout the rock mass but tend to occur in zones or clusters. Typical discontinuities include sedimentary features (e.g., lithological layering/bedding, cross bedding, erosion unconformities, etc.), sedimentary and intrusive rock type contacts (e.g., facies changes, intrusive dykes, etc.) and geological defects created during structural deformation of the rock mass (i.e., normal, reverse and thrust faults, shear zones, bedding, foliation and cleavage planes, joints, mineralized veins, etc.). There may be several phases of structural deformation, resulting in a complex structural pattern.

Mining often modifies some pre-existing factors e.g. the water table may be drawn down. In fact, this drawdown may be a necessity to provide dry working conditions in the pit, to reduce blasting costs and improve fragmentation, to enhance ground stability and to provide part of the water required for mining activity. The ground immediately adjacent to mine workings may be blasting disturbed, although the severity of this could be minimized by appropriate blasting practices. Zones of stress concentration and tension as well as strata displacements will be induced in the ground.

Mine slopes are temporary excavations. To reduce the cost of waste rock removal, pit slopes are mined as steep as possible. An appropriate understanding of: the pre-mining physical, structural and geotechnical attributes of the ground, the statistical variability in these attributes across a project area, spatial distribution of significantly different geotechnical 'domains' around the mine workings and likely mining-induced impacts; are basic requirements for the design of interim and final pit slopes and quantification of stability risks.

Existing nearby facilities (e.g., waterways, water supply dams, roads and other civil infrastructure) as well as the ones that need to be constructed as part of mine development (e.g. haul roads, tailings dams, waste dumps, in-pit and ex-pit crushers, mineral processing plant, etc.) impact on slope design. Depending on their location and proximity to the pit workings, due consideration and quantification of these is needed to determine the stability risks that will be acceptable for various slopes around the mine perimeter.

CONCEPTUAL MODELS

The geological and geotechnical models for a mine often evolve and are progressively updated over a period of time. Sometimes, these models may only become fully resolved as the mine nears its end of life. Table 1 details the type of data that needs to be collected for stability risk assessments.

Initial Model

At the outset of a mining project, the model may be solely based on existing regional topographic and geological maps, air photo interpretation, cored (and, perhaps, structurally orientated) borehole data and limited geological mapping of scant rock outcrops within the project area. Viewed simply, the mine site geological model is a subset of the regional geological model. At a later date, this database may be supplemented by geological mapping of bulk samples or trial excavations.

Borehole data has its limitations. There is an inherent bias in the sampling, with 'blind' sampling zones (i.e., defects aligned semi-parallel to the drilling direction) and the swamping and distortion of the resulting struct-ural model with disproportionate numbers of relatively short (say, ≤100mm to 200mm) defects that may have little practical impact on pit slope design. Experience on many mining projects suggests that, unless extreme care and diligence are exercised by the driller in achieving reliable 'core orientation' marks and the geologist / engineer logging the core is likewise fully dedicated to achieving a good logging outcome, structurally orientated core data may have a low reliability. The sampling bias and limited reliability are demonstrated by the fact that the structural defect patterns ensuing core results are often difficult to reconcile with those based on slope mapping data. Some core orientation devices are better than others. The standard Craelius pin device is basically limited to subhorizontal holes and is totally unreliable for holes declined steeper than 20^o to 30^o from the horizontal. The modified Van Ruth Craelius pin device is much more versatile and reliable and has been successfully used in boreholes drilled as steep as 80^o or more from the horizontal. Other techniques such as spears, acid etch, imprint packer, etc. are also reported to have been successful on various projects.

In recent years, considerable advances have been made in using geophysical and video camera (e.g., RaaX) techniques to determine downhole geological defect patterns. The writer's experience with the latter method on several civil and mining projects suggests that this method is especially successful. Also, investigation objectives are achieved at a significantly lower (say, 60% to 70% less) overall cost than incurred using conventional orientated core drilling, especially when the cost of the structural core logging and processing of this data is taken into consideration. Whilst cored boreholes are still required to obtain representative rock samples from within the deposit/ore, the surrounding overburden and pit floor strata, not all holes may be necessary for that purpose. Some holes could be open-holed and then scanned using the RaaX system.

Updated Model

As mining commences, the geological database expands or should expand rapidly due to slope face mapping data. The geological and geotechnical models are progressively updated as new data accumulates. For geotechnical analysis and design purposes, the slope face mapping daa is typically the more reliable. To be statistically most useful, geological and structural defects data should be collected systematically as the pit workings expand laterally and increase in depth.

Future Mine Areas

Future mine areas may be located at considerable distance (say, 200m to 500m) from the expanding pit perimeter or very deep below the floor of the current pit workings. Such areas can only be realistically investigated by drilling. Without drilling, the conceptual model must rely on the extrapolation of data from the existing pit areas. Whilst the practice of extrapolation is commonly used, the extrapolation distances may sometimes limit the confidence in such conceptual models. It is essential that the extrapolated model conditions are checked by an on-going program of slope face mapping as the pit workings advance towards these distant/deeper areas.

GENERAL SLOPE DESIGN APPROACH

The slope design approach that has been typically used or should have been used on the majority of open cut mine projects is a systematic multi-step process. Many aspects need to be considered, often in a relatively sequential manner, and the basics of this process are best illustrated by means of flowchart diagrams.

The flowchart in Figure 3 broadly overviews the key steps involved. The flowchart in Figure 4 expands on the key steps. It presents a more detailed breakdown of the associated tasks. The reader should examine this flowchart closely before proceeding with the rest of this text.

Each task represented by a flowchart box in Figure 4 often requires considerable analysis effort. As an example, Figure 5 expands on Box B of Figure 4 to illustrate the basics of the kinematic stability analysis process to identify potential slope failure modes.

Figure 6 expands on Item B-2 in Figure 5 (also a subset of Box D of Figure 4) to show the kinematic stability analysis involved in identifying a potential

Conceptual Model		Regional	Mine Site
Mine Plan	Layout of deposit; likelihood of underground mine; layout of open cut pit workings; layout of existing civil and proposed mine infrastructure; mining schedule (locations, volumes, depth); location of critical slopes		✓
Ground Conditions	Topography	✓	✓
	Landform development history (e.g., ancient + recent landslides)	✓	✓
	Surface drainage patterns (rivers, creeks, swamps, rainfall, flow regime)	✓	✓
	Soil overburden characteristics (soil types, depths, shear strength)	✓	✓
	Rock types, geological history, contacts, etc	✓	✓
	Intact rock geotechnical properties (1)		✓
	Geological deformation history (i.e., number of phases, characteristics)	✓	✓
	Through-going structures (> 100m to 500m) characteristics (2)	✓	✓
	Major structure (15m to 100m long) characteristics (3)	✓	✓
	Minor structure (0.3m to 15m long) characteristics (4)		✓
	Rock mass classifications (RQD, fracture frequency / m, RMR or Q)		✓
	Rock mass geotechnical parameters (5)		✓
	Groundwater conditions (depth to water table, rock permeability, storativity, transmissitivity, aquifers, aquitards, flow regime, recharge, seasonal fluctuations, drawdown characteristics – pump testing)	✓	✓
	Stress regime (i.e., from in-situ measurements or based on structural relationships, experience on other projects in region, etc.)	✓	✓
	Seismicity (ie., history of events – occurrence date, geographic location, depth, magnitude and duration, magnitude return period, etc.)	✓	

Footnotes:	
(1) Intact rock properties	1. Unconfined compressive strength (UCS) – check for anisotropy in strength relative to bedding / foliation (this could be as much as 200% to 400%), strength reduction with increasing degree of rock weathering etc. 2. Brazilian tensile strength 3. $I_{S(50)}$ Point-load strength index (axial, diametral, 'irregular lump' samples) 4. Strength ratio between UCS and $I_{S(50)}$ 5. Rock density 6. Elastic modulus 7. Dynamic modulus 8. Poisson's ratio 9. Triaxial compressive strength
(2) Through-going structures	1. Structure type – normal, reverse, thrust faults, shears and / or shear zones, regional folding, intrusive dykes or dyke swarms 2. Geological deformation history – sequence of events, phases of deformation and their characteristics, relationship between phases 3. Other airphoto lineaments (not immediately apparent as structures on the ground surface) 4. Structure attributes – orientation, number of sets, lengths, widths, spacings, infill types, extent of more intense deformation / fracturing in close proximity to these structures, evidence of recent movement on them 5. Shear strength based on infill types and back-calculated from existing slides / ground failures
(3) Major structures	1. As above, for (2) through-going structures 2. Location and relative occurrence of "zones" of closely spaced "joints" / minor structures

Table 1 Conceptual Model requirements.

(4) Minor structures	1. Structure type – fault, shear, intrusive dyke, bedding, foliation, joint, vein, rock type contact 2. Number of differently orientated defect sets FOR EACH DEFECT SET, to allow STEPSIM4 'step-path' shear strength assessment, sufficient data needs to be collected to develop a confident statistical model (i.e., statistical distribution type – normal, lognormal, exponential, etc., population mean, mode, median, standard deviation, minimum, maximum values) for: 3. Orientation (dip direction / dip angle) – ideally, stereographic projection plots comprising ≥300 to 400 data 4. Relative % of defect types within particular orientation grouping (i.e., faults, shears, foliations, joints,etc) 5. Probability of occurrence within rock mass (i.e., % of areas that defects occur in) 6. Length 7. Spacing 8. Probability that defects terminate within intact rock or are cut-off by other defects 9. Small scale defect surface roughness (i.e., Barton's 1 to 10 scale over 100mm surface distance) 10. Large scale defect surface roughness (i.e., undulation wavelength and amplitude) 11. Infill type (e.g., none / clean, "weak" – clay, chlorite, talc, graphite, breccia, gouge, "strong" – iron oxides, sulphides, calcite, quartz, etc.) 12. Base friction angles (i.e., laboratory determined by direct shear testing of defects)
(5) Rock mass parameters	1. Hoek-Brown empirical equations determined shear strength (friction and cohesion) for blasting disturbed and undisturbed ground conditions 2. Rock mass elastic deformation parameters (modulus, Poisson's ratio) 3. Rock mass bulk density 4. Rock bulking factor on blasting 5. Rock fragmentation characteristics

Table 1 continued Conceptual Model requirements.

tetrahedral wedge failure mode and the critical geological defect sets defining the base / sliding surfaces of such a wedge.

By itself, the kinematic stability analysis cannot determine whether a slope failure will occur or not. It can only flag the potential for such a failure mode to develop in a particular mine slope. As shown in Figure 4, the designer needs to assess the elements in flowchart boxes H, I, J, K and L before a stability analysis can be undertaken.

In essence, before embarking on the stability analysis, the designer must firstly assess the:

- shear strength (i.e. effective peak friction angle and cohesion, residual friction angle) for the geological defects defining potential wedges,
- groundwater conditions in the slope (including the impact of potential recharge and development of artesian pressures in the slope due to water or tailings dams or water sumps that may be located within close proximity of the slope crest),
- impact of other external factors on stability (e.g. seismic loadings, reduction in defect shear strength due to blasting-induced damage to slopes, surcharge loadings such as waste dumps located within close proximity of slope crests), and
- 3D geometry of the slope to be assessed.

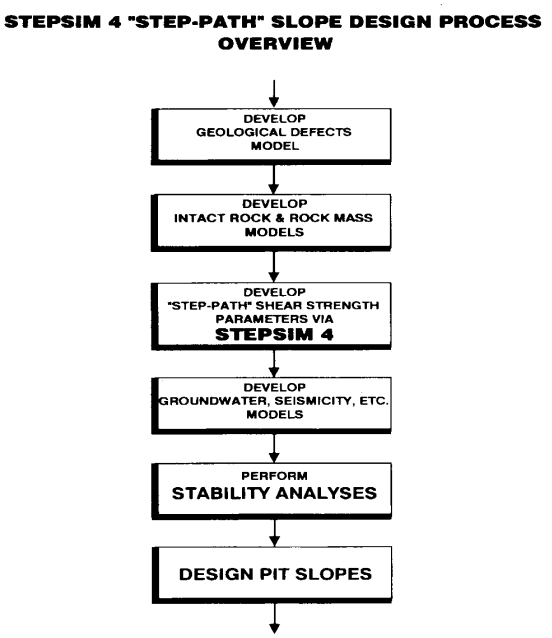

Figure 3 Broad overview of key design systems

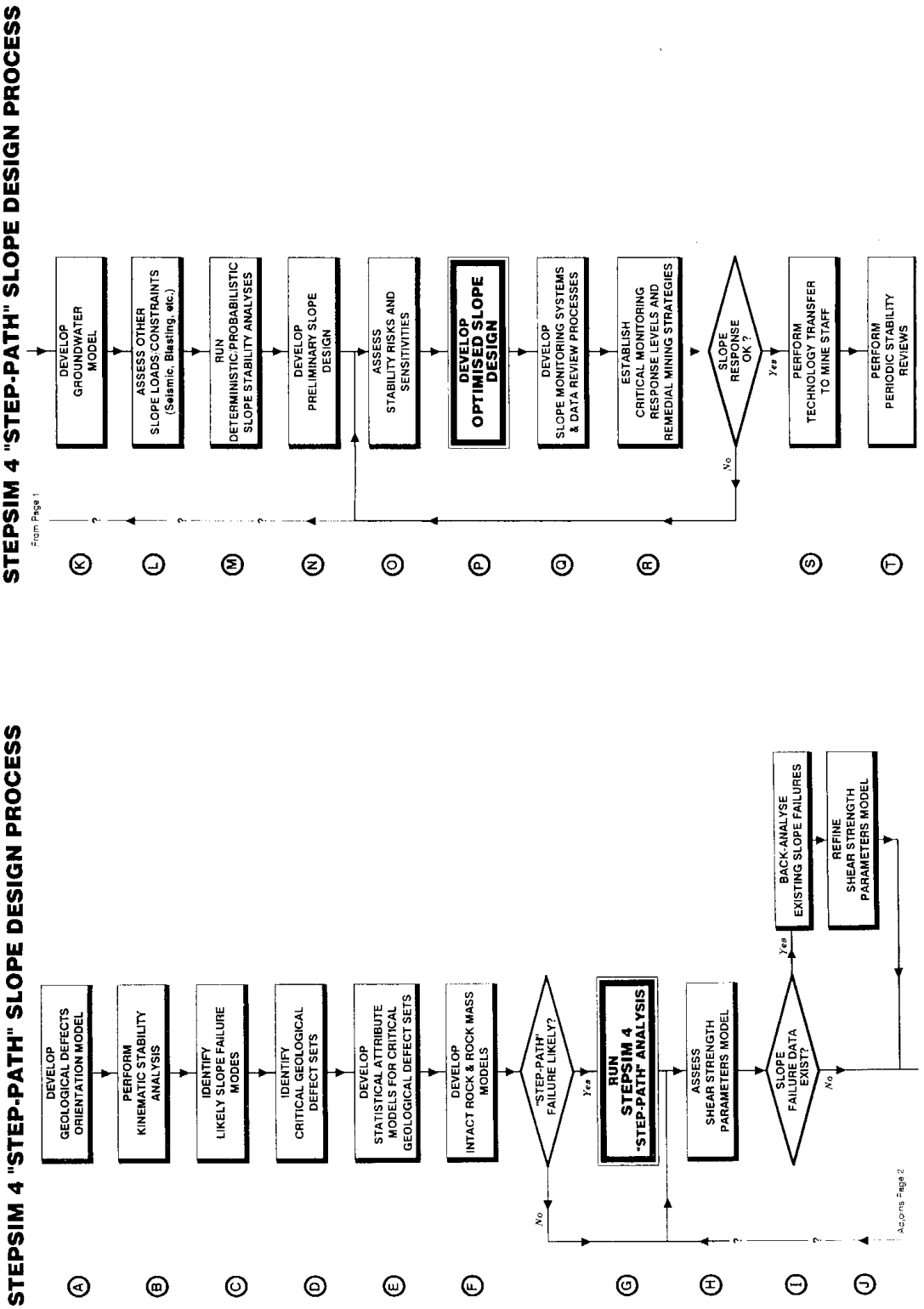

Figure 4 Expanded overview of key design tasks.

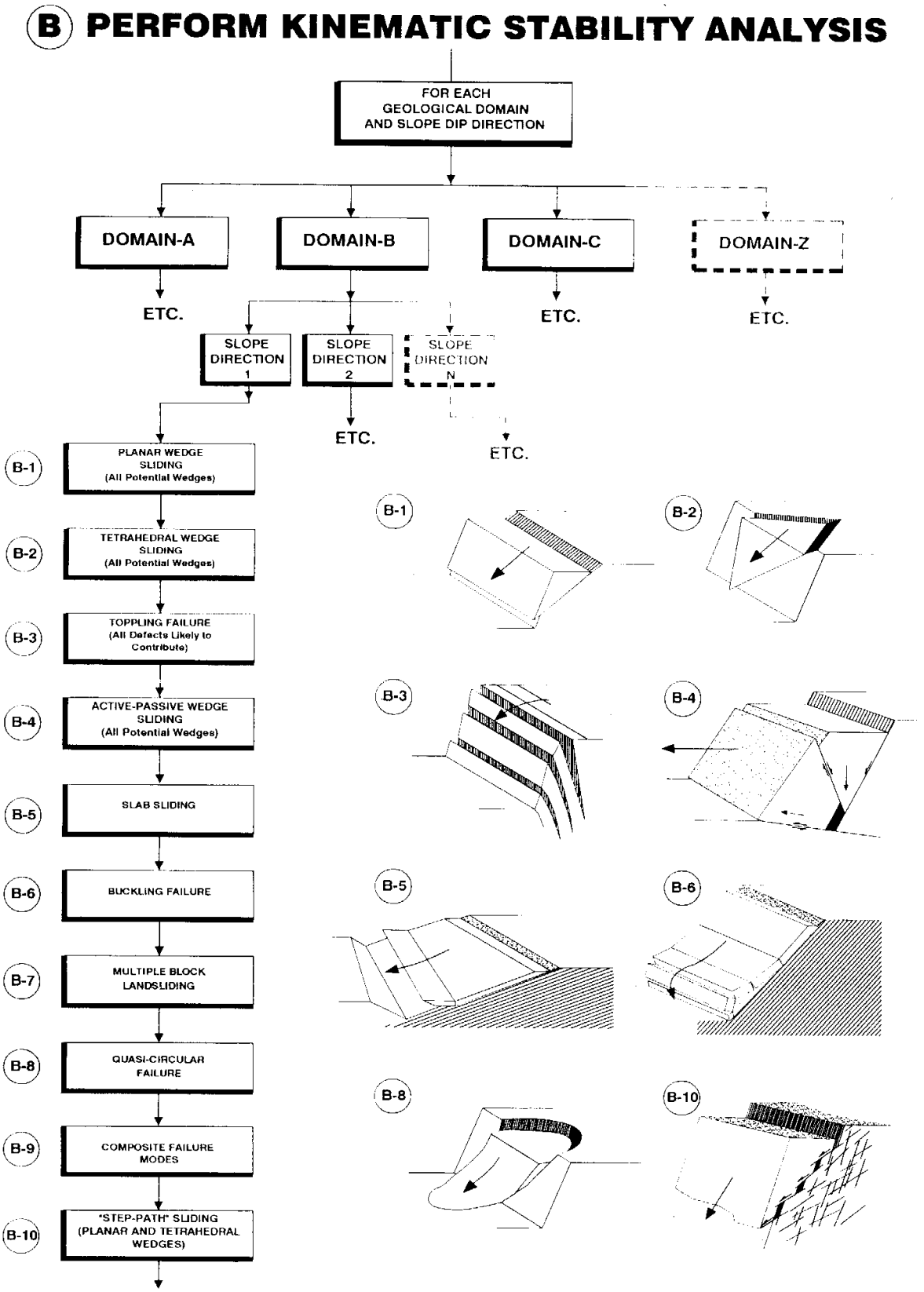

Figure 5 Elements of kinematic stability assessment.

Shear strength of geological defects is one of the key inputs, if not the overriding input, to the stability analysis process. In many instances, a realistic assessment of this parameter is not straightforward.

Even where the potentially unstable ground results from one or more through-going geological defects (faults, shears, dykes, etc.), assessing the shear strength may not be an easy task. However, there is now probably sufficient information published in geotechnical textbooks, technical journals, conference proceedings and case studies to provide some guidance in assessing order of magnitude shear strength values for such geological structures. Whilst published values may be adopted for purposes of preliminary design, such values must be validated by relevant site-specific geotechnical investigations in the project area.

As open cuts are mined deeper, progressively higher slopes need to be assessed, where potential instabilities may not necessarily be totally defined by through-going geological defects only. As shown in Figure 7 (reproduced from Baczynski, 2000e), potential slides may be complex and be characterized by occurrence of multiple failure modes within them, with overall sliding along a composite failure path through the rock slope.

In many situations, less continuous individual defects or zones of closely associated such defects may impact on overall and partial (e.g. single and multiple bench height) slope stability. For example, the following combinations of geological defects may define the two slip surfaces of potential tetrahedral wedges:

- both surfaces/sides are defined by through-going defects,
- one surface/side is defined by a through-going defect; the other by a set of defects where the individual defects are discontinuous but tend to occur in a broadly through-going zone, and
- each surface/side is defined by a different set of defects, where the individual defects are discontinuous but tend to occur in a broadly through-going zone.

Because of the discontinuous nature of individual defects, such zones often have considerable inherent cohesion due to existence of intact rock or rock mass 'bridges' between many of the defects within the zone. Such zones defined by one or more defect sets are commonly referred to as 'step-paths' through mine slopes. The shear strength of 'step-paths' can only be realistically assessed by systematic and detailed geological mapping of slope faces.

STEPSIM4 'STEP-PATH' SHEAR STRENGTH

The basic 'step-path' methodology was reviewed in Baczynski (2000e).

Dr Barry MacMahon conceptualized the 'step-path' approach for slope design at the Bougainville copper mine in PNG in the late 1970's. Over the last three to four years, the writer (NB) has applied an enhanced and extensively modified version of the 'step-path' technique (i.e. STEPSIM4 software) at the Ok Tedi, Kidston and Mount Owen mines in PNG, Qld and NSW, respectively. The results of this work reside in company files and reports, e.g., Little, Cortes and Baczynski (1999, 2000), Baczynski and Smyth (2000) and Baczynski (1998 to 2001). A similar but less formal approach to the determination of the contribution of intact rock 'bridges' to shear strength along critical paths was also applied to the design of some slopes at Leigh Creek in SA during the 1980s and early 1990s, e.g., Baczynski (1990, 1992) and Choros (1992).

Basic inputs to the 'step-path' shear strength determination are those parameters listed under 'Ground Conditions' and 'Footnotes (1) to (5)' in Table 1. Many of the elements of Footnotes (1) and (5) and all elements of Footnote (4) are considered in the shear strength assessment via the STEPSIM4 software. STEPSIM4 statistically simulates potential 'step-paths' through mine slopes. The achieved simulation reflects the inputs, notwithstanding the assumptions, constraints and limitations inherent in the STEPSIM4 method. The purpose of this analysis is to derive a statistical model for shear strength (i.e., the mean and standard deviation for the effective friction angle and cohesion).

As shown in Figure 8, the STEPSIM4 approach envisages potential failure paths through rock masses as a system of adjacent ground 'cells'.

In determining the shear strength, each cell is statistically associated with one or more of the following failure modes:

- sliding along members of an adversely orientated defect set (Set 1),
- 'stepping-up' along another set of steeper dipping defects (Set 2),
- direct shearing through all intact rock or rock mass 'bridges', and
- shearing through the rock mass in those 'cells' without Sets 1 and 2 defects.

The STEPSIM4 simulation assumes that Set 1 and Set 2 defects occur independently within a rock mass. This simulation involves the following basic computational procedure.

- The user selects a target 'step-path' length (e.g. 100m, 250m, 500m). For each simulated path, the geological defect and strength characteristics are statistically assigned to each 'cell' on the basis of the input parameter models.
- 'Step-paths' start at the slope toe; the first 'cell' in the simulation process. 'Cell' size should be statistically meaningful. Ideally, it should mirror the size of the 'data windows' used to structurally map faces, a convenient length section of line traverses or perhaps bench heights. If this is not possible, an arbitrary 'cell' size (say, 5m x 5m or 10m x 10m) may be selected.

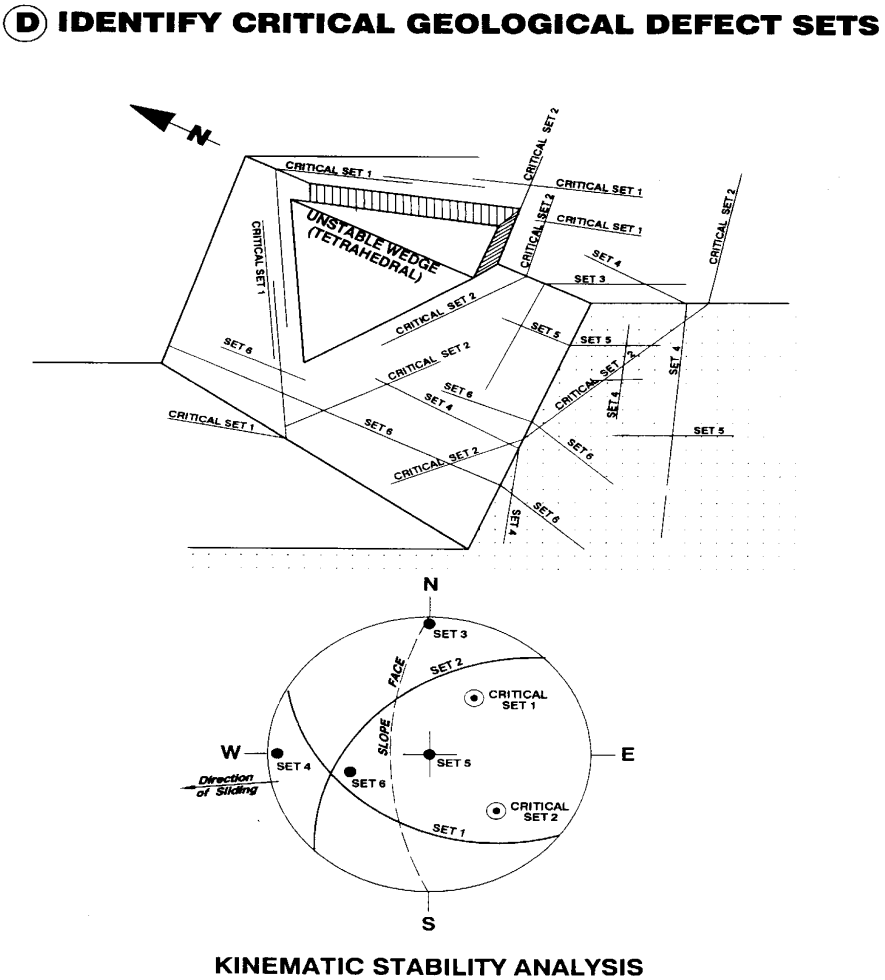

Figure 6 Example of Kinematic Stability Assessment for Tetrahedral Wedges.

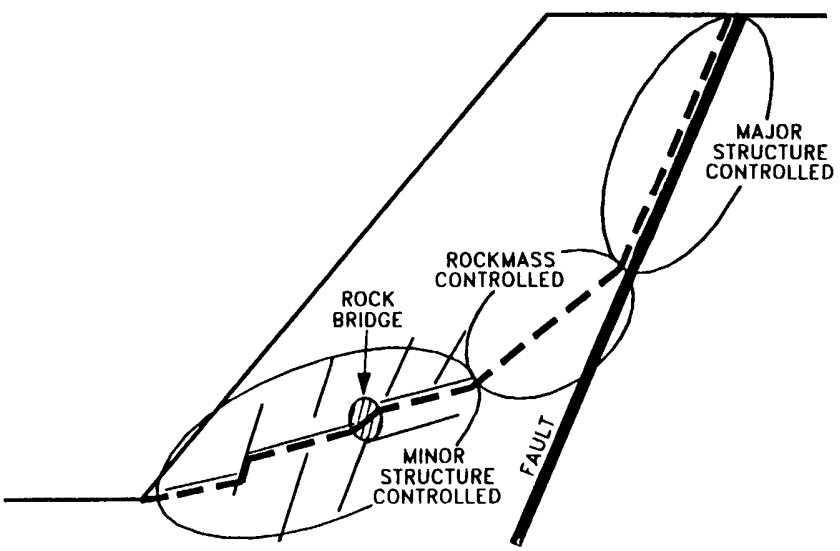

Figure 7 Composite Failure Path Through Rock Slope.

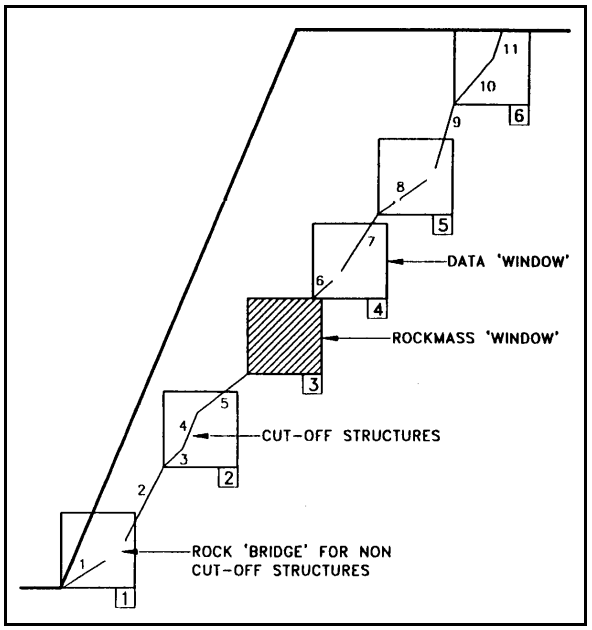

Figure 8 Conceptual STEPSIM4 Model.

- Based on the statistical model for the 'probability of occurrence' for Set 1 and Set 2 determined for the rock mass, STEPSIM4 uses a 'random number' generating algorithm to check whether one, both or none of the defect sets should be simulated in the first 'cell'. If neither set occurs, rock mass properties are assigned.
- If the first, the second or both defect sets occur, then the 'Monte-Carlo' process is used again to systematically generate the respective defects within the first 'cell'. Based on the input statistical model for defect 'types' (e.g., fault or joint, joint with 'weak' infill or one with 'strong' infill, etc), a 'type' is Monte-Carlo assigned to the first defect. A similar process is used to assign orientation (dip), length and shear strength for the first defect and to check whether this defect terminates in intact rock or is 'cut-off' by another defect within the simulated rock mass. If the first defect is 'cut-off', then the second defect will start at the end of the first defect. If the first defect is not 'cut-off', then an appropriate length rock 'bridge' is Monte-Carlo simulated at the end of the first defect, with the second defect starting at the end of this rock 'bridge'. Depending on their size, 'bridges' may be assigned either intact rock or rock mass shear strength parameters. If both Sets 1 and 2 occur in the first 'cell', then the Monte-Carlo process is used to decide whether the next structure to be generated should be a Set 1 or a Set 2 member. This process is iterated until the last generated defect or rock 'bridge' either terminates at the perimeter of the current 'cell' or outside it.
- The bottom left-hand corner of the second 'cell' coincides with the end of the last generated defect or rock 'bridge'. The above process is repeated for the second 'cell'.
- Successive 'cells' are processed until the target 'step-path' length has been simulated. The shear strength is computed for the first simulated path.
- A large number of target length paths are simulated (i.e., usually, 2000 to 5000). The statistical shear strength model is computed.

The STEPSIM4 derived shear strength model provides the basic input to conventional and risk based slope stability analyses. STEPSIM4 is simply a software tool. It provides a logical and transparent approach for statistically combining several types of related data to assess shear strength variability along critical 'step-paths' through rock slopes. It does not provide magic answers. STEPSIM4 is intended to complement existing geotechnical approaches.

STABILITY RISK ASSESSMENT PROCESS

Stability risk assessment is a multi-step process. The computed risks are only meaningful if the conceptual geological model being assessed is representative of actual site conditions. The geological model for a particular slope may be simple or complex, but its complexity must not exceed the stability analysis capability of existing 'state-of-the-art' software.

Rosenblueth Method

The risk assessment for simple cases where only a few parameters need to be considered is easiest handled by Rosenblueth's method of (statistical) moments, such as outlined below. This approach assumes that each parameter is an independent variable. The stability analysis determines a factor of safety (FOS) for every combination of +1 standard deviation (+1SD) and -1 standard deviation (-1SD) value for each parameter. The ±1SD, ±2SD and ±3SD intervals encompass 68.26%, 95.46% and 99.73% of the values about the population mean, respectively.

A FOS is defined as the ratio of the resisting force (i.e. stabilizing the system) to the activating force (i.e. destabilizing or causing the system to fail). A FOS of <1, 1 and >1 means that the system is unstable, just stable and stable, respectively. A FOS of 1.3 means that the resisting force is 30% higher than the activating force.

If the conceptual model comprises three parameters (say, defect dip angle, friction angle, and cohesion), then 2^3 or 8 stability analyses need to be performed. If there are 4 or 5 parameters (say, groundwater, seismic loadings as well as previous considerations), then the number of stability analyses required will increase to 16 and 32, respectively.

After the suite of stability analyses is completed, ensuing FOS values are statistically processed to derive their mean and ±1SD. The stability risk is equivalent to the percentage of FOS values <1.

'Monte-Carlo' Simulation

As the number of parameters to be considered increases, the Rosenblueth stability analysis task becomes very onerous. Normally, this method would not be used for more than 6 parameters (i.e., >64 stability analyses). Such models are easier handled by 'Monte-Carlo' simulation techniques.

The inputs to the 'Monte-Carlo' technique are similar to those for the Rosenblueth method. Each parameter is described in terms of its mean and ±1SD. Using a random number generator, the 'Monte-Carlo' software statistically samples relevant statistical populations for the parameters. It then performs the stability analysis and determines the FOS for the conceptual model based on the sampled values.

The computer software iterates this statistical sampling and stability analysis process a large number of times, usually several thousand times (5,000 to 10,000). The ensuing FOS is again statistically processed to determine the risk of a FOS <1.

The 'Monte-Carlo' method is quite versatile. It allows the stability risk assessment of quite complex models comprising significant number of independent parameters.

Example Planar Wedge – Rosenblueth Stability Risk Assessment

The risk assessment procedure is easiest illustrated by a simple example — the planar wedge shown in Figure 1. Table 2 details the assumed design parameters.

There are four (4) statistically variable parameters in this risk assessment – dip of the geological defect, rock density, friction angle and cohesion along the defect. Hence, the Rosenblueth method requires 2^4 or 16 analyses. Table 3 shows the combinations of +1SD and –1SD parameters that need to be assessed and the resulting FOS.

The statistical FOS model for the above analyses is 1.67 ± 0.63. The risk of instability (i.e. FOS <1) is 13.5% or 0.135. The risk of a FOS <1.2 is about 23% or 0.230.

Multiple Wedge Type Failures

The above principles may be readily extended to more complex situations where slope stability is impacted by several wedge types and/or by several different slope failure modes. The stability risks for each wedge type and failure mode must be assessed separately. The individual stability risks are then combined. As an example, assume a case of three wedge types with stability risks R_1, R_2 and R_3, respectively. The overall risk R_O for the slope may be derived in the following manner:

Table 2 Details of Example Planar Wedge.

Depth of Excavation	6m
Excavation Face Angle	75^o
Dip of Geological Defect / Base	$48^o \pm 6^o$
Crest to Toe Wedge Height	4m
Rock Density	$2.4\pm 0.1 t/m^3$
Defect Peak Friction Angle	$26^o \pm 2^o$
Defect Cohesion	2 ± 1kPa
Groundwater	Dry Slope

$$R_O = R_1 + [\,(1 - R_1) \times R_2\,] + \{(1 - R1 - [(1 - R_1) \times R_2\,]\,) \times R_3\}$$

If the three risks were, say, 0.3, 0.2 and 0.6, respectively,

then the overall slope failure risk will be:

$$R_O = 0.3 + [\,(1 - 0.3) \times 0.2\,] + \{(1 - 0.3 - [(1 - 0.3) \times 0.2]) \times 0.6\}$$

$$R_O = 0.3 + 0.14 + 0.336$$

$$R_O = 0.776$$

Simple addition of the individual risks will yield an incorrect answer. In the above case, such addition would have resulted in a risk of 1.1, an impossibility as the maximum risk cannot exceed 1.0 (i.e. 100%).

Complex Models

As shown in Figure 7, slope failure may be complex. The backscarp may be defined by a through-going geological defect (i.e. fault, shear, dyke, etc.), the toe region may comprise a 'step-path' traverse through a network of discontinuous geological defects, whereas the central section of the slide base may involve shearing through the rock mass. Each of the three regions along the slide base would need to be characterized by appropriate shear strength parameters.

Limitations

To achieve meaningful stability analysis results, whether using conventional analyses or risk based ones, the conceptual geological model must reflect actual ground conditions and probable slope failure mode(s), i.e. the outcome of the kinematic stability assessment must be valid.

If the conceptual model is wrong, then the stability analysis will have little chance of being valid. No amount of 'state-of-the-art' stability analysis software or statistical processing will alter this poor outcome.

Analysis No.	+1SD and -1SD Combinations				FOS
	Base Dip	Density	Friction	Cohesion	
1	+	+	+	+	2.28
2	–	+	+	+	2.16
3	+	–	+	+	2.57
4	+	+	–	+	2.22
5	+	+	+	–	1.01
6	–	–	+	+	2.30
7	+	–	–	+	2.50
8	+	+	–	–	0.95
9	–	+	–	+	2.07
10	+	–	+	–	1.11
11	–	+	+	–	1.12
12	–	–	–	+	2.20
13	+	–	–	–	1.05
14	–	+	–	–	1.02
15	–	–	+	–	1.16
16	–	–	–	–	1.06
				Rosenblueth FOS =	1.67 ± 0.63

Table 3 Rosenblueth FOS for Example Planar Wedge

Table 4 Inputs for example joint

WIDER APPLICATION OF ROSENBLUETH METHOD

The Rosenblueth method has wider applications than discussed so far. It may be used to derive statistical models for some parameters input to the STEPSIM4 simulation process, e.g., Barton and Choubey (1977) friction angle for joints and Bieniawski (1976) rock mass rating (RMR) index.

Joint Friction Angle

The Barton and Choubey (1977) equation for the effective peak friction angle of joints may be extended to include the 'large scale surface roughness' component. The extended equation is:

$PFA = JRC \times Log_{10} (UCS / NS) + BFA + LSSR$, where:

PFA = Peak friction angle
JRC = Barton's joint roughness coefficient, where the JRC = SSSR x 2 – 1, and
SSSR = Small scale surface roughness (1 to 10)
Log_{10} = Logarithm to base 10
UCS = Unconfined compressive strength of the rock adjacent to the joint
NS = Normal stress acting on the joint surface (i.e., joint dip and depth in slope related)
BFA = Base friction angle (material along joint surface, without including SSSR)
LSSR = Large scale surface roughness of joint surface, i.e., ATAN [amplitude / (0.5 wavelength)]

For a particular normal stress scenario, four input parameters (i.e., SSSR, UCS, BFA, LLSR) vary statistically. Tables 4 and 5 present inputs and outputs for an example joint.

RMR Index

The RMR Index considers five input parameters — i.e. the unconfined compressive strength (UCS or $I_{S(50)}$ point-load index), rock quality designation (RQD) index, joint spacing, joint condition (i.e., infill and length attributes) and groundwater. These input parameters vary statistically. Tables 6 and 7 present inputs and outputs for an example rock mass.

BFA (base friction angle)	$30^o \pm 2^o$
JRC (i.e., SSSR x 2 – 1)	7.4 ± 2.0
UCS (intact rock strength)	49 ± 24MPa
LSSR (large scale surface roughness)	$4^o \pm 3^o$
NS (normal stress on joint surface)	3.2MPa

Table 4 Inputs for example joint.

UCS (intact rock strength)	60MPa and 160MPa (8, 14) *
RQD (rock quality designation)	32% and 100% (7, 20)
Joint Spacing	0.15m and 3.05m (8.5, 20)
Joint Condition	Slickensided and Fresh / Rough (10, 30)
Groundwater	Dripping and Dry (4, 15)

Table 6 Inputs to RMR Index for Example Case

* *-1SD condition and +1SD condition (– 1SD RMR rating, +1SD RMR rating)*

Analysis No.	+1SD and -1SD Combinations				Friction Angle
	BFA	JRC	UCS	LSSR	
1	+	+	+	+	51.8
2	–	+	+	+	47.8
3	+	–	+	+	46.3
4	+	+	–	+	47.4
5	+	+	+	–	45.8
6	–	–	+	+	42.3
7	+	–	–	+	43.8
8	+	+	–	–	41.4
9	–	+	–	+	41.8
10	+	–	+	–	43.4
11	–	+	+	–	40.3
12	–	–	–	+	39.8
13	+	–	–	–	37.8
14	–	+	–	–	37.4
15	–	–	+	–	36.3
16	–	–	–	–	33.8
Rosenblueth Joint Peak Friction Angle =					42.3 + 4.6

Table 5 Rosenblueth Peak Friction Angles for Example Joint

Analysis No.	+1SD and -1SD Combinations					RMR Index
	UCS	RQD	Spacing	Condition	Water	
1	+	+	+	+	+	99.0
2	–	+	+	+	+	93.0
3	+	–	+	+	+	86.0
4	+	+	–	+	+	87.5
5	+	+	+	–	+	79.0
6	+	+	+	+	–	88.0
7	–	–	+	+	+	80.0
8	–	+	–	+	+	81.5
9	–	+	+	–	+	73.0
10	–	+	+	+	–	82.0
11	+	–	–	+	+	74.5
12	+	–	+	–	+	66.0
13	+	–	+	+	–	75.0
14	+	+	–	–	+	67.5
15	+	+	–	+	–	76.5
16	+	+	+	–	–	68.0
17	–	–	–	+	+	68.5
18	–	–	+	–	+	60.0
19	–	–	+	+	–	69.0
20	+	–	–	–	+	54.5
21	+	–	–	+	–	63.5
22	+	+	–	–	–	56.5
23	–	+	–	–	+	61.5
24	–	+	+	–	–	62.0
25	+	–	+	–	–	55.0
26	–	+	–	+	–	70.5
27	–	–	–	–	+	48.5
28	–	–	–	+	–	57.5
29	–	–	+	–	–	49.0
30	–	+	–	–	–	50.5
31	+	–	–	–	–	43.5
32	–	–	–	–	–	37.5
					Rosenblueth RMR Index =	68 ± 15

Table 7 Rosenblueth RMR Index for Example Case

RISK ASSESSMENT EXAMPLES

KEY FACTORS		4 MINE				
		All Slopes, Ok Tedi, PNG	**East Wall, Eldridge Pit, Kidston, Qld.**	**All Slopes, Pit A, Mount Owen, NSW**	**M6 Terrace Mining Box Cut, Leigh Creek, SA**	**M10 Pit, Trial Slope, Leigh Creek, SA**
Slope Heights Assessed	Overall (highwall)	600–850m	290m	250m	220m	95m
	Partial	50 – 350m	70 – 150m	45 – 150m	50 – 150m	–
	Bench (single / multiple)	15m / 45m	35m	15m / 45m	12m / 36m	12m / 24m
Slope Angle	Overall (highwall)	35^o – 50^o	42^o	48^o – 62^o	35^o – 40^o	50^o
	Partial	30^o – 50^o	46^o – 57^o	65^o – 75^o	50^o	–
	Bench (single)	65^o	65^o	90^o	70^o	70^o
Geotechnical Domains (Number)		36	5	12	12	3
Slope Directions (No. per domain)		3 – 6	1 – 3	1 – 3	1 – 2	1
Through-going Structures	Normal Faults	✓	✓	✓	✓	✓
	Thrust Faults	✓		✓	✓	
	Shear Zones		✓		✓	
	Dykes			✓		
	Skarn Zones	✓				
	Bedding Shears			✓	✓	✓
	Foliation Shears		✓			
	Closely Jointed Zones	✓	✓	✓	✓	✓
Joint-fault defined ‘Step-paths’		✓	✓	✓	✓	
Intact Rock & Rock Mass Strength		✓	✓	✓	✓	✓
Groundwater (Several Options)		✓	✓	✓	✓	✓
Seismicity		✓	✓	✓	✓	
Blasting Disturbance of Slope		✓	✓	✓		
Slope Failure Modes	Planar Wedge	✓	✓	✓	✓	✓
	Tetrahedral Wedge	✓	✓	✓	✓	✓
	Active-Passive Wed		✓		✓	✓
	Circular	✓	✓	✓	✓	✓
	Quasi-Circular	✓	✓	✓	✓	✓
	Toppling	✓	✓	✓	✓	✓
	Slab Buckling				✓	✓
	Composite Mode	✓	✓	✓		

Table 8 Factors impacting on slope risks: Case studies. This table details the geological factors that influence the development of conceptual models and stability risk analyses for pit slope design at four mines.

Tables 9 to 11 present indicative statistical inputs and shear strength outputs from the STEPSIM4 'step-path' analysis for an example slope area at a case study mine.

Attribute	Statistical Model	Median (Mean)	-1 SD	+1 SD	Other Design Details
Orientation	Bivariate Normal	Domain 1 250 / 55	–	–	Design 250 / 55 ± (12/12)
		Domain 2 245 / 60	–	–	Design 245 / 60 ± (12/12)
		Domain 3 260 / 75	–	–	Design 260 / 75 ± (9/9)
		Domain 4 300 / 80	–	–	Design 300 / 80 ± (9/9)
Length	Lognormal	Domains 1-4 1.30m (Mean=2.2m)	0.46m	3.6m	8% risk > 5m 2% risk > 10m <1% risk > 20m
Spacing (between adjacent J1 joints)	Lognormal	Domains 1-4 0.44m (Mean=1.38m)	0.10m	2.00m	5% risk >5m 2% risk >10m 0.5% risk >20m
Probability of Occurrence in Rock Mass (5m Windows)	Domains 1, 2	75%	–	–	Domains 1-4 Design 75%
	Domain 3	70%	–	–	
	Domain 4	65%	–	–	
Probability of 'cut-off' by another structure	Domains 1, 2	50%	–	–	Design 50%
	Domain 3	75%	–	–	Design 75%
	Domain 4	50%	–	–	Design 50%
Rock 'bridges' for fractures 'not cut-off'	Lognormal	Domains 1,2,4 0.170m (Mean=0.294m)	0.060m	0.485m	5% risk > 1m 1% risk > 2m 0.1% risk > 5m
		Domain 3 0.114m (Mean=0.166m)	0.048m	0.270m	0.5% risk > 1m 0.05% risk > 2m 0.01% risk > 5m
'Small scale' Roughness Index (1–10)	Normal	Domains 1,2,4 4	2	6	Design 4 ± 2
		Domain 3 3	2	4	Design 3 ± 1
'Large scale' Fracture Surface Roughness Angle	Normal	Domains 1, 2 7°	0°	14°	Design 4° ± 3°
		Domains 3,4 4°	1°	7°	Design 4° ± 3°
Infill Type	N/A	Domains 1,2,4 None 55% Ca and/or Fe 40% Weak 5%	–	–	Design 5% joints with weak infill, plus 60% joints with friction only and no cohesion
		Domain 3 None 40% Ca and/or Fe 40% Weak 20%	–	–	Design 20% joints with weak infill, plus 40% joints with friction only and no cohesion

Table 9 Example of Statistical Defect Attributes input to STEPSIM4.

Domain(s) in A-11 Mine Area	Statistical Parameter	UCS (MPa)	Elastic Modulus (laboratory) (GPa)	RQD Index	RMR Rating	Hoek-Brown (1988) Parameters			
						Undisturbed Rock Mass		Blasting-Disturbed Rock Mass	
						m	s	m	s
Domain 3	-1 SD	3	1.0	22	31.5	0.928	0.00092	0.0985	0.0000382
	Median	8	3.0	47	41.5	1.268	0.00177	0.1661	0.0000796
	+1 SD	13	5.0	72	51.5	1.893	0.00859	0.4109	0.001104
Domains 1,2,4	-1 SD	10	2.0	88	66.0	3.014	0.02893	0.9515	0.006884
	Median	31	6.0	96	73.5	4.134	0.09211	1.930	0.03653
	+1 SD	52	10.0	100	81.0	5.253	0.1553	2.908	0.06619

Table 10 Example of Statistical Inputs to Hoek-Brown (1988) Empirical Equations.

Model 1 - "Typical": Probability of Fracture Occurrence = 60%					
Step-path Length (m)	Failure Depth	Step-path Friction Angle (°)		Step-path Cohesion (kPa)	
		Mean	+1 SD	Mean	+1 SD
15	Shallow	51.9	6.2	1017	1205
	Deep	47.6	5.9	1057	1190
100	Shallow	51.9	2.4	1017	467
	Deep	47.6	2.3	1057	461
200	Shallow	51.9	1.7	1017	330
	Deep	47.6	1.6	1057	326

Model 2 - "Zonal": Probability of Fracture Occurrence = 100%					
Step-path Length (m)	Failure Depth	Step-path Friction Angle (°)		Step-path Cohesion (kPa)	
		Mean	+1 SD	Mean	+1 SD
15	Shallow	50.6	5.9	339	252
	Deep	44.5	4.7	345	259
100	Shallow	50.6	2.3	339	96
	Deep	44.5	1.8	345	100
200	Shallow	50.6	1.6	339	69
	Deep	44.5	1.3	345	71

Table 11 Example of Statistical STEPSIM4 Shear Strength Outputs for Sandstone.

GEOTECHNICAL DESIGN PHILOSOPHY

Apart from superficial ground reinforcement (e.g. cablebolting), ground conditions at open cut mines cannot be altered. Reinforcement is costly. Depending on the geometry of the deposit, mine life and final pit depth, ground support is not always the best mining solution; less aggressive slope angles are often adopted instead. Flatter overall slope angles incur a cost penalty — more overburden/waste rock must be mined. It is in the economic interests of the mine to make slopes as steep as safely possible.

The final pit layout is dictated by the geometry of the deposit, and thus, the trend and height of final slopes is predefined. The layout and development of interim slopes reflect the mining plan and schedule.

Several factors, listed in their approximate order of importance, impact on interim and final slope stability:

- ground conditions with respect to slope direction, angle and height,
- crest surcharge (e.g., waste dumps),
- groundwater,
- surface water erosion / undercutting of slopes,
- seismic loadings,
- mining practices (e.g., blasting disturbance, pre-splitting, direction of mining), and
- regional stress regime.

The geotechnical engineer cannot alter the deposit layout, ground conditions, seismicity and stress regime. However, some factors can be successfully controlled. Waste dumps can be constructed further back behind the slope crest. Overall slopes can be mined flatter. Groundwater levels can be reduced. Interim slopes can be mined in more favourable directions. Blasting practices can be improved to limit ground disturbance. In most instances, slope flattening and groundwater control are the key factors in slope design. The extent of drawdown needed for an acceptable FOS and stability risks can be iteratively computed for given overall slope angles and pit depths. These analyses (slope angle versus water level) provide the basis for deciding the best slope design option.

SLOPE DESIGN VALIDATION

As shown in Figure 2, good slope design is an iterative process.

Typically, the conceptual geological and geotechnical models developed at the early stages of a mine project are based on limited data. While slope design often relies on ground conditions extrapolated over considerable distances. The ensuing preliminary slope design and risk predictions cannot be more reliable than the input data.

All key slope design assumptions must be validated by on-going geotechnical investigations and monitoring. Ground movements and water levels must be monitored to demonstrate that both are consistent with design assumptions and predictions. The type and intensity of on-going work and monitoring will be dictated by slope design issues at particular mine sites. There is no single plan of action that suits all mines; the requirements need to be considered and established on an individual basis.

The process of conceptual model validation and monitoring should be proactive rather than reactive (i.e. after adverse situations have developed). Typical design issues that need to be confirmed are listed.

- Location, orientation and shear strength attributes of all through-going (>100m long) and major (15m to 100m long) geological defects (faults, shears, bedding plane 'weak' seams, dykes, etc.) likely to daylight within the slope face or occur a short (say, < slope height) distance behind the final pit wall. Drilling may be required to confirm the latter situation.
- General geological defect pattern and shear strength attributes for each geotechnical design domain in interim and final slopes around the pit perimeter. Individual slope face mapping requirements will be dictated by the nature and variability of ground conditions, pit depth, aggressiveness of the overall slope angles, slope function (e.g. contains haul road), severity of impact of instabilities on mine operations and slope design life. Good geotechnical practice is to carefully inspect ground conditions in all slopes on a regular basis and to selectively line traverse map the face of every second or third bench in interim slopes and all bench faces in final slopes. Line traverse data should comprise the information listed under footnotes (1) to (5) in Table 1.
- Groundwater conditions in mine slopes. Water has a key stability impact on most slopes. Groundwater drawdown characteristics should be established in the project area by testing prior to mining. The FOS of saturated slopes may be 0.3 to 0.4 less than for equivalent dewatered slopes. A measure of drawdown is usually a pre-requisite to achieving the designed overall slope angles. Water levels should be systematically monitored at several key locations around the pit final perimeter to ensure that the necessary drawdown will be achieved by natural or assisted (e.g. horizontal drains) drainage at all stages of pit slope excavation.
- Ground control monitoring. The rock mass is an elastic medium within a stress field. Pit excavation redistributes the ground stresses and results in the elastic rebound of the ground into the workings. The magnitude and direction of movement will be a function of the elastic properties of the ground, pit geometry and depth, and the pre-mining stress field. Displacements could be considerable; two and three-dimensional numerical modeling has predicted elastic movements in excess of 1m for 800m deep pits. Non-elastic displacements associated with shearing displacements along geological defects within the

rock mass may be several times greater. Ground displacements must be monitored to ensure that pit slope movements are generally consistent with the anticipated elastic ones. Greater than elastic and/or accelerating displacements may be indicative of pending ground instability, and these areas require more intense monitoring.

To be of practical use, all structural mapping data must be assessed and interpreted as it is collected. The updated geological model must be compared with previous design assumptions. Unless this is done, the mapping effort and associated costs will have been wasted. Similar requirements apply to groundwater and ground control monitoring data.

CONCLUSIONS

Geological hazards represent geological systems close to their limit equilibrium for stability. Small changes in the external environment may render these systems unstable. Mining activity alters the external environment and often reduces the equilibrium of the geological system. Mining involves the creation of temporary openings in the ground. Geological defects are exposed and undercut by the opening, stresses are redistributed and concentrated around the opening and the groundwater regime is affected.

Slope stability risks in open cut mines can be qualified and quantified by a systematic approach to the analysis. The task of assessing pit slope design risks is a multi-step process. Statistical techniques exist to facilitate this assessment. Considerations and limitations in the risk analysis have been introduced and discussed in this paper. Examples have been provided to illustrate the methodology that has been applied at several open cut mines. Indicative results have been presented.

ACKNOWLEDGEMENTS

Slope design investigations at most mines are collaborative efforts between mine staff and their consultants. The writers gratefully acknowledge this valuable assistance and contribution on the cited projects.

REFERENCES

BACZYNSKI, N.R. (1990) “M10 Highwall Steepening Trial at Leigh Creek Coalfield, Hollingsworth Dames & Moore, Progress Report HOD0049, 1 May 1990, 30p. 21 Figures + 1 Drawing, Appendices A to C.

BACZYNSKI N.R. (1992) “Leigh Creek Coalfield, S.A., Terrace Mining Project: M6 / M7 Boxcut Highwall: “GSLOPE Stability Analysis”. Dames & Moore Report, Project 13230-019-70 (DOD0288), April 1992, 22p. + 18 Figures + Appendices A and B.“Structural Mapping – Line Traverses”. Dames & Moore Report, Project 13230-019-70, 30 June 1992, 15p. + 8 Figures + Appendices A and B.“Stability Impact of Slope Steepening & Cablebolting”. Dames & Moore Preliminary Report, Project 13230-019-70, 12 June 1992, 8p. + Appendix A.

BACZYNSKI, N.R. (1998) “Geotechnical Review of Mine Slopes at Mount Owen Mine, NSW”, BHP Eng. Memorandum. (Ref. 12015) to Mt Owen Mine (Thiess Contractors), 9 Feb 1998, 5p. “Phase 2 Geotechnical Study”, BHP Engng Report RE-052000 to Thiess Contractors, April 1998, 21p, 1 Figure, Appendices A to E.

BACZYNSKI, N.R. (1999) “Mount Owen Mine, NSW – Phase 3 Geotechnical Study”, Douglas Partners Report (Project No. 21945) to Thiess Contractors, April 1999, 29p, 9 Figures, Appendices A to D “Phase 5 Geotechnical Study”, Douglas Partners Report (Project No. 33030A) to Thiess Contractors, December 1999, 25p, 6 Figures, Appendices A to I.

BACZYNSKI, N.R. (2000a to d) “Mount Owen Mine, NSW – Phase 6 Geotechnical Study”, Douglas Partners Report (Project No. 33030B) to Thiess Contractors, May 2000, 36p, 16 Figures, Appendices A to F.“ Phase 6(D) Geotechnical Study – Stability of In-Pit Spoil Dumps, Mount Owen Mine, NSW”, Douglas Partners Report (Project 33030C) to Thiess, June 2000, 20p, 22 Figures, Appendices A and B.“Phase 7 Geotechnical Study”, Douglas Partners Report (Project 33030D) to Thiess, Nov. 2000, 14p, 1 Figure, Appendices A to D.

BACZYNSKI, N.R.P. (2000e) STEPSIM4 “Step-Path” Method for Slope Risks”, GeoEng2000 Conference, Melbourne, November 2000, pp. 1-7.

BACZYNSKI, N. R. & SMYTH, M. (2000) “Geotechnical Assessment: Eldridge Pit East Wall Stability at Kidston Gold Mine, Qld”, Douglas Partners Report 33100, July 2000, 17p. + 5 Figures + Appendices A to G.

BACZYNSKI, N.R. (2001) “Mount Owen Mine, NSW – Phase 9 Geotechnical Study”, Douglas Partners Report (Project No. 33030E) to Thiess, April 2001, 12p, References, 1 Figure, Appendices A to N.

BARTON, N. & CHOUBEY, V. (1977) “The shear strength of rock joints in theory and practice” Rock Mechanics, Vol. 4, pp. 1-54.

BIENIAWSKI, Z. T. (1976) “Rock mass classification in rock engineering.” in *Proc. Symp. Exploration for Rock*

Engineering (edited Z.T. Bieniawski), Johannesburg, Nov. 1-5, pp. 97-106.

CHOROS, E. (1992) "Assessment of the Risk for Footwall Landslides based on Pit Geometry at Leigh Creek Coalfield", The Electricity Trust of South Australia (ETSA), Internal Report EC9134, 15 Feb 1992, 22p. +17 Figures.

HOEK, E. & BROWN, E .T. (1988) "The Hoek-Brown failure criterion – a 1988 Update." *Proc. 15th Canadian Rock Mech. Symp.*, Toronto, October 1988, pp31-38.

LITTLE, T.N., CORTES, J.P. & BACZYNSKI, N.R. (1998) "Risk-Based Slope Design Optimization Study for the Ok Tedi Copper-Gold Mine – Executive Summary: Final Report." OTML Internal Report, 30 May 1998, 12p. "Geotechnical Slope Design Constraints for the Ok Tedi Mine." OTML Internal Report, 2nd Draft, 30 January 1998, 46p.

LITTLE, T.N., CORTES, J.P. & BACZYNSKI, N.R. (1999) "Risk-Based Slope Design Optimization Study for the Ok Tedi Copper-Gold Mine – Vol.1: Project Scope and Site Description." OTML Internal Report, 30 August 1999, 79p. + Appendices A to D. "Vol. 2: Rock Strength Testing." 42p. + Appendices A to C."Vol. 4: Geological Structures and Models." 104p. + Appendices A to D."Vol. 5: Geotechnical Models and Failure Modes." 111p. + Appendices A to F."Vol. 6: Deterministic Slope Design Analysis." 135p. + Appendices A to E."Vol. 7: Probabilistic Design Analysis and Sensitivity Studies." 104p. + Appendices A to E.

LITTLE, T.N., CORTES, J.P. & BACZYNSKI, N.R. (2000) "Risk-Based Slope Design Optimization Study for the Ok Tedi Copper-Gold Mine – Vol. 8: Risk-Based Slope Design Optimization." OTML Internal Report, dated 30 August 2000, 160p. + Appendix A.

ROSENBLUETH, E. (1975) "Point estimates for probability moments." *Proc. Nat. Acad. Sci. USA – Mathematics*, Vol. 72, No. 10, pp. 3812-3814

.

SESSION SIX — UNDERGROUND HAZARDS I

Geological hazards — The impact to mining 15-16 November 2001, eds Doyle, Moloney, pp 175-182

Quantification of Fault Uncertainty and Risk Management in Longwall Coal Mining: Back-Analysis Study at North Goonyella Mine, Queensland

R. DIMITRAKOPOULOS & S. LI

W H Bryan Mining Geology Research Centre, The University of Queensland, Brisbane Qld 4872,
e-mail:brc@uq.edu.au; http://www.minmet.uq.edu.au/~bryan/

A method for fault uncertainty and risk assessment based on the concept of stochastic simulations is used to back-analyse data from mined out longwall panels at North Goonyella mine, Queensland. The results from back-analysis show that (i) fault risk can be quantified; (ii) quantified fault risk can be integrated into longwall design and assist decision making; and (iii) if the simulation technologies were available earlier, geological risk at North Goonyella would have been substantially better understood, therefore could have had a major positive economic impact. Lastly, a comparison between North Goonyella and a specific part of the Goonyella-Riverside area suggests that the latter is less risky for a comparable longwall design. The study shows the contribution of the quantified risk approach to reducing coal mining investment risks and facilitating more informed decisions.

INTRODUCTION

Fault uncertainty and risk have widely recognised adverse impacts on the exploration and mining of underground coal deposits, especially for longwall mining. Geological uncertainties may cause significant delays in production schedules, impose substantial changes to mine plans, reduce expected recoverable coal quantities, adversely affect safety, and heavily influence the financial viability of a mine. As Australia's coal mining industry is becoming increasingly reliant upon longwall mining, there is a need to implement: more effective quantitative and practical approaches to geological risk modelling, uncertainty assessments, and integration of risk management. This will enable mining companies to better plan underground exploration activities and longwall operations.

The recently completed ACARP project C7025, "Quantification of fault uncertainty and risk management in underground coal mining" contributes to meeting the above needs. The methods developed, case studies and tests are detailed in Dimitrakopoulos et al (2001), and the tools assisting the implementation of the methods are presented in Li et al (2001).

A key aspect of the above project is the back-analysis at the North Goonyella mine. Back-analysis aims to:

- assess the effectiveness and validity of methods for fault uncertainty and risk quantification developed by the project in a mined out part of the mine, where all faults have been mapped in detail,
- show that if the technologies from the above project were available earlier, the fault related risk at North Goonyella would have been more accurately understood, therefore improving decision-making, and
- complementary to the above is the comparison of quantified risk at North Goonyella to that of Goonyella-Riverside.

These three aspects of the ACARP project are presented in this paper.

The results reported here are based on a new method developed for modelling fault uncertainty and quantifying risk. The method and the back-analysis are based on the concept of spatial stochastic simulations. The key idea in stochastic fault simulation is that from an initial set of fault data, one can generate multiple equally probable models (realisations) of the faults within a study area. The combination of these equally probable models provides the means to quantify fault risk. Characteristics of fault simulations include:

- fault realisations are based on and reproduce all the available data and geological interpretations available, and
- realisations reproduce the statistical characteristics of the fault data including the key "power-law" relationships of fault size distributions and length versus maximum throw of the fault data.

For further information on the method, the reader is referred to the ACARP C7025 project report available from ACARP.

BACK-ANALYSIS: STEPS AND ASSUMPTIONS

North Goonyella mine is located in the Bowen Basin, Central Queensland. Back-analysis uses mined out longwalls of the mine where faults have been mapped in detail. Geological interpretations or other information are not available. Figure 1(a) shows the available and completely known dataset. The steps involved in back-analysis are as follows:

- the completely known fault data are sampled to generate a sample fault dataset as shown in Figure 1(b),
- 50 fault simulations are run, based on the sample fault data set and its statistical characteristics,
- fault probability maps derived from the simulations are compared to the complete fault dataset, and
- a longwall design is used to quantify fault risk and is compared to the known risk of longwall panels in the study area.

The back-analysis study assumes that there would be a reasonable level of exploration carried out in the parts of the area to be considered, and that the proportion of known smaller faults reflects the levels to which such faults are known after typical exploration activities.

FAULT SIMULATION, UNCERTAINTY ASSESSMENT AND RISK MAPPING

Two simulated realisations of the fault populations in the study area are shown in Figure 2. The comparison to the complete dataset in Figure 1(a) provides an insight to the concept of fault simulations. The specifics of the fault simulation within the study area are beyond the scope of this paper and are given in the C7025 project report. Figure 3(a) shows the fault probability map generated from the 50 fault realisations used here. The fault probability map can be assessed and compared against the completely known fault dataset.

Figure 3 compares various fault probability maps, showing that the technologies used in this study can predict risk particularly well. More specifically, Figure 3(b) shows the probability map based upon the faults in the sample dataset alone (70 faults with throw ≥1m). As discussed earlier, the quantification of risk based on the sample data seems severely reduced in comparison with that seen in Figure 3(a), which is the probability map resulting from 50 fault realisations (about 207 faults with throw ≥1m). Figure 3(c) presents the probability map from the completely known fault dataset (231 faults with throw ≥ 1m). The fault simulation technologies are able to use an exploration-like level of information to generate a more reasonable assessment of fault risk throughout the study area when compared to the spatially limited and incomplete sample dataset alone that could be any "exploration data".

The probability map based upon 50 fault realisations, shown in Figure 3(a) can be compared to the probability map of the complete data set in Figure 3(c). In Figure 3, locations numbered with '1' highlight an actual high-risk part of the study area that is predicted by the fault simulation methods developed in this project. Number 2 highlights a part of the study area in which risk is overestimated by the fault simulation methods. Number 3 highlights a part of the study area in which a high-risk area (in the probability map based upon the realisations) is slightly shifted with respect to its position in the completely known fault dataset.

It should be noted that the risk assessments based strictly on the sample dataset underestimate risk within the mining area, as is expected. The probability map resulting from the fault realisations provides a substantially closer estimate to the actual risk scenario than that based upon the sample dataset.

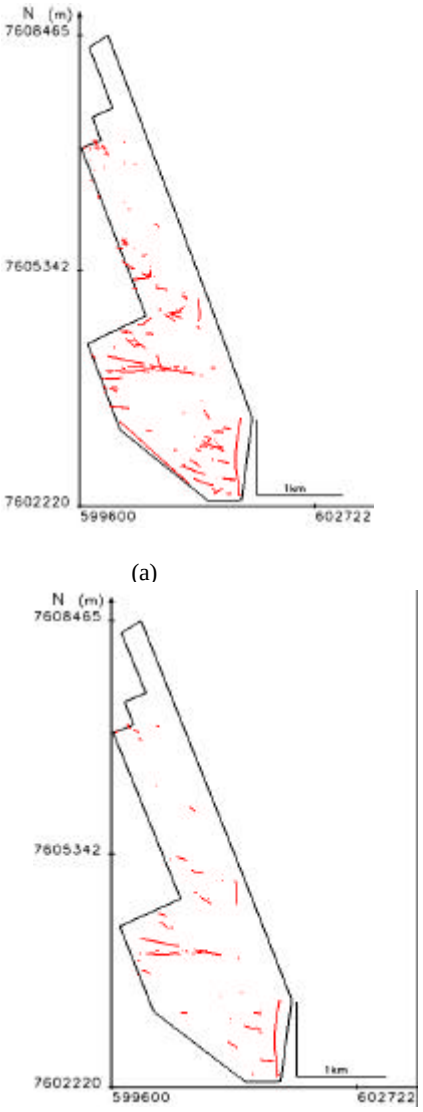

Figure 1 (a) Mapped and completely known fault dataset from mined out part at North Goonyella mine; (b) sample fault dataset (faults shown have a throw ≥ 1m).

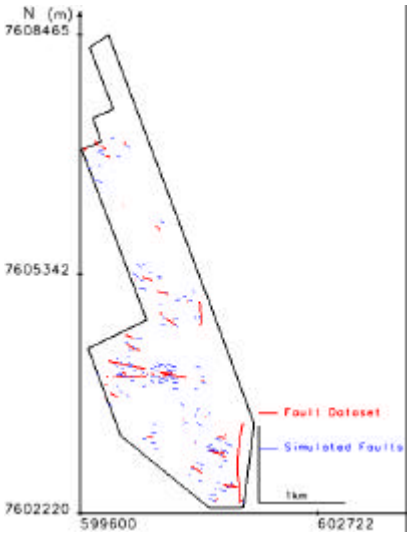

(a)

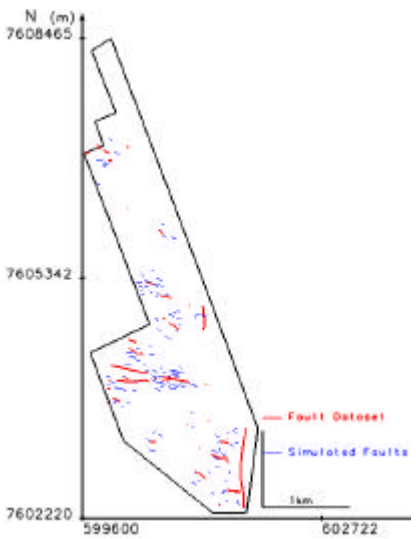

(b)

Figure 2 Two fault realisations using the sample fault dataset at North Goonyella mine (faults shown have a throw ≥ 1m).

Data collection expenditure (drilling or geophysical surveying) is one additional example where quantification of geological risk has the potential to improve current practices. For instance, if one considers Figure 3, the expenditure for further seismic surveys may be prioritised and there may be two or three approaches to the task. The first involves the targeting of low risk panels to verify the simulation predictions. Secondly, if an ambitious approach is decided upon, the risky parts of the area may be investigated to determine if indeed there are significant faulting concerns or not. Thirdly, as the middle values of fault probability (eg 40 to 60%) reflect those areas about which the least is known, they can be explored (their exploration may be prioritised) and then classified with greater certainty.

INTEGRATION OF QUANTIFIED RISK IN LONGWALL DECISION MAKING AT NORTH GOONYELLA

The levels of risk associated with a longwall layout used at North Goonyella mine are assessed in this section. In all cases presented here, risk is calculated and reported for an equivalent longwall panel size of 200m x 2000m. Risk is calculated and reported for a given (constant) longwall panel size in order to be physically and statistically meaningful and can be calculated for any longwall panel sizes as needed.

Figure 4 shows the probability and risk associated with the mine and the longwall panels when all faults within the completely known dataset with throws greater than or equal to 1m are considered. This is the 'true risk' scenario. Figure 5 shows the fault probability and risk associated with the mine and the longwall panels based upon the probability map obtained from fault simulation. Spatial distribution of risk, the histogram of the risk distribution and the related descriptive statistics are shown. The assessment of risk shown in Figure 5 is very close to that of the actual scenario shown in Figure 4.

Figure 6 shows the fault probabilities and risk associated with mine longwall panels based upon the sample fault dataset only. The spatial distribution of risk, the histogram of the risk distribution and the related descriptive statistics are shown. Figure 6 shows a fault risk assessment that could be anticipated at a relatively early stage of exploration without the use of computerised fault modelling technologies. By comparing Figure 6 with the risk distribution of the completely known fault dataset in Figure 4, it can be seen that the use of exploration data alone results in severe underestimation of geological risk.

Comparison of Figure 4 and Figure 5 suggests that the use of fault simulation technologies provide an excellent assessment of the actual fault risk levels in the North Goonyella example. A comparison of Figure 4 to Figure 6 shows that the estimated fault risk is far closer than that obtained using the sample fault dataset alone. Exploration provides fault data, which is commonly used 'as is' which implicitly corresponds to the level of risk in the faults identified in the dataset. If technologies such as seismic methods are used, faults below resolution are not detected and as a result any 'risk' assessment based on the dataset 'as is', will underestimate the true risk. The opposite is also possible, for example, other geophysical methods such as aeromagnetics are highly interpretative and may result in the over representation of interpreted faults which if used 'as is' will produce an overestimated risk assessment.

Qualitative risk assessments are, in addition to the above, difficult to use because they implicitly reflect fixed information similarly to the use of the dataset 'as is'. Furthermore, quantitative assessments are highly subjective and a relative measure, not a physically meaningful probability to be used for risk assessment.

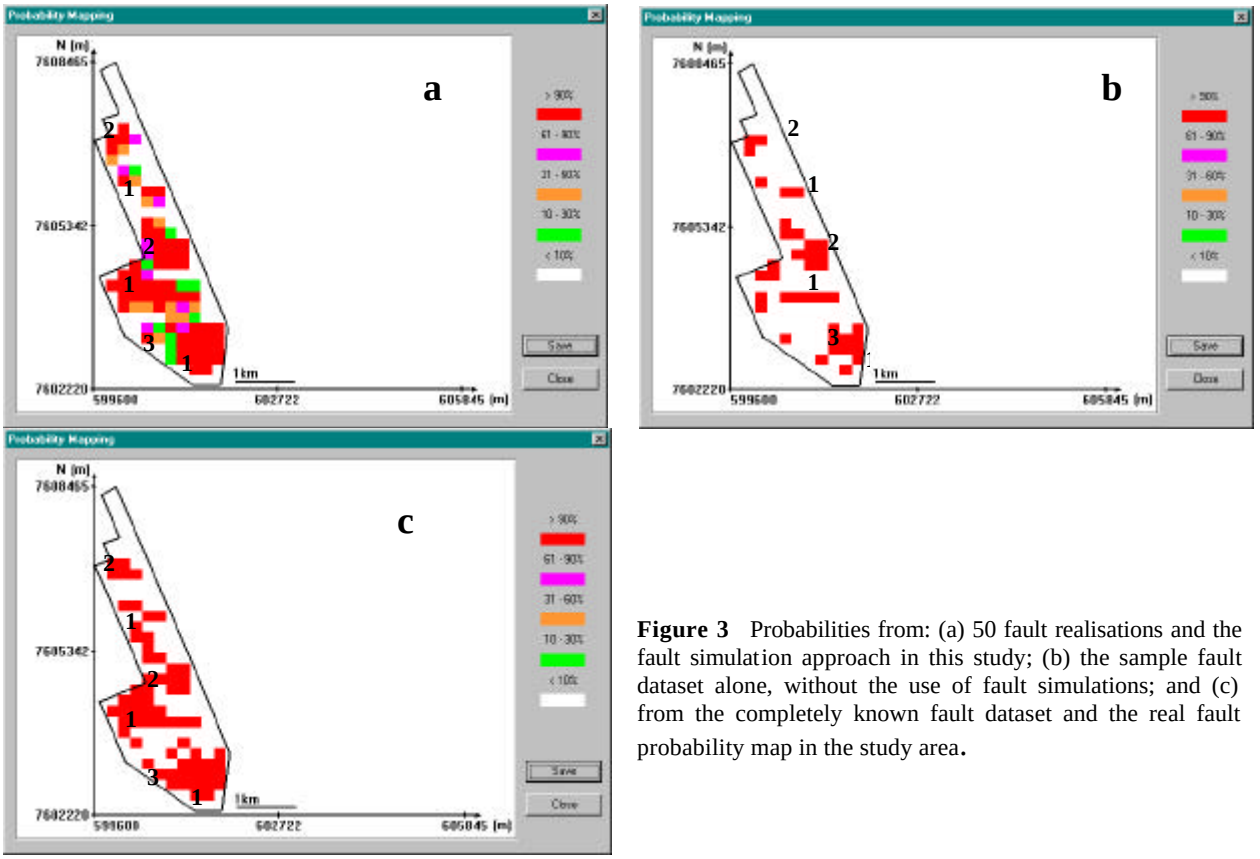

Figure 3 Probabilities from: (a) 50 fault realisations and the fault simulation approach in this study; (b) the sample fault dataset alone, without the use of fault simulations; and (c) from the completely known fault dataset and the real fault probability map in the study area.

This is perhaps obvious, but also useful to recall in uncertainty modelling and risk assessment. To enhance the understanding of an area, further exploration could be carried out which may be costly and would not guarantee uncertainty reduction or the optimisation of data collection. Using fault simulation technologies provides a means to utilise exploration data to gain a more complete and quantitative understanding of a relatively unknown area than would otherwise be achievable (from qualitative investigations). Simulation technologies such as those developed in this project could be utilised in combination with the information acquired from remote sensing surveys. Although the example presented here is simple, it shows that probabilistic models, in combination with current exploration, offer a way to obtain a more complete picture.

IS A LONGWALL MINE AT GOONYELLA-RIVERSIDE AS RISKY AS NORTH GOONYELLA MINE?

A comparison can be made between the levels of risk at North Goonyella Mine and a potentially mineable part of Goonyella-Riverside. The histograms of risk associated with a longwall panel layout can be seen in Figure 7. The longwall layout shown for North Goonyella Mine is the same as that used above in the quantification of fault risk. The layout shown for the Goonyella-Riverside area has been designed without consideration of quantified geological risk — while the "exploration data" is available. Using the basic map of fault locations, it is apparent that risk is fairly high and may be classified as such using a qualitative approach. It is only through quantifying risk using true probabilities that the difference in geological risk between the two areas can be grasped. Using the longwall layouts presented, the average fault probability at North Goonyella is 61%, and for the study area in Goonyella-Riverside it is 39%. The comparison shows that the longwall layout designed for Goonyella-Riverside has, on average, a substantially reduced level of risk compared to the mined-out parts of North Goonyella. Using the quantified risk assessment provided by the technologies developed in this study, it is possible to redesign the longwall layout of both locations to reduce risk. The quantitative approach is the only method that can determine which parts of the mineable area have lower risk and lead to an optimal redesign of the layout.

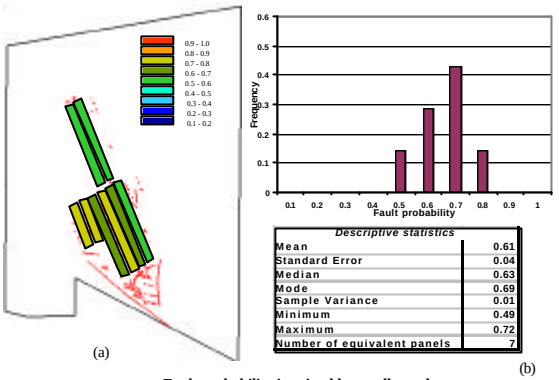

Descriptive statistics	
Mean	0.61
Standard Error	0.04
Median	0.63
Mode	0.69
Sample Variance	0.01
Minimum	0.49
Maximum	0.72
Number of equivalent panels	7

Fault probability in mined longwall panels
a) spatial distribution; b) histogram distribution
(fault throw >= 1m, panel size 0.2x2.0km)

Figure 4 Spatial distribution of fault probability and 'true' risk in a longwall layout at North Goonyella in (a); histogram and descriptive statistics of same in (b) using the completely known dataset.

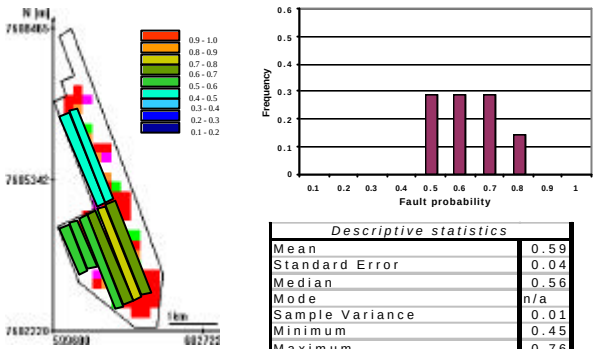

Descriptive statistics	
Mean	0.59
Standard Error	0.04
Median	0.56
Mode	n/a
Sample Variance	0.01
Minimum	0.45
Maximum	0.76
Number of equivalent panels	7

Fault probability and risk in North Goonyella mine
based on the simulated fault probability using a sampledataset
a) spatial distribution; b) histogram distribution
(fault throw >= 1m, panel size equivalent 0.2 x 2.0 km)

Figure 5 Spatial distribution of fault probability and risk in a longwall layout at North Goonyella mine in (a); histogram and descriptive statistics of same in (b) as calculated using the fault probability map generated from realisations based on the sample fault dataset.

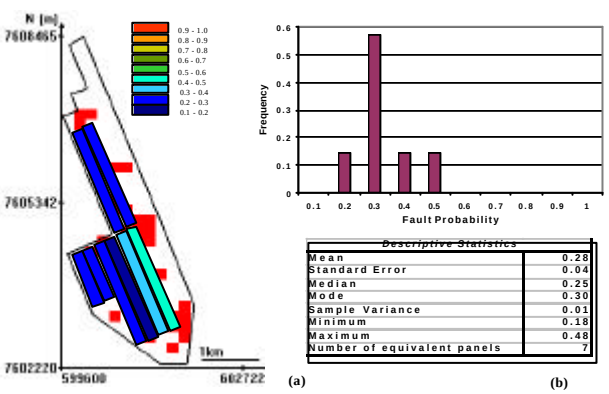

Descriptive Statistics	
Mean	0.28
Standard Error	0.04
Median	0.25
Mode	0.30
Sample Variance	0.01
Minimum	0.18
Maximum	0.48
Number of equivalent panels	7

Fault probability for a longwall layout at NorthGoonyella mine
based on the sampledataset
a) spatial distribution; b) histogram distribution
(fault throw >= 1m, panel size equivalent 0.2 x 2.0 km)

Figure 6 Spatial distribution of fault probability and risk in a longwall layout at North Goonyella mine in (a); histogram and descriptive statistics of same in (b) as calculated based on the sample dataset only.

FAULT UNCERTAINTY AND MINEABLE COAL RESERVE RISK

To link the quantification of fault risk to mine economics, the risk associated with the mineable coal reserve can be calculated. In all cases presented here, calculations assume; an equivalent longwall panel size of 200m x 2000m, an average coal seam thickness at North Goonyella Mine of 4.5m, and a coal relative density of 1.60. Figure 8(a) shows a histogram of the classification of quantities of mineable coal reserve at various risk levels as calculated using the completely known fault dataset. This is the true risk scenario. Figure 8(b) shows a histogram of the classification of quantities of mineable coal reserves and their fault risk levels based upon the fault simulation technologies in this study. Figure 8(c) shows a histogram of the classification of quantities of mineable reserve using only the sample dataset.

Figure 8(a) can be compared to Figures 8(b) and 8(c) to evaluate the impact of considering quantified geological risk on mineable coal reserves. The estimate generated from the fault simulation technologies (Figure 8(b)) is very close to that of the "true" scenario (Figure 8(a)). Risk is underestimated when only the available data is used (Figure 8(c)). When mine design and planning is conducted without the explicit consideration of risk, it is in fact conducted as if the risk levels were those shown in Figure 8(c) (i.e. largely underestimated). A comparison with Figure 8(a) shows that the real risk situation is not reflected by a sample fault dataset. The results in Figure 5 and Figure 8(b) provide information that could have been used in the decision-making processes at the time of the original longwall layout design.

CONCLUSIONS

The back-analysis study at North Goonyella mine shows that the quantification of fault uncertainty is feasible and contributes to the implementation of risk management strategies, both in terms of exploration and mine planning. In addition, it shows that the technologies generated in ACARP project C7025 work very well.

The real risk of faults in longwall panels in North Goonyella is particularly well predicted from a subset of faults (sample dataset) within the same area and the fault simulation method. More specifically, this means that if the technologies from this project were available at the time North Goonyella Mine was designed, subsequent substantial fault related risk could have been better analysed. Providing the opportunity to 'design out' the impact of faulting.

The comparison of mined out longwalls at North Goonyella to a potential longwall mine located in the Goonyella-Riverside area provides an eloquent example of the use of quantified uncertainty and risk for investment decision-making. The ability to compare risk in a longwall layout at Goonyella-Riverside to that in North Goonyella is uniquely based on the quantification of geological risk.

The back-analysis study also shows that the traditional use of geological data from exploration programs 'as is' may severely underestimate geological risk. Qualitative risk assessments, although technically simpler, may be misleading and difficult to use because they implicitly reflect information similar to that from exploration programs taken 'as is'. Furthermore, qualitative assessments are highly subjective and do not provide an objective "number" (probability) as needed for risk comparison.

Qualitative risk assessments are generally difficult to link meaningfully to mine design and planning, whereas quantitative risk assessments that incorporate local geological understanding offer accurate risk assessments and can be used directly and routinely in longwall mine design and planning.

Coal reserve risk is a specific topic that the methods and examples presented in this paper can be applied to. Reserves can be classified based on their fault risk level and the possibility of not being recovered from mining.

Cost effective data collection, be it additional drilling or geophysical surveys, can be supported and strategies for prioritised data gathering developed based on fault risk quantification.

Lastly, technologies developed in this project can serve as a starting point for further development of risk quantifying technologies that can offer an inexpensive method to acquire information to substantially assist decision-making in both longwall exploration, longwall mine design, mine development and operations.

ACKNOWLEDGEMENT

Acknowledgements are in order to the Australian Coal Research Association for selecting and funding this research project, Anglo Coal, Newlands Coal Mine for additional funding and collaboration; BHP Coal, CSIRO, North Goonyella Mine and MIM Holdings for support and collaboration. Thanks are in order to the project monitors: A. Wilson, P. Forrestal, S. Peau, D. Mathew, P. Cuddihy and J. Sleeman. We appreciated their dedication and pragmatic views. We thank D. Dunn and B. Coutts, (BHP Coal), A. Laws (Anglo Coal), M. Barker (Newlands) and T. Britten (North Goonyella Coal Mines), as well as CSIRO's J. Esterle, G. LeBlanc Smith and R. Sliwa for technical collaboration and data provision. The support and contribution of P. Hatherly (CSIRO/CMTE), particularly in the conception of this project, was greatly appreciated. Last but not least, we thank Bruce Robertson (Anglo Coal) and Alan Davis (BHP Coal) for supporting and encouraging the undertaking of ACARP C7025.

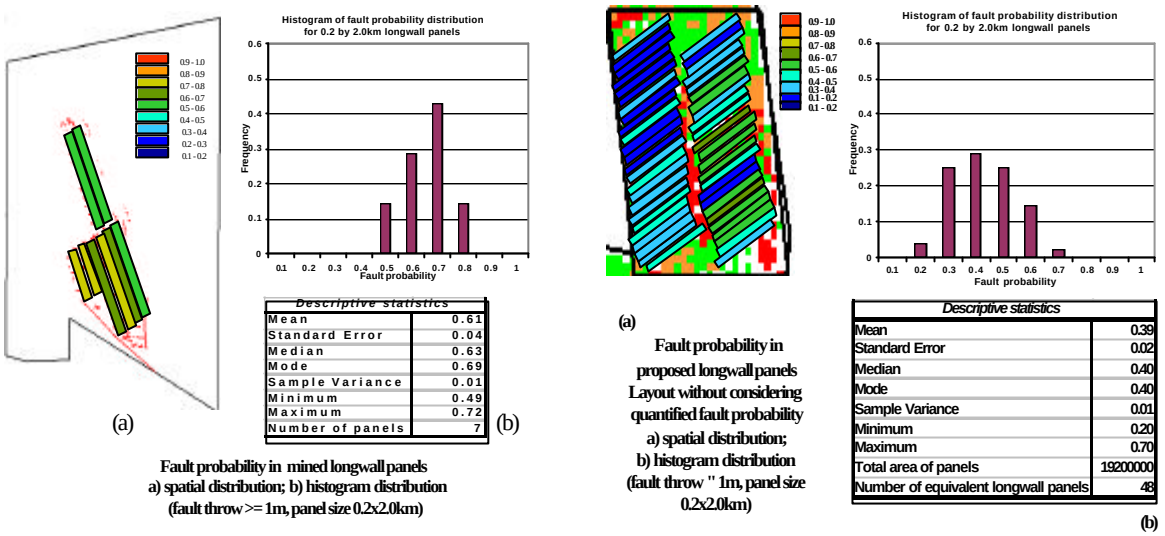

Figure 7 Spatial distribution of fault probability and histograms of risk for North Goonyella Mine (left) based on mined out dataset and for part of the Goonyella-Riverside area (right) based upon simulations using the available sample dataset and calculated for given layouts and a panel size equivalent of 200m x 2000m.

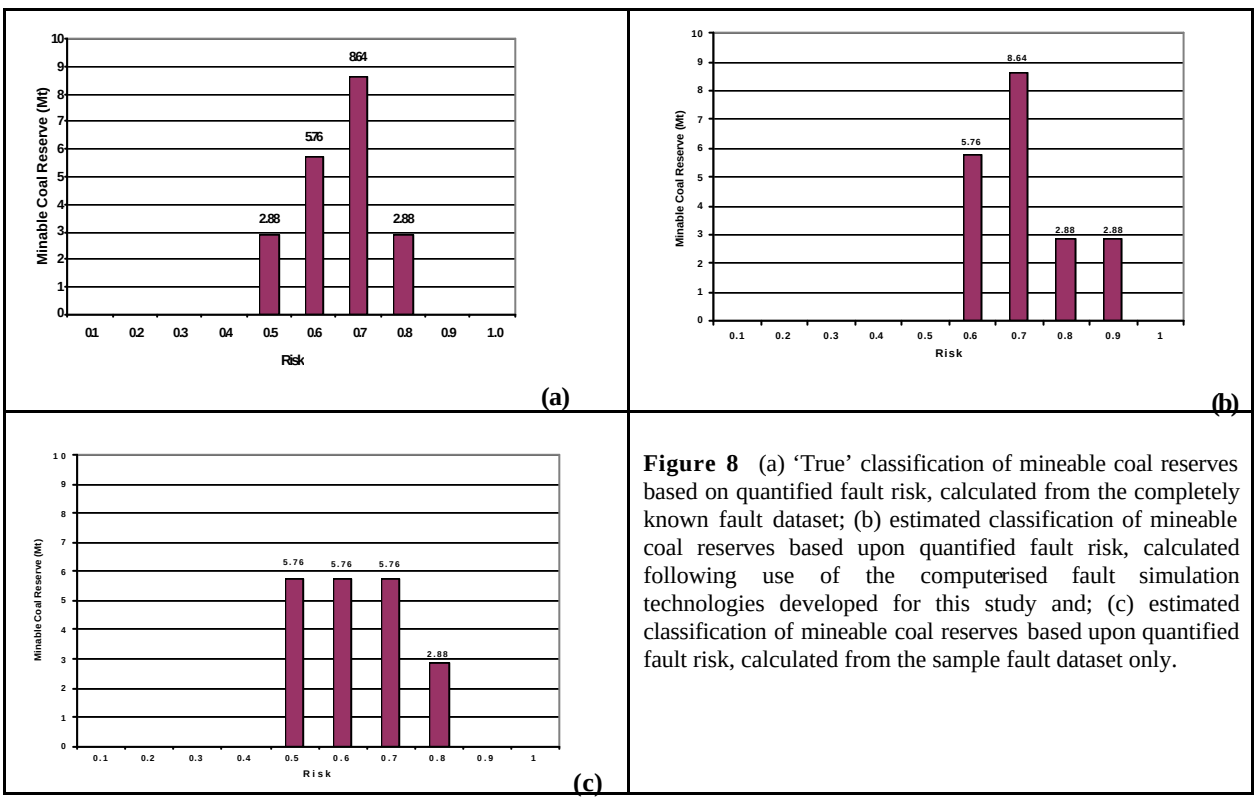

Figure 8 (a) 'True' classification of mineable coal reserves based on quantified fault risk, calculated from the completely known fault dataset; (b) estimated classification of mineable coal reserves based upon quantified fault risk, calculated following use of the computerised fault simulation technologies developed for this study and; (c) estimated classification of mineable coal reserves based upon quantified fault risk, calculated from the sample fault dataset only.

REFERENCES

DIMITRAKOPOULOS, R., LI, S., SCOTT, J. & MACKIE, S. 2001. *Quantification of Fault Uncertainty and Risk Management in Underground Longwall Coal Mining*, ACARP Project C7025 Report, Volume I, W H Bryan Mining Geology Research Centre, The University of Queensland, 215p.

LI, S., DIMITRAKOPOULOS, R., SCOTT, J. & MACKIE, S. 2001. *Quantification of Fault Uncertainty and Risk Management in Underground Longwall Coal Mining*, ACARP Project C7025 Report, Volume II, W H Bryan Mining Geology Research Centre, The University of Queensland, 88p.

Geological hazards — The impact to mining 15-16 November 2001, eds Doyle, Moloney, pp 183-196

A Method of Determining Longwall Abutment Load Distributions for Roadway and Pillar Design

K.W. MILLS

Senior Geotechnical Engineer, Strata Control Technology

This paper describes a method to determine abutment loads on longwall chain pillars and adjacent roadways. The method is based on: observation of subsidence behaviour, field measurements of abutment load distributions, and considerations of total overburden load about one or more longwall panels.

Surface subsidence data is used to deduce how far the overburden strata can transfer overburden weight and the total abutment load required to be distributed for any particular depth and longwall geometry. To be of practical use in roadway and pillar design, the shape of the abutment load distribution is also required as a function of distance from the goaf edge. Direct field measurement using high quality, three dimensional stress monitoring instruments is considered to provide the most reliable method of determining the magnitude and shape of the abutment load distribution at various stages of longwall mining.

The abutment load distribution determined at any one site by field measurement can be scaled horizontally to account for changes in overburden depth and vertically to account for changes in total abutment load. Thus, within the limitations of extrapolating data from one site to another, the abutment load distribution can be estimated for different depths and longwall geometries. Pillar loading and the vertical stress acting on adjacent roadways can then be determined from the measured load distributions, or scaled versions thereof, for any particular stage of mining, longwall geometry or depth of overburden.

INTRODUCTION

This paper describes a method that has been successfully used to determine the vertical loading on longwall chain pillars and adjacent roadways. Vertical loading is useful as a general indication of roadway and rib performance, as well as input for more detailed numerical modelling studies of roadway performance at various stages of mining. The approach described is based on observation of subsidence behaviour, field measurements of abutment load distributions and considerations of total overburden load about one or more longwall panels.

Field measurement allows this method to be as site specific as circumstances allow. However, the strength of the approach is that, when access is not possible, loading conditions can be estimated from measurements elsewhere and applied to new sites through consideration of subsidence observations, overburden depth and general overburden behaviour. The estimated distribution can subsequently be confirmed when mining commences.

The general concept of using subsidence information to estimate abutment loading has been recognised for some time (Wilson 1972). The potential to refine this relationship even further has now become available through recent detailed measurements of surface subsidence and of sub-surface overburden behaviour.

Stress monitoring instrumentation has also improved in recent years to overcome some of the limitations of earlier systems. Now it is possible to measure changes in the full three dimensional stressfield with a high degree of confidence. Best results are obtained by making the measurements in the stronger roof strata typically found immediately above the coal seam. Equilibrium considerations require that the vertical stress in the immediate roof is equal to that in the pillar, but in the stronger strata above a coal pillar, instruments can survive at vertical loads beyond those at which boreholes in coal become overloaded. When borehole breakout occurs in boreholes that become overloaded, the results of uniaxial stress monitoring systems required to be located within the pillar may be compromised. For example, such instruments typically do not register increased vertical load beyond the load at which breakout occurs. With improved instrumentation systems in stronger strata it is possible to follow the loading to higher stress levels. Furthermore, confirmation through independent checks on the correct function and integrity of the instruments at any stage of the monitoring boost confidence in the quality of the results. The recent elimination of time related creep that has been an issue with some types of instrument has also boosted confidence in the results

obtained.

The full benefit of improved prediction of vertical loading is realised through numerical modelling. Numerical modelling not only provides a method to predict roadway and pillar performance for various scenarios before mining commences, but also provides a framework in which to interpret observations made during actual mining.

BACKGROUND

The principal source of vertical load in underground coal mining environments is the weight of overlying strata. Mining removes coal from one area causing the load it previously supported to be transferred to another area. The ability of the strata to transfer weight and the distance that weight can be transferred are characteristics of the overburden strata. These characteristics are of interest to understanding the vertical stresses that act on chain pillars and gateroad developments.

In typical Australian coal mining environments, the coal seams are flat and more or less horizontal so the average pre-mining vertical load can be estimated with reasonable confidence from the weight of overburden strata. For each 40m of overburden depth, the average vertical stress increases by approximately 1MPa. Although geological structures such as faults and dykes, and rapid variations in surface topography are recognised to locally modify this pre-existing vertical stress environment, equilibrium requires that, overall, the average is maintained.

On development, and in other non-caving geometries, the tributary area method of load redistribution is an effective method of estimating pillar load. The method is well used and works by redistributing all the original weight onto the remaining pillars on a pro-rata areal basis.

With the onset of caving, pillar load estimation is complicated by the uncertainty as to how much load is carried by the fallen goaf. Through a process of deduction from observations of surface subsidence, it becomes possible to separate the weight carried on the abutments from the weight supported on the goaf, and that process is the beginning of a method of determining pillar loading about longwall goafs.

IMPLICATIONS OF SUBSIDENCE MEASUREMENTS

Surface subsidence measurements provide a basis to separate the proportion of overburden load supported on the solid abutments around a total extraction mining area, from the load supported on the goaf. This section describes the deductive process that leads to a practical method of separating these two components.

In the centre of a longwall panel of supercritical width, the subsidence profile measured over a solid goaf edge is of the form shown in Figure 1(a). Over the solid, far away from the panel edge, there is zero subsidence and the full weight of overburden strata is clearly supported on the unmined coal. Likewise, far away from the panel edge over the goaf, there is full subsidence (as implied by supercritical width) and all the weight of overburden strata in this area is now fully supported on the goaf. In between, there is a transition zone and the size of this zone provides a direct measure of the distance that the overburden strata can transfer load.

The relationship between load and subsidence can be illustrated by considering the surface at three locations indicated in Figure 1 by trees. The weight of the tree on the left is fully supported on the solid coal. There has been no downward movement, so there can be no transfer of weight. Similarly, the tree on the right is fully supported on the goaf. This tree has undergone the full amount of subsidence and further mining does not cause it to move downward any further, so by implication, its full weight must be supported on the goaf.

The middle tree is located in the transition zone. While the face is in position A, the tree is not fully subsided. When the face has moved to position B, the tree has fully subsided and its weight is therefore supported fully on the goaf. The key question is, what was holding it up when the face was in position A? The only thing that has changed is that the face has moved from position A to position B. Therefore the coal that was between positions A and B had to be contributing to the support of the middle tree. Since the tree was being supported, at least in part, by the coal on the face, the tree must have been contributing to the load on the face when the face was in position A.

By the time the longwall face has moved to position B, as shown in Figure 1(b), the tree is fully supported on the goaf. Therefore the weight of the tree is not supported on the longwall face. The point at which load ceases to be transferred onto the longwall face is that point out from the goaf edge at which full subsidence is first reached.

Figure 2 shows an example of surface subsidence profiles measured at frequent intervals during longwall retreat. The profiles show that for each metre of longwall coal mined, there is a corresponding shift in the subsidence profile. The surface lies down incrementally behind the longwall face. The distance from the longwall face to the point of maximum subsidence, the “maximum load transfer distance”, remains essentially constant. This distance is the maximum distance that this overburden strata can transfer weight at this overburden depth.

Figure 3 shows subsidence data for a range of overburden depths in essentially the same overburden strata. The horizontal distance is normalised with respect to distance from the goaf edge and subsidence is normalised with respect to seam thickness mined.

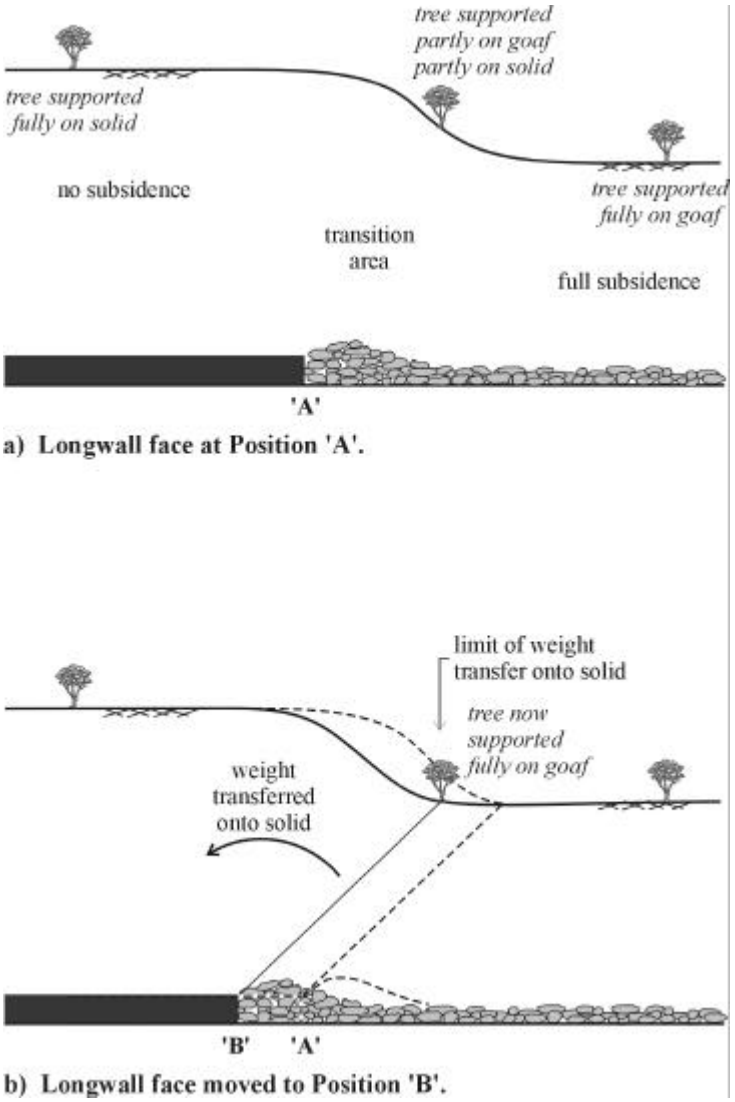

Figure 1 Implications of the subsidence profile behind a retreating longwall face, of supercritical width, for determining the maximum lateral distance that overburden strata can transfer weight.

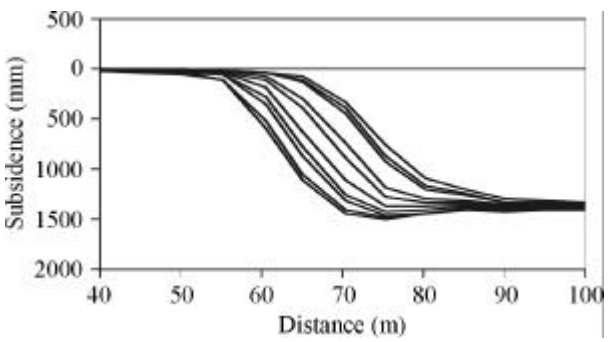

Figure 2 Close spaced subsidence monitoring, showing surface subsidence profiles behind a retreating longwall face and the constant "maximum load transfer distance".

The distance to the point of maximum subsidence is more of less constant and falls within the range 0.5-0.7 times depth, even though the overburden range captured in this data set ranges from 25m to 230m.

Figure 3(a) shows subsidence data from over the longwall face. Figure 3(b) shows data from over solid edges on the sides of the panel. The range of distances that the overburden strata can transfer load from the goaf to the solid is essentially the same in both cases. This result suggests that the distance that horizontal load is transferred is not a characteristic of the caving process, which would be different behind the longwall face compared to off the sides of the panel, but rather a characteristic of the overburden strata itself.

When subsidence results from different overburden strata are plotted in the same way as Figure 3, it is found in most cases that the variation from one overburden strata type to another is surprisingly small. Some strata types are able to bridge more effectively, but once full subsidence is generated, the profiles seem to be generally similar.

A key aspect of the subsidence profiles shown in Figure 3 is that the distance from the goaf edge to the point at which maximum subsidence is first reached is a linear function of overburden depth (as implied by normalisation with respect to depth). For any overburden depth, the distance to full subsidence divided by overburden depth remains a constant in the range 0.5-0.7 times depth.

Given this linear relationship and the inference that the point at which maximum subsidence is first observed is the maximum distance that the overburden can transfer load, the load distribution through the overburden strata is constrained to be a triangular distribution as illustrated in Figure 4. The volume of material above the line 'AB' represents material that is supported on the solid abutment. The volume of material below the line represents material that is supported on the goaf.

This triangular load distribution should not be confused with the development of fractures within the overburden strata or caving behaviour. It is simply a way of dividing up the overburden load between the goaf and the solid abutment that is consistent with subsidence observations.

Sub-surface extensometer monitoring (Mills & O'Grady 1998) demonstrates that the weight distribution is located inside the zone of large downward movement identified as defining the edge of the caving zone as illustrated in Figure 5. This is consistent with the expectation that subsiding strata on the fringes of the caving zone are supported partly on the goaf and partly on the solid abutment.

The delineation of the various zones is illustrated by physical modelling of longwall caving behaviour (Hall 1982). In these physical models, the strata on the fringes of the caving zone deform as a series of beams. For beams of this type, the load is supported more or less equally at both ends. Figure 6 shows a composite diagram that illustrates the effect. The edge of the zone of large downward movement and the edge of the zone where strata is clearly resting fully on the goaf are shown. The line that delineates the load carried on the goaf from the load carried on the abutment is within the zone defining the edge of large downward movement, but outside the fully subsided zone. This line should not be regarded as the fringe of the caving zone or as representative of any fracture surfaces, it is purely a division between load carried on the goaf and load carried on the solid abutment.

So far, only panels of supercritical width have been considered. However, sub-surface monitoring (Mills & O'Grady 1998) and computer modelling (Gale 2001) indicates that essentially similar processes occur within the overburden strata even when the surface has not fully subsided.

TOTAL ABUTMENT LOAD

The implications of subsidence data discussed above provide a basis to estimate total load on chain pillars fully isolated in the goaf. Figure 7 the load distribution that is inferred for different overburden depths. At shallow depths, the weight is low and derived from the weight of overburden strata near the panel edges. At moderate depths, the abutment load on each side of the panel remains independent of the load supported on the other side of the panel. At great depths, the overburden load supported on the goaf is only a small proportion of the total overburden load. The bulk of the load is shared between the abutments on each side of the panel.

In some geological settings (and stress environments), strong units within the overburden strata are able to bridge more effectively and can change the way that load is redistributed. For instance in the Southern Lake Macquarie area, massive conglomerate strata are able to bridge across 100m wide longwall panels so that almost the full overburden load has to be supported on the chain pillars, more or less as defined by tributary area.

ABUTMENT LOAD DISTRIBUTIONS

Subsidence behaviour provides a method to estimate the magnitude of the total abutment load as, described above. However for this information to be useful for estimating loads on pillars and roadways there are two further issues that need to be addressed. The first is the three dimensional distribution around the corners of the longwall panel and under full side abutment loading, and the second is the shape of the load distribution as a function of distance from the goaf edge.

The three dimensional distribution around the corners of the longwall panel can be addressed by considering, in three dimensions, the overburden weight transfer from over the goaf shown in Figure 4.

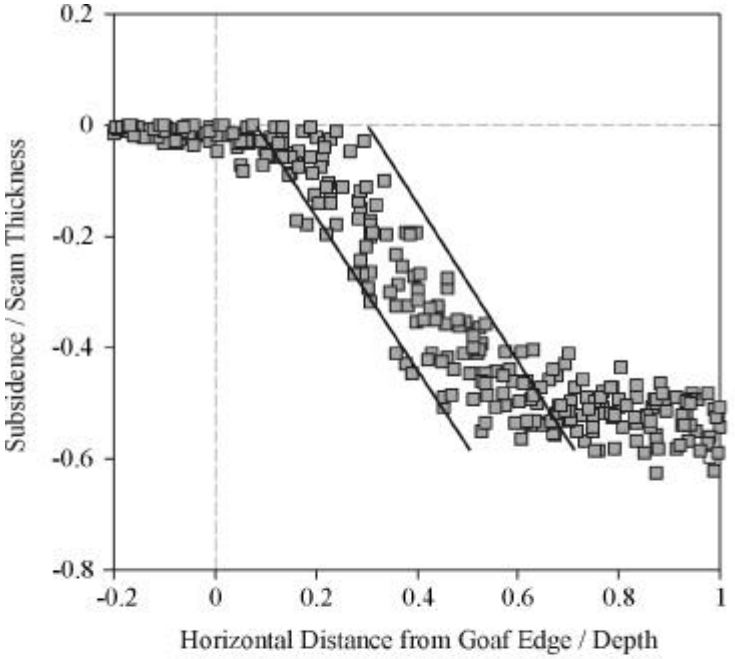

a) Subsidence measurements over longwall face at one mine site for a range of overburden depths up to 240m.

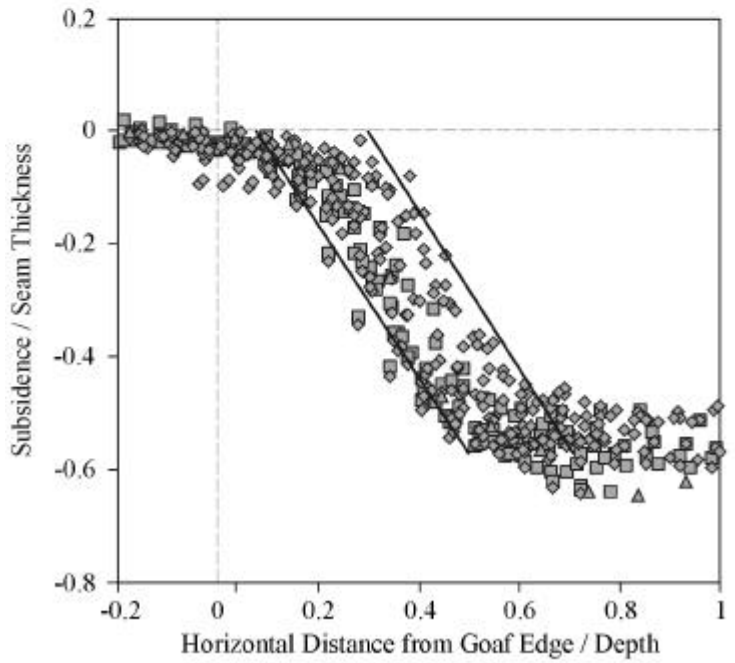

b) Subsidence measured over panel sides at same mine site for a range of overburden depths up to 240m.

Figure 3 Subsidence measurements from a single mine site with essentially constant overburden geology, but variable overburden depth for: a) longitudinal profiles behind the longwall face, and b) cross-panel profiles over the sides of longwall panels.

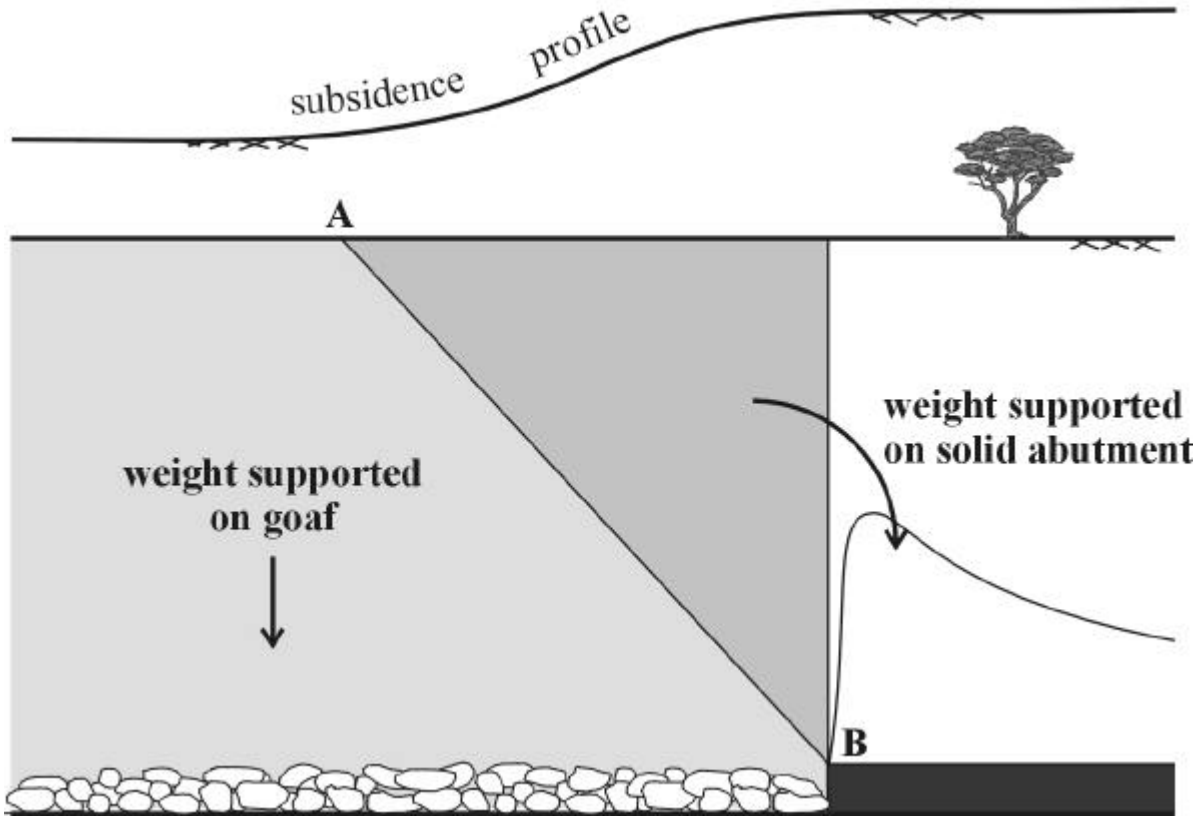

Figure 4 Results of extensometer monitoring at Clarence Colliery showing the edge of the zone of large downward movement and the extent of load transfer indicated by subsidence monitoring.

Subsidence data shown in Figure 3 indicates that the triangular load distribution inferred to exist ahead of the face is also valid over the sides of the panel. In the corners of the panel, the overburden load can be distributed to the face and to the panel sides. The magnitude of the abutment load in these corner areas is therefore less than the full side abutment loading where the entire load is distributed onto the chain pillar

Figure 8 shows how the triangular load distributions ahead of, and to the side of, the panel interact to form a tent shaped division of overburden load. The load inside the tent shaped surface is supported on the goaf. The load above the tent shaped surface has to be supported on the solid abutments and chain pillars.

The actual magnitude of the loading in the panel corners and the distribution of the load away from the goaf edge is determined directly and most effectively by; field monitoring of stress changes during longwall retreat, or direct field measurement in the case of an existing goaf. The geometry of longwall panels and the relatively rapid retreat rate of most longwall operations make it relatively straightforward to monitor the abutment loading using only a small number of instruments.

There are two basic monitoring strategies that have been found to be effective. These are illustrated in Figure 9. Both involve arrays of three dimensional stress monitoring instruments installed well ahead of the longwall face in areas where the pre-existing three dimensional stressfield has been measured (or is adequately known).

The first strategy involves installing instruments in a linear array across the chain pillar and out above the block of the next longwall panel as shown in Figure 9(a). These instruments are monitored as the longwall retreats past the site. The position of the instrument array changes relative to the goaf as the longwall panel retreats. By plotting the measured stresses relative to the goaf (as if the longwall was actually stationary and the instruments were moving), the array of instruments effectively sweeps down the edge of the panel determining the stress distribution at each stage of mining as it does so. The completeness of the distribution of three dimensional stress changes at each stage of mining is simply a function of how often the instruments are read during retreat and their lateral distribution from the goaf edge.

The second strategy is similar, but instead of deploying the stress change instruments to the side of the longwall face, the instruments are installed in the block ahead of the approaching longwall face. To reduce the drilling distances involved the instruments are located near the outbye end of the panel. Two groups are best, one near the centre of the block and a second near the maingate corner. This arrangement is shown in Figure 9(b).

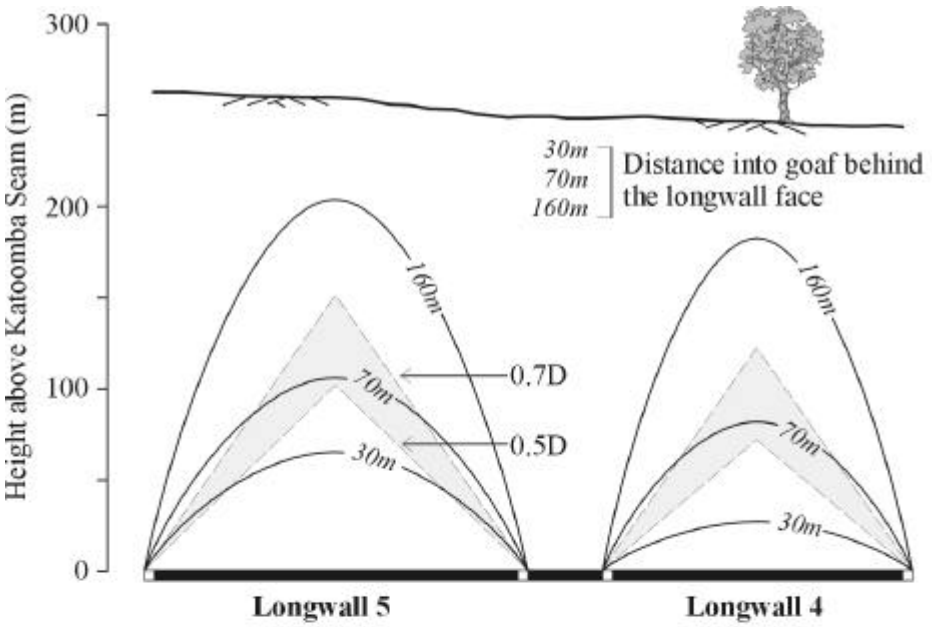

a) Cross section through Longwalls 4 and 5 at Clarence Colliery showing zones of large downward movement and load division for overhang distances of 0.5 and 0.7D *(Mills and O'Grady, 1998).*

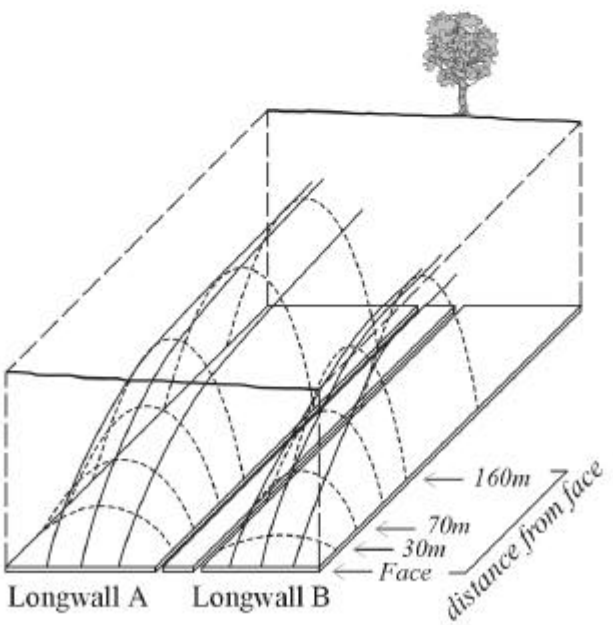

b) Schematic isometric of completed longwalls showing zones of large downward movement over each panel.

Figure 5 Results of extensometer monitoring at Clarence Colliery showing the edge of the zone of large downward movement and the extent of load transfer indicated by subsidence monitoring.

The instruments are again monitored during longwall retreat. With this approach, each group of instruments is able to detect the full load distribution about the retreating longwall face providing a measurement of the load distribution curve that is free from the local effects of the chain pillars, roadways and cut-throughs.

The first strategy is more useful for directly measuring the effects of the side abutment load on the chain pillars and adjacent roadway. However, it is typically more difficult to place the instruments sufficiently far away from the goaf edge to get a full measure of the extent of the load distribution. The second strategy provides a better indication of the full extent and form of the load distribution free from the influence of roadways and pillar concentration effects but is most suited to panels of supercritical width. A combination of both strategies provides the most comprehensive measure of load distribution about a longwall panel.

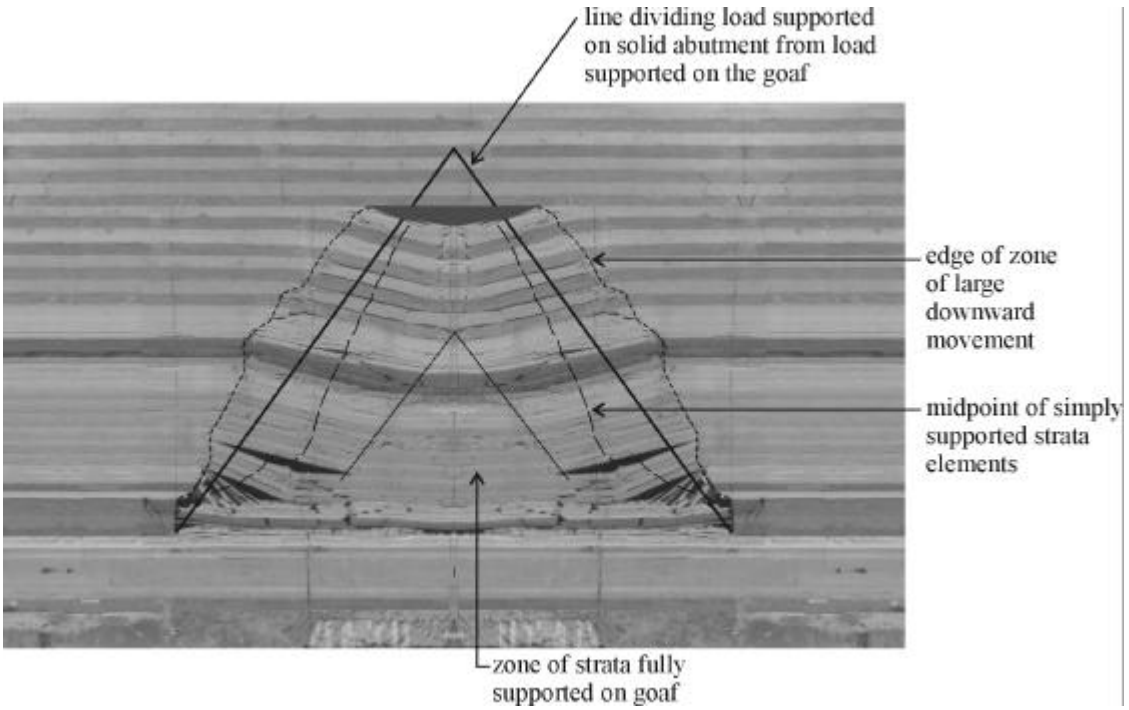

Figure 6 Results of extensometer monitoring at Clarence Colliery showing the edge of the zone of large downward movement and the extent of load transfer indicated by subsidence monitoring.

Of course direct measurement of the in situ stresses at various distances from the edge of an existing goaf is also possible. This strategy typically provides high quality data of the side abutment distribution close to the goaf edge, but there are several significant disadvantages:

- measurement costs are typically higher,
- three dimensional effects about the corner of the panel cannot be measured with the same instruments that measure the side abutment loading, and
- it is also difficult to determine the lateral extent of the load distribution, not only because it can be a long way to drill, but also because it is difficult to differentiate between random measurement variability and the small changes in load that occur at large distance from the goaf edge.

Figure 10 shows some examples of the load distribution measured for full side abutment loading at overburden depths from 100m to 250m. While all of similar form, peaking near the goaf edge and exponentially decreasing with distance from the goaf edge, there is a significant range in the magnitudes of the peak loads and the area under each curve. Mills & Doyle (2000) present the results of monitoring load distribution ahead of the longwall face and its application to estimating load on other chain pillar geometries and at great depth.

PILLAR LOADS AT VARIOUS STAGES OF LONGWALL RETREAT

Once the loading distribution has been determined for any particular site and overburden conditions, it is helpful to be able to extrapolate this distribution to other depths and longwall geometries. This can be achieved, at least as an approximation, by scaling the measured distributions to account for variation in the overburden depth, load magnitude and stage of mining, thus allowing the one set of field measurement to be applied to other areas of the mine.

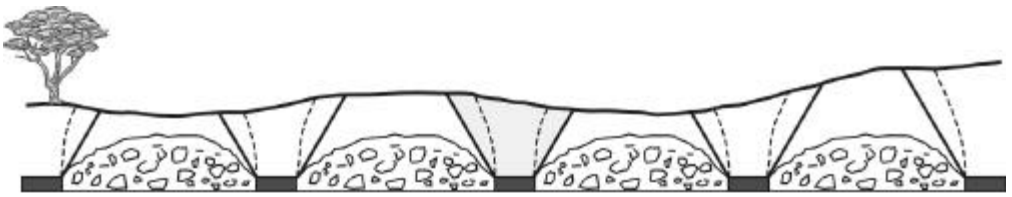

a) Shallow longwalls.

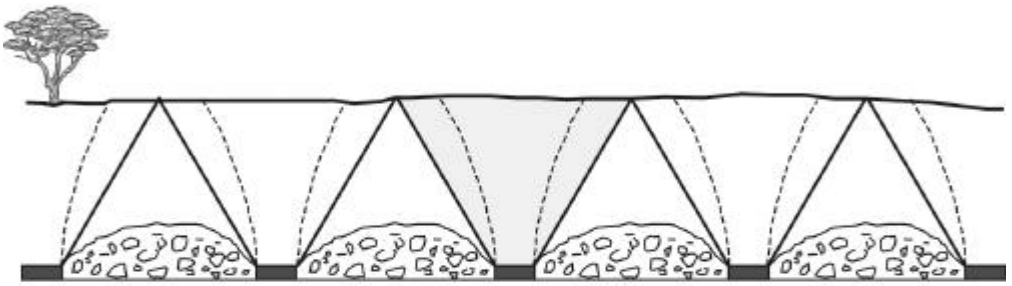

b) Critical width longwalls.

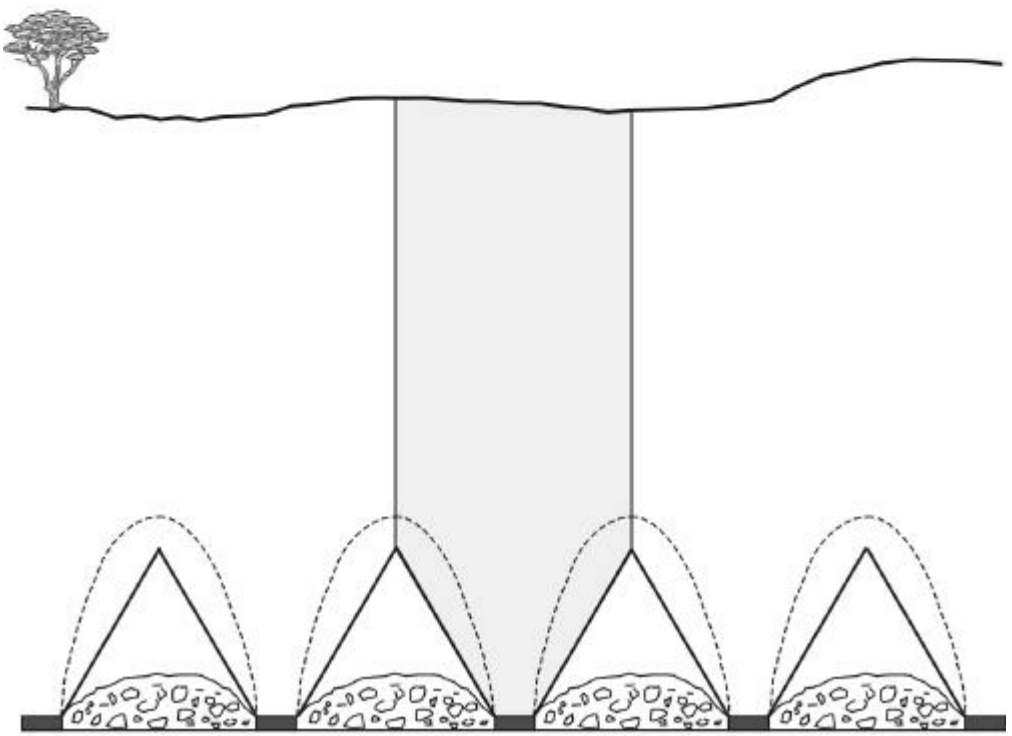

c) Deep longwalls.

Figure 7 Total pillar loading determined from subsidence information for pillar fully isolated in the goaf at various overburden depths.

As illustrated in Figure 11, the load distribution can be scaled horizontally to take account of changes in overburden depth, if the lateral extent of the abutment load is assumed to be linearly proportional to overburden depth. Field measurements consistently show that the vertical abutment loading first becomes perceptible to stress change monitoring instruments when the goaf edge approaches within a distance from the instruments of half the overburden depth. This observation suggests that the assumption of proportionality with depth is reasonable.

The area under the abutment stress curve is equal to the total overburden load. As the total abutment load changes with changes to longwall geometry or increasing overburden depth, the vertical stress values can be scaled so that the total load equals the total abutment load calculated from consideration of subsidence data.

For most practical purposes, it is useful to know the vertical loads on pillars and roadways at five stages of longwall mining: on development, at the maingate corner of the longwall panel, under full side abutment loading, at the tailgate corner of the longwall face, and for long term subsidence impacts, when the chain pillars are fully isolated in the goaf.

By measuring the load distribution at the corner of the longwall panel and under full side abutment loading, it becomes possible to estimate the load at all these stages of mining.

The load on development is estimated from tributary area considerations. At the maingate corner and under side abutment loading, the abutment load distributions are available directly from field measurements or from appropriate scaling of measured distributions.

The maximum vertical and horizontal stress increases at the maingate corner of the panel are typically of interest for design of reinforcement suitable to maintain roadway stability at the maingate/longwall face corner. These values are available directly from field measurement and are estimated for other depths and longwall geometries by appropriate scaling for depth and abutment load.

Under side abutment loading conditions, the principal design issues relate to the stress conditions experienced by the travel road inbye of the face (future tailgate roadway) and the stability of the chain pillar. The vertical stress at any given distance from the goaf edge, in this case the width of the chain pillar, is determined directly from the measured stress distribution or from appropriate scaling of the measured distribution for different geometries or overburden depth.

The vertical load on the chain pillar under side abutment loading is estimated by integrating the area under the stress distribution curve above the chain pillar. The load determined by integration over the pillar width is then adjusted to account for the tributary area effect of the cut-throughs to give the total pillar loading.

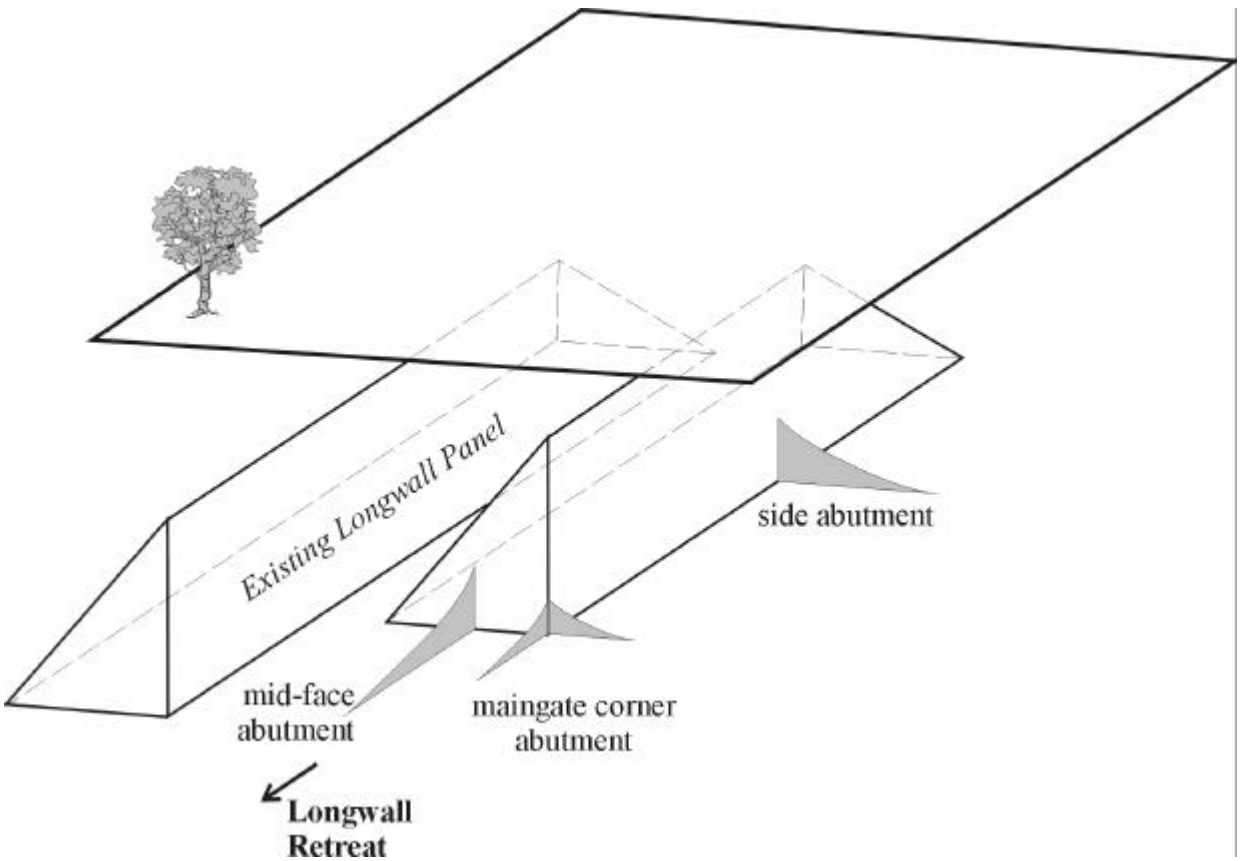

Figure 8 Distribution of overburden weight about longwall panels in three dimensions.

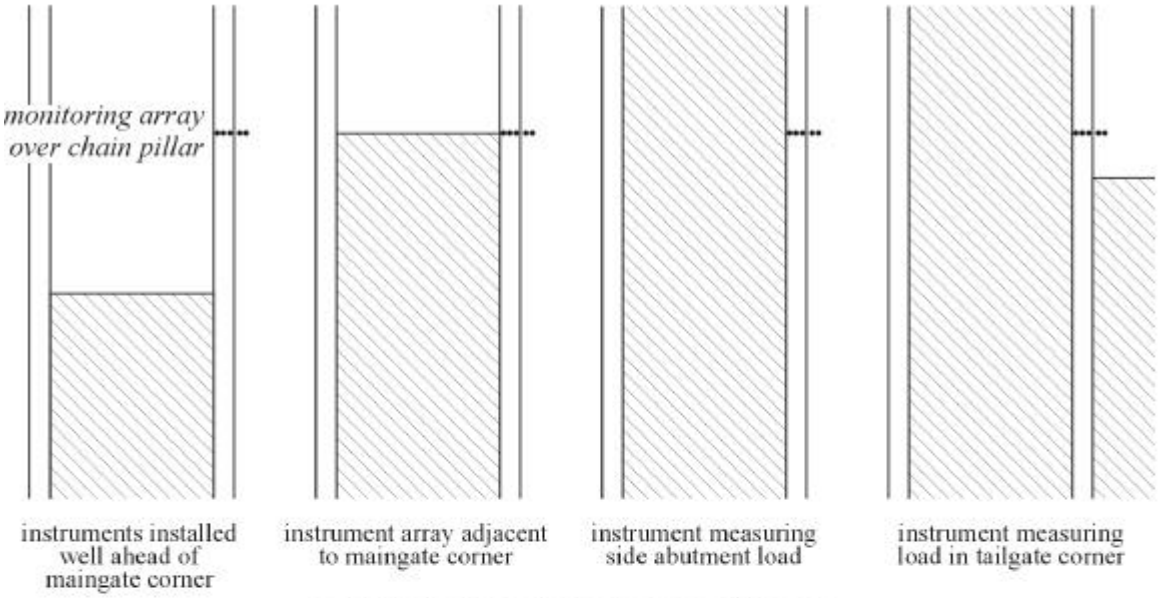

a) Side abutment monitoring strategy.

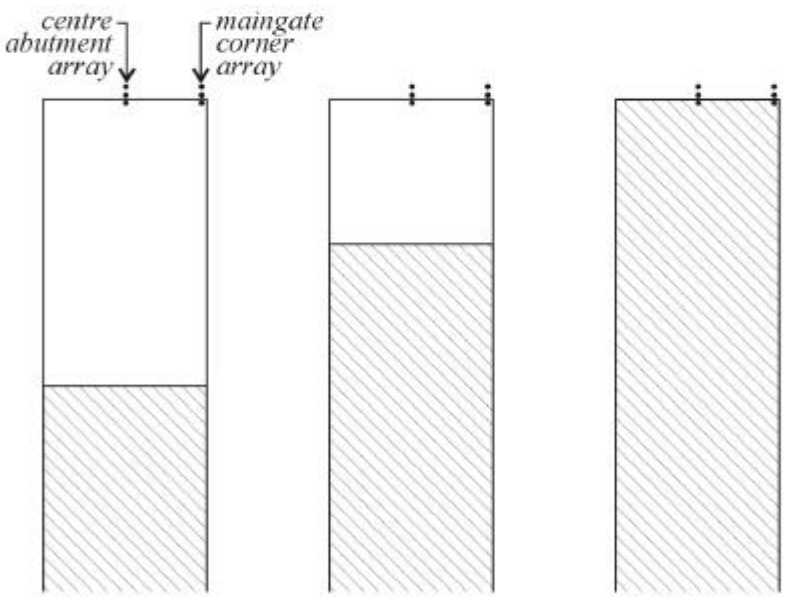

b) End abutment monitoring strategy.

Figure 9 Illustration of strategies to monitor longwall abutment loads using stresscells capable of measuring three dimensional stress changes.

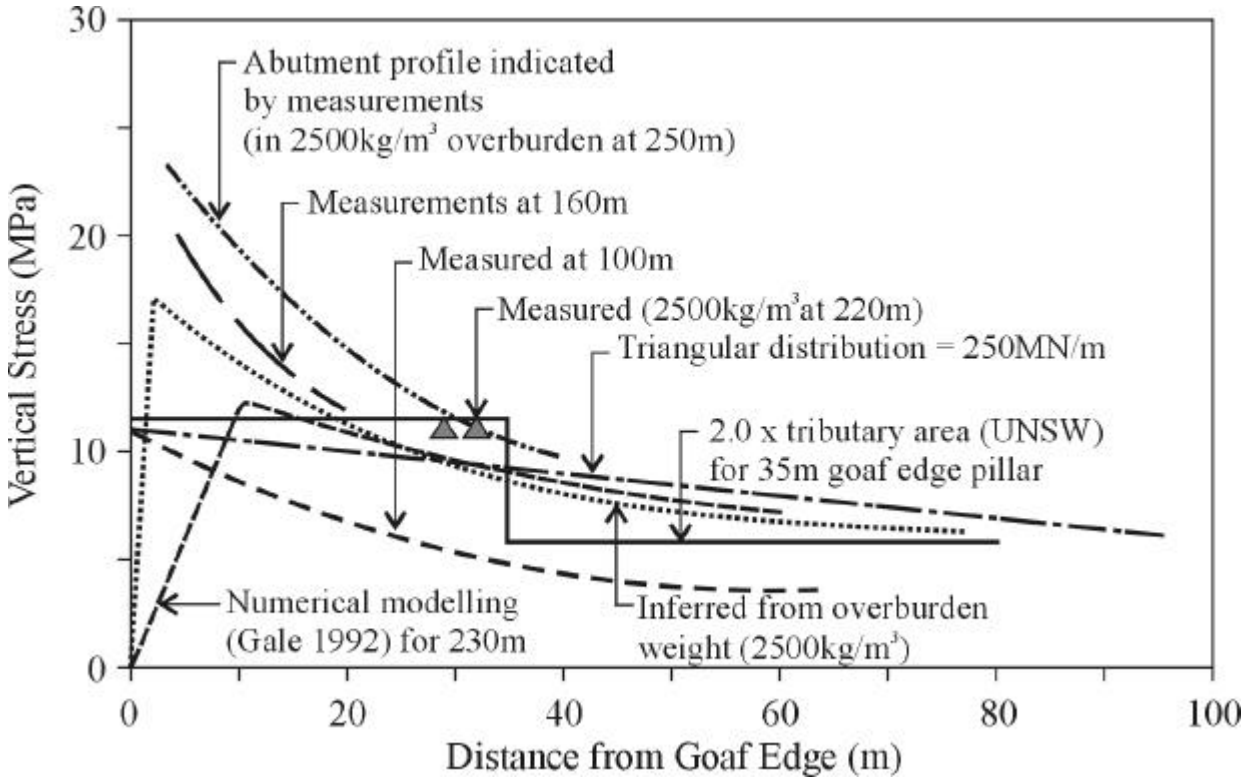

Figure 10 Examples of full side abutment load distributions measured at overburden depth ranging from 100m to 250m.

This load can then be compared directly with the nominal strength of the chain pillar to assess pillar stability.

In the tailgate corner of the longwall face, the vertical loads experienced by the roadway reach a maximum in terms of roadway support requirements. The magnitude of the pillar stresses, and assuming a uniform distribution, the stresses on the tailgate roadway as well, are estimated by adding the full abutment load about the corner of a longwall panel, to that proportion of the side abutment load supported by the chain pillar. The rest of the side abutment load is assumed to be supported on the solid coal in the block ahead of the longwall face. The average pillar load is calculated as the sum of these two components added to the original vertical stress. The average vertical stress is then concentrated using tributary area theory to take account of the cut-through spacing. The approach assumes that the average load at the tailgate corner is the sum of the various components divided by the area available to support it.

When the chain pillar is completely isolated in the goaf, the total load is no longer important for the assessment of roadway conditions, but the stability or otherwise of the pillar can be important for controlling surface subsidence impacts. The load acting on a chain pillar isolated in the goaf is calculated by adding the original vertical stress to twice the magnitude of side abutment loading and concentrating this total using tributary area theory to take account of the cut-through spacing. Pillar stability is estimated by comparing this load to the nominal pillar strength.

Although the pillar loading can be estimated with reasonable confidence, there is another issue that impacts on the stability assessment of pillars isolated in the goaf. The nominal pillar strength can be difficult to determine with confidence because of the confining effects of the adjacent goafs. The confinement provided by the goaf material is likely to significantly increase the actual strength of the pillars compared to the strength calculated if the pillars were free to deform into an adjacent roadway. At the load levels typically experienced by a chain pillar isolated in the goaf, it is difficult to keep stress monitoring instrumentation alive. Confirmation of the behaviour of chain pillars isolated in the goaf is likely to require further work.

CONCLUSIONS

A method to determine abutment loads on pillars and roadways has been described. The approach involves using surface subsidence data to establish how far the overburden strata is able to transfer overburden weight. Using this information and applying some deductive reasoning, the total magnitude of abutment load can be estimated for any particular overburden depth and overburden strata conditions.

In order for the abutment load to be used for practical benefit in roadway and pillar design, it is necessary to establish how the abutment load is distributed as a function of distance from the goaf edge.

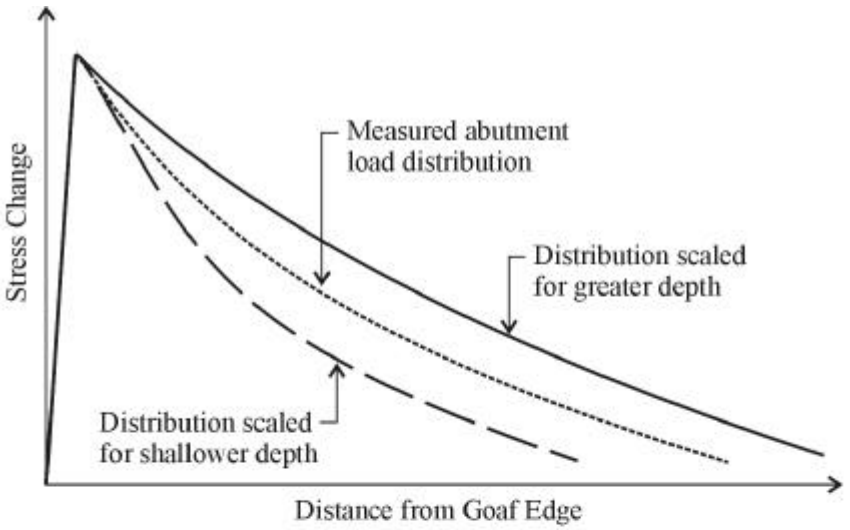

a) Horizontal scaling of abutment load distribution to account for changes in overburden depth.

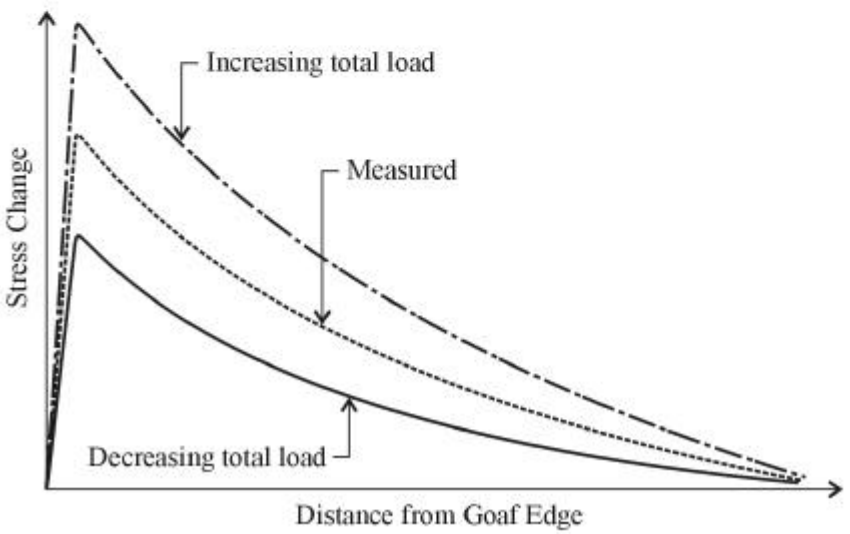

b) Vertical scaling of vertical stress to account for changes in stress magnitude.

Figure 11 Illustration of the method of scaling abutment load distributions.

Direct field measurement using high quality, three dimensional stress monitoring instruments is considered to provide a sound method of determining the abutment distribution.

The abutment load distribution determined at any one site can be scaled horizontally to account for changes in overburden depth and vertically to account for changes in total abutment load. Thus, within the limitations of extrapolating data from one site to another, the abutment load distribution can be estimated for different depths and longwall geometries.

Pillar loading and vertical stress acting on adjacent roadways are determined by superimposing the measured load distributions, or scaled versions thereof, for each stage of mining.

The method described in this paper is considered to provide a valid method for assessing pillar loading and vertical stress levels at all the various stages of longwall mining.

REFERENCES

GALE, W.J. 2001. "Advances in the understanding of complex mining problems." DC Rocks 2001 Keynote Address.

HALL, R. 1982. "A physical model to study longwall extraction in the Woodlands Hill Seam at the proposed United Colliery." ACIRL Report No 08/1146. (unpubl.).

MILLS, K.W. & O'GRADY, P. 1998. "Impact of longwall width on overburden behaviour." Proceedings of 1st Coal Operators Conference 18-20 February 1998, Wollongong N.S.W. ISBN 0 86418 477 8.

MILLS, K.W. & DOYLE, R. 2000. "Impact of vertical stress on roadway conditions at Dartbrook Mine." Proceedings of 19th Conference on Ground Control in Mining, Morgantown, eds S.S. Peng and C. Mark pp. 291-296.

WILSON, A.H. 1972. "Research into the determination of pillar size." The Mining Engineer, 131, Part 9, pp. 409-417.

Geological hazards — The impact to mining 15-16 November 2001, eds Doyle, Moloney, pp 197-202

The use of the acoustic energy meter concept to detect potentially unstable ground conditions during mining and tunnelling operations

BRIAN CLIFFORD, RUSSELL FRITH & TIM BRITTEN

Rock Mechanics Technology (UK), Strata Engineering (Australia) & Strata Engineering (Australia)

The detachment of relatively small pieces of rock continues to be the primary safety hazard related to ground instability in mining. Almost all personal injuries and a significant number of fatal accidents fit into this category. The associated business costs are substantial and in certain states, the Mining Inspectorate have made it clear that the full measure of the law will be brought to bear against those involved in safety breaches.

As a rock mechanics problem, this is an area that cannot be effectively covered by many of the more high profile topics such as support effectiveness, rock testing methods, numerical modelling and the like. It is an operational problem in that the instability cannot generally be predicted in advance of mining and similarly, cannot always be seen when the rock surface is exposed as it is often the result of hidden rock defects.

One control strategy is to install full mesh over all exposed roof and rib surfaces in order to provide a hard barrier between the hazard and mine workers. This is highly effective but not always practical to implement.

In response, momentum is gathering with the use of a hand-held instrument that was developed in the UK some 14 years ago when segmental concrete linings were being used in deep coal mines. The "Acoustic Energy Meter" (AEM) was developed with the intent of being able to remotely identify voids behind such linings where backfilling was incomplete.

This paper details recent successful work in South African coal mines and also tunnelling applications in both the UK and Finland whereby the AEM has been used for identifying areas of potentially unstable roof strata and/or tunnel linings as well as void detection behind tunnel linings.

The paper describes the fundamental basis of the AEM and its current evaluation within the Australian coal mining industry.

CONSTRUCTION AND OPERATION OF THE ACOUSTIC ENERGY METER

Method

It is well established that voids within a solid structure can be detected by listening to the variation in sound when the surface is struck at varying locations. This is the historical basis of roof "sounding" in underground mining that has been in use for many years.

A problem with roof sounding and the "qualitative" assessment of the response of the struck object is that operator judgement is required in interpreting the outcome. In particular, whilst extreme conditions may be readily identified, marginal conditions have proven to be more difficult to reliably detect in this manner. Unfortunately, such marginal conditions have also resulted in falls of ground and associated accidents despite the area being sounded and assessed to be competent.

Essentially, the principle of roof sounding is proven, simply that the interpretation of the outcome is not fully reliable.

The AEM has been designed to monitor the response of a solid body to a hammer blow in a quantifiable and reproducible manner in order to attempt to improve the reliability of sounding outcomes.

The attributes of the sound made when a surface is struck can be quantified in terms of:

- amplitude,
- frequency, and
- reverberation.

Of these three, various research studies have established that amplitude and frequency are influenced to some degree by such variables as the initial impact energy and the velocity of sound in the material (which is a function of elastic modulus and small-scale density). This makes both parameters difficult to use when a reproducible measure is the required sounding output.

The reverberation attribute is a measure of the rate at which the impact energy is absorbed by the material. It depends largely on the geometry of the structure and the internal friction of the bulk material. In general, the greater the amount of material involved, the faster the

energy is absorbed.

It has been found that the presence of voids within the structure being sounded slows down the rate at which impact energy is absorbed. It is this mechanism by which the AEM can detect the presence of such voids.

Apparatus

The apparatus consists of a transducer which is in contact with the surface of the structure, a prescribed method of striking the surface close to the transducer and a detector connected to the transducer. The detector provides an output which is directly related to the reverberation time of the surface.

Figure 1 shows a schematic circuit diagram of the AEM principle. The traces in the figure represent the variation in voltage (vertical scale) as a function of time (horizontal scale).

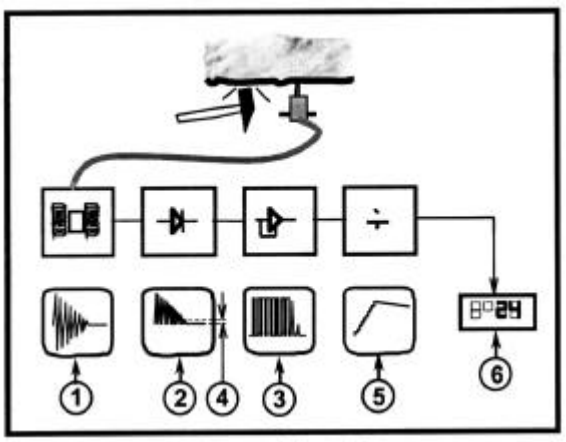

Figure 1 Schematic Diagram of the AEM Concept .

The various traces are now described:

- ¬ geophone output,
- ↑ rectified geophone output,
- → amplified to saturation,
- ↓ all pulses above a defined small threshold are converted to square pulses of equal amplitude,
- ° pulse integration to give output, and
- ± visual indicator of output.

The RDL3 AEM

The RDL3 is a hand-held version of the AEM consisting of a geophone and readout unit housed in a single case. It also has automatic arming and reset functions and features a "traffic light" LED alarm display as well as a digital readout (see Figure 2).

The operation of the AEM is straightforward consisting of holding the geophone to the surface, either directly or through the use of an extension pole according to the working height. The surface is struck within 0.5m of the geophone and a reading stored on the digital display. An average of three readings is usually taken for the area being tested.

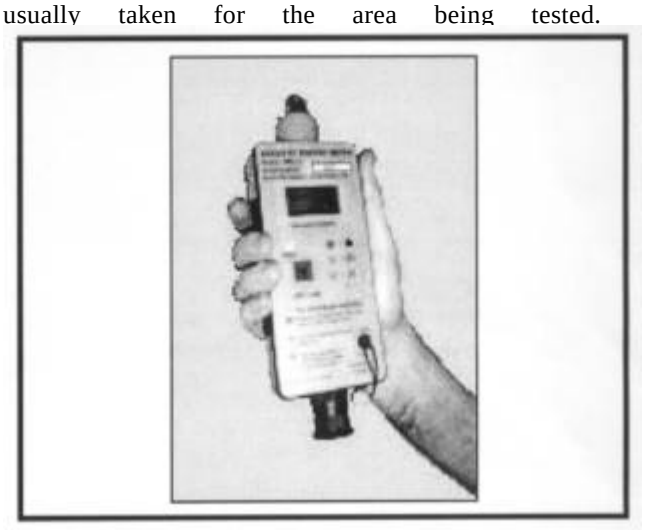

Figure 2 RDL3 Acoustic Energy Meter.

INSTRUMENT PERFORMANCE PARAMETERS

As stated previously, the AEM reading is a numeric value related to the rate of absorption of impact energy by the test material. The values obtained have relative rather than absolute significance such that on-going calibration and site assessment is a vital part of its use.

Underground proving and calibration trials have confirmed that AEM readings are consistent (within a reasonable range) and repeatable for wide range of surfaces. Intact and loose surfaces result in significantly different outputs with few intermediate readings, indicating excellent discrimination of surface condition.

The effect on reverberation of damping from the operators hand holding the instrument in place has been shown to be negligible.

Field investigations have been undertaken to check the sensitivity of the AEM to the energy in the hammer blow by varying both the strength of the blow and the position of the blow relative to the geophone.

Figure 3 shows the graphical output from these investigations and the following points are made.

- Three different hammers of various sizes were used, one being spring-loaded (ie Schmidt Hammer).
- For a solid sandstone surface, all hammers gave low readings with the largest being obtained using a 2kg hammer.
- The 2kg hammer was used to investigate the effect of blow distance from the geophone and no effect was found for distances between 0.25m and 1m.
- In areas containing known bed separation, the results using conventional type hammers showed close agreement with those found from solid sandstone roof conditions.
- It was noted that the energy of the hammer blow had a minimal impact upon the measured AEM output, as evidenced by the close correlation of the curves for Hammers 1 and 2 in Figure 3.

- In contrast to the solid surface, the Schmidt Hammer results were inconsistent in character, presumably due to the dynamics of the spring-loaded mechanism affecting the surface in a manner that is not achieved with the use of conventional hammers.
- A hammer weight of around 1kg is needed to obtain consistent results.

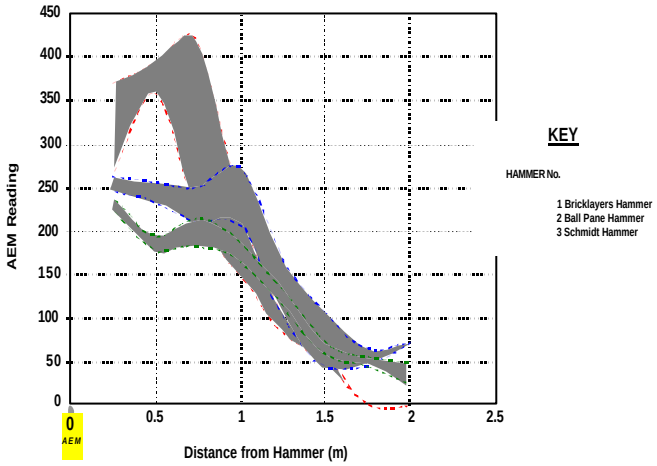

Figure 3 Plots of AEM Reading with Respect to Hammer Type and Hammer Impact Point.

Based on all of the initial proving trials, it was decided that a normal operating mode would consist of Hammer Number 1 (ie a short-handled 1kg hammer) being used to impact the surface at a nominal standard distance of 0.25m from the geophone.

FIELD RESULTS

The AEM has undergone several field trials for various applications in recent times, including:

- South African coal mines for the detection of incompetent roof (SIMRAC funded research),
- UK tunnels to assess the competency and extent of back-filling/voids associated with a number of lining types (eg steel, brick and concrete segments), and
- The assessment of the competency of sprayed shotcrete linings in Finnish underground caverns.

Each of these will now be described in more detail.

Detection of Incompetent Roof in South African Coal Mines

Under a SIMRAC funded project, the AEM was evaluated in some 11 underground coal mines. The objective was to assess its reliability in detecting potentially incompetent roof that may have otherwise remained undetected.

Altounyan and Minney (2000) describe the project outcomes in detail. The following summary is given.:

- The AEM output magnitude in stable areas varied according to roof type (ie as low as 20 for sandstone and as high as 100 for coal). This was as expected but highlights the need for geological input and site calibration with the use of the AEM.
- Abnormal readings were recorded up to 1000 but typically twice that of the normal readings for the roof type in question. Intermediate readings between the two conditions were relatively infrequent.
- For high range abnormal readings, poor roof conditions were usually visible and could be heard when sounding. However, for lower range abnormal readings, poor roof conditions were not generally visibly or audibly apparent. This is the "grey-area" in which it was hoped that the AEM would prove to be effective.
- The AEM was highly successful in identifying potential slip planes (ie angled joints), the presence of detaching laminated slabs within the immediate roof as well as depositional features known locally as "sandstone drums" that can fall out with little or no obvious warning.
- Variations in AEM readings in different roadways showed good correlation with the known state of *in-situ* stress.

Figure 4 shows the outcomes of a detailed AEM survey of a roadway passing through a dyke.

Overall, the research study demonstrated that the AEM could indeed identify potentially incompetent immediate roof conditions in underground coal mining operations as well as give guidance on a number of other related issues. As a result, the AEM has been commissioned into full operational use and is already credited with having saved lives by those mines that use it. It is about to be evaluated in the South African metalliferous mining industry as the next step in its use.

Assessment of Tunnel Linings and Associated Backfilling in the UK

Cartwright et al (2001) describe a number of field evaluations in UK tunnels. Steel, brick and concrete segmental tunnel linings have been assessed, in particular the detection of substantial voids behind such linings.

Steel Linings

Figure 5 shows the outcomes of an AEM survey in a steel-lined circular water tunnel. The purpose of the survey was to detect any voids in the grout behind the tunnel lining.

AEM outputs were found to vary from between 3500 for the 45mm thick steel tube in air to below 50 for a well grouted lining.

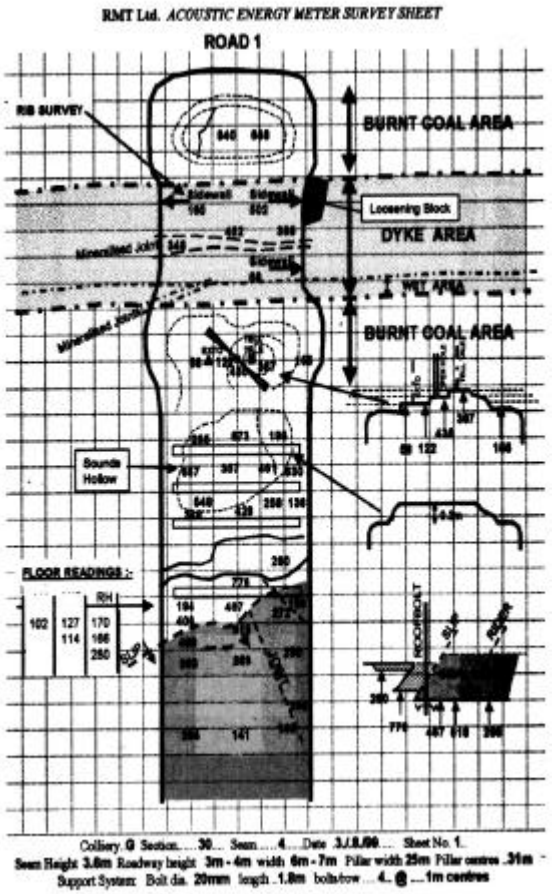

Figure 4 Sample AEM Survey Output.

The results are shown as a contour plot in Figure 5 and areas of potential voids behind the linings are clearly evident. It is noted that in other areas of the same tunnel, AEM surveys were conducted and revealed no readings greater than 50.

It was concluded that the AEM is effective in assessing grout coverage behind steel linings.

Brick Linings

The AEM has been used to inspect the brick linings of Victorian railway tunnel in the UK. Many voids are present behind these linings, either existing since original construction or having developed following movement of the lining or water damage and deterioration of the rock background.

Surveys were carried out at selected locations by obtaining mean AEM readings from 13 positions, equally spaced around the tunnel section at intervals of 5m along the tunnel length.

Figure 6 is an example output from a 250mm thick brick lined tunnel in South Wales in which both known and suspected voids behind the lining were confirmed.

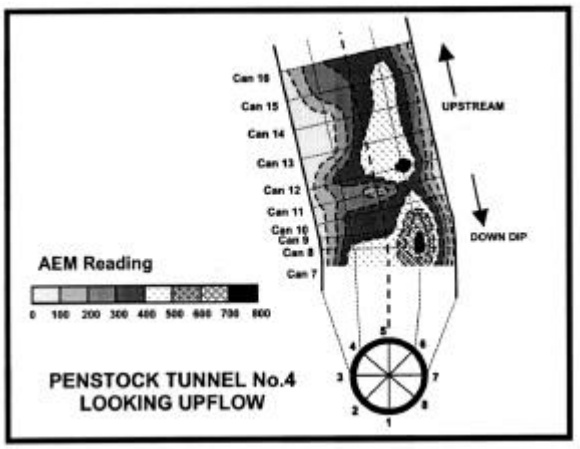

Figure 5 Relief Plot in Plan View Showing Contours of AEM Readings.

Figure 6 AEM Survey Results – Brick Lined Tunnel.

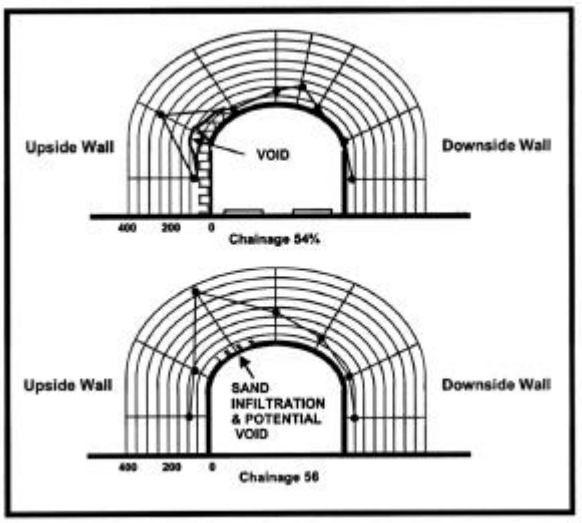

It was concluded that the AEM accurately detected the presence of voids behind the lining and /or bulging or loose brickwork.

Concrete Segmental Linings

The original AEM prototype was used extensively by British Coal between 1987 and 1992 to inspect 240mm thick concrete segmental linings in 5m diameter tunnels.

Again, the AEM was successful in detecting voids behind such linings after grouting and additional grouting of these areas prevented further stability problems occurring. Figure 7 shows an example of a segmental lining survey with a void clearly indicated at the left-hand shoulder position.

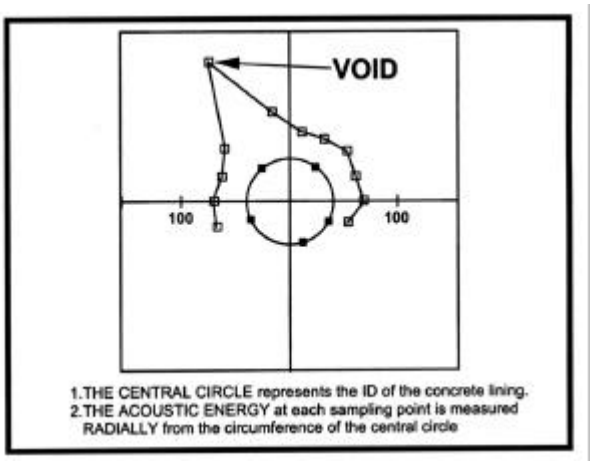

Figure 7 AEM Survey Result – Concrete Segmental Lining.

Application to Shotcrete Linings

In Finland, the use of the AEM to examine shotcrete tunnel linings is an area which has been investigated by Geotek Oy during enlargement excavations of the Viikinmaki underground municipal wastewater plant in the Helsinki area.

The integrity of a 75mm thick shotcrete lining was evaluated using the AEM after the lining had been subjected to blast vibrations and deformations. Initial test measurements were followed up by further tests after four months to reveal any changes in shotcrete lining quality caused by subsequent excavation work.

Test configuration and average results of the initial and repeated tests are shown in Figure 8.

The results indicated that the detached shotcrete areas, which were surrounded by visible fractures and later confirmed by drilling, could be revealed by using the AEM which gave a high output value (average around 150). In contrast, intact shotcrete gave a very low measurement or no triggering of the instrument at all.

Two hidden drain pipes in the shotcrete could also be located by the AEM (see Figure 8).

The repeated tests confirmed that the shotcrete lining was unaffected by the blasting vibrations. It was also found that the detached side of any given fracture could be identified by comparing the readings taken on either side of it (as was also the case of slips within the roof of coal mine roadways).

CONCLUSIONS AND FUTURE DEVELOPMENTS

It is evident that the AEM concept has undergone a significant amount of testing and evaluation in a wide variety of applications and geotechnical settings.

Its ability to provide a representative and reproducible measure of reverberation within solid structures has been well established. Furthermore, the method is inexpensive and relatively simple to undertake. A proven testing methodology in terms of hammer type and blow location is now available.

The use of the AEM to-date has also shown a very strong correlation between voids within structures and measured reverberation (ie AEM output). This has allowed potentially unstable areas of coal mine roofs and shotcrete linings to be detected as well as significant voids behind full tunnel linings.

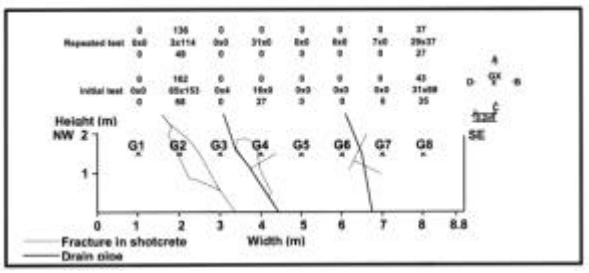

Figure 8 Test Configuration and Results from the AEM Test Profile in a Pillar with a Shotcrete Lining.

The one area of uncertainty with the use of the instrument relates to local geological conditions as this can result in threshold or trigger values changing. As such, the use of the AEM must always be in conjunction with a full appreciation of the specific geological or tunnel lining environment.

Within Australia, a Joint Coal Board funded research project has just commenced to examine the use of the AEM in underground coal mines, with a similar objective to the SIMRAC funded study in South Africa.

It is intended that in addition to reproducing the outcomes of the SIMRAC funded work, the project will also seek to clarify such issues as:

- its suitability and application in a range of local strata conditions, primarily sandstone and conglomerate, in which low bolting densities are traditionally used,
- the use of detailed borescope observations within the roof strata in areas associated with abnormal readings in order to observe and quantify the location and extent of local voids,
- defining a maximum distance into the roof strata that the AEM can reliably detect the presence of voids, and
- gaining full approval for the use of the AEM in Australian underground coal mines.

The project is due for completion by the end of 2001.

REFERENCES

ALTOUNYAN, P. & MINNEY, D. 2000. Field Experience of Measuring the Acoustic Energy from a Hammer Blow to Coal Mine Roof and its Relationship to Roof Stability. Proc 19th Int. Conf. on Ground Control in Mining, Morgantown, WVA, pp. 12-18.

CARTWRIGHT, P., CLIFFORD, B., ARMANEN, E. & VUORI, A. 2001. Application of the Acoustic Energy Meter for Assessment of Tunnel Lining Condition. Paper to be presented to Eurock 2001.

Geological hazards — The impact to mining 15-16 November 2001, eds Doyle, Moloney, pp 205-214

Understanding the influence of geological structures on outburst risk — a new modelling approach

M. B. WOLD & S. K. CHOI

CSIRO Petroleum, PO Box 3000, Glen Waverley, Victoria, 3150

A new approach to numerical modelling of coal gas outburst is presented in which geological structures are quantitatively represented on both large and small scale. Important geomechanical and reservoir variables together with their coupled interactions are modelled. These include strength, deformability, gas desorption and diffusion, porosity, permeability and 2-phase flow. The paper reviews the observed association of geological structures with outburst risk, and demonstrates quantitative modelling of outburst initiation mechanisms involving structures such as cleats, shear zones and dykes. Requirements for improved geologic structure assessments and methods for modelling of outburst evolution are discussed.

INTRODUCTION

Gas outburst has been recognised as a potential hazard for underground miners of gassy coal seams in Australia since at least 1895, when the first recorded outburst happened at Metropolitan Colliery in the Southern Coalfields of New South Wales. Many outburst events have since occurred in New South Wales and Queensland, with loss of life, mine closure and severe cost to the community.

Over the last decade outburst risk has been brought under control in Australia by the introduction of in-seam gas drainage ahead of mine development and production. Drainage to meet statutory safe gas content threshold values (THV's) is carried out in all mines assessed as at risk. This concept is based on the work of Lama particularly with respect to the outburst problems at West Cliff Colliery (Lama, 1995). Two decades ago, before the advent of the THV concept, severe outburst problems and fatalities led to the closure of Leichhardt Colliery in the Bowen Basin. While the current THV's have been set primarily based on Bulli seam experience, mines in areas such as the Hunter Coalfield and the Bowen Basin are now operating at increasing depth, with increasing gas contents, and in some cases with high CO_2 composition. There is a re-emerging need to determine safe working criteria for these operations, while seeking optimum mine development and production rates.

Geology and Outburst Hazard

A majority of the gas outbursts that have occurred in Australian underground coal mines have been associated with the presence of geological structures in the coal and the surrounding rocks, having a range of physical scales from millimetres to metres. Efforts to understand and manage the problem have been hindered by: the complexity of the physical mechanisms involved, the difficulty in determining the various contributing factors and how they interact, and the need to continuously measure and monitor underground conditions as mining progresses. The mechanisms by which geological structures contribute to outburst risk are influenced not only by geomechanical variables such as strength, in situ stress and mining induced stress concentrations, but also by coal gas reservoir variables which include fluid pressure, porosity, intrinsic permeability, relative permeability to gas and water, and sorption properties of the component gases.

Recent advances in computer modelling now enable some quantitative simulations of outburst events, including the contribution of geological structures to the physical mechanisms. The new approach is based on coupling of geomechanical, fluid flow and reservoir models. Using quantitative reservoir and geomechanical data from Australian coal mines, the potential influence of geological structures on outburst mechanisms is demonstrated in this paper by the model. This is presented in the context of geological observations, made by others, of outburst events in the Sydney and Bowen Basins. The paper also discusses properties of geological structures pertinent to outburst risk, but for which little or no quantitative data are available.

OBSERVATIONS AND EXPERIENCE

The Manifestation of Gas Outburst

A gas outburst is an essentially dynamic event in which coal and/or rock is projected into a mine opening, accompanied by a rapid release of gas. In Australian experience, the mass of coal/rock may range from small (less than 1t) to very large (greater than 400t), and volumes of gas released may be very large (greater than 5000m^3 at atmospheric pressure). Although frequently characterised as sudden or instantaneous, the time scale may span many seconds for a large outburst, suggesting a progressive event. It appears that a key element is the presence and role of compressed gas in the initiation of the burst and in the transport of material. This distinguishes a gas outburst from rockbursts which are dynamic failures resulting from mechanical stress alone.

Cavity Volume and Gas Source

Outburst cavities can vary from small cone shaped cavities of typical dimension 1m, with apparently well-defined boundaries, to large rubble filled zones of the order of 20m across. The latter may encompass associated geological structures, and have irregular geometries extending into the roof and floor. The extent of large outburst cavities may not be apparent until mined through, and the full extent of the affected zone and immediate gas source may be considerably larger than the visible cavity. This can be inferred from mass balance considerations of estimated pre-burst gas content, volume of fragmented material removed, and amount of gas released during the event.

Specific gas release intensities (de-gassing factors) of greater than 100m^3/t of rubble have been reported from European events. For the Collinsville outburst in 1954, which was at 250m depth and associated with a reverse fault structure, the factor was estimated at 28m^3/t of fragmented coal.

Geological Factors

The vast majority of outbursts in the Bulli Seam have been associated with geological structures within 2.5m of workings (Lama, 1995). Although coal has natural structures across a range of scales down to the microscopic, the geological structures considered here are primarily faults, shear zones and igneous intrusions, with characteristic length dimensions greater at least than the prevailing seam thickness. Reverse and strike slip faults have historically been outburst prone in both the Southern Coalfields and the Bowen Basin (Shepherd and Rixon, 1983).

At a smaller scale, coal cleat can result in strength anisotropy and permeability anisotropy. At Leichhardt Colliery, face cleat planes with strike length greater than 1m were systematically spaced at about 2m, many extending the full seam height (Hanes and Shepherd, 1981). These were paralleled by minor face cleats spaced down to 1-3mm. In bright coal bands, butt cleat intersected the face cleat, but had very short persistence, and frequently contained secondary mineralisation.

Particularly if aligned parallel to the mined face, face cleat can allow preferential tensile failure into the opening. The face cleats also can result in enhanced permeability along their strike direction, facilitating easier gas flow to the face region, which has been de-stressed in the perpendicular direction. Gray (1980) pointed out that butt cleat could result in improved face drainage and a reduction in gas pressure, reducing the likelihood of failure initiation. It is noted that closely spaced cleavage fracturing was induced by mining at Leichhardt, and was associated with outburst occurrence. When cleavage of dull coal was absent, outbursts did not occur. Hanes and Shepherd (1981) reported that cleavage formation was independent of the pre-existing face cleat. However, most bursts occurred with their axes perpendicular to the prominent face cleat. Reservoir and geomechanical aspects of this occurrence are discussed below.

Reservoir and Geomechanical Factors

Gas content

Gas content generally increases with depth, but at any depth the value will depend on the coal type, gas composition, reservoir pressure, and degree of saturation at that pressure. Undrained gas contents likely to be associated with outbursts in the Bulli seam at Appin Colliery are typically 13m^3/t (mainly CH_4), and reservoir pressures of 4.2MPa have been measured by well testing from the surface. This represents a hydrostatic head of 420m at a seam depth of 453m. Lama (1995) reported gas contents approaching 19m^3/t and maximum reservoir pressure of 4.6MPa. At Leichhardt Colliery, the Gemini seam was mined at depths 350-410m. Gas contents up to 16m^3/t (mainly CH_4) were measured at pressures up to 3.6MPa, which approximated the hydrostatic head.

Gas composition

For a given coal type and gas composition, gas content is a function of pore fluid pressure, as quantified by the adsorption and desorption isotherms. It is widely known that for single component gases (100% CH_4 or 100% CO_2), the storage capacity of CO_2 at a given pressure is generally more than twice that of CH_4. Therefore, if an outburst occurs, coal saturated in CO_2 will release much greater amounts of gas than if saturated with CH_4 at the same pressure. For similar gas contents, 100% CO_2 is found to desorb more rapidly than 100% CH_4.

Desorption rate

The process of diffusion from the micropores to the cleat or fracture system is driven by gas concentration gradient, following Fick's law. The time taken for desorption increases strongly with increasing particle size. A particle 10^{-3}mm in diameter will typically desorb most of its gas in less than 2s, whereas a 1mm diameter particle will take up to 30d. Desorption rate is also strongly correlated with gas content.

Williams (1997) presented data from 30s desorption of crushed coal that shows gas volume release rate to be directly proportional to gas content. The rate for >90% CO_2 is greater than that for >90% CH_4. The formation of mylonite and granulated porous coal on thrust and strike-slip faults therefore provides a mechanism for more rapid desorption.

Permeability

Permeability is a key factor controlling drainage rates of water and gas, either via drill-holes or into the advancing mine roadway. For given gas content and rate of roadway development, pressure gradients forming behind the face are inversely related to the permeability.

Low permeability causes high pressure-gradients, which result in high body forces behind the newly exposed face. For stability, these forces must be resisted by the strength of the coal. High gas pressure gradient is widely recognised as a critical variable in the initiation of outbursts.

Relative permeability

Effective permeabilities for 2-phase gas-water flow are lower than the intrinsic permeability, which acts in the case of single-phase flow, gas or water. Whilst hydrostatic water pressure may act to prevent gas desorption, the presence of the water phase in the coal at pressures below desorption pressure may greatly reduce the permeability to the gas phase.

Wood and Hanes (1982) concluded that free water in emission test holes was historically associated with burst prone conditions, and that its occurrence indicates the low effective permeability of a coal face. A discussion of 2-phase flow and outburst was presented by Gray (1987a,b).

Permeability and stress

Low permeability at the coal face may also be caused by mining-induced stress concentration. Permeability is strongly dependent on the effective stress acting on the coal. A number of studies have shown an inverse non-linear relationship of permeability with effective stress (McKee et al., 1987). Discussing the Bulli seam, Lama (1995) stated that dykes and faults influence a decrease of fracturing ahead of the face and lower the permeability, resulting in the build up of higher pressure gradient. Hanes (1995) noted that at Leichhardt, outbursts commonly occurred after signs of "hardening" in which the ribs and face stood solidly with no evidence of crushing.

Stress, strength and structure

In contrast to the predominant influence of major geological structures observed in Bulli seam outbursts, the Leichhardt experience demonstrated the effect of *in situ* stress and mining-induced stress in more homogeneous coal conditions. Highly anisotropic stresses were measured in the sandstone roof; σ_H = 30MPa, σ_h = 20MPa and σ_V = 10MPa. Arched roadways driven by an Alpine miner produced less outbursts, apparently as a result of increased stability by stress 'arching' and decreased stress concentrations around the face. Unconfined compressive strengths varied from 5-20MPa for bright to dull coal, respectively. Compared to Bulli seam conditions, coal structure at a much smaller length scale promoted the failure mechanism.

A NEW MODEL FOR THE SIMULATION OF GAS OUTBURSTS

Coupled Model

A new modelling approach has been developed, the main objective of which is to couple the various reservoir and geomechanics processes that contribute to the evolution of the outburst mechanism. The physical and mathematical basis of the model is presented by Choi and Wold (2001). SIMED (Stevenson, et al.,1994) and FLOMEC (Choi, 1996) can each model some of the defined processes, and together they can model all the processes. The simplest way to develop a model which can model all the processes without making any significant modification of the two codes is by 'linking' SIMED and FLOMEC through sharing information of the coupling parameters (Choi, 1998), which in this case are fluid pressure and stresses. This is shown schematically in Figure 1.

SIMED is a two-phase (gas and water), three-dimensional, multi-component, single or dual porosity reservoir simulator. The coal matrix is considered to be the low permeability, high storage capacity, primary porosity system. The cleat system is analogous to the high permeability, low storage capacity secondary porosity system. Desorption of gas from the coal is governed by the Langmuir model, and diffusion of gas through the matrix is modelled by Fick's law. Fluid flow in the cleats is described by Darcy's law. Flow in fractures is modelled by high conductivity zones. Drainage of gas from progressively mined faces can be modelled.

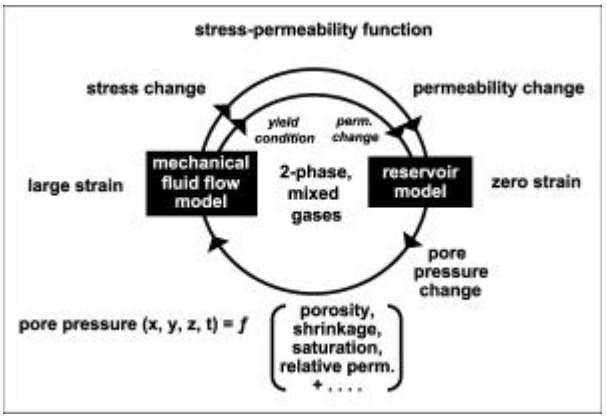

Figure 1 New outburst model: interaction of reservoir and geomechanics – fluid flow models.

FLOMEC is an enhanced version of a three-dimensional finite difference/finite element program (Choi *et al*., 1991), for analysis of coupled fluid flow - mechanical processes in rock containing joints, faults and aquifers. Large deformations and two-phase (gas and water) fluid flow in discrete structures can be modelled. Progressive mining followed by the formation and consolidation of goaf can also be modelled. The Mohr-Coulomb criterion is used for the intact material (rock and coal). This is the conventional model used to represent shear failure in geomaterials. For the major geological discontinuities, joint properties are assigned which include joint friction angle, cohesion, and dilation angle. Large deformation (finite strain) is modelled using an updated Lagrangian scheme. In the approach, the geometry of the material is updated continuously, and the strain measure is based on the geometry just prior to the current one.

For a highly jointed material, the ubiquitous joint model can be applied. It is an anisotropic plasticity model that assumes the existence of closely spaced weak planes of specific orientations, embedded in a Mohr-Coulomb solid. Failure can occur along any set of the weak planes or in the intact material, or both, depending on: the stress tensor the properties of the intact material and the weak planes, and the orientations of the planes.

The elastic properties of the jointed material depend on the number and the orientations of the sets of weak planes. If there is only one set of planes, the elastic properties of the material can be represented by the conventional elastic transversely isotropic model. For more complex sets of the planes, the elastic properties of the material can be derived using homogenisation techniques, mixture or effective media theories.

DEMONSTRATING THE MODEL

The model is demonstrated here in 2-dimensional form using composite data and observations from the Bulli and Gemini seams. Data assembled by Lama (1996) relating observed outburst occurrence to gas content and composition are given in Figure 2, for the Bulli Seam. THV criteria applied to two mines working this seam are superimposed. They incorporate a significant margin of safety, with many of the outbursts recorded at gas content values approaching virgin, undrained conditions.

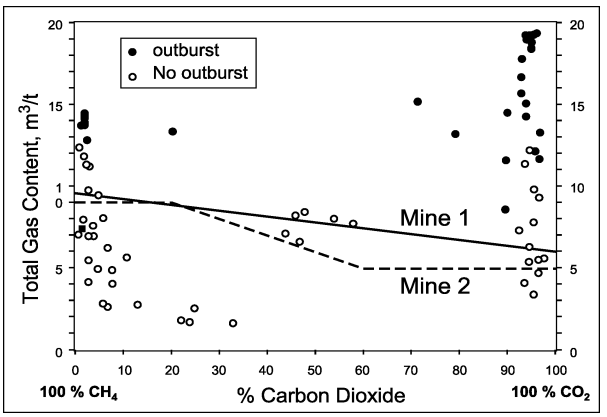

Figure 2 Outburst experience in the Bulli Seam, with imposed THV's for two mines working the seam (after Lama, 1996).

The main model variables are as follows:

- opening geometry,
- mining advance rate,
- vertical stress based on depth,
- horizontal stresses based on field measurement and depth,
- intrinsic permeability and permeability anisotropy based on field measurement,
- desorption isotherms from laboratory measurement,
- initial reservoir pressure based on depth, or reduced to various pressures to represent drainage or under-saturated conditions,
- sorption times based on production well history matching,
- CH_4/CO_2 composition in the range 0-100%, and
- coal strengths from laboratory measurements.

Sensitivity to Gas Content

'Outburst' behaviour in the model takes the form of rapidly occurring, very large deformations of a localized region of the excavated face or rib. It is apparent that gas pressure is a major driving force for the large deformations observed. However, experience with the model has also confirmed that model outburst is also dependent on the interactions of permeability, coal strength, in situ stress and roadway dimensions. Sensitivity to these variables may depend on the state of other variables in the area of interest. For example, sensitivity to coal strength may be low unless the state of stress and gas pressure are near to critical outburst condition. The modeling approach taken is to bring the model to near-critical state in one or more dominant

variables, and then parametrically change the variable of interest. This approach is presented in greater depth by Wold and Choi (1999), including details of input data and results from parametric studies.

Sensitivity to the level of pore pressure is illustrated in Table 1, in which the reservoir pressure and desorption pressure are reduced 'along the isotherm'; i.e. the coal formation is assumed to be almost gas-saturated, and the pressure is reduced until the model does not 'burst'. For the given model conditions, 'critical' pressure occurs at a saturated gas content of 12.6m^3/t, which lies within observational experience in the Bulli seam (Figure 2).

The distribution of pore fluid pressure with distance from the mined face is shown in Figure 3 for the four model cases of Table 1. The model curve for critical burst condition lies just below the pressure distribution measured under outburst conditions in the Gemini seam (Wood and Hanes, 1982). These results support the hypothesis that pore pressure gradient is one of the key factors in outburst initiation. For the excavation sequence and geometry modelled, outburst generally does not initiate until after several excavation stages, resulting from the interaction of mining-induced mechanical stress with pore pressure fields.

Sensitivity to Permeability Anisotropy and Cleat Orientation

The Gemini seam pressure measurements implied that the major systematic cleat system affected the gas pressure distribution close to the working face. The maximum gas pressure gradient was found to be perpendicular to the major systematic cleat, which indicates that the minimum permeability component lay in this direction. Permeability anisotropy associated with structure can also be evident in the drainage rates from in-seam drainholes of different orientations. In the work presented here, parametric variation of permeability is modelled in terms of, magnitude of the geometric mean permeability, and the presence and orientation of anisotropy. The maximum anisotropy ratio in the horizontal plane is about 3:1.

These particular models assume initially undrained, gas-saturated conditions. For the base case, the maximum permeability component is aligned perpendicular to the roadway axis, parallel to the face, representing the direction of the face cleat system in the model. The lower permeability in the butt cleat direction leads to the formation of higher pore pressure gradient near the face than for the case where the anisotropy is reversed (Figure 4). The change in permeability component direction results in a major change in outburst mode; the face outburst is replaced by rib outburst. These cases quantify the mechanisms by which small-scale structures such as cleats, through their effect on directional permeability, and drainage rates, can influence the initiation of outburst.

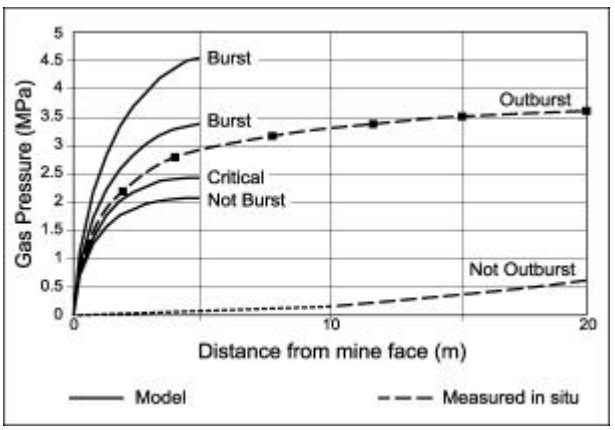

Figure 3 Pore fluid pressure profile measured in Gemini Seam under outburst conditions (adapted from Wood and Hanes, 1982), compared with model predictions for conditions given in Table 1.

Reservoir pressure MPa	Desorption Pressure MPa	Gas Content m^3/t	Model response
4.85	4.79	15.2	Burst
3.47	3.41	14.0	Burst
2.48	2.41	12.6	Critical
2.10	2.03	11.8	Not burst

Table 1 Variation of reservoir pressure 'along the isotherm' and model 'burst' response

Mining Towards Large Scale Structures

The great majority of outbursts recorded in Australia have occurred at the working face of roadways close to or at intersections with geologic structures such as fault zones and intrusions. These structures provide discontinuities in strength, fluid storage coefficient, permeability, fluid pressure and effective stress, but observation data have not been found which adequately quantify the various strength, porosity, permeability and desorption properties required for modelling outbursting structures.

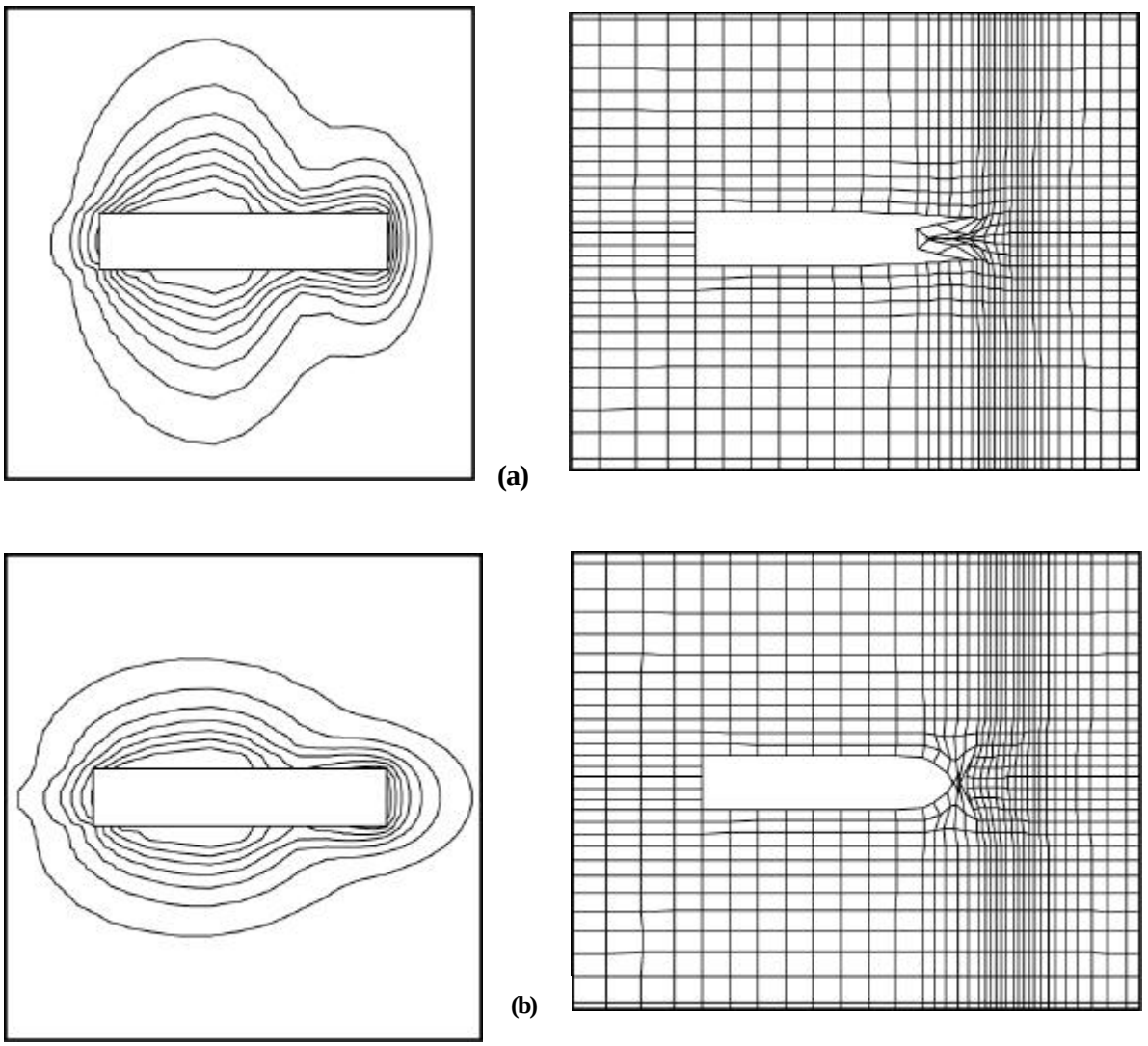

Figure 4 Pore pressure contours and 'burst' displacements with minimum permeability component aligned (a) parallel to the roadway axis (b) perpendicular to the roadway axis.

Permeable Shear Zone

Model pore pressures, changing with time around a newly excavated roadway, are shown in Figure 5. In this example, a roadway of 5m width is extended progressively towards a 1.0m thick shear zone. This zone is assumed to initially have high permeability, low strength, and a high fracture-porosity that is gas-saturated. At a length of 25m outburst is initiated as the shear zone is reached.

The low strength promotes outburst initiation and the highly permeable, highly porous structure provides high energy storage in the free gas. Rapid extension of the pressure depletion zone occurs along the shear zone as the outburst develops. The drainage of gas from coal remote from the excavation adds to the 'hazard' of the event. The model computes the flux of gas at the free surface, i.e. the time rate of gas migration across unit surface area. For this case, the amount of gas released is 7 times that released from a 'normal' outburst. The enhanced drainage mechanisms seen in the model may explain the very large degassing factors that have been observed *in situ*.

Impermeable Dyke

A low permeability barrier such as a dyke may help to maintain apparently stable conditions while confining high pore pressures behind it. Quiescent conditions prior to outburst occurrence have been variously reported. The dyke model assumes a 1.0m thick zone normal to the heading axis, having low porosity and very low permeability. In contrast to the shear zone model, the dyke stores very little free gas and acts as an impermeable barrier to both flow and drainage from the coal as the heading approaches.

Impermeable Dyke

A low permeability barrier such as a dyke may help to maintain apparently stable conditions while confining high pore pressures behind it. Quiescent conditions prior to outburst occurrence have been variously reported. The dyke model assumes a 1.0m thick zone normal to the heading axis, having low porosity and very low permeability. In contrast to the shear zone model, the dyke stores very little free gas and acts as an impermeable barrier to both flow and drainage from the coal as the heading approaches.

The mechanical properties of the dyke can significantly affect the potential outburst behaviour to be encountered. A relatively stiff, high strength, stiff dyke 'attracts' stress but resists failure because of its high strength. However, the dyke model exhibits an unanticipated result. If the dyke is of sufficient stiffness and strength it can 'shield' the coal on the new face after the dyke is mined through, and actually inhibit the coal from outbursting. The effect is seen when comparing two model cases with low strength (same geomechanical properties as coal) and high strength, respectively.

For the low strength dyke, the coal face outbursts through the gap in the dyke, shown in time sequence in Figure 6. For the high-strength dyke, coal outburst does not occur. Insight to the mechanism is provided by the stress vectors and yield zones around the face. Figure 7 shows that the very strong dyke reduces the coal yield zone, and the stress abutment is close to the face. For the low strength dyke, the stress abutment is located several metres forward of the face, beyond the low-stressed zone.

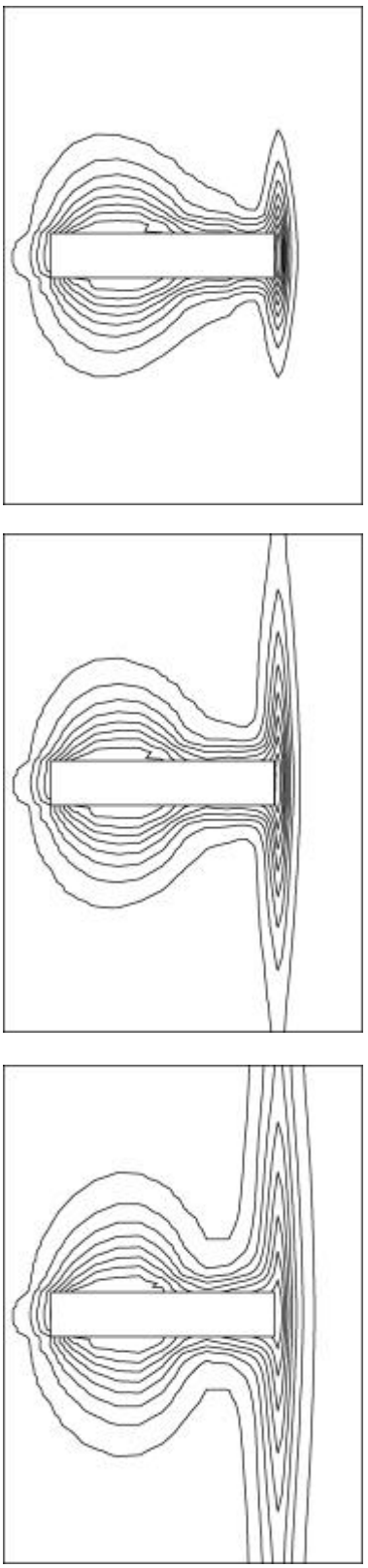

Figure 5 Pore fluid pressure contours with increasing time, at intersection of advancing model roadway with low strength, high permeability 'shear zone'

DISCUSSION AND CONCLUSIONS

Considering the geomechanics of outburst mechanisms, it is evident that: geological structure, stress conditions and strength of coal are strongly interactive, and attention has also been drawn in this paper to size scale effects. At the larger scale, the model can explicitly represent these interactions on discrete discontinuities. On the smaller scale, ubiquitously distributed or 'smeared' properties are used to represent cleat and other macrostructures. Engineers and geologists have gained experience and confidence in the use of various geomechanical models, and may have a good 'feel' for the geomechanical properties of coal seams and coal bearing formations. Nevertheless, improved estimates of strength and deformability under fluid saturated, effective stress conditions are required. In the case of coal reservoir properties, experience has been gained via applications of reservoir simulators to gas drainage, predominantly SIMED, but the level is relatively less than for the geomechanics.

With respect to outburst mechanisms, the models described here are new and are undergoing further development. There is a strong need to improve the reservoir data base, and to develop methods of measuring or estimating the reservoir properties of the geological structures that are relevant to outburst mechanisms.

Considering first the large-scale structures (faults, shear zones, intrusions) the model clearly shows the importance of mechanisms related to strength, energy storage capacity, gas transport from more distant parts of the reservoir, and barriers to flow. However, the quantitative results remain limited because they are based on estimated properties of the structures, rather than physically measured data. In terms of risk analysis, further model work could help classify the degrees of hazard associated with these structures. For instance with respect to their geological setting; a strike-slip fault in a thin seam, or a low angle thrust fault in a thick seam may both potentially access and transport very large volumes of gas to an outburst site.

At a smaller length scale, strength of 'intact' coal can be related to cleat and other macrostructures.

When in the near-critical gas state, the model demonstrates that both permeability anisotropy and coal shear strength can significantly affect outburst initiation. Comparative risk assessment from site to site could therefore benefit by considering the permeability and strength of intact coal. It is also noted that high strength intact coal is often associated with low permeability, a contributor to high pressure-gradients and increased risk factor.

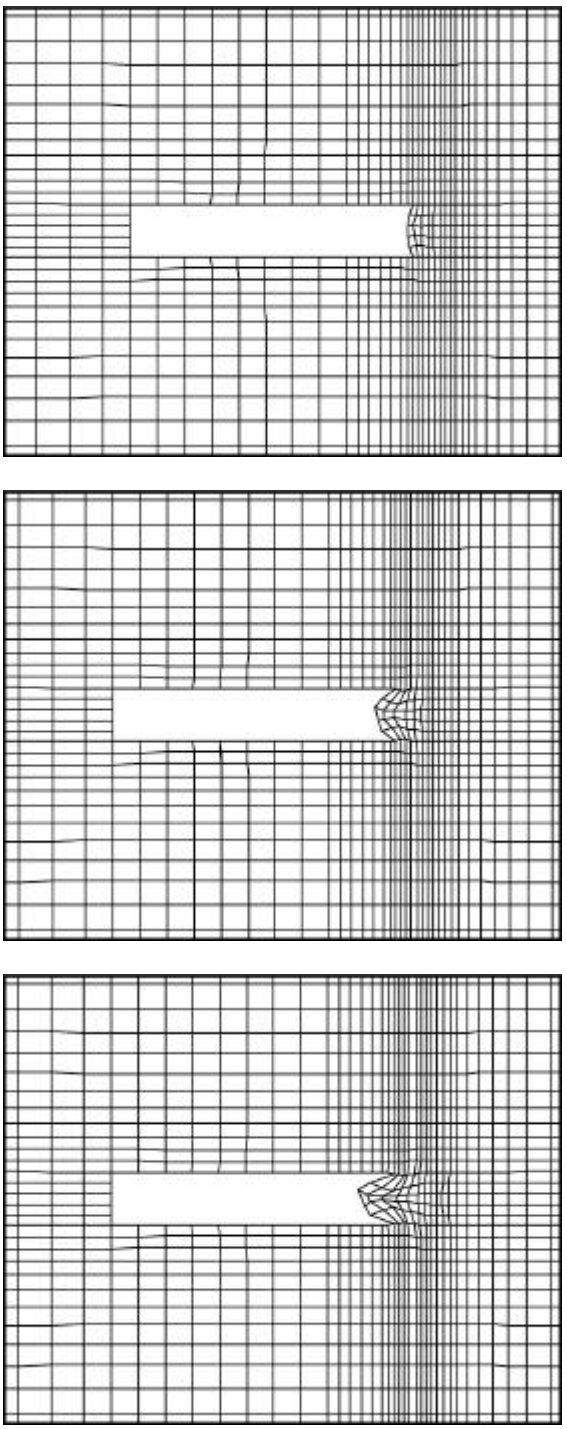

Figure 6 Model mesh deformation with time from 'burst' initiation, after mining through impermeable dyke (low strength case).

Modelling of Post-Initiation Outburst Dynamics

The manifestation of gas outburst is an essentially dynamic event. The advances in modelling technique developed and demonstrated in the current work primarily deal with conditions for outburst initiation.

However, the essential dynamics of outbursts are derived from the energy released and consumed after the event has initiated. The major hazards derive from the rate of energy release, transport of fragmented coal, and the volume and rate of release of noxious gases.

A more adequate model for the evolution of the dynamic event is under development at CSIRO Petroleum, focussing on the prediction of the violence of an outburst, the likely volume of coal that can be expelled, and the volume of gas that can be emitted. This takes account of induced coal fragmentation, increased desorption rate as a function of fragmentation, increased desorption rate as a function of fragment size, and information on mixed gas sorption characteristics.

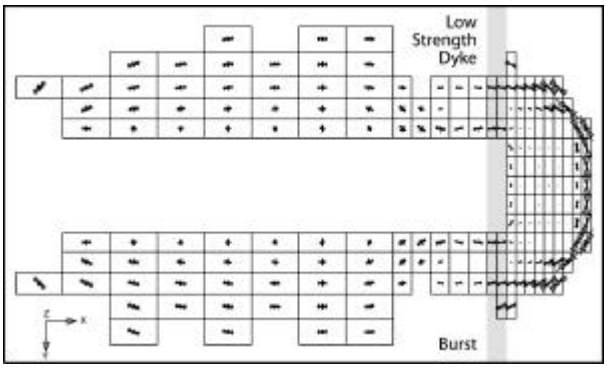

Figure 7 Yielded region and vector components of total stress, after mining through (a - above) low strength dyke - 'burst' initiated (b - below) high strength dyke – no burst occurs.

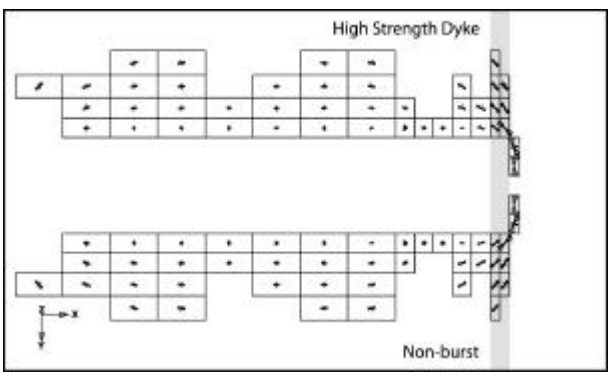

RECOMMENDATIONS

Based on the outcomes of the work discussed in this paper, it is recommended that research and development be undertaken for:

- the application of quantitative modelling of this type for improved outburst risk assessment techniques,
- measurement of coal seam reservoir variables, and the assemblage of reservoir and geomechanical data bases for mine sites, in parallel with geological and structural data which are generally constructed,
- the assessment of geomechanical and reservoir properties of geological structures, particularly with respect to their strength, fluid conductivity and potential-energy storage characteristics, and
- development of an outburst strength criterion and a practical measurement method for this variable.

ACKNOWLEDGEMENTS

The authors acknowledge the support of ACARP, BHP Billiton Pty. Ltd., Anglo Coal Australia Pty. Ltd., and CSIRO Petroleum for this work. They are grateful for the information and data provided by staff in these organisations and in particular for the most valuable insights and discussions provided by Mr. Jeff Wood of BHP Billiton Pty. Ltd.

REFERENCES

CHOI, S.K. (1996) Personal communication.

CHOI, S. K. (1998) Personal communication.

CHOI, S.K., WOLD, M.B., CROTTY SISSON, J.M. & LEE, M.F. (1991). 3-dimensional analysis of underground excavations – two new programs applied to a mining problem. In Beer, G. and Carter, J.P. (eds.). *Computer Methods and Advances in Geomechanics*, A.A.Balkema /Rotterdam/Brookfield 1991, pp. 1287-1292.

CHOI, S. K. & WOLD, M. B. (2001). Advances in simulation of gas outburst conditions in underground coal mines, in Proc. 2001 International coal Bed Methane Symposium, University of Alabama, Tuscaloosa, May 2001, pp. 283-294.

GRAY, I. (1980). The mechanism of, and energy release associated with outbursts, *Symp. on Occurrence, Prediction and Control of Outbursts in Coal Mines*, AusIMM, Brisbane, pp. 111-125.

GRAY, I. (1987a) Reservoir Engineering in coal Seams: Part 1 - The Physical Process of Gas Storage and Movement in Coal Seams, *SPE Reservoir Engineering*, pp. 28-34.

GRAY, I. (1987b) Reservoir Engineering in coal Seams: Part 2 - Observations of Gas Movement in Coal Seams, *SPE Reservoir Engineering*, pp. 35-40.

HANES, J. & SHEPHERD, J. (1981) Mining induced cleavage, cleats and instantaneous outbursts in the Gemini Seam at Leichhardt Colliery, Blackwater, Queensland. *Proc.AusIMM.No.277*, March 1981, pp. 17-26.

HANES, J. (1995). Outbursts in Leichhardt Colliery: lessons learnt. In Lama, R.D. (ed.) *International Symposium-cum-Workshop on Management and Control of High Gas Emissions and Outbursts in Underground Coal Mines.* Wollongong, NSW, March, pp. 445-464.

LAMA, R. D. (1995). Safe gas content threshold value for safety against outbursts in the mining of the Bulli Seam. Lama, R.D. (ed.). *International Symposium-cum-Workshop on Management and Control of High Gas Emissions and Outbursts in Underground Coal Mines.* Wollongong, NSW. March, pp. 175-189.

LAMA, R.D. (1996). Assessment of Threshold Values for Safety Against Outbursts of Gas and Coal in the Bulli Seam at Appin Colliery. TechEffect, Kembla Coal and Coke Pty Limited, October 1996.

STEVENSON, M. D., PINCZEWSKI, W. V., MEANEY, K. & PATERSON, L. (1994). Coal seam reservoir simulation. *APEA Journal* 34, pp. 114-120.

MCKEE, C.R., BUMB, A.C. & KOENIG, R.A. (1987) Stress dependent permeability and porosity of coal, presented at the *Coalbed Methane Symposium*, Tuscaloosa, November. pp. 183-193

SHEPHERD, J. & RIXON, L.K. (1983) Contribution discussion to “Instantaneous outbursts of gas and coal - a review by Alan Hargraves (Proceedings No. 285, March 1983)”. *Proc. AusIMM. No.287,* Sep. 1983, pp. 71-73.

WILLIAMS, R. (1997). Definition of outburst threshold limits from core testing, *Symposium on Safety in Mines: The Role of Geology*. Doyle, R., Moloney, J., Rogis, J. and Sheldon, M. (eds.). Newcastle, NSW. November. pp. 85-90.

WOLD, M. B. & CHOI, S. K. (1999). Outburst Mechanisms: Coupled Fluid flow – Geomechanical Modelling of Mine Development. ACARP Project C6024 Final Report, CSIRO Petroleum, Australia, December 1999, 94 p.

WOOD, J. H. & HANES, J. (1982). Development of Protection Techniques for Mining in the Outburst Prone Central Bowen Basin. NERDDC Project 80/0223 Final Report, July 1982.

Geological hazards — The impact to mining 15-16 November 2001, eds Doyle, Moloney, pp 215-220

The Impact of Coal Properties on Gas Drainage Efficiency

LILA W. GURBA[1], ANDREW GURBA[2], COLIN WARD[1], JEFF WOOD[3], ANDREW FILIPOWSKI[4] & DAVID TITHERIDGE[5]

[1]The University of New South Wales, School of Geology, [2]AGURBA Pty Ltd, [3]BHP Billiton Illawarra Coal, [4]Coal Geotechnical Services Pty Ltd, and [5]Tahmoor Colliery

Access to underground coal reserves is conditional on the reduction of coal gas content to below the regulatory outburst threshold limit. Reduction of gas content is currently achieved by pre-drainage of the seam using underground drainage systems. Several mines in the Southern Coalfield of New South Wales have recently encountered areas in which drainage of gas has proved to be very difficult. As a part of an ongoing ACARP funded research project, a petrological study of coal properties has been undertaken on selected coal samples from the Bulli seam (Southern Coalfield). The purpose of this project is to determine the nature and origin of very low drainability areas within the coal seam, as well as to characterise the mass differences in the coal between normal and difficult drainage areas. The initial results of this project have shown that some differences in coal properties may be directly related to gas drainage efficiency. Several micro-markers have been identified that appear to have an impact on the gas content and gas drainage characteristics.

INTRODUCTION

The problem of outbursts and high gas emissions must be controlled ahead of mining operations in line with established safety requirements. Gas content threshold values for safe mining of a coal seam are applied across the underground coal mining industry. These values are achieved by pre-drainage of the seam using underground drainage systems. Yet in many operations high gas content and low drainability areas are a major obstacle in achieving economic longwall development rates.

Areas with coal of high gas content and low permeability are encountered within the Southern Coalfield at West Cliff, Appin and Tahmoor Collieries, and more recently at Tower Colliery. Such difficult drainage areas are expected to become increasingly important in other underground coal operations both in NSW and Queensland. Large changes in gas drainage characteristics are reported to occur even over relatively short distances (tens of meters) within the Bulli seam.

In order to determine the nature and origin of the very low permeability areas within the coal seam, as well as to characterise the mass differences between the coal of areas with normal drainage and areas with slow or difficult drainage conditions, a petrological study has been undertaken as a part of a research project funded by the Australian Coal Association Research Program (ACARP C10011). The aim of the project is to determine coal properties that might affect gas drainage efficiency. The project aims to quantify the directional changes in coal properties due to regional stress and the stress induced during intrusion, and to investigate the impact of faults and igneous intrusions on coal properties such as microstructure, mylonitisation and mineralisation. The objective is to develop a simple means of detecting such difficult/low drainability areas well in advance of actual mining, so that appropriate drainage strategies can be developed.

The paper aims to discuss some of the specific microscopic characteristics of coal identified as being directly related to gas drainage difficulties in particular areas of the mines. Prior to the commencement of the ACARP project, a number of samples from Tower and West Cliff Collieries were also investigated to determine the nature and origin of very low drainability areas within the Bulli seam (Gurba et al., 2000).

METHODOLOGY

Sampling

A set of coal samples was obtained from the Bulli seam in the collieries of the Southern Coalfield, and a study undertaken of the variation in coal properties that may be related to difficulties with gas drainage in particular areas. To develop a better understanding of the influence of coal properties on gas drainage characteristics, a series of oriented sample pairs were collected in close proximity and from the same section of the seam representing normal and difficult drainage areas. In some coal mines it was not possible to obtain such a specimen pair; in these cases coal samples with

difficult and normal drainage characteristics were taken from drilling. The coals cover the high to low volatile bituminous rank range, with the exception of some very high rank heat-affected coals collected in proximity to igneous intrusions.

Experimental

The tools used in the project include the optical microscope, electron microprobe and X-ray diffractometer. Oriented 1-3cm coal blocks with 3 polished orthogonal faces were used for reflectance, micro-structural observation and other optical studies. This is a departure from conventional practice, which involves either unoriented blocks or crushed coal samples.

The samples were prepared for microscopic examination as epoxy impregnated blocks according to Australian Standards (Standards Australia, 1989a). The polished samples were examined using a Zeiss Axioskop reflected-light microscope, fitted with both white (50W halogen) and blue-violet (HBO) light sources. Maximum and minimum reflectance of vitrinite (telocollinite) was measured following the Australian Standard (Standards Australia, 1989b). All measurements were taken using monochromatic light of 546nm wavelength and in oil immersion.

Additional microscopic studies on the coal samples were directed at describing:

- the development of coal microstructure (development of micro-cleats, slits and pores), and associated mineralisation,
- the pattern and significance of reflectance anisotropy,
- the fluorescence properties, and
- the development of coke mosaic structures.

Electron Microprobe Analysis

Selected coal samples were analysed using electron microprobe techniques. The electron microprobe is a powerful tool, which allows quantitative chemical evaluation of both the organic matter and the mineral matter simultaneously. The electron microprobe investigates a 2-5 micron diameter spot to produce a chemical composition analysis. More detailed description and application of the technique in coal research is given by Gurba and Ward (2000).

RESULTS AND DISCUSSION

Several differences in optical properties have been identified between the coal of normal and difficult drainage areas. These differences are related to the presence of some specific micro-markers identified in the bad drainage areas, such as:

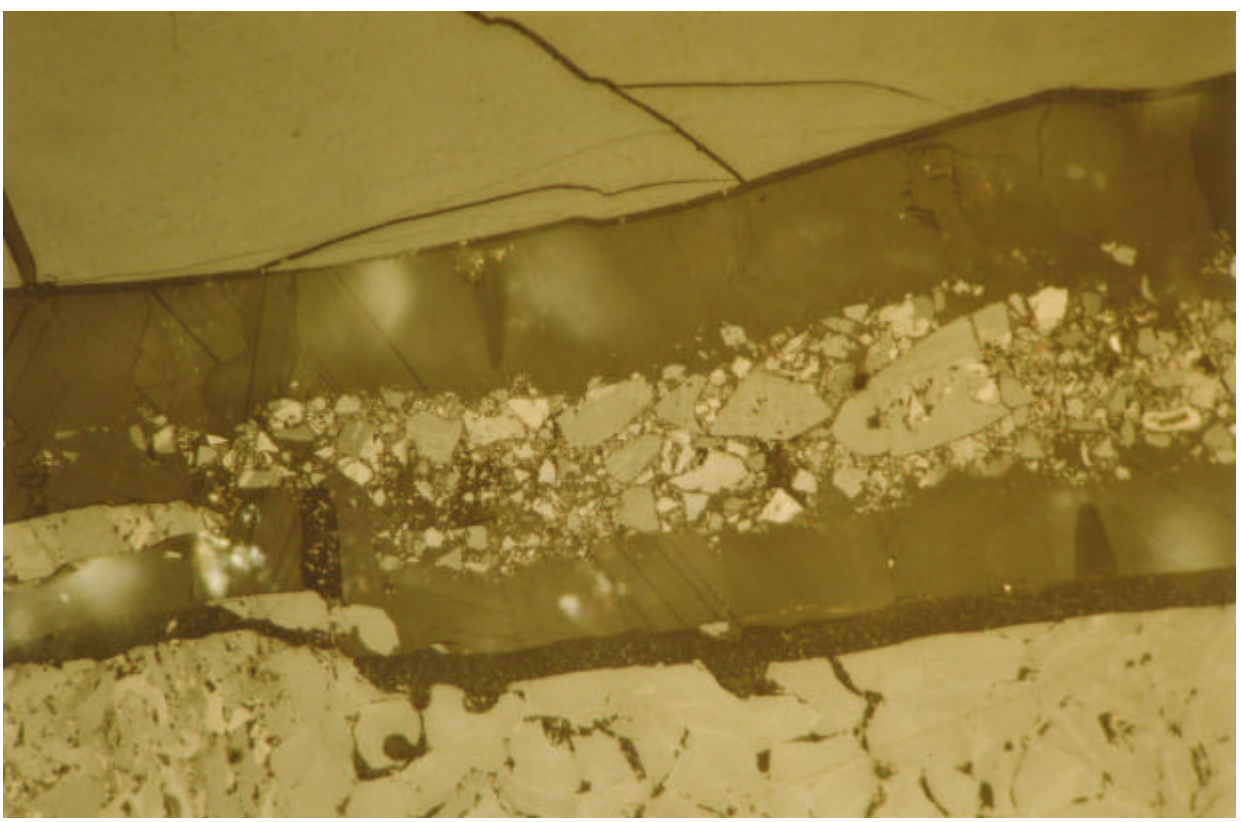

Figure 1 Microphotograph showing coal from a low/difficult drainability area as observed in a bedding plane section. Note large micro-cleat filled with calcite, and in the central part with brecciated coal (mylonite). Reflected light, oil immersion, field of view is about 0.22mm.

mylonitisation of the coal,
- development of micro-cleat and its mineralisation,
- the mode of occurrence of minerals in coal macerals,
- development of vitrinite reflectance anisotropy,
- the presence of oil and solid bitumen in coal macerals,
- the presence of heat-affected coals, and
- the presence of pyrolytic carbon.

Some of these micro-markers are discussed below.

Mylonite (Brecciated Coal)

Microscopic examination of coal samples from difficult drainage areas has revealed the presence of powdered or brecciated coal (mylonite) in vertical and horizontal micro-cleats (Figure 1). This form of mylonite is invisible in hand specimen and occurs in solid-looking coal. Such mylonitic coals have probably been subjected to deformation caused by nearby faults and/or dykes.

Mylonite has been reported to occur, or to be associated with, almost all outbursts in the Southern Coalfield of New South Wales (Lama and Bodziony, 1998). At Leichhardt Colliery, Blackwater (Queensland) the presence of vitrinite-rich mylonitised coal and an inertodetrinite-rich coal were also responsible for a methane/coal outburst (Beamish and Crosdale, 1998). This mylonite can be identified at a macroscopic scale, and usually occurs as an infilling of structures/fractures in the coal seam or as bands several centimeters thick within the seam.

However, in the samples studied from the Bulli seam, the mylonitised coal identified in difficult drainage areas occurs in micro-cleats. It is cemented by carbonate (calcite or dolomite) or clay minerals, and is invisible in hand specimen. The mineralisation may have an impact on gas flow and gas drainage efficiency. This type of coal will retain its gas content due to a resulting slow diffusion rate. Cao et al. (2000) suggest that the higher gas content of outburst coals results from the greater surface area for gas adsorption associated with mylonitised, granular, or cataclastic coal, and the higher tectonic pressure in the geologic environment that contributed to the entrapment of gas in the coal seam.

According to Lama and Bodziony (1998) seams where the structure of the coal has been damaged or completely obliterated are most liable to outbursts. As stated by Cao et al. (2000) two important geological observations related to outburst occurrence are (1) that nearly all outbursts occur in the deformed coal layers within tectonically deformed zones, and (2) that outburst coals have higher gas contents than non-deformed coals.

The presence of mylonite in the micro-cleat indicates that the zones related to geological structures, such as shear zones, fault zones or the presence of dykes, extend over much larger areas than can be identified by normal geological observation. In areas where mylonite occurs in micro-cleats the outburst proneness may increase due to difficulties in extracting gas from the coal matrix.

Microstructure and Mineralisation

The presence of cleat and its open nature and mineralisation are of fundamental importance to the development of coal permeability. Permeability of coal is a critical factor in the extraction of methane from coal seams. Systems of fractures in coal may provide permeable conduits for reservoir drainage, if the fractures are sufficiently open to fluid flow.

When observed under the reflected light microscope with magnification about 500X, coals from the Bulli seam were found to contain a characteristic microstructure, consisting of micro-cleat (apertures ranging from 2-10µm to more than 300µm), slits (2-5µm to 30µm in size) and devolatilisation pores.

Microscopic investigations have shown that in coal with good drainage characteristics the micro-cleats are mostly empty, or only partly filled with calcite or dolomite (Figure 2). A system of slits parallel to the micro-cleats was also found in the better drainage areas. These slits are preferentially developed in the telocollinite layers, and would also be expected to enhance permeability. As reported by Gurba and Weber (2001), the micro-cleat systems can be developed in both macerals of the vitrinite group (telocollinite and desmocollinite), but the slit pattern is developed preferentially within telocollinite. Slits have been found to enhance seam permeability (Gurba and Weber, 2001).

In poor drainage areas, calcite (or dolomite) completely fills the cleat voids, and, in addition, the micro-cleats are often filled with mylonite (Figure 1). As revealed by electron microprobe analysis the breccia (mylonite) is cemented by calcite, dolomite or kaolinite. Mineralised micro-cleat can become impermeable to gas, forming a screen and blocking methane migration. The micro-cleat system can also be a source of anisotropic permeability, as micro-cleat development and its mineralisation in some samples seem to follow preferential directions. Thus the mineralisation in micro-cleats and the presence of mylonite probably play a major role blocking or slowing down gas drainage.

Abundant siderite nodules (Figure 3) have also been identified in the coal from difficult drainage sites. These may block the micro-pores in the maceral cells; ie they reduce the void spaces for gas permeation.

Oil and solid bitumen

The presence of oil droplets and abundant fluorescing material has been discovered in the cell cavities of the coal macerals in difficult gas drainage areas. The fluorescing material in the cell cavities may represent mineral matter or solid bitumen residues. The

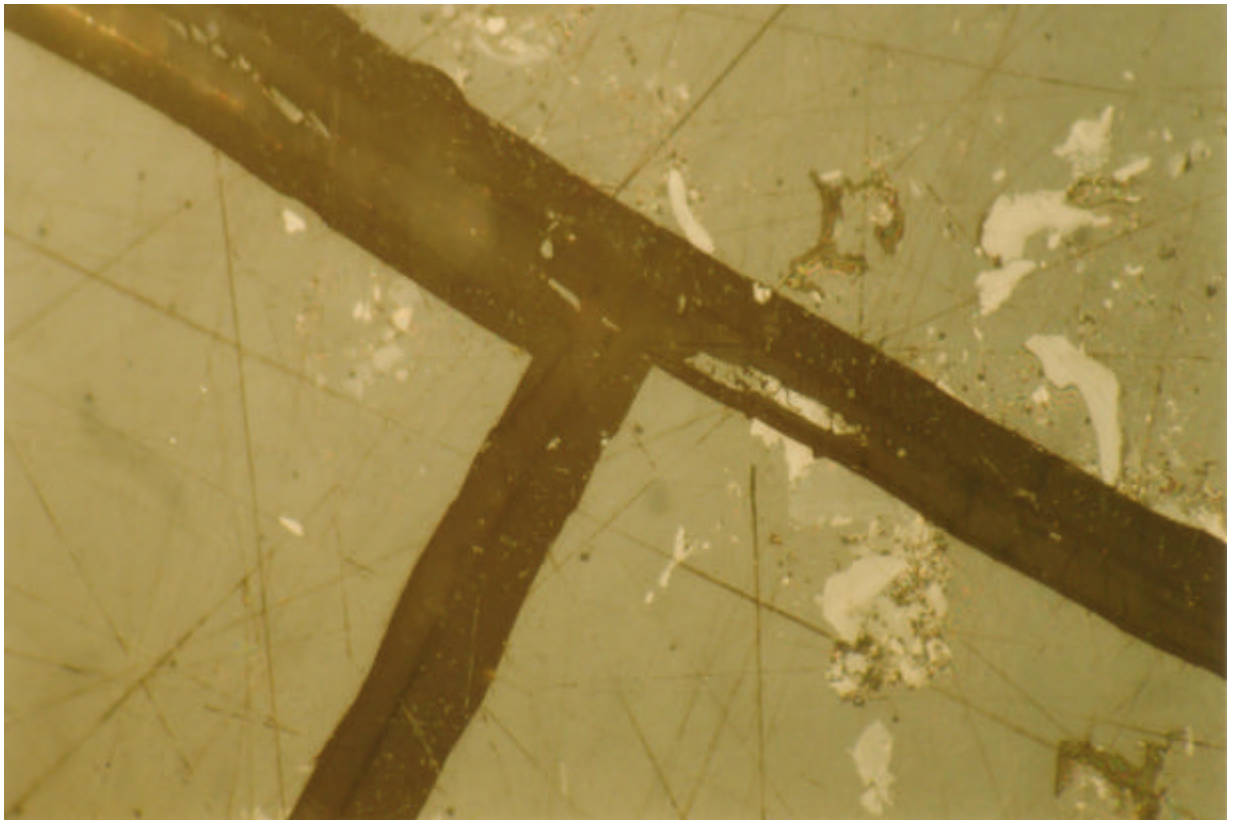

Figure 2 Microphotograph showing coal from normal drainage area observed in a bedding plane section. Note large, only partly mineralised micro-cleats (black). Reflected light, oil immersion, field of view is about 0.22mm.

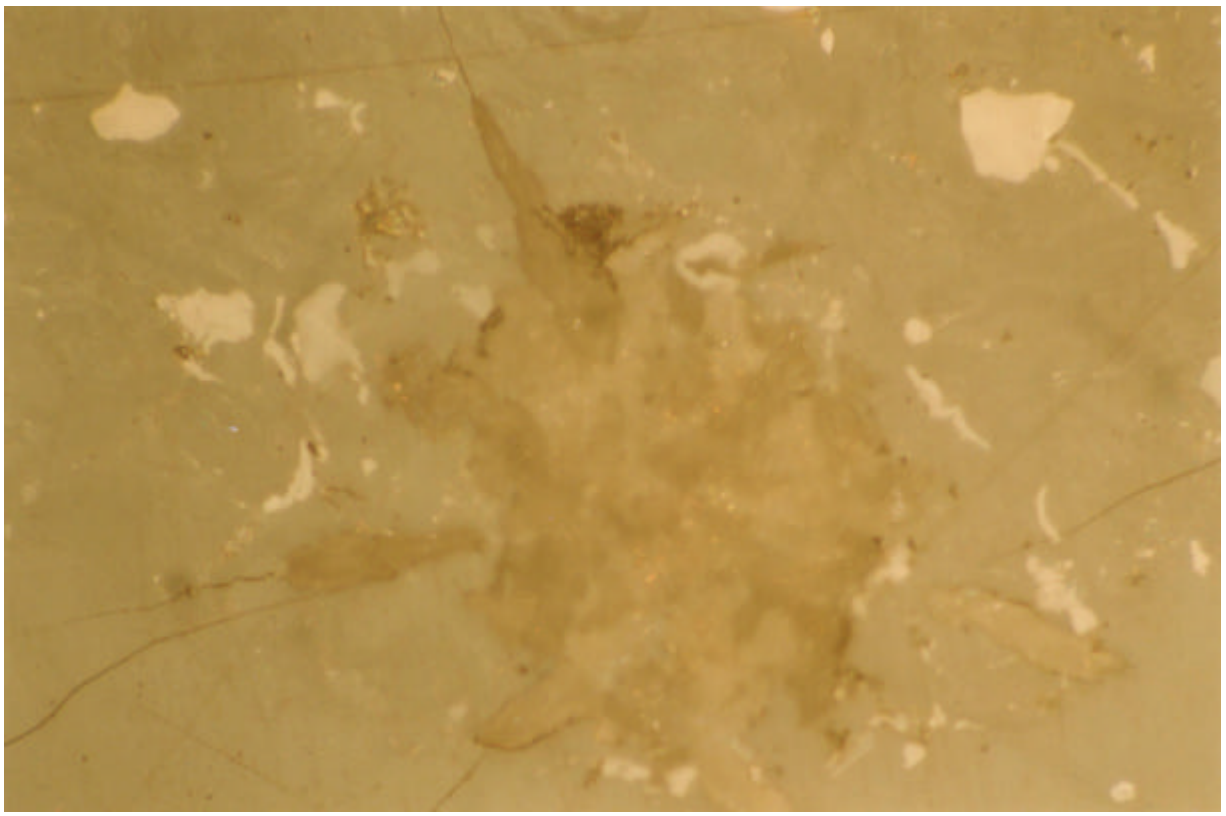

Figure 3 Microphotograph showing coal from a low/difficult drainability area as observed in a bedding plane section. In the central part is a large siderite nodule. Reflected light, oil immersion, field of view is about 0.22mm.

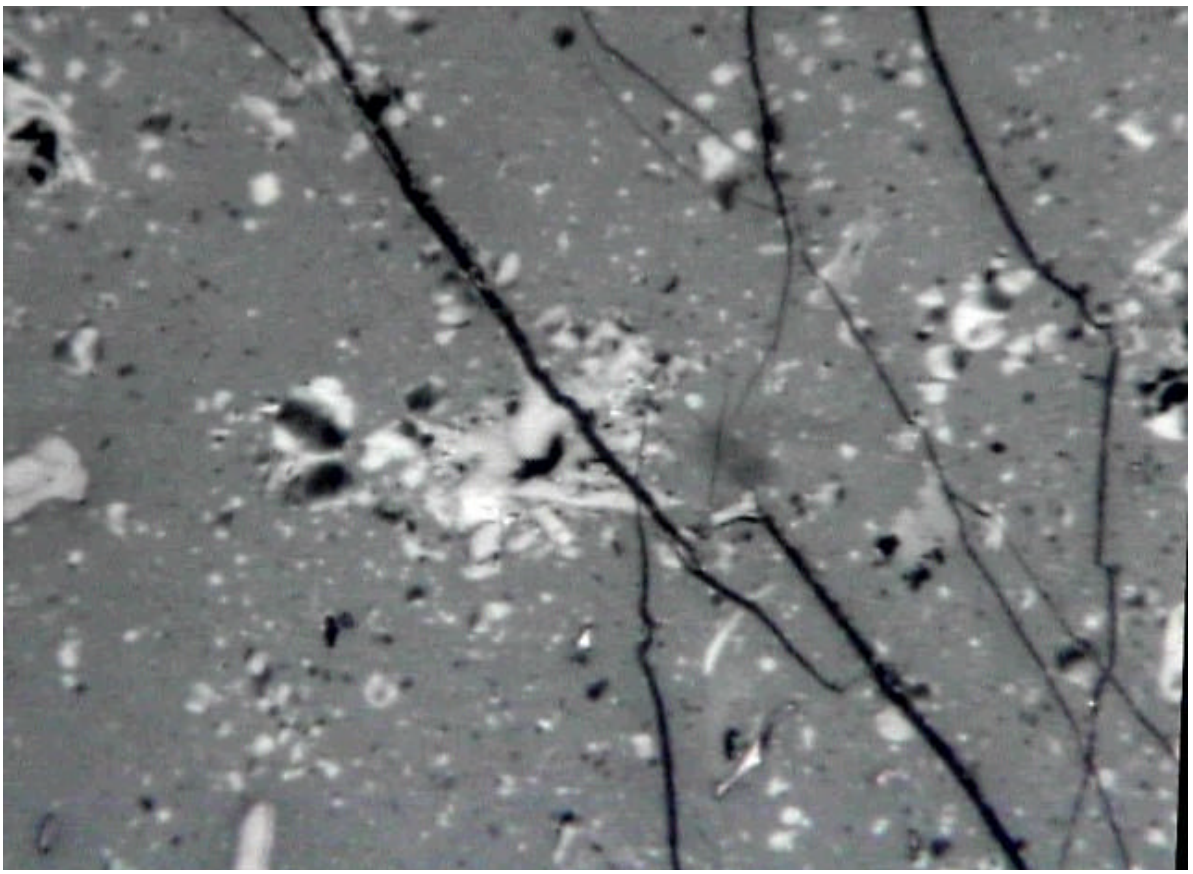

Figure 4 Microphotograph showing coal from a low/difficult drainability area as observed in a section perpendicular to bedding plane. Grey background is vitrinite, white, strongly anisotropic grains are pyrolytic carbon. Reflected light, oil immersion, field of view is about 0.22mm.

presence of the droplets may indicate the presence of liquid hydrocarbons (oil) in the coal. Such oils may migrate into macropores, or may permeate into the vitrinite microstructure. The oil or the solid bitumen (residues of the oils?) may also reduce coal seam drainage characteristics by restricting or closing the pore throats and filling the pore spaces.

Pyrolytic Carbon

Pyrolytic carbon has also been found in some coal samples (Figure 4), indicating that the relevant coals might be within alteration zones associated with igneous bodies. The pyrolytic carbon was probably deposited from the gas phase as a result of chemical cracking of volatiles generated during intrusion. Pyrolytic carbon can be found some distance away from known intrusions, indicating a possible long migration path for the volatile matter displaced from the intruded coal seams.

CONCLUSIONS

The results of the ongoing research include the following aspects.

- Microscopic examination has revealed a fine powdery structure of the coal in micro-cleat of the samples analysed in low drainability areas. The mylonite seems to have an impact on the gas content and drainage characteristics in the collieries of the Southern Coalfield. The micro-cleat aperture and its mineralisation may play a major role in blocking gas drainage.
- Coal seam drainage can also be reduced by the presence of oil and solid bitumen in cell cavities restricting or closing the pore throats and filling the pore spaces.
- Siderite nodules have also been identified in the coal. These may block the micro-pores in the maceral cells, ie reduce the void spaces for gas permeation.
- These changes in coal properties, as seen under the microscope, occur over a much larger regional volume than that in which the relevant features can be observed macroscopically at core scale (e. g. mylonitisation, micro-cleat mineralisation, cindering of the coal).

The seam gas flow from the micropore system to the cleats must rely upon the effectiveness of the microstructure system in coal for gas migration. The extent and the rate of gas flow through the coal will be influenced by coal microstructures, especially the micro-cleat openings and infillings. Efficient drainage is achieved if the gas is able to migrate through the coal seam at a satisfactory rate down a reasonable pressure gradient. The presence of some micro-markers identified in bad drainage areas can retard the rates of gas flow through the coal by blocking flow paths and as a consequence slowing down the gas drainage process. The micro-markers identified from this study clearly have an impact on the gas content and drainage characteristics.

ACKNOWLEDGMENTS

Funding for the project has been provided by the Australian Coal Association Research Program (ACARP Project C10011). Financial assistance was also provided by BHP Billiton Illawarra Collieries prior to the commencement of the ACARP project.

We would like also to acknowledge Tahmoor Colliery, and Tower, West Cliff and Appin Collieries (BHP Billiton Illawarra Collieries) for assistance with sampling and gas drainage information. Rod Doyle is thanked for constructive comments on the manuscript.

REFERENCES

BEAMISH, B. B. & CROSDALE, J. P. 1998. Instantaneous outbursts in underground coal mines: An overview and association with coal type. *International Journal of Coal Geology* **35**, pp. 27-55.

CAO, Y., MITCHELL, G D., DAVIS, A. & WANG, D. 2000. Deformation metamorphism of bituminous and anthracite coals from China. *International Journal of Coal Geology* **43**, pp. 227-242.

GURBA, L.W. & WARD, C. R. 2000. Elemental composition of coal macerals in relation to vitrinite reflectance, Gunnedah Basin, Australia, as determined by electron microprobe analysis. *International Journal of Coal Geology*, **44,** pp. 127-147.

GURBA, L. W., WARD, C.R. & GURBA, A. 2000. Petrographic and mineralogical analysis of coal samples. Unpublished Report for BHP Collieries Division.

GURBA, L. W. & WEBER, C. R. 2001. The relevance of coal petrology to coalbed methane evaluation, using the Gloucester Basin, Australia as a model. Proceedings of 2001 International Coalbed Methane Symposium. The University of Alabama, Tuscaloosa, Alabama, May 14-18, pp. 371-382.

LAMA, R.D. & BODZIONY, J. 1998. Management of outburst in underground coal mines. *International Journal of Coal Geology* **35**, pp. 83-115.

STANDARDS AUSTRALIA. 1989a. Preparation of coal samples for incident light microscopy. *Australian Standard **2061***: 4p.

STANDARDS AUSTRALIA. 1989b. Methods for microscopical determination of the reflectance of coal macerals. *Australian Standard* **2486**: 12p.

Geological hazards — The impact to mining 15-16 November 2001, eds Doyle, Moloney, pp 221-230

The Development and Implementation of the Moonee Colliery Windblast Warning and Control System

NEWLAND[1], R. CAMPBELL[2] & C. MACDONALD[3]

1. Principal Consultant, Newtuk Consulting Pty Ltd, 2. Manager Moonee Colliery, Coal Operations Australia Pty Ltd, 3. L/W Coordinator Southland Colliery (Formerly Projects Coordinator Moonee)

This paper will describe how Moonee Colliery has controlled the mine workforce exposure to windblast at Moonee Colliery by using seismic monitoring, hazard control plans and hydrofracturing. These measures have enabled Moonee to continue longwall production under a thick conglomerate roof, which caves naturally only over large areas therefore creating a windblast hazard.

INTRODUCTION

Moonee Colliery restarted as a longwall operation in late 1997 after being closed as a bord and pillar extraction colliery in the early 1990's. Moonee Colliery longwall blocks are narrow by most standards 90m with 40m chain pillars due to surface subsidence restrictions caused by the old Pacific Highway and the Munmorah State Recreation area. The longwall extraction area for the first 6 or 7 longwall blocks is overlain by thick conglomerate which has a tendency to hang up for some time with a result that when it finally falls a windblast may be generated.

In early 1998 a goaf fall occurred which generated a strong windblast which injured a number of mine workers. Mining was stopped until a method was found to warn mine workers of impending goaf falls. It was discovered that ISS Pacific had a seismic monitoring system that had been used at Newstan Colliery to monitor and warn mine workers of seismic activity associated with impending goaf falls under a conglomerate channel roof. The ISSP seismic system is also widely used at a number of metalliferous mines to monitor seismic activity.

The Newstan ISSP system was no longer in use so could be purchased from Powercoal Pty Ltd, the operators of Newstan Colliery, and transported to Moonee. The system was setup and operating in less than two weeks, therefore enabling Moonee to restart production after finalising its windblast management plan.

In April 1999 longwall production was again halted, after a mineworker was injured by a goaf fall. No warning, either audible or seismic, of the fall was given. The mine was unable to recommence production until the management and Mines Inspectorate were satisfied that an additional system to the seismic monitoring system was in place to prevent injury due to windblast.

As a result of this the safety systems already implemented under the Windblast Management plan were revised, a Microseismic Plan was developed and a system of hydrofracturing the mine roof in the goaf was developed in conjunction with SCT Australia Pty Ltd and the CSIRO Petroleum Division.

THE WINDBLAST CONTROL AND MONITORING SYSTEMS

ISSP Seismic Monitoring System

The seismic monitoring system uses geophones to detect seismic noises caused by roof movement in the goaf. The seismic events are processed using the ISSP software, which calculates the size and position of each seismic event. Based on certain criteria strata alarms can then be given to the longwall crew via the Citect mine monitoring system, allowing the crew to move to safe havens for protection from windblast.

Seismic System Hardware

The Moonee ISSP monitoring system, from Feb 1998 to Mar 1999, used PS seismic boxes located in a purpose-built underground cabinet connected through the mine optic fibre communication system to a surface Silicon Graphics processing computer. Each PS box gathered data from one triaxial geophone.

During March 1999 the PS boxes were exchanged for MS boxes which have the capability of running three triaxial geophones per box. The PS or MS boxes and the geophones are connected by shielded cable with an approved safety barrier isolating the geophones and the boxes. Four geophones are used, two each side of the longwall block ideally straddling the area of longwall extraction.

A further system change occurred in Aug 2000 when the Silicon Graphics surface-processing computer was exchanged for a standard PC running the ISSP seismic processing software under Redhat Linux 5.0.

Diagrams of the seismic system and the geophone layout in relation to the mine workings are shown in Figures 1 and 2.

Seismic System Software

ISSP have developed seismic monitoring software over many years originally to monitor seismic activity caused by ground movement in deep South African gold mines. The software consists of numerous programs and is extremely configurable to individual mine situations.

The MS boxes underground run the RTS (Run Time System) part of the software which gathers the seismic triggers from the geophones and does some initial processing of the seismic data, before it is sent up to the surface-processing computer.

The seismic operators use only a few of the software programs eg 'xmts' (the seismic processing program) and 'xdi' (the seismic graphical parameter program). Other programs, such as 'chncon' are used to change geophone sites as the longwall mining progresses.

COAL IT personnel and ISSP wrote Linux scripts to provide audible warning to the seismic operators when a seismic trigger or communication loss occurs. A Linux script (auto) was also written by COAL IT personnel to initiate an auto alarm (used when the operator has to leave the seismic control room).

Seismic Alarm Criteria

When the seismic monitoring system was used at Newstan a warning system was devised based purely on frequency of events with the longwall face mine workers being evacuated for the rest of the shift after a seismic alarm.

Moonee Colliery by comparison withdraws the longwall crew for two hours after a trend alarm or stops production for 20 minutes with the crew staying in safe havens on the face after a frequency or magnitude alarm.

At Moonee the alarm criteria have been developed and refined by back analysing the seismic data. The criteria were at first a purely frequency based alarm system as at Newstan but are now more sophisticated warning criteria based on frequency, magnitude and trends. A summary of alarm criteria is shown in Figure 3.

It needs to be emphasised that the seismic alarm criteria were developed for Moonee Colliery geological situation and would need to be redefined for different geological situations.

A total of 127 goaf falls producing significant wind velocities have occurred since seismic monitoring commenced. For these falls seismic alarms have given warnings longer than 12 seconds in 84% of cases. Figure 4 summarises fall warning times, while figure 5 indicates the magnitude of seismic events.

Strata Alarm Initiation

The strata alarm can be initiated in a number of ways. This can be by the seismic operator when strata alarm criteria are met, by an auto alarm, by the longwall crew if they believe a fall is imminent or by chock leg pressure when three adjacent chocks exceed 350bar.

When a strata alarm is initiated all HT power is disconnected therefore stopping the shearer, AFC, crusher and belts, strobe lights flash along the longwall face and at the DCB and sirens go off. As soon as this occurs the longwall crew make their way as quickly as practicable to safe havens which are located at intervals along the face and in the maingate. Figure 6 shows the paths of the strata alarm signal being sent from the surface Citect computer to underground.

Windblast and Microseismic Plan Controls

A windblast as shown in Figure 7 is generated by a goaf fall which results in mass air movement that causes injury and/or seriously disrupts ventilation or is greater than 20m/sec. The premise of 20m/s is derived from the fact that terminal velocity is of the order of 50m/s and the force due to wind drag varies in proportion to the square of velocity. It follows, therefore, that a drag force equal to 15% of self-weight would be occasioned by an air speed of the order of 20m/s. It is provisionally assumed that the sudden application of a force equal to, or more than, 15% of self-weight would give rise to the possibility of an individual in an upright mode being knocked over. In Moonee's case any velocity greater than 20m/s is classified as a significant velocity. The velocities and overpressures are measured by equipment designed by Dr Chris Fowler at UNSW.

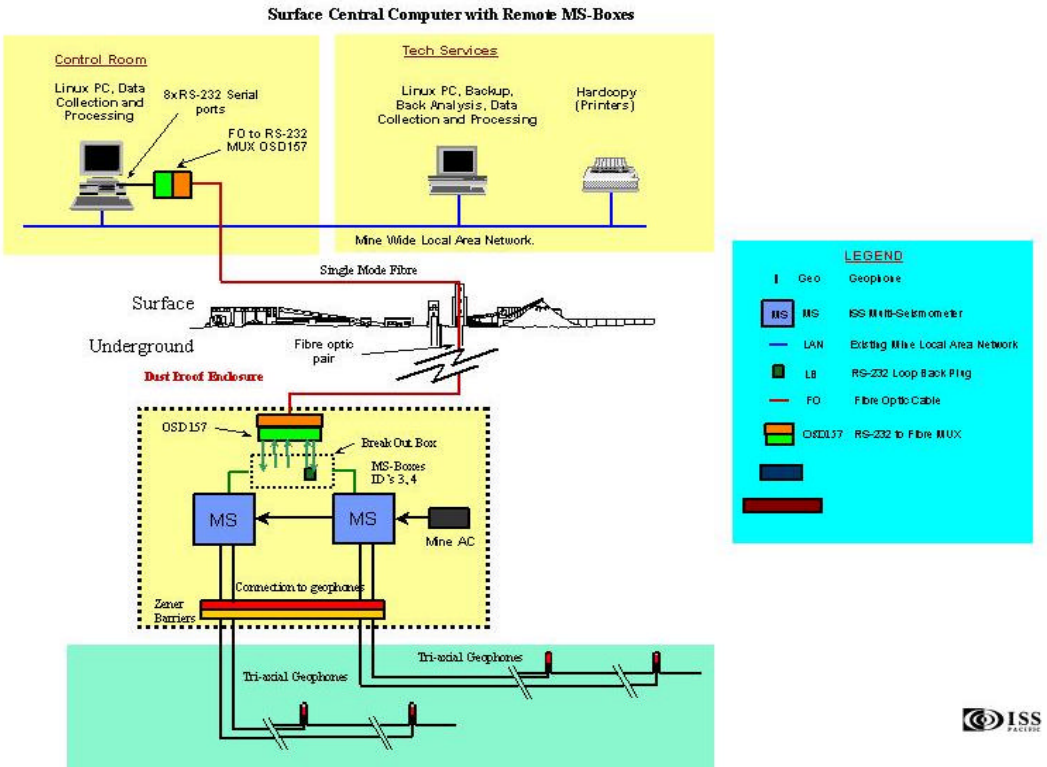

Figure 1 Seismic system for Windblast monitoring at Moonee Colliery.

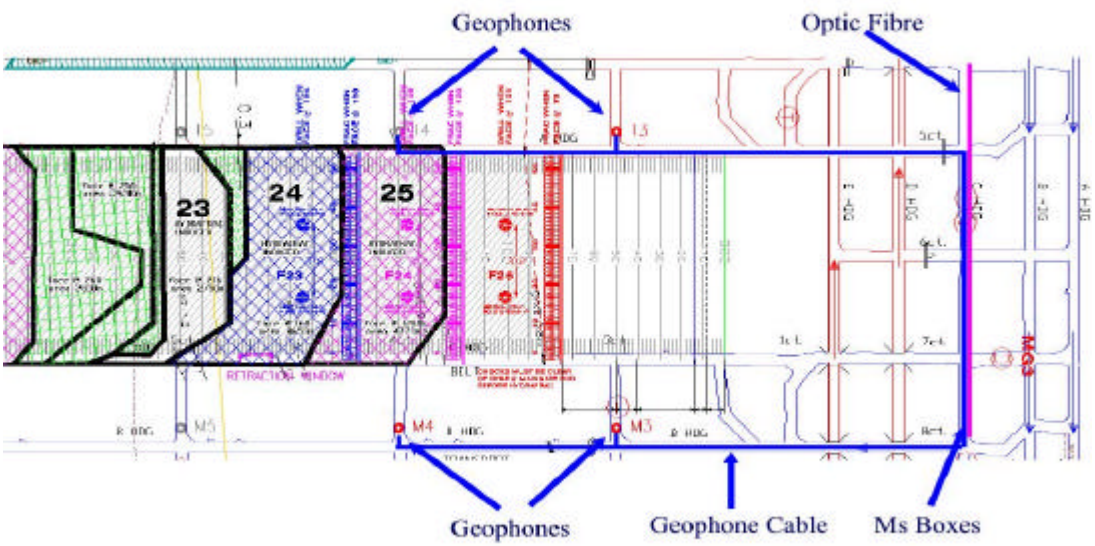

Figure 2 Geophone Layout for Moonie Colliery, also showing goaf fall areas.

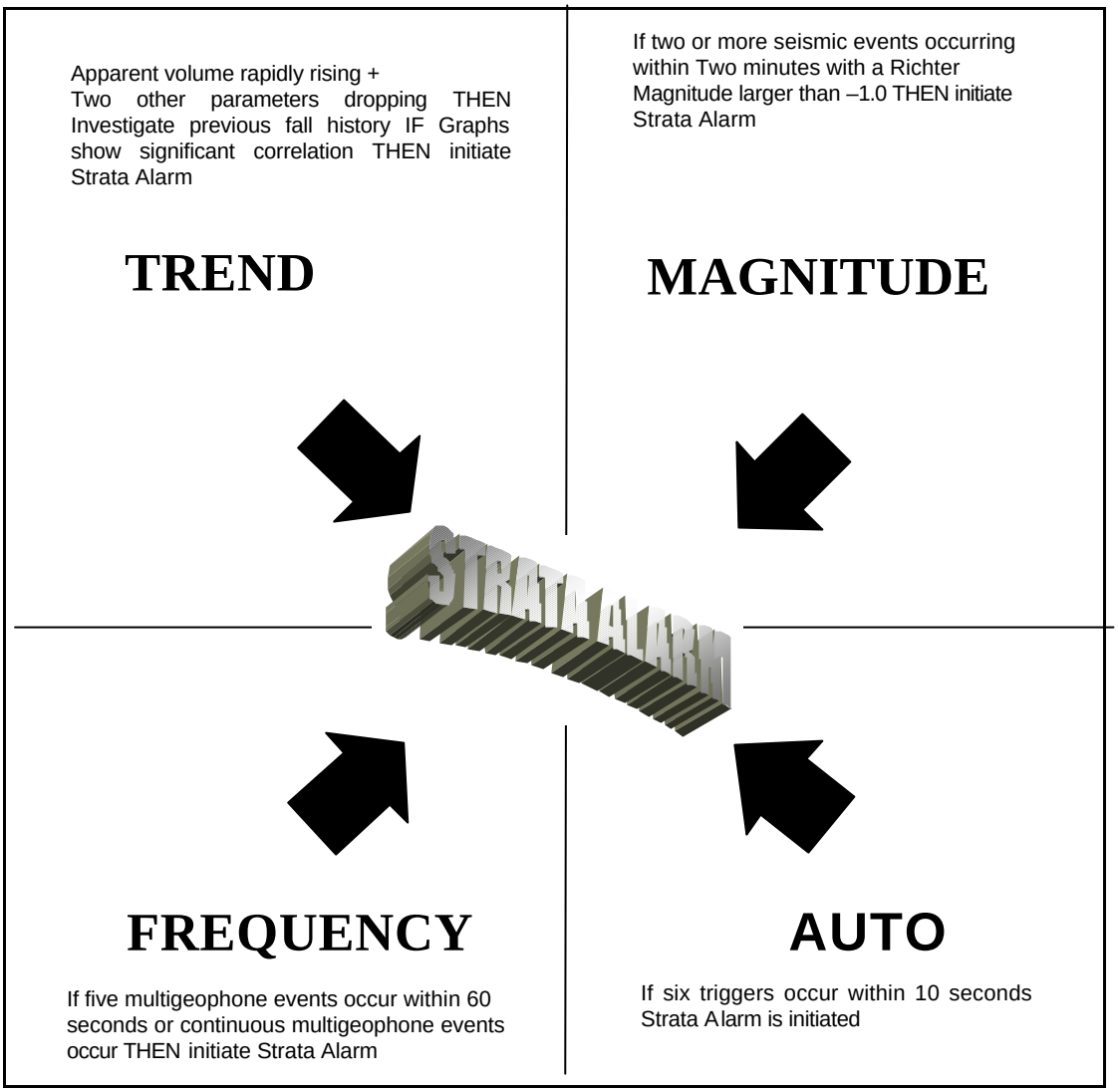

Figure 3 Summary of Seismic Strata Alarm Criteria

In the Mines' Windblast Management and Microseismic Plans, there are a number of controls used to minimise the exposure of the longwall crew to danger of windblast caused by a goaf fall. Some of the controls include the following aspects.

- Continuous Seismic Monitoring when any personnel are within the Windblast Zone of Influence.
- Windblast Zoning – Red Zone (>20m goaf standing), Green Zone (<20m goaf standing).
- Seismic Activity Levels (High and Low). These activity levels control where the longwall crew can move around the face area, limit certain tasks and control access through the longwall zone of influence.
- Windblast Zone of Influence. This is the area of the mine likely to be effected by a significant air velocity if a goaf fall causes a windblast.
- Windblast Task Procedures. These are procedures developed to enable work tasks to be undertaken within the windblast zone of influence.
- Seismic Alarms (Strata Alarms). These are caused by trend, frequency, auto or magnitude criteria being met in the seismic system or by longwall crew or chock leg pressure.
- False Alarms. These are alarms that have not met the seismic alarm criteria.
- Leg Pressure Alarms. These are caused by 3 adjacent chock legs exceeding 350 bar pressure.
- Pre Shift Inspection Procedures.
- Post Fall Procedures.
- Wind Flap.

The purpose of the wind flap is to cut all 3.3kV power to the longwall face machinery and conveyor belt when a windblast occurs. Two windblast flaps are situated at the remote inbye point of the Longwall DCB. These windblast flaps have been engineered to provide a positive trip. This has been achieved by utilizing reed type switches which physically pull apart

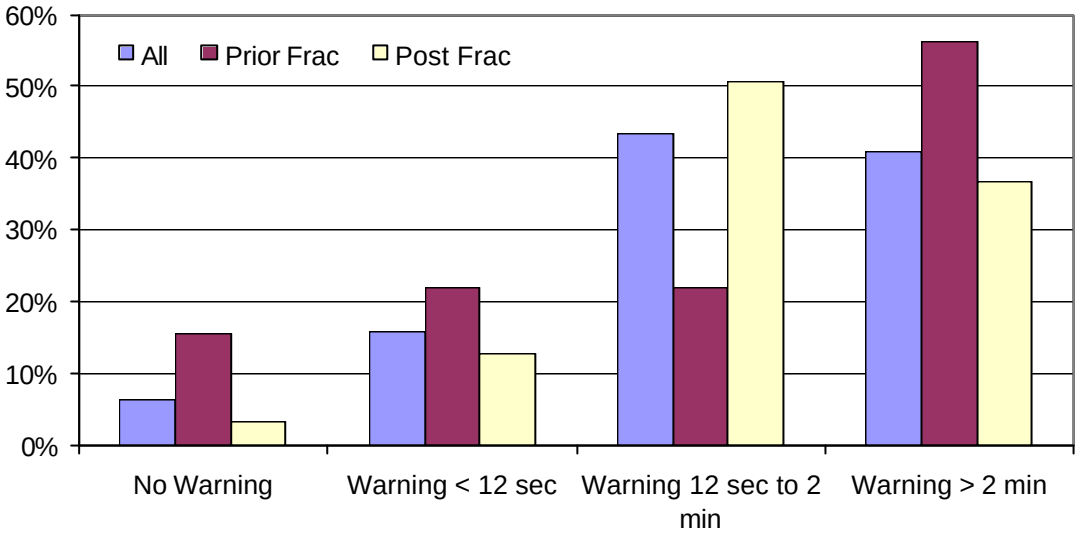

Figure 4 Summary Fall Warning Times to 21/08/01. A total of 127 goaf falls producing significant wind velocities have occurred since seismic monitoring commenced. For these falls seismic alarms have given warnings longer than 12 seconds in 84% of cases. Figure 4 summarises fall warning times.

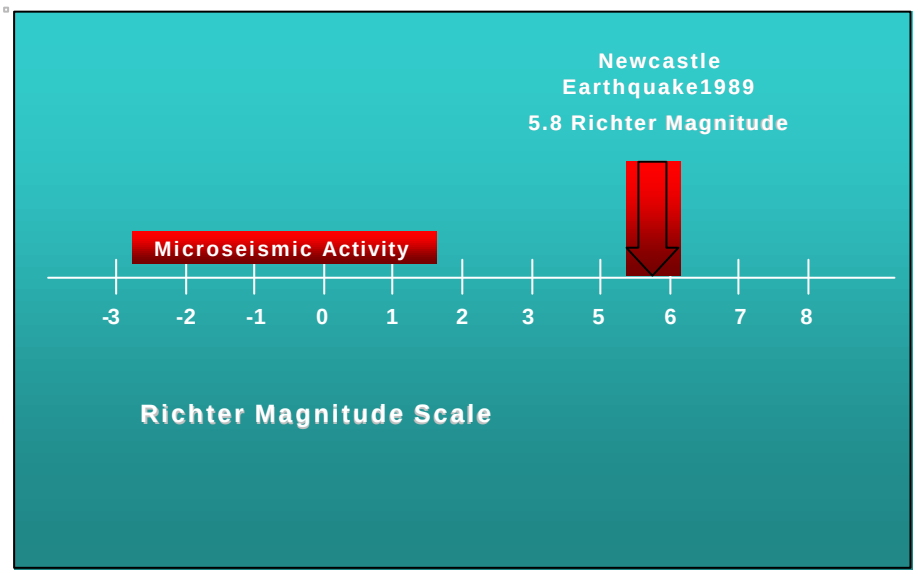

Figure 5 Size of seismic events recorded at Moonee Colliery. This figure shows the size of seismic events recorded at Moonee Colliery can be seen to be many orders of magnitude smaller than more familiar events such as the Newcastle Earthquake of 1989.

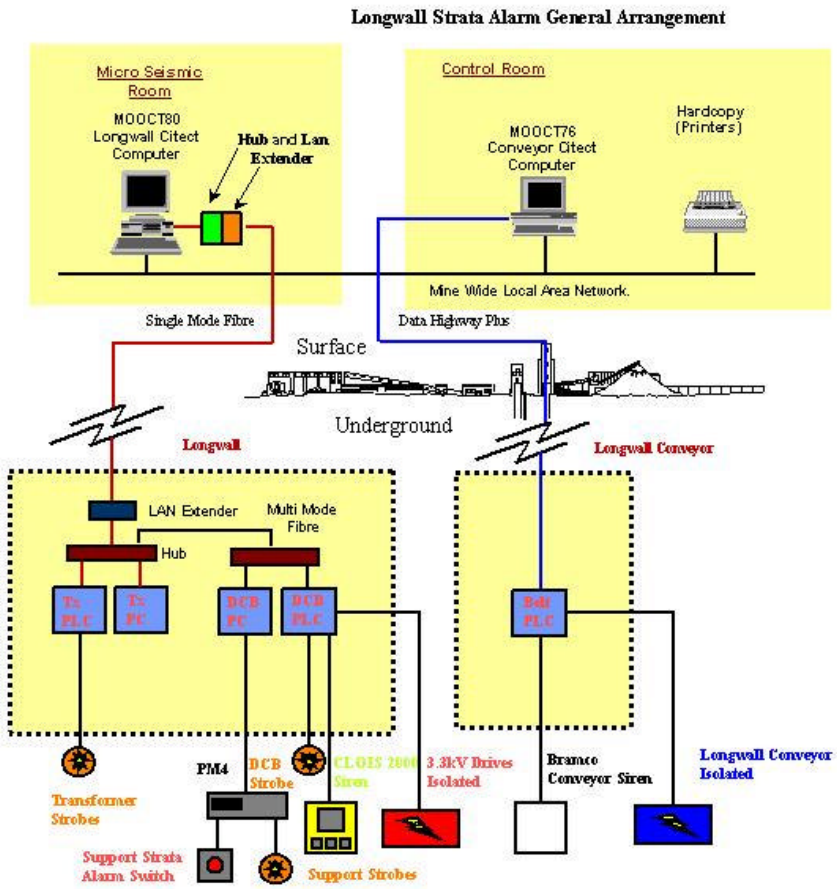

Figure 6 Longwall Strata Alarm General Arrangement.

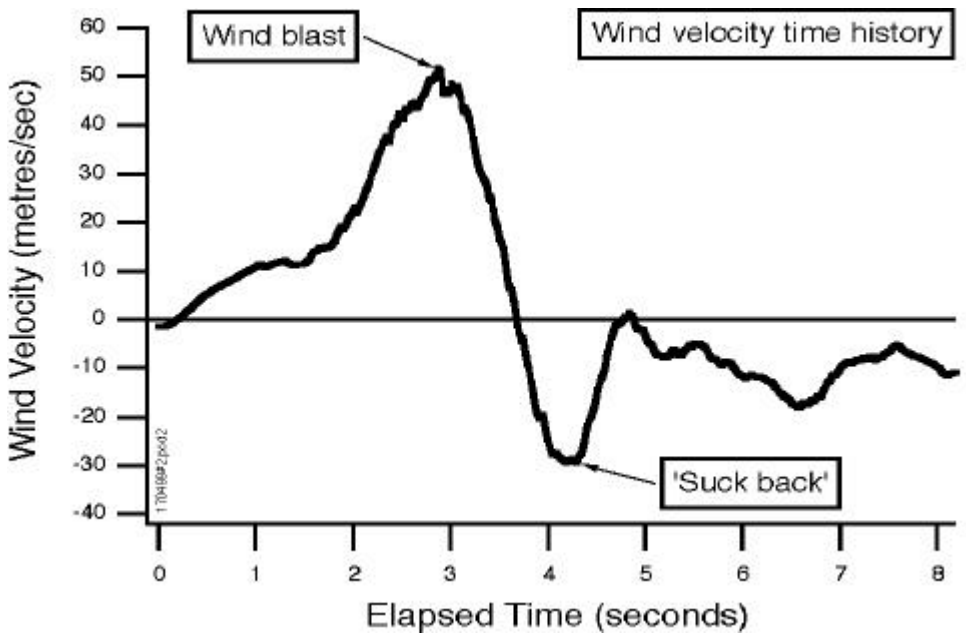

Figure 7 A typical windblast event

when activated and must be plugged back together before re-energising power.

Figure 8 shows the windflap and reed switches on the DCB. Figure 9 shows safety equipment required in the red zones.

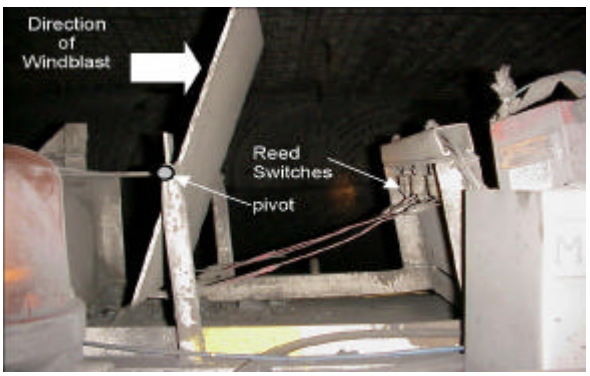

Figure 8 Wind-flap with reed switches position on DCB in Maingate

A safe haven is a place for persons to retreat to immediately before a major fall. Safe havens are positioned at the DCB in the maingate, the crib room cut through, the pump station cut through, the boot end and every second roof support. Figure 10 shows views of the roof support safe havens.

Figure 9 Personal safety equipment required in red zone.

Hydrofracturing

Strata Control Technology (Australia), CSIRO Division of Petroleum and colliery personnel developed the hydrofracturing system used. Moonee Colliery personnel run the system in-house on whichever shift a hydrofrac is required to be undertaken.

The hydrofracturing system currently operates in the following manner.

- Three boreholes are drilled vertically into the roof after 20m advance since the last fall and fraccing hoses grouted into the roof. (See Figures 11 & 12).
- Hoses are connected to the boreholes and are continuously fed out into the area behind the chocks as the face advances.
- When the longwall face advances to the predetermined frac distance (usually 60m) the hoses are connected to the fraccing valve bank and the longwall crew withdraws from the face to the surface.
- Solsenic is pumped into the hole to initiate the hydrofracture using the shearer water pump to finish the hydrofracturing and instigate the goaf fall.

The entire hydrofracture procedure is conducted from the surface, see Figure 13 using software written for the Citect control system. This software allows the Frac Coordinator to control all aspects of the control of pumps and valves and monitor flow rates and uphole pressures from the Citect computer located in the seismic monitoring room.

The initial frac on Longwall 6 successfully used crosslinked gel pumped from the surface to produce a successful hyrofracture failure. This was the first initial frac to fall on demand for any longwall since hydrofracturing has been used.

Figure 14 shows the pumping into the three holes in turn, the resulting pressure drops in the holes, and the subsequent goaf fall. All the data from the hydrofracturing procedure is recorded and kept for further analysis by Moonee personnel, SCT (Australia) and CSIRO Petroleum.

CONCLUSIONS

Longwall mining has been able to continue at Moonee Colliery under difficult geological conditions due to the use of the hazard management plan system, the seismic monitoring system and the hydrofracturing system to reduce windblast hazard. Without the commitment from the whole workforce at Moonee Colliery, the seismic contractors from Newtuk, MEGS, ISS Pacific, personnel from SCT (Australia) and CSIRO, the ongoing operation of Moonee Colliery would not have been possible.

ACKNOWLEDGEMENTS

The authors acknowledge the assistance from: Coal Operations Australia Pty Ltd for permission to publish this paper, all the personnel of Moonee Colliery, John Edwards (formerly of Coal Operations Australia), James Langdon of ISS Pacific, Van Zyl Brink (formerly of ISS Pacific), Ken Mills of SCT (Australia), and Rob Jeffrey of CSIRO.

Figure 10 Roof support Safe Havens

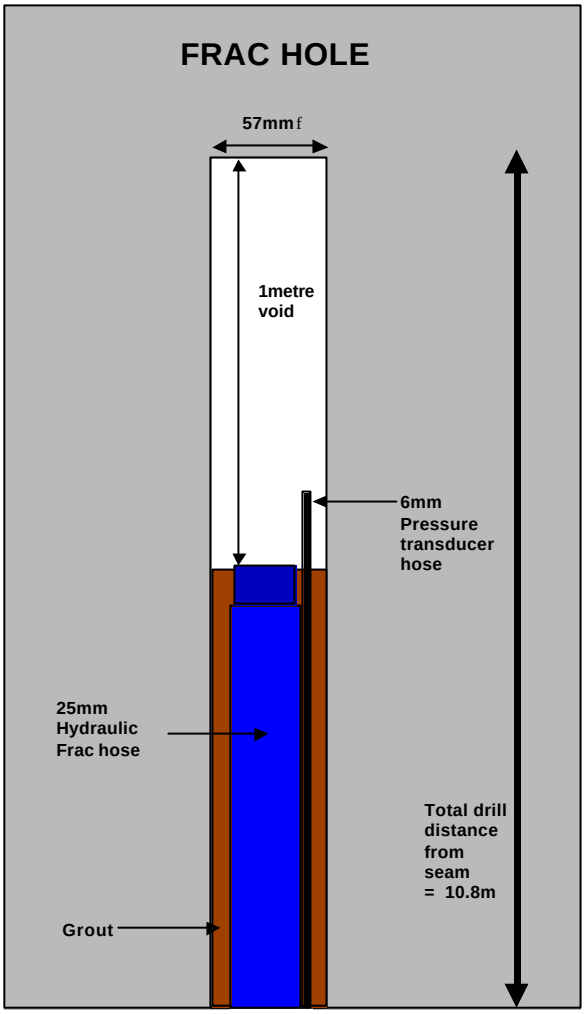

Figure 12 Hydrofrac hole layout.

Figure 11 Drilling of Hydrofracture Boreholes

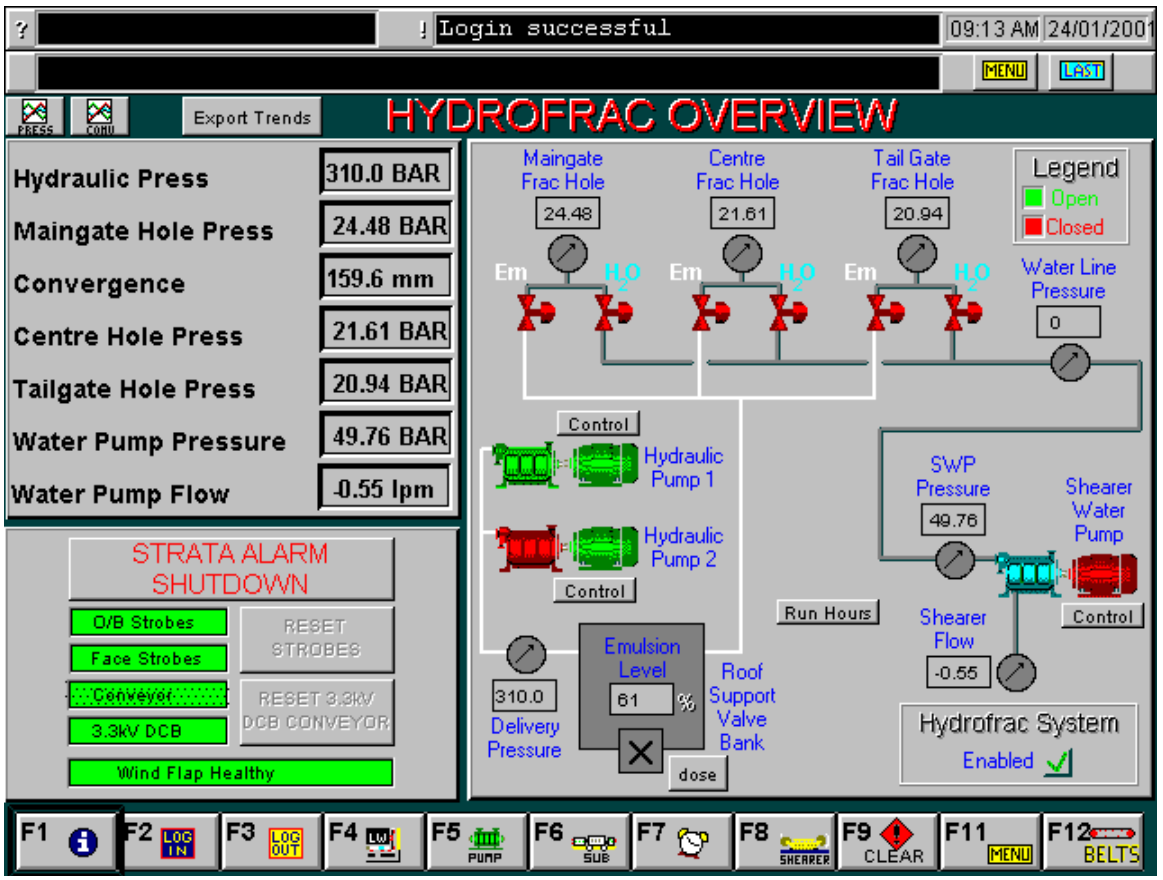

Figure 13 Citect Hydrofrac Control Screen

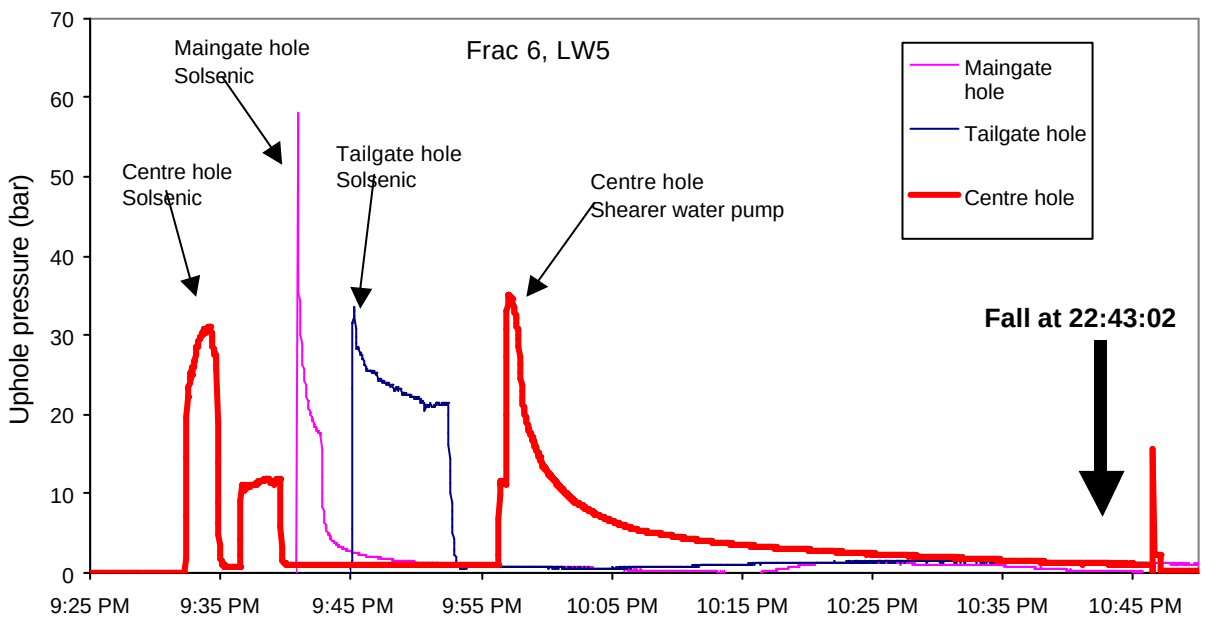

Figure 14 A Typical Frac Plot on 30/01/2001.

BIBLIOGRAPHY

FOWLER, J.C.W. & SHARMA, P. 2000 The dynamics of windblasts in underground coal mines. Project report no.4. University of New South Wales. ISBN0733407005.

JEFFREY, R.G. & MILLS, K.W. 1999 Hydraulic fracturing at Moonee Colliery. Internal report for Coal Operations Australia Ltd.

MACDONALD, C. 2001 Windblast Management at Moonee Colliery AJM Conference 2001.

MICROSEISMIC MANAGEMENT PLAN MSP-01 Coal Operations Australia Pty Ltd Moonee Colliery.

WINDBLAST CODE OF PRACTICE MDG No.1003 Moonee Colliery Internal Reports.

WINDBLAST MANAGEMENT PLAN WMP-01 Coal Operations Australia Pty Ltd Moonee Colliery.